Tooth Mobility, Periodontal Ligament Space, and the Alveolus During Periodontal Health, Disease, and Disuse

Atriya Salamati

A dissertation

submitted in partial fulfillment of the

requirements for the degree of

Doctor of Philosophy

University of Washington

2016

Reading Committee:

Susan W. Herring, Chair

Zi-Jun Liu

Katherine Rafferty

Johan Aps

Program Authorized to Offer Degree:

Oral Health Sciences

University of Washington

Abstract

Tooth Mobility, Periodontal Ligament Space, and the Alveolus During Periodontal Health, Disease, and Disuse

Atriya Salamati

Chair of the Supervisory Committee:
Professor Susan W. Herring
Department of Orthodontics and Oral Health Sciences

Teeth move during mastication and this mobility is structurally governed by the periodontium (including PDL and alveolar bone) supporting the teeth and functionally by the forces that are generated during mastication and transferred to the teeth via the masticatory muscles. The extent of this mobility is clinically used to determine the prognosis for teeth. However, the range of tooth movement and its direction under functional loads are largely unknown for either periodontal health, disease, or disuse.

The objective of this study was to investigate *in vivo* tooth mobility during mastication and masticatory muscle stimulation in pigs and its relationship to the periodontal ligament (PDL) space. A periodontal disease model was created and these diseased pigs were compared with healthy controls. However, it was not possible to create a pig disuse model, so instead quality of the alveolar bone supporting the molar teeth was assessed in a rabbit disuse model.

The assessment of magnitude and direction of mobility of molar teeth during mastication and masticatory muscle stimulation utilized ultrasound signaling in the form of small implantable piezoelectric transducers placed inside and around the maxillary molars of young pigs. Periodontal disease was induced over 8-week period using silk ligatures with a cocktail of four bacteria. μCT images were used to quantify the PDL space around the molars and histology was used to observe the general organization and pattern of the PDL fibers during health and disease. μCT images were also used to assess the alveolar bone density of the molar bearing region of the alveolus during disuse conditions in rabbits.

Tooth mobility ranged from 20-322μm for both mastication and masseter stimulation. Mobility did not differ between healthy and diseased pigs. PDL space width measurements were in the range of 116-1690μm around the root circumference and at the furcation locations and did not differ for health and disease. The PDL space at the root's apex, was larger ranging from 329-1,833μm and was greater in diseased teeth.

These results show that functional tooth mobility caused by masticatory muscle contraction is extensive, approximating the entire periodontal space especially at the furcation. The molar typically showed intrusive and lateral (either buccal or palatal) movements during mastication. The intrusive movements appeared to be limited by the height of the PDL space at the furcation of the molars. Although it was not possible to characterize the functional tooth mobility during disuse conditions, bone density was significantly reduced ($P < 0.05$) after unloading via muscle paralysis, which could affect the tooth mobility. Future studies are needed to further investigate the functional tooth mobility during disuse.

TABLE OF CONTENTS

LIST OF FIGURES

LIST OF TABLES

ACKNOWLEDGEMENTS

As the saying goes “it takes a village to raise a child”, and here I would like to thank everyone in the village who has helped me through this journey to get to where I am today.

First and foremost, I am extremely grateful to my mentor, my highly knowledgeable, enthusiastic, motivational, and ethical, research and professional role model: Dr. Sue Herring. She has always encouraged me to think outside the box and to push my limits, and become a better critical thinker and writer. She never hesitated to listen to me and support me and my ideas, even when my idea for my research direction was not within the research grant and it was not funded by NIH F30 grant. Instead she motivated me to never give up and be persistent and apply for more funding resources. My persistence ultimately enabled me to win the Sunstar Preventative Dentistry Award in November of 2014. This funding made it possible for me to form and carry out the research questions presented in Chapter 2. This supported the purchase, husbandry, induction of periodontal disease, and CBCT imaging of the eight pigs used in Chapter 2, and also the follow-up future projects using the periodontal pigs from this method.

I also want to thank my other wonderful committee members who patiently and generously devoted their time, knowledge and energy to educate and guide me the past 3 years of completing my doctorate degree: Dr. Zi-Jun Liu (co-advisor), Dr. Richard Darveau, Dr. Katherine Rafferty, Dr. Johan Aps, and Dr. Avina Paranjpe (GSR). I would like to thank Dr. Liu for his generous grant support for the tooth mobility aspect of this project and obtaining the μCT scans. I would like to thank Dr. Darveau for generously allowing me to use his laboratory for growing bacteria culture for induction of periodontal disease in pigs and for providing the antibody for IHC and neutrophil staining of my pig samples. I am very grateful for the unlimited help and guidance that his lab

members: Dr. Jenny To, Dr. Tom Kantrong, and Ana Chang provided me for learning how to grow bacteria, and IHC technique. I want to express my special thanks to Dr. Johan Aps, Dr. Liu, Dr. Rafferty, and the UW Department of Comparative medicine for staying late hours and making it possible to take CBCT scans of the pigs that were properly secured in a customized car seat; a contribution from Dr. Gerry Hish from Department of Comparative Medicine.

I am thankful for the help and support of many individuals who played an important role in assisting me through the surgery experimental sessions. Our wonderful and kind lab technician Dr. Qin Bai who has helped tremendously with teaching me how to handle the pigs, and preparing the histological slides. I would also like to thank our vising scholar from China: Dr. Jie Chen who assisted me during the surgeries and handling the pigs. Special thanks to Dr. Casey Self for teaching me how to use polarized light microscopy. Additionally, I am thankful for the help of many other volunteers and members of Herring, Liu, and Rafferty labs for their help along the way.

The privilege of doing research that sparked my interest in choosing it as part of my professional and career goal was initiated during my undergraduate studies. I would like to express my deepest gratitude to my first research mentors and advisors Dr. Celeste Berg (UW Department of Genome Sciences) and Dr. Raymond Huey (UW Department of Biology) who played an incredible role and instilled in me early on the values that research plays in advancing science and our understanding of life.

I would also like to acknowledge the University of Washington Department of Oral Health Sciences and the Oral Biology program for giving me the opportunity to obtain my doctorate degree from such an outstanding and leading research institution in the nation. Dr. Richard Presland, Dr. Timothy DeRouen, Dr. Douglas Ramsey, Dr. Chuck Spiekerman, Dr. Tracy

Popowics, Dr. Linda LeResche, Jenifer Kohn, Kathy Hobson, Rosale Meriales, Eileen Kakida, Carol Wiesenbach, MaryBeth Cunningham, Kseniya Savva, and many others have contributed significantly to assist me with applying and getting funding opportunities and I would like to thank them all. I want to thank Seattle Children's Research Institute and Dr. Timothy Cox and Dr. Murat Maga for training me with the micro-CT scanner.

This work would not have been possible without the multiple funding sources listed below: The National Institute of Health (NIH/NIDCR T90 DE021984-03) for UW institutional training grant that supported me for all my 7 years of DDS/PhD. The SunStar Americas, for the generous research financial support through the Sunstar Preventative Dentistry Award in November 2014. The Magnuson family for the Warren G. Magnuson Scholarship that was awarded to me in 2015. NIH/NIDCR PHS DE018142 awarded to Dr. Herring that funded the Botox® study. NIH/NIDCR R21 DE023127 awarded to Dr. Liu that supported the tooth mobility, μCT scans, and the cost of the pigs in the healthy control group. And the NIH/NIDCR R01 DE023453 awarded to Dr. Darveau that supported the bacteria growth and maintenance for creating periodontitis in pigs, and IHC for neutrophil staining of the healthy and periodontally diseased tissues.

To my wonderful friends, you have all been an important part of my journey. I have met brilliant individuals from all over the world during my past 7 years as a DDS/PhD student and have made life-time friendships that I am sure will help us all collaborate as colleagues through our careers as future researchers and scholars in our respective fields.

And last, but not least, I would like to express my deepest and sincere gratitude to my wonderful, loving, and caring parents, Behnaz Kavoosi and Iraj Salamati, and my sisters, Nayrika, Annahid, and my wonderful, charming niece Annette. They have all been beyond amazing in loving me and believing in me during this whole journey, especially when I was going through

hard times and failed results. They have always supported my dreams and encouraged me to never give up and always advance to the peak of success.

I am very lucky and blessed to have you all in my life and I will always carry the values that my parents and my mentors instilled in me to the best of my power and will never give up to reach my dreams and make them into reality.

DEDICATION

I would like to dedicate this work to the most important figures and role models in my life. My beloved, hard-working, amazing parents, Behnaz Kavoosi and Iraj Salamati who have always made education my top priority. I also would like to dedicate this to my kind grandma Memejoon Khorshidbanoo, and my beloved grandparents who may not physically be in this world anymore, but they have been and will always be with me spiritually: Memejoon Morvarid, Babajoon Karimdad, and Babajoon Aghajoon Mehraban. You have all taught me the real values in life: to think good thoughts, do good deeds, and say good words, to be compassionate and caring towards others, and to always strive for the best that life has to offer and never give up.

Babajoon Karimdad you were a math teacher in a small village in Yazd, Iran and I still remember all the stories that you used to tell me which encouraged me early on to want to become an educator like you. I remember you used to always tell us that education is the wealth that no one can steal from us and the most important power we should ask for. Babajoon Aghajoon Mehraban, I always looked up to you as you carried out your duties as a medical doctor and educator in Yazd and then in Tehran, and helped so many patients. You all taught me very early in life to never give up, always stand up for what I believed in, care for others and treat others as I want to be treated. I still have a long road ahead of me to learn more, educate and care for my patients, and I always will carry the values you taught me with me. Memejoon Morvarid, thank you for all your prayers and kindness and love as I grew up.

Mom and Dad I love you both beyond words can express. THANK YOU for all the sacrifices you both made so I could achieve my goals and make my dream a reality, and be who I am today.

CHAPTER 1

Introduction

"*Teeth have a certain degree of motion, which is of great benefit in mastication, thereby preventing that injury which might arise from concussion consequent on the breaking of hard substances*." Joseph Fox, 1833, was one of the pioneers commenting on the mobility of teeth during mastication [1].

Teeth have certain degree of physiological movement within their bony sockets that increases or decreases in magnitude with age, periodontal disease, diet change, and many other factors. However, the magnitude of physiological tooth movement is not known under either healthy or diseased conditions. In order to better understand the movement of the teeth within their bony sockets in response to functional, parafunctional, and external loads, under healthy and periodontal disease states, it is important to understand each of the determinants of tooth movement and their contributing factors, such as gingival tissues, periodontal ligament, and the alveolar bone.

Therefore, in this chapter, after reviewing what is known and what is not known about tooth mobility in humans and other animals, I will focus on four sections: (1) tooth mobility, (2) ligature-induced periodontitis, (3) animal models for my project, (4) specific aims of this project.

1.1 Background on Tooth Mobility

All mammalian teeth move in response to occlusal forces, environmental stressors, and loads, unless they have been ankylosed [2]. This physiological movement is called fremitus or functional mobility [3]. Evolutionarily, teeth are essential for survival. Thus their health and

maintenance are important. Almost all periodontists and general dentists use tooth mobility as a guideline to determine the prognosis of and establishment of a treatment plan [4],[5]. In clinical dentistry, every day, clinicians make treatment plans involving extraction of 'very' mobile teeth on the assumption that the prognosis for such teeth is poor. The mobility assessment of the teeth used in clinical practice is very subjective and highly variable among clinicians [6]. The decision of retention and treatment *vs.* extraction of mobile teeth depends on the clinician's understanding of whether the observed mobility is reversible (i.e. with periodontal or occlusal treatment) or irreversible, which requires clear diagnosis and understanding of the etiology behind certain patterns of tooth movement, as it changes constantly [7],[8]. Although clinically tooth mobility increases with periodontal disease, excessive mobility might not be a valid indicator for extraction, as mobility is also an intrinsic protective and adaptive response of the tooth to the environmental stressors and functional loads. Thus, effective treatment planning requires an understanding of normal tooth mobility during function.

Lack of research assessing tooth mobility during mastication and elucidating how much teeth move during function, highlights the complexity of such *in vivo* functional measurements. Among the reasons for lack of a better tooth mobility clinical assessment tool, is lack of evidence in the literature for what the normal range of movement is during mastication for a given tooth, and how to measure that practically in everyday use [8],[9]. This information would be useful in assessing what would be considered as pathological range of movement. Additional contributing reasons are lack of recent studies using good animal models which mimic the human masticatory pattern, and the dynamic and three-dimensional nature of tooth movement that changes continuously due to many biological and functional factors [11]–[14]. Most of the studies that have attempted to measure tooth displacement, both in animals and humans, use external forces

that are hoped to resemble those of functional masticatory forces [2], [15]–[19]. However, there are a few studies that have attempted to measure tooth displacement during mastication [20]–[22].

As already mentioned, the magnitude and direction of tooth movement under functional loads, such as mastication, is relatively poorly understood, however, it is presumed that the movement is confined to the alveolar socket boundaries [14]. Forces that are produced during mastication are by far the largest short-duration forces acting on the teeth [10], [23]. Tooth movement during mastication occurs within the periodontal space defined by the tooth root cementum and alveolar bone. The thickness of this space and the characteristics of the bone are then crucial in defining the limits for tooth mobility [24]–[26]. The intensity of tooth displacement depends partially on the type of diet and the extent of attrition on dentition [27]–[29], which could be a clue to the extent of parafunctional habits as well as the diet. Mobility is also one of the common clinical manifestations of occlusal trauma [13].

In the first section of this chapter, I will discuss (1) biological tissues surrounding the tooth that are essential in guiding the tooth movement, and then I will (2) review some of the existing literature regarding various tooth mobility measurement techniques and methods.

1.1.1 Biological Tissues Guiding the Tooth Mobility

1.1.1.1 Gingival Tissues

Gingiva is a protective layer that covers the alveolar bone and part of the tooth. It provides a mechanical seal around the teeth from the oral cavity via the junctional epithelium [30]–[32]. The junctional epithelium, which follows the cemento-enamel junction (CEJ) in healthy states, is composed of non-differentiated stratified squamous epithelium, has a very high

cell turnover rate [30], and is important in mechanical support of the tooth. This epithelial attachment complex provides actual attachment of the gingival tissues to the tooth structure [30]. In humans, during periodontal health, the gingiva covers up to about 2mm of the tooth enamel structure [32], and its various fiber groups, namely the dentogingival, alveologingival, dentoperiosteal, and the periosteogingival fiber groups, attach the gingiva to the alveolar bone and the tooth [32]. The semicircular, circular, transseptal, and transgingival fiber groups connect the adjacent teeth to each other. The transseptal fibers have been shown to play a major role in the mesial drift of the teeth [33], [29], [30].

Besides the various fiber groups, the junctional epithelium and the gingival sulcus have blood vessels, lymphatics, and nerves to carry out their physiological protective role. During inflammation and disease there is an increase in the venous plexuses that reside in the junctional epithelium and thus also an increase in levels of neutrophilic granulocytes [32], [34], [35]. However, it is important to note that even during healthy states, there is a sub-clinical level of neutrophils which is a sign of slight inflammation [31], [36]. In healthy periodontium the depth of the gingival sulcus, or the periodontal pocket depth, is usually 1-3mm, and the periodontal probe tip, which is one of the tools used clinically to assess the periodontal health, does not reach beyond the apical portion of the junctional epithelium [37]. During periodontal disease, inflammation damages the attachment points and structural integrity of the junctional epithelium, resulting in more apical placement of the gingival attachment and deeper periodontal pocket depths [30]. If the inflammation persists, as the gingival sulcus moves apically, the inflammatory mediators will also start causing alveolar bone destruction. The longer the disease process persists, the more tissue destruction will occur, leading to an unfavorable crown to root ratio and increased mobility of the dentition [4]. There is a statistically significant correlation between

tooth mobility and Clinical Attachment Loss (CAL) for the central and lateral incisors, but not for other teeth [4].

1.1.1.2 Periodontal Ligament Space

The space between the tooth root cementum and the alveolar bone is called the periodontal ligament space. Various tissue types are found within this space including: the periodontal ligament (PDL), other soft fibrous connective tissues such as collagen, oxytalan elastic fibers, blood vessels, nerves, and various other cells that mainly include fibroblasts, but also osteoblasts, osteoclasts, epithelial cell rests of Malassez, macrophages, monocytes, cementoblasts, odontoblasts, and undifferentiated mesenchymal cells [30], [38],[39]. In addition to the hemodynamic pressure of the blood vessels that create damping effect to help the tooth in withstanding the occlusal loads [40], another component of the PDL space is the fluid that is in the space and contains low and high molecular weight ground hydrophilic molecules of glycosaminoglycans (GAGs), that act as shock absorbers and thus are thought to play a role in dissipating the occlusal loads received by the tooth [41]–[45].

The blood vessels in the PDL occupy about 1-2% of the space and they tend to run parallel to the long axis of the root. They are important not only in providing nutrients, but also in producing fluid pressure that has been implicated in the eruption and support of teeth [10], [38], [46], [11]. In the absence of occlusal forces on the tooth, the pulsation in the arterial blood vessels causes the tooth to rise and fall essentially with the heart beat [10], [14], [21], [23], [40], [47]–[49].

PDL occupies 53-74% of the periodontal membrane space [10]. In the presence of occlusal loads, the PDL acts as a shock-absorbing substance to spread the occlusal loads to the

surrounding alveolar bone [50],[10]. As a suspensory ligament, the PDL attaches to the tooth root cementum on one end and the alveolar bone on the opposite end. The insertion points of PDL collagen fiber bundles into the cementum and alveolar bone are called Sharpey's fibers. The Sharpey's fibers insertion points into acellular cementum are completely mineralized [30]. The insertion of PDL collagen into the root cementum do not show a specific pattern, but the fibers that insert into the alveolar bone are found mainly at convex and flat surfaces [51]. Studies in dogs and rats have shown that the thickness of the fiber bundles varies on the cementum and alveolar bone ends [38], [52]. The PDL fiber bundle thickness varies from 3-10 micrometers close to cementum to 10 -20 micrometers close to the alveolar bone surface [38],[53]. This difference of insertion point thickness could have important mechanical properties for transferring the occlusal loads from the teeth to the bone, as it may suggest greater concentration of force at the bone-PDL interface. Also, since the bone has a higher turnover rate than cementum, the thicker inserting bundles of PDL principal fibers into the bone ensures that the bundles stay in partial contact with the bone as it remodels and as individual strands of collagen turn over. The quantity of PDL fiber insertion points and the surface area of tooth root that is covered by PDL are mechanically important. This is one of the reasons why healthy multi-rooted teeth show less mobility than single-rooted teeth [12],[15]. The direction, organization, and the volume of the PDL fibers change as they go from the cervical portion of the tooth root to the apex. In rats, the PDL collagen bundles are organized in sparse and dense sheets with spaces in between them. The dense sheets tend to be on the side of the tooth that is thought to be under tensile loads, while the sparse sheets are found on the compressive loading side of the tooth [51].

In general, the width of the PDL space is relatively narrow in the middle third of the root and furcation areas (Figure 1-1) [30], [38], [54]–[58]. PDL width decreases with age, and teeth

that are out of occlusion or impacted have narrower PDL space than those in full masticatory function (Table 1-1) [30], [54], [57], [59], [60]. One of the first studies to look at human PDL width at different ages was by G. V. Black who reported the PDL space width was different among individuals and among different teeth, but he noticed that with age it got smaller [59], [61].

Although the width of PDL space varies among different species and different teeth, and decreases in response to decreased fremitus, space does not disappear unless injury occurs, resulting in ankyloses [62]. In humans the thickness of periodontal membrane is reported to be around 150-300μm [61]. There is a relationship between the magnitude of tooth movement and the width of the PDL space: usually PDL width is larger in teeth that are in function [15], [54], [57],[63],[64]. Table 1-2 shows histological PDL width measurements under different states of function, obtained from a 38 year old man who died and had periodontitis [57]. Table 1-1 shows that when forces applied to the tooth change, the width of the PDL space changes as well. Due to its specialized functions in withstanding the forces, PDL needs to remain un-mineralized. To date, there are still studies investigating how the PDL can stay un-mineralized, while trapped in between two mineralized tissues [62], [65]–[67]. Among the suggested answers is that proteins such as Msx2 repress the activity of Runx2/Osf2 and therefore, inhibit the osteogenic differentiation of the PDL fibroblasts [66]. A more recent study shows that on the tension side of the tooth, where bone formation is up regulated, another protein, scleraxis (Scx), is up regulated in the PDL fibroblastic cells to inhibit the mineralization of the PDL, and thus maintain the PDL patency [68].

It has also been shown that reduced functional loads also affect the mechanical and therefore, functional properties of the PDL fibers [69]. Under reduced loads, the PDL turnover

rate decreases and the PDL collagen fibers show less birefringence, which means the fibers are less organized and less dense [15], [69]. In humans, the PDL fiber bundles lose their organization in hypo-functional and unloaded teeth. The latter explains teeth becoming loose or hyper-mobile [57]. Furthermore, rat studies show that under reduced functional load, the diameter and number of the PDL blood vessels decrease as well as the number of fibroblast cells and there is an increase in the collagen remodeling of the PDL [70]–[73] .

The complex nature of the PDL contributes to the difficulty of studying tooth movement. One of the characteristics of PDL that plays an important role in load transfer is the waviness or 'crimp' appearance of this tissue [74]. Due to PDL's high flexibility compared to its surrounding mineralized tissues, namely alveolar bone and tooth cementum, PDL has a very important role in regulation of magnitude and direction of tooth movement [75],[76],[77]. Under load, the tooth goes through two phases of movement [15]. The initial phase of mobility exists only in *in vivo* conditions and is mainly due to the presence of the flexible PDL (Figure 1-2 and Figure 1-3) [15], an effect that is demolished when the teeth have been fixed, presumably because the crimp is no longer capable of being stretched out (Figure 1-3) [10], [21], [78]. In the initial stage of tooth movement, displacement requires little force (0-0.5N), and this is explained by the movement of the root within the socket with extension of the crimp and displacement of the normal soft tissues. The tooth is presumably supported mainly by the fluid phase of the PDL (Figure 1-2) [2], [10], [21]. This initial tooth mobility is not determined by the width of the PDL space [12], [15]. With increase in the load on the tooth (500 grams), the second phase of tooth movement happens, which shows less displacement with increased force application [21]. In this second phase of tooth movement, it is presumed that collagen fibers have straightened from their

original crimp shape to transfer the force to the alveolar bone, and more elastic deformation of the bone occurs [2], [10], [12].

Like the gingiva and the alveolar bone, the PDL has a high turnover rate at its different locations, ranging from 2-45 days in rats, which may be related to the importance of this tissue in bearing the occlusal forces and facilitating tooth movement [38], [70], [79]. The turnover rate of PDL at the cervical area is much faster than the apical area of the root [80], and the turnover rate is faster close to the alveolar bone surface than to the tooth surface [81].

1.1.1.3 Alveolar bone

One of the important components of tooth movement regulation is the alveolar bone. As a connective tissue, the alveolar bone contains blood vessels, nerve fibers and various cells that help in maintaining homeostasis and bone remodeling as needed. An important role of the bone in regulation of tooth movement comes from the interaction between the periodontal ligament fibers and the bone.

As mentioned above, the PDL inserts on one side to the cementum, which has low metabolic activity, and on the opposite end, it inserts into alveolar bone, which is a very active tissue with a high remodeling rate [23]. The PDL fibers that insert into alveolar bone (Sharpey's fibers) become mineralized at their insertion points [29],[30], [82]. There is a thin layer of bone, about 100μm-200μm in thickness, the "bundle bone", covering the interior of the socket where this occurs [29], [30], [83]. Where the bone undergoes resorption (e.g. orthodontic forces), osteoclasts excavate the bundle bone and the underlying supporting bone, and in doing so, the insertion points of PDL attachment are lost. After the resorption process is over, a cement line [84] is produced, the fibroblasts start secreting thin collagen fibrils to be attached to the existing

PDL fiber bundles, and the osteoblasts start forming bone in between the fiber bundles as they remineralize into Sharpey's fibers [85], [86].

Another contribution of alveolar bone in regulation of tooth movement within the physiological range is the height of the bone [7], [28]. If the alveolar bone height is close to the CEJ, the increased tooth mobility that results from occlusal trauma is considered to be reversible with treatment. If the alveolar bone height covers less than 30% of the root, then the attached PDL is reduced along with the physical support of bone around the tooth, and the treatment is less likely to be successful [7].

The bone can respond differently under different occlusal forces. One of the biomechanical properties of the bone that helps it withstand various forces is that the bone has certain degree of flexibility which is thought to support the tooth movement and help in resisting the forces transmitted to the bone through the tooth [87], [88]. Under orthodontic forces, there is a pattern for bone resorption and bone apposition [89]–[91]. On the compression side, in the direction of applied forces, and thus the direction of tooth movement, osteoclasts induce bone resorption. On the tension side, osteoblasts lay down mineralized bone [7],[92]. Two weeks of experimental tension on rat molars produced deposition of new bone 3.5µm-5µm thick which included Sharpey's fibers [89]. Like PDL, the alveolar bone responds to occlusal loads by increasing or decreasing its volume. Under reduced occlusal forces, the alveolar surface area is reduced and trabecular cortex is much thinner compared to rats who are on hard diets (Table 1-1) [64]. This difference was more pronounced in the apical areas of the roots and less evident in the cervical measurements. A possible explanation could be that rats on soft diet will have less loading on the teeth, and thus less force is being transmitted via the PDL to the bone, hence the latter will be less stimulated and thus have a lesser rate of bone apposition.

1.1.2 Factors Contributing to Tooth Mobility

Occlusal trauma (hypofunction and hyper-function), inflammation, loss of periodontal support, pregnancy, and orthodontic tooth movement may result in increased tooth mobility by alteration of the periodontal tissues [2], [12], [13], [75], [93]. During pregnancy for example, even with healthy gingiva, tooth mobility is still increased [94], [95]. Mühlemann explains that this could be due to biophysical changes in the connective tissue of the periodontium such as increased hydration, which is not histologically evident [12]. Other factors such as increased expression of hormones such as relaxin contributes to increased tooth mobility during pregnancy [96]. Most authors believe that more mobility is associated with increased periodontal breakdown and poorer long-term prognosis [5], [12], [16]. It has also been shown that losing interdental contact points and occlusal contact points (hypofunction) increases the mobility of the teeth [12], [97], [17].

1.1.3 Methods for Assessing Tooth Mobility

Most of the studies on tooth mobility have also aimed at developing a technique to help clinicians assess it. However, as evident in today's clinical practice, almost all dentists mainly use Miller's clinical assessment of tooth mobility to establish treatment plans. Currently the only used clinical tooth mobility assessment tools are the (1) Miller Mobility Index, which is by far the most common method taught in the dental schools and used clinically, and (2) the Periotest, which is more objective but its values are based on Miller mobility classifications, and it is used mainly by periodontists [98].

The Miller Mobility Index (MMI) is determined by manipulating the tooth between two mirror handles and pushing the tooth labio-lingually [6],[36],[69]. MMI is subjective and depends widely on the experience of the dentist [6]. It is also crude, scoring a tooth as moving more or less than 1 mm. The 3 MMI are defined as follows (Table 1-3) [93].

Schulte's Periotest instrument is used to some extent in clinical settings, but mainly for clinical research purposes. The Periotest uses gentle tapping on the teeth, registers the dampening effect of the PDL, and gives it a score [Periotest value (PTV)] in the range of 0-100. The PTVs are then associated with different MMI [99]–[102]. Schulte also compared the Periotest technique with the mechanical dial periodontometer that Mühlemann had introduced to show how the two systems were correlated with each other [102]. Mühlemann used a microperiodontometer and a macroperiodontometer, for his tooth mobility measurements. The small indicator could be used in the molar area but its values were less reproducible than the larger device which had higher reproducibility but was better suited for anterior teeth and premolars [75].

Obtaining more accurate measurements of tooth mobility is complex, and through the years many researchers have developed mechanical, electronic, vibratory, and optical devices to measure and evaluate tooth mobility more precisely (Table 1-4) [2], [4], [15], [75], [93], [101]–[109]. Most of these studies have utilized external, quasi-static force on the tooth [75],[108],[110], which is unlike masticatory loading. Niedermeier (1993) measured tooth mobility mechano-electronically using a quasi-static method called 'Desmodontometry' in patients. External forces of 150 grams were applied in buccal and palatal directions and apically on different teeth to measure their displacement. He reported that canines had minimum horizontal mobility, whereas multi-rooted posterior teeth had minimum intrusive movement [17].

The majority of human studies focus on the anterior teeth, which are seldom important in mastication [4],[74],[77],[93]. The range of mobility for incisors might not be a good estimate for the range of mobility of multi-rooted teeth [111] which are under more occlusal stress resulting from masticatory or parafunctional loads. To date there is no direct measurement of molar displacement during mastication in humans or other animals.

1.1.4 Long Term Adaptation of Tooth Movement- Orthodontic Forces

There has been extensive research on tooth movement as a consequence of orthodontic force applications [2],[8],[9],[114]. Although this type of tooth displacement is not the focus of this paper, orthodontic forces create increased tooth mobility. If the forces transmitted to the tooth exceed a 'certain' threshold, the movement of the tooth is no longer confined to the PDL space defined by the alveolar bone boundaries [50],[114]. In such a case the bone has clearly reached a yield point, implying injury. It is under these extreme forces that the stresses in the PDL will trigger events leading to bone remodeling, and the tooth movement permanently changes the tooth's position and enters a new phase, which is sometimes called translation through the bone [50],[68],[115]. Orthodontic forces applied to the tooth are unidirectional and will create a pressure and a tension side. On the pressure side, there will be osteoclastic bone resorption and thus decrease in the density of the interseptal bone. On the tension side, there will be bone apposition and thickening of the cellular cementum in order to re-establish the PDL space [13],[68],[114],[116]. While the bone is remodeling, the PDL also remodels, as the fibroblasts will be synthesizing and degrading collagen simultaneously to maintain the PDL space width [117].

More recently it has been suggested that the interaction of the tooth and alveolar bone in the furcation area of multi-rooted teeth is critical in guiding and limiting orthodontic tooth movement (Figure 1-4) [118]. The close contact point or very narrow PDL space (at least in rats) between the tooth and the alveolar bone at the furcation could be one explanation as to why the mobility of multi-rooted teeth (Table 1-4) is typically less than the mobility of single-rooted teeth.

1.1.5 Short Term Adaptation of Tooth Movement- Physiological Tooth Movement

As mentioned earlier, tooth mobility is governed functionally by occlusal loads transmitted through masticatory muscles to the teeth [13]. The greatest forces transmitted to the teeth are during mastication [10],[23]. The magnitude of these forces varies depending on many factors such as gender, age, plane of occlusion, the food item being masticated, muscle strength, etc. [119],[120]. Occlusal loads can reach up to about 50 Kg during mastication [13], [18],[112]. Unlike unidirectional orthodontic forces, functional and parafunctional forces tend to be exerted upon teeth in all directions, and thus it could be assumed that during functional loads some of the PDL fibers will be reacting as they do under pressure and some will act as if they are under tensile forces [13],[120].

Most *in vitro* studies of tooth mobility have looked at the movement of single rooted teeth (Table 1-4), but a few have dealt with multi-rooted teeth in response to forces intended to mimic those of mastication (Table 1-4). Data show that different tooth types have different degrees of mobility. Naveh *et. al.,* 2012, used Electronic Speckle Pattern Interferometry (ESPI), an optical metrology method, to study the different responses obtained from teeth in a mandible *versus* teeth embedded in epoxy [56]. Under axial loads of up to 75N, the first molar of the

minipig in the mandible and in epoxy both showed the same see-saw displacement pattern, however the magnitude in epoxy (about 2.7μm) was half that of in the mandible [56].

Under axial loads, the single rooted lower incisors of the macaque monkeys in a mandible and macaque monkey incisors embedded in epoxy, both showed the same cantilever-like pattern of movement, mainly in the bucco-lingual direction, and barely in the apical direction, but similar to the multi-rooted molars mentioned above, the epoxy embedded teeth showed lower magnitudes of displacement [26], [56]. By applying known forces of 100 grams and 500 grams [22] and using the force meter, Mühlemann recorded the movement of human teeth *in vivo* and showed that for the incisors this movement was from 100-120μm, for canines about 50-90μm, for premolars 80-100μm and for molars it was reported as 40-80μm [75]. The lower reported number by Mühlemann for the molar tooth displacement is most likely due to the smaller PDL space that is available in the furcation of the multi-rooted molar teeth compared to the PDL space around the roots, which both single and multi-rooted teeth share.

One of the early studies, and one of the very few that included mastication, was by Parfitt. He used a transducer [21] that would only have contact with the labial surface of the tooth to avoid interference with speech or the mastication of food. He applied 500 grams of force to periodontally healthy right upper central incisors, and reported their movement to be 40μm when the force was applied in the labial direction and 30μm when the force was in the lingual direction [22]. During mastication and incising of various foods, he reported that the most amount of movement for the incisor was during incising into a celery which resulted in 52μm of labial movement [22]. The numbers reported by Parfitt for incisors are lower than those reported by Mühlemann, however, this could be due to the different techniques that were used and the great variability among individuals of age and periodontal status. Mastication was also

investigated by Picton, who used data from Anderson [121], consisting of dynamometer measurements of forces during chewing and wire strain gauges to record the movement of teeth. He concluded that during chewing the first molar tooth tends to be displaced apically and mesially by about 100µm in the socket due to regular forces of mastication, with incomplete recovery between cycles [20]. He noted that recovery of the tooth after application of forces happens in two phases and this was true for both horizontal and axial directions of movement [20].

Hypo- and hyper-functional teeth were investigated under applied loads by Niedermeier. The range of mobility for the posterior teeth in normal conditions was 50µm-100µm. He also reported that teeth that were loaded hyper-functionally had greater amount of movement in all directions by about 60-75% compared to normal teeth. The mobility was smaller for the canine teeth[17] even though canines are single rooted, perhaps due to their long roots. For teeth that were loaded hypo-functionally, he showed that the mobility was increased two-fold compared to the hyper-functionally loaded teeth and three-fold in comparison with the normally loaded teeth [17]. It was not clear why both over- and under-loading increased tooth mobility.

In order to understand the mechanics of tooth movement, it is important to also evaluate what occurs biomechanically at the interphase of PDL with bone and tooth. To do this, digital image correlation (DIC) of micro CT images was used while applying loads *in* vitro in rats. Five N forces, caused predominantly vertical displacement of 35µm, followed by 40µm at 10N, and 50µm at 20N. The overall tooth movement was described as a screw-like motion at lower load rates (5N/s), and rotational movements at higher rates (10-20N/s) [122]. Areas of concentrated strain within the PDL were mainly located at the furcation, apical and cervical regions of the PDL, *i.e.* the extremes of the sockets. Rat teeth made hypofunctional using a soft diet showed

disorganized PDL fibers [69], but in spite of this the displacement in the apical and rotational directions decreased substantially [69], a finding that contrasts with that of Niedermeier [17].

1.2 Analyzing the biological findings in ligature-induced periodontal disease and specifically considering events that may occur at the apex of the root

Periodontal disease, or periodontitis, by definition is a complex multifactorial chronic immunoinflammatory disease of the periodontium, initiated by subgingival biofilms and a shift from gram-positive aerobic bacteria to gram-negative anaerobic bacteria [123], [124]. Systemic diseases such as diabetes mellitus influence the course of periodontal disease, most likely by modifying the host immune response, but are not the etiological factor for the inception of the disease [125]–[128]. Furthermore, there is an association between systemic disease such as cardiovascular disease and periodontitis [129], [130]. In addition to microbial challenge and systemic diseases, environmental factors such as smoking, stress, and various genetic traits can affect the host response to the disease. According to the 2009 and 2010 data from the National Health and Nutrition Examination Survey (NHANES), the prevalence of periodontitis is more than 47% for the adults over the age of 30, and more than 64% for individuals 65 years and older [131]. Patients diagnosed with periodontal disease demonstrate a cascade of events ranging from progressive loss of gingival tissue, PDL, adjacent supporting alveolar bone, loosening of the teeth, loss of chewing function, and ultimately loss of the affected teeth [132]–[134]. Lack of masticatory function will alter the food choice and diet of the partially edentulous individuals, and thus impact their systemic health as well.

In periodontal health there are many species of commensal bacteria that reside in the oral cavity. Homeostasis of these commensal bacteria is not only required for the maintenance of the health of the periodontal tissue and preserving the teeth, but also for the general health of the individual. Disruption in the microbial biofilm will result in imbalance in expression of inflammatory mediators that are active even during healthy states, resulting in bone and tissue destruction around the teeth [132], [135], [136]. The bacteria associated with periodontal health are mostly gram-positive, facultative anaerobes, cocci, and primarily non-motile [137]–[139]. Most of these commensal bacteria are members of the *Streptococcus* and *Actinomyces* genera. However, *Fusobacterium nucleatum* and a few other species are gram-negative [137], [138]. *F. nucleatum* is a bridging organism between early and late colonizers, and is found in periodontal disease as well. It co-aggregates with various other bacteria to elicit inflammation and alveolar bone destruction in periodontal disease [140]–[144].

In human periodontal disease there are three main pathogens: *Porphyromonas gingivalis, Treponema denticola,* and *Tannerella forsythia* which are described as "red complex" species [132], [145]–[147]. The hallmark of bacteria identified as red complex is the high level of protease activity, which is responsible for the epithelial barrier loss in the mouth [148]. Studies in mice have shown that presence of *P. gingivalis*, a black pigmented gram-negative anaerobic bacterium that resides in the subgingival crevice, is essential for advancement of periodontal disease and thus it has been named a keystone pathogen [149]–[152]. However, *P. gingivalis* by itself is not able to induce the disease and the associated bone loss, and it needs the presence of other bacteria in in significant levels in the oral biofilm [141], [148], [153], e.g. *Aggregatibacter actinomycetemcomitans, F. nucleatum, Streptococcus* and *Actinomyces* species [154]–[158]. Many of these are secondary colonizers and require early colonizers as a scaffold to which they

can attach. In addition to *F. nucleatum*., *Streptococcus gordonii* is an early colonizer that is present in the initial plaque formation and binds to receptors in the pellicle, providing a bridge for the secondary colonizers and their growth [159].

In order to understand (1) the evolution of periodontal disease, (2) the mechanisms by which different bacteria induce inflammatory responses that cause tissue damage and (3) how the host responds, we need animal models. However, it is also important to select a model that resembles the course of the disease in humans. This section discusses (1) various animal models used to induce experimental periodontitis, (2) various methods used in inducing experimental periodontitis, with focus on ligature-induced periodontitis, (3) biological changes in the periodontium associated with the ligature induced experimental periodontitis, and (4) the effect of experimental periodontitis on tooth mobility in animal models.

1.2.1 Animal Models for Experimental Periodontitis

It is important to understand the process of periodontitis and its treatment in an appropriate animal model. Most periodontal studies have been in rats, mice, and ferrets, but hamsters, rabbits, minipigs, sheep, cats, dogs, and primates have been used as well. With regard to ligature induced periodontal disease research, the following six animal models have been used.

1.2.1.1 Rodents

Rodents, and specially rats and mice, are economically more accessible and ethically more acceptable than alternative animals. Rats have been the most widely used rodent in periodontal research [160]. Furthermore, the genetic background of mice and rats is well studied,

and there are models for various systemic diseases such as diabetes so that periodontal disease can be studied in relation to systemic diseases [161]. Periodontal disease does not naturally occur in rats, which could be due to the fact their molars show continuous attrition and exfoliation [160], [162], and that they don't live long enough. Nevertheless, lesions can be induced by using high carbohydrate diet, ligatures with bacteria, oral gavage, lipopolysaccharide (LPS), or a combination of these [163]–[167]. Periodontal pathogens such as *A. actinomycetemcomitans, F. nucleatum, P. gingivalis, Capnocytophaga, Eikenella corrodens, Actinomyces viscosus,* and *Streptococus sorbinus* can induce periodontitis in rats [163].

In hamsters and rats, periodontitis is not spontaneous and is diet dependent, unlike humans. The inflammatory response is limited and consists of only neutrophil activity. Furthermore, studies have shown that osteoclastic activity and alveolar bone loss occurs on the palatal and lingual alveolar crests of the affected molars and in the interproximal regions more than the inter-radicular areas, causing a horizontal pattern of bone loss [168], [169].

1.2.1.2 Rabbits

Rabbits have been used for studying periodontal microbial interactions, periodontal regeneration, and testing biomaterials. Their oral microorganisms resemble those of humans [170]–[172].Periodontitis can be induced by ligatures with or without bacterial inoculation [170], [173]–[175]. However, since rabbits have ever-growing molars with high eruption rates, it is difficult to assess bone loss and PDL regeneration [173].

1.2.1.3 Dogs

Using dogs for periodontal disease studies was once very common, but it is less frequent now. Dogs have open occlusal contacts in their premolar region and open proximal contact between the teeth, and their composition of periodontal plaque and calculus is different than that of humans [176]. In dogs, like humans, periodontal disease progresses with age. However, the genetic variation among dogs makes some breeds resistant to development of natural periodontitis [170], [177]. Ligatures are easy to place and are a common method to induce periodontitis in dogs [178]. Once periodontitis is established, the cellular infiltrates in the PDL are composed of large numbers of lymphocytes, plasma cells, and osteoclasts. Vertical bone defects result [179], and apical bone loss is seen as well (Figure 1-9) [180].

1.2.1.4 Ferrets

Ferrets, like humans and dogs have primary and permanent teeth. Periodontitis can be induced naturally or by using ligatures in about 4 weeks. Similar to humans, the connective tissues show high levels of neutrophils, lymphocytes and plasma cells, and there is a high level of osteoclastic activity and bone resorption [181].

1.2.1.5 Non-human Primates

Non-human primates are the best animal model since they so closely resemble human anatomy and pathophysiology [182]. There are numerous studies in monkeys, since they have immunological, microbiological and histological responses similar to humans and naturally develop gingivitis and periodontitis [182]–[185].

Producing experimental periodontitis in monkeys using silk ligatures around the circumference of the tooth is relatively easy [183], [185]–[189]. Kornman *et. al*., 1981, reported

that the microbial community for *Macaca fascicularis* experimental disease is very similar to that of human chronic gingivitis and advanced periodontitis. Progression of the ligature-induced periodontitis has been described in these monkeys up to 17 weeks [183]. The active destructive part of the disease takes place 4 to 7 weeks after placement of the ligatures, and then from 8 to 17 weeks post ligation the conditions stabilize and no further bone loss is observed [183], [189]. In specimens collected from squirrel monkeys at 2, 10, 26, and 52 weeks after placement of the ligatures, Kennedy and Polson, 1973, measured the distance from CEJ to the alveolar bone crest and to the termination of the junctional epithelium [188]. They reported that most of the damage occurred in the first 2 weeks after placement of the ligature, and after that the progression of disease slowed down until no more significant bone loss was detected between weeks 26 to 52 [188]. Adams *et al.,* 1979, also reported that in monkeys periodontal destruction was at its peak from 0-2 weeks post ligature placement, and by week 8 there was a balance and a significant reduction in the neutrophil population [185]. However, the use of monkeys as animal models is not common anymore due to ethical and economic issues [170], [177]. In all these investigations, the periodontal changes at the crest of the alveolar bone and junctional epithelium were the focus of the studies. No studies looked closely at histological and morphological changes at the furcation of the multi-rooted teeth or at the apex of the examined teeth [160], locations of special interest for tooth mobility.

1.2.1.6 Pigs

Up until 1982, pigs were not popular for periodontal research studies [160]. However, more recently minipigs have been used in studies on periodontal regeneration, dental implants, salivary gland research, and for *in vitro* assessments of material properties [111], [177], [190]–

[193]. Besides being relatively good mimics of human mastication, minipigs have a similar progression of periodontitis to that of humans and show signs of natural development of gingivitis starting at age six months and periodontitis by the age of 16 months [194]–[198]. Periodontitis can be induced in minipigs using ligatures inoculated with *A. actinomycetemcomitans, P. gingivalis, and Streptococcus mutans* [193] in 4-8 weeks. After this period, the disease stabilizes until about week 20 [199]. Induction of experimental periodontitis in pigs has been achieved by using a combination of surgical removal of bone, ligature, and soft diet [191], [192], [199]–[201]. However, pigs seem to have very good immune systems, as the probing pocket depth measurements (PPD) and CAL decreased significantly 3 weeks after removal of ligatures [199]. Pigs are a relatively cost effective large animal model and therefore were chosen for the present study.

1.2.2 Inducing Experimental Periodontitis

Various methods have been reported in the literature to induce experimental periodontitis in animal models, and there are implications for each of the methods. The methods to cause chronic or acute experimental periodontitis include: 1) ligature, 2) oral gavage, 3) LPS, 4) surgical bone removal and 5) soft diet [147], [177], [191], [202]. The choice of each of these methods depends on the nature of the scientific questions asked and the animal model used. Often a combination of these methods is used, but this manuscript will focus on ligature induced periodontitis.

Ligatures are usually placed around the circumference of the tooth and slightly subgingival. Different types of ligatures have been used in various studies, ranging from cotton, silk, or nylon sutures, to stainless steel orthodontic wires, orthodontic elastic rings, and sutures

that have been twisted with wires [125], [141], [142], [166], [167], [178], [183], [188], [189], [192], [202]–[207]. Ligatures help in the induction of periodontal disease by retention of bacterial biofilm and acting as a niche for accumulation and colonization of periodontal pathogens. They also introduce mechanical damage to the cervical gingival tissue. Depending on the method of placement of the ligature, the extent of this damage varies. However, the mechanical damage of the ligature alone does not seem to cause experimental periodontitis. This was first shown in 1966 in a study of germfree and conventional rats [125]. Studies in monkeys have also showed that loss of attachment and alveolar bone are more related to the subgingival biofilm than to the mechanical trauma from the ligatures [182], [208]. Often, ligatures have been soaked with periodontal pathogens to intensify the inflammatory response [142].

Although most ligatures have been silk or cotton [207], the use of different materials elicits different inflammatory responses. Figure 1-10 shows the immunohistochemical staining of ED1, an inflammatory marker, from a rat study that showed that silk ligatures and elastic bands induced a greater inflammatory response than NiTi coil springs when used as ligatures or in between teeth [205]. In monkey molars cotton and silk ligatures caused more tissue damage and inflammatory response than nylon ligatures [207]. In mice nylon ligatures (knotted mesio-buccally and repositioned twice weekly as necessary) around the maxillary molar teeth were the most effective method to produce a high inflammatory reaction and interproximal alveolar bone loss 7, 15, and 30 days after placement (Figure 1-11) [209].

1.2.2.1 Biological Changes Associated with Ligature-Induced Periodontitis

The goal of experimentally induced periodontitis is to replicate the events that occur during natural periodontitis, but in a more controlled manner, in order to study the effect of certain variables or to elucidate pathways that lead to tissue damage.

The biological events seen in humans during spontaneous periodontal disease start with apical migration of the junctional epithelium proceeding to increased periodontal attachment loss and periodontal pocket depth, and ultimately alveolar bone and root cementum resorption. The inflammatory mediators released by the host to destroy the pathogenic bacteria are thought to have a role in periodontal tissue destruction long-term.

In the following section some of the existing literature regarding the biological changes associated with ligature-induced periodontitis is reviewed, with focus on inflammatory changes, alveolar bone changes and changes in the PDL.

1.2.2.2 Inflammatory Changes and Neutrophils in Ligature-Induced Periodontitis

In the state of periodontal disease, the normal defense mechanism of the host is challenged and changed. To fight the microbial challenge the host immune system increases expression of selected mediators called E-selectins, in addition to other molecules such as interleukin-8 (IL-8) and intercellular adhesion molecules (ICAMs), which result in movement of neutrophils to the gingival crevice where they form a barrier between the dental plaque biofilm and the host tissue [132], [210]. The porous architecture of the junctional epithelium facilitates the migration of the neutrophils to the sites of infection [31]. The sources of inflammation are mainly neutrophils, monocytes, and macrophages [211] which reside in the infected tissues. An increase in their number during periodontal inflammation results in overproduction of cytokines,

which disrupts the balance between the osteoblasts and osteoclasts and lead to bone resorption [212]–[215].

Histologically, neutrophils are very abundant in gingival connective tissue, periodontal pockets, and junctional epithelium during periodontal disease and cause damage to these tissues via releasing matrix metalloproteases and reactive oxygen species [216]–[218]. Any imbalance in the neutrophil count can contribute to the severity of the periodontal disease [219]. However, as reported by Rovin *et. al*., 1966, polymorphonuclear neutrophils (PMN) and leukocytes are found in the connective tissues subjacent to the crevicular epithelium and supra-epithelial aspect of the crevices in both germfree and conventional healthy rats that had no ligatures [125]. The presence of neutrophils in the healthy tissue and their gingival crevicular fluid [32], [132], [136], [220], [221] perhaps is an indicator that the crevicular epithelium is always ready as a defense mechanism and inflamed to a certain degree because of being exposed to normal flora and the plaque biofilm. In rats neutrophils near bone can cause osteoclastic alveolar bone destruction via expression of receptor-activated of nuclear factor-kB ligand (RANKL) [150] synthesized. In response to increased expression of cytokines such as tumor necrosis factor (TNF) and IL-1ß [132].Four weeks after placement of ligatures around molar teeth, the expression of gingival neutrophils increased by ten-fold in conventional rats, but not in germfree rats [125]. Figure 1-12 shows the level of expression of neutrophils (arrows) after 26 weeks of molar ligation in germfree and conventional rats compared to controls [125].

1.2.2.3 Alveolar bone loss in Ligature-Induced Periodontitis

The alveolar bone loss seen during periodontal disease varies in severity in different experimental periodontal disease induction models and in different animal models. For example,

comparison of periodontal tissue destruction using oral gavage with *P. gingivalis* and *F. nucleatum versus* ligature induced periodontitis in mice reveals more apical migration of the gingival epithelium accompanied by inflammation and interproximal and inter-radicular bone resorption than in the ligature model after 45 and 60 days (Figure 1-13) [142], [158]. Induction of periodontitis by inoculation of *P. gingivalis* in mice resulted in increased osteoclastic activity and alveolar bone loss especially in the furcation areas [152], [166], a decrease in osteoblast number, but interestingly an increase in compensational osteoblastic bone formation [152]. Periodontal bone loss caused by ligatures soaked with *P. gingivalis* occurred as early as 10 days in mice (Figure 1-14) [166]. Crater-like bone loss occurs 6-8 weeks post infection [163]. although bone loss induced widened PDL spaces in the furcation and apical regions (Figure 1-11) [209], have not been further investigated.

Alveolar bone loss is seen in healthy mice as well. Comparison between germ-free (GF) mice and specific-pathogen-free (SPF) mice has shown that SPF mice have physiological alveolar bone loss as a result of the immune system's regulatory mechanisms [222]. Natural bone loss was especially seen on the lingual and palatal surfaces. Correspondingly, the expression of RANKL and neutrophils and number of TRAP(+) cells were much higher for SPF than GF mice at the junctional epithelium [222].

Alveolar bone loss (up to 50%) has been followed in dogs after copper band ligatures were placed around the mandibular premolar teeth (Figure 1-9B) [180]. Histological examination indicated some degree of recovery or adaptation. Osteoclasts appeared by the third day and were increased by day 7, but after 3 weeks were relatively sparse (Figure 1-15) [206]. This study also suggested that osteoclasts were more active on the bone surface facing the gingiva than the lingual alveolar bone. A decrease in the number of the osteoclasts with disease progression and

compensational osteoblastic bone formation have also been shown in monkeys, starting 14 days after placement of the ligatures [208]. Molon *et. al*., showed increased alveolar bone loss in mice around the maxillary first molar after ligature compared to oral gavage. Their histological and μCT images show a clear increase in the PDL space and bone resorption in the apical region of the ligated tooth (Figure 1-13 B' and B'1 red arrows), although this was not discussed. The study suggested that the inflammatory response and alveolar bone resorption rate decreased after day 45. All these examples of stabilization may relate to the fact that as the alveolar bone resorbs, the periodontal tissues tend to migrate apically, and if the ligature is not pushed apically to re-introduce trauma, the tissue will reach a stabilization point by physiological remodeling [142], [204], [223], [224].

A pattern of apical bone loss is not unique to mouse studies; a similar pattern is visible in a work by Bhattarai *et. al.*, but was apparently not noticed, because only interproximal and inter-radicular areas were examined [225]. Lindhe and Svanberg (1974) reported bone loss around the apex of dog mandibular premolars subjected to a combination of surgical bone removal, copper banding and soft diet. The area around the apex of the root was surrounded by an undulated bony socket characterized by absence of inflammatory cells and presence of a large number of small blood vessels (Figure 1-9) [180]. Similarly, Lin *et. al.*, found increased PDL space in ligated rat molars not only in the inter-radicular region, but also in the distal apical region (Figure 1-16) [226].

1.2.2.4 PDL in Ligature-Induced Periodontitis

Besides the alveolar bone destruction, another target of periodontal inflammation is the PDL. As a highly vascular and fibrous suspensory ligament [134], the PDL attaches to the tooth root cementum on one end and to the alveolar bone on the opposite end. The PDL is a shock-

absorbing material that spreads the occlusal loads from the teeth to the surrounding alveolar bone [50]. The PDL contains a wide variety of cells, a fluid component and a fibrous network mainly composed of type I collagen [38], [51]. The PDL cells include epithelial and endothelial cells, nerve cells, myofibroblasts, fibroblasts, osteoblasts and cementoblasts [134], [227]. During the inflammatory phase of periodontal disease, pathologic alterations to the fibroblasts occur. Under attack from periodontal disease, the highly organized PDL fiber bundles in the marginal gingiva lose their organization and orientation [228]. Because of the active bone and cementum resorption, the Sharpey's fibers become detached [30]. Where increased infiltration of the inflammatory cells is seen, vascularity increases and collagen fibers decrease [35], [202]. The transseptal fiber bundle, on the other hand, regenerates continuously and migrates apically as the disease progresses [202].

In dogs the histological examination of the ligated teeth shows that the PDL fibers are intact on the cementum insertion points, but not on the alveolar bone end, which could suggest that PDL fiber disorganization and destruction during periodontal disease might not be a direct effect of the inflammatory process of the PDL, but a result of alveolar bone destruction [206]. However, it is not clear whether these observations can be extrapolated to other species.

Ligated rat molars show disorganization of the fibers in the interdental epithelium compared to the controls. However, in the distal apical regions the fibers are more organized and more elongated with less crimped morphology and with sparse distribution. With the progression of the periodontal disease in rats there is an increase in the PDL collagen turnover, leading to a looser fibrous tissue between alveolar bone and cementum. Such a morphology would have less dampening effect, resulting in increased tooth mobility [226].

After long-standing ligation, inflammatory cells are no longer present in the PDL and a more chronic, non-inflammatory phase of the disease becomes dominant [180], [189].

1.2.3 Periodontitis and Tooth Mobility

Although some experimental and clinical studies have shown that tooth mobility increases during periodontal disease [229]–[231] there are limited data as to how much, or how this mobility compares with the healthy state in different species and different teeth, or whether the relative tooth mobility is in relation to the severity of the disease [230], [232]. In beagle dog experimental periodontitis, affected teeth had increased horizontal mobility (49µm and 78 µm) compared to the control teeth (10µm and 16.5µm) in response to external horizontal loads of 100 and 500 grams respectively [180]. In addition, the authors indicated an increase in axial tooth mobility for affected teeth compared to the control teeth, but no value was given for this. Similar findings have been reported for ligated rat teeth, with intrusive movement increasing from 50µm in healthy molars to 85µm in diseased teeth [226], [233]. Interestingly, the mobility of the control teeth stayed unchanged, despite the 50% reduction of bone volume horizontally (Figure 1-17) [180]. This results suggests that alveolar bone height might not be an accurate predictor of tooth mobility, or that bone loss elsewhere (e.g. the apex or furcation) or periodontal destruction is what leads to increased mobility of the teeth [234].

1.3 ANIMAL MODELS

Animal models have distinct advantages in mimicking complexities that occur *in vivo* in humans, and are more realistic than *in vitro* studies. However, no animal model is 'identical' to

humans [160]. Simply due variations in diet, genetics, activities, tissue composition and architecture, immune system response, life span, and many more factors, it is not possible to find a perfect animal model for humans. However, with specific questions in mind, it is possible to find a more suitable animal model to investigate that area. In this project, I propose to use a juvenile pig model to investigate functional tooth mobility in the healthy state and compare it to periodontally diseased conditions for the first three aims of the proposal. Pigs have similar immunology [24], [235], mastication pattern, and dental anatomy to humans and are the most accepted and well-described model for primate mastication. Their multi-rooted posterior teeth are similar to those of humans [236].

There have been numerous studies over many years attempting to shed some light on the displacement of the tooth within its bony socket. While most of the focus has been on the anterior teeth during load application, and on displacement of teeth during experimental orthodontic tooth movement, some studies have attempted to measure the movement of teeth during mastication, but data are not as clear. The PDL and alveolar bone are important in distributing the force and governing the extent of tooth displacement, based on *in vivo* and *in vitro* load application studies. However, there are almost no data available as to how the periodontium controls the tooth movement during mastication. Thus, studying tooth movement under a physiological load, such as mastication, and especially in multi-rooted teeth of an animal model that is close to humans in anatomy and masticatory pattern, such as a molar of a pig [24], [193], [235]–[239] remains of importance and interest.

In order to study tooth mobility during periodontal disease in a specific model, it is important to understand the events that lead to periodontitis that are also determining factors for displacement of the teeth during function. It is therefore essential to investigate the events that

occur at the apex and furcation areas of diseased teeth, since these may be major influences on how a tooth responds to functional loads and how the mobility changes during periodontal disease. Little to no information is available on inflammatory, PDL, and bone changes that occur at the apex and furcation regions of the tooth root when periodontal disease is induced by ligatures. Most studies focus on the junctional epithelium and coronal aspect of the teeth, with only a few recent contributions dealing with the furcation area [142], [225]. One reason for this neglect is the assumption that the soft and hard tissue destruction starts from the coronal part of the tooth and advances apically. Thus studies focus on the events that occur at the most coronal levels. However, there are suggestions that bone loss and PDL destruction in the apical and furcation regions may be especially significant for tooth mobility. Most of the recent studies have used rodents as the model to investigate these areas, however, when it comes to measuring functional parameters such as tooth mobility during mastication, pigs are better mimics of human physiology.

For the last aim presented in this dissertation, the work was initiated in the rabbit model a few years ago. Because pigs are resistant to Botox® [240], rabbits were used as model organisms for the human bone remodeling process. Rabbits require strong masseteric activity to chew their hard-pelleted diet. Moreover, similar to humans, rabbits have a transverse chewing stroke, and this makes them good models for studying masseter activity and hypertrophy [241].

1.4 Specific Aims

1.4.1 Aim 1: Determine range of movement of the mesiobuccal root of the last maxillary deciduous molar (Dm3) during mastication and masticatory muscle stimulation in periodontally healthy pigs. Establish normative data on alveolar bone height and % root coverage by bone, PDL width, and root morphology.

Expectation: I expected that owing to the buccal-to-palatal excursion of the lower molars across the upper molars during chewing, and the apical pressure during power stroke of mastication, the teeth will displace three dimensionally with the coronal part of the tooth moving in the buccal-palatal and apical direction. Furthermore, the maximal excursion will be close to the width of the PDL space in these directions.

Strategies: Ultrasound crystals were used to measure the magnitude and direction of movement during natural chewing and stimulation of masticatory muscles. μCT images were used to examine periodontal space width, periodontal space volume, and root perimeter for the mesiobuccal (MB) and mesiopalatal (MP) roots of the last maxillary deciduous premolar (Dm3). Micro CT images were also used to measure the alveolar bone height housing the Dm3. *Histological sections stained with H&E were examined for location of presence of neutrophils and comparison with micro CT images and to determine if and where bone resorption occurs around these roots in periodontal health.*

1.4.2 Aim 2: Establish a pig model of periodontal disease.

Expectation: I expected to induce periodontal disease in juvenile pigs in 4-8 weeks, defined by 2-4 mm of alveolar bone loss and 4-6 mm of periodontal pocket depth around the Dm3.

Strategies: Periodontitis was induced using silk ligatures inoculated with *P. gingivalis, S. gordonii, F. nucleatum*, and *A. actinomycetemcomitans.* Success of the model was assessed by measuring the bone level using periapical (PA) radiographs and periodontal probing.

1.4.3 Aim 3: Establish parameters of mobility in a pig periodontal disease model by measuring tooth mobility during mastication and masticatory muscle stimulation and establish the associated changes in alveolar bone height and % root coverage by bone, PDL width, and root morphology.

Expectation: I expected a greater range of motion due to loss of bone and periodontal attachment, as compared to Aim 1.

Strategies: In pigs with periodontitis (pocket depths 4 mm- 6 mm and at least 2- 4 mm of bone loss) ultrasound crystals were used to measure the magnitude and direction of tooth movement as in Aim 1. Micro CT images were used to look at alveolar bone height, periodontal space width, periodontal space volume, root perimeter, and % bone coverage of the roots for the MB and MP roots of the Dm3 during periodontal disease for comparison to Aim 1. *Histological sections will be prepared for comparison with healthy pigs.*

1.4.4 Aim 4: Establish changes in alveolar bone modeling in a rabbit disuse model.

Expectation: I expected that reduction of occlusal load would reduce the bone density around the mandibular molars.

Strategies: A disuse rabbit model was created by single and three-repeated injections of Botox® into the superficial masseter muscle unilaterally *vs.* control injections of saline. Micro CT of alveolar

bone samples from Botox®-treated and saline-treated rabbits after 4 (single injection), 12 (single injection), and 36 (3-repeated injections) weeks were used to compare the alveolar bone density.

1.5 FIGURES

Figure 1-1: Micro CT of a coronal section of a rat mandibular first molar tooth.

Legend for Figure 1-1: The arrows show the thickness variability of the PDL space in different areas of the section. Scale bar= 500μm. [Figure modified from Naveh, 2012 [56]].

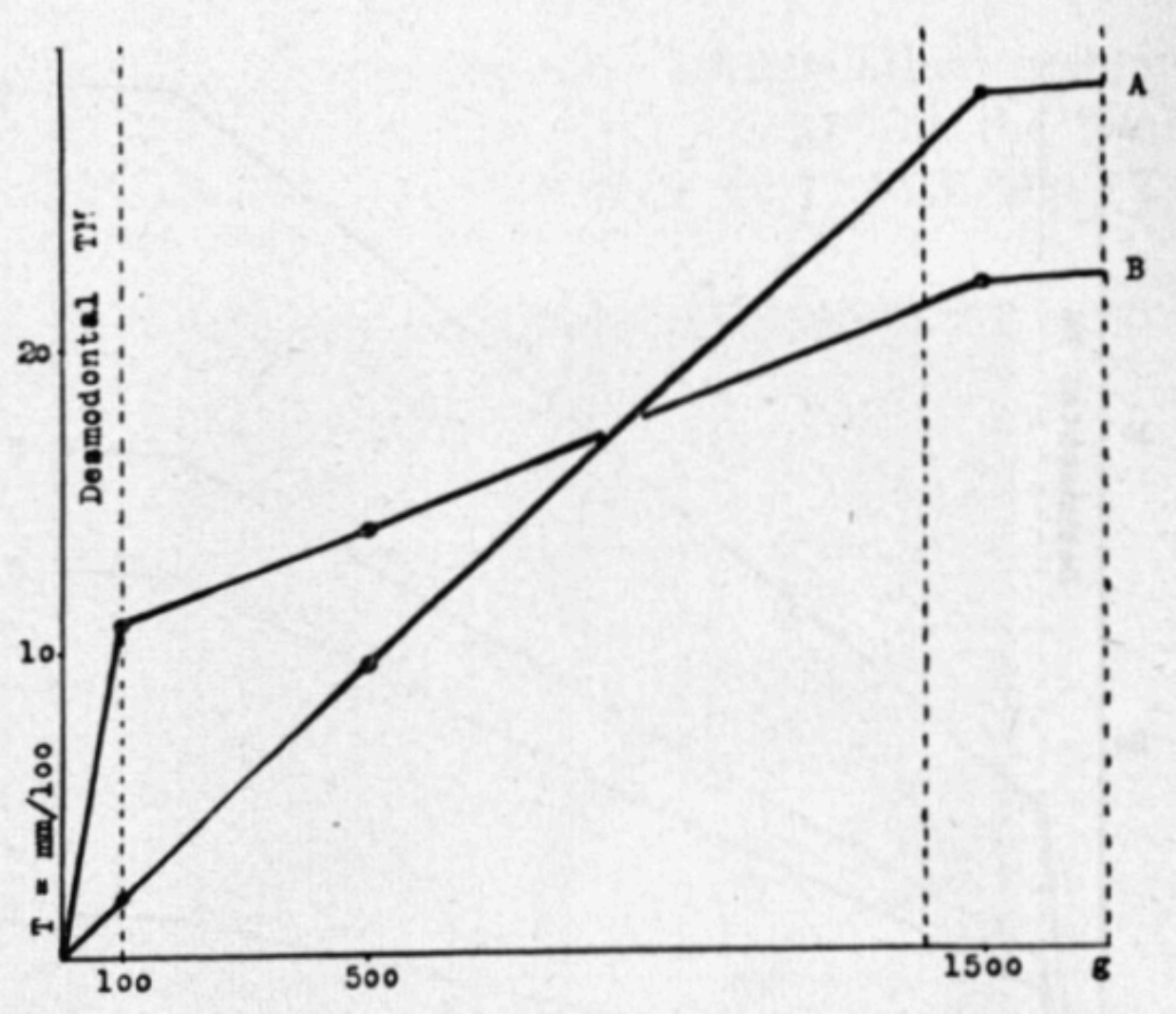

Figure 1-2: Tooth movement of 2 different incisors of the same person.

Legend for Figure 1-2: A: tooth movement of a replanted incisor, with no PDL attached. This is missing the initial phase of movement. B: intact incisor that has PDL, and thus is showing the two phases of tooth movement upon application of force. [Figure is from Mühlemann 1951 [2]].

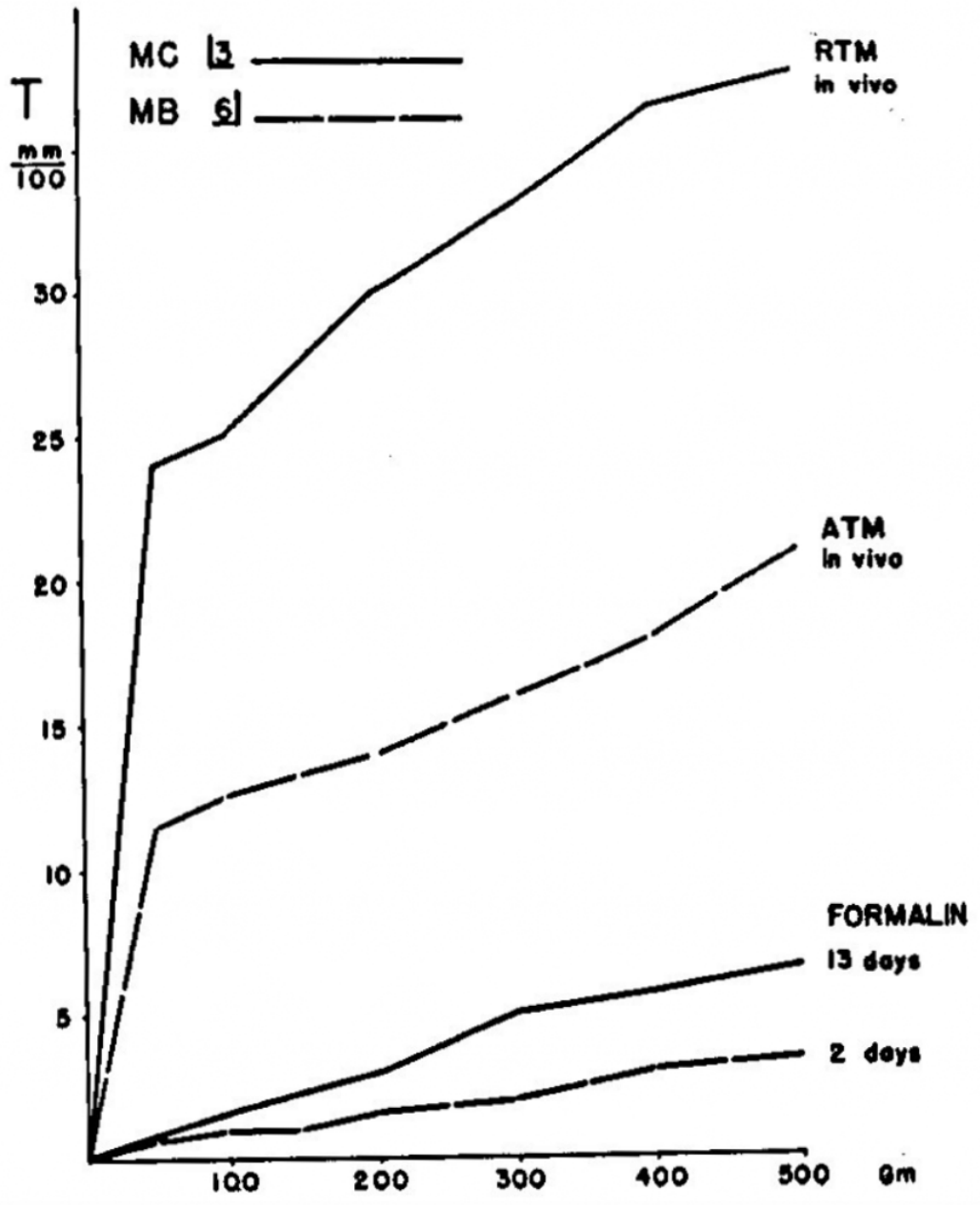

Figure 1-3: Initial and secondary tooth mobility in monkeys.

Legend for Figure 1-3: Loss of initial tooth mobility and decrease in secondary tooth mobility of monkey teeth after treatment with formalin. RTM: Rest Tooth Mobility. ATM: Activated Tooth Mobility [97]. [Figure is from Mühlemann 1954 [78]].

A

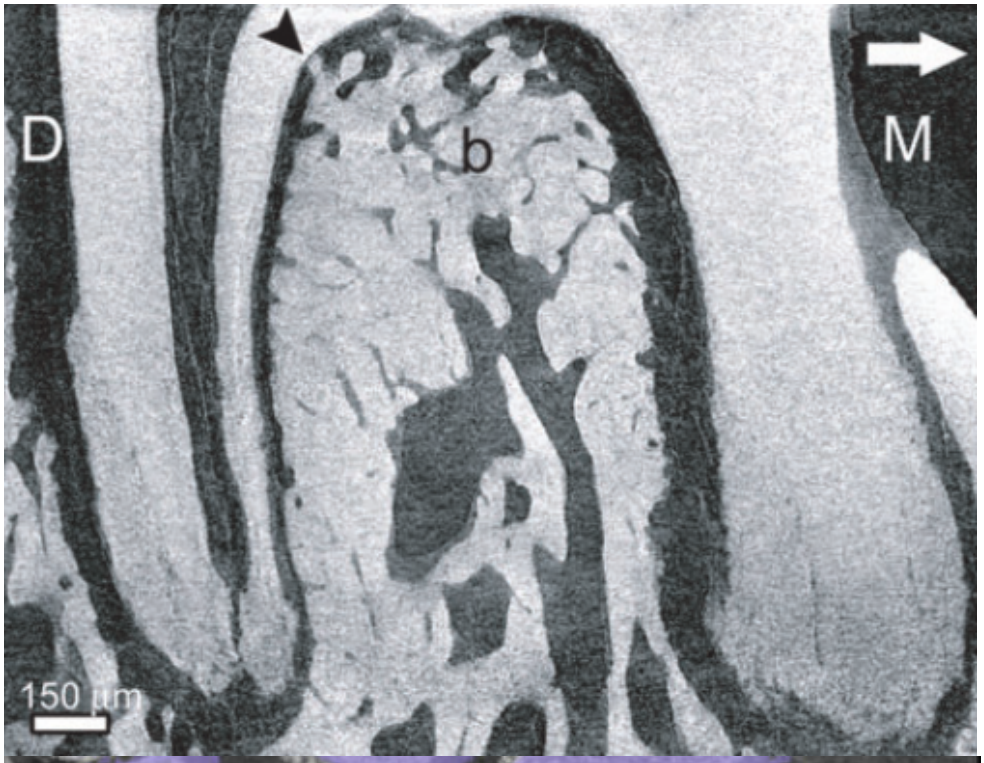

B

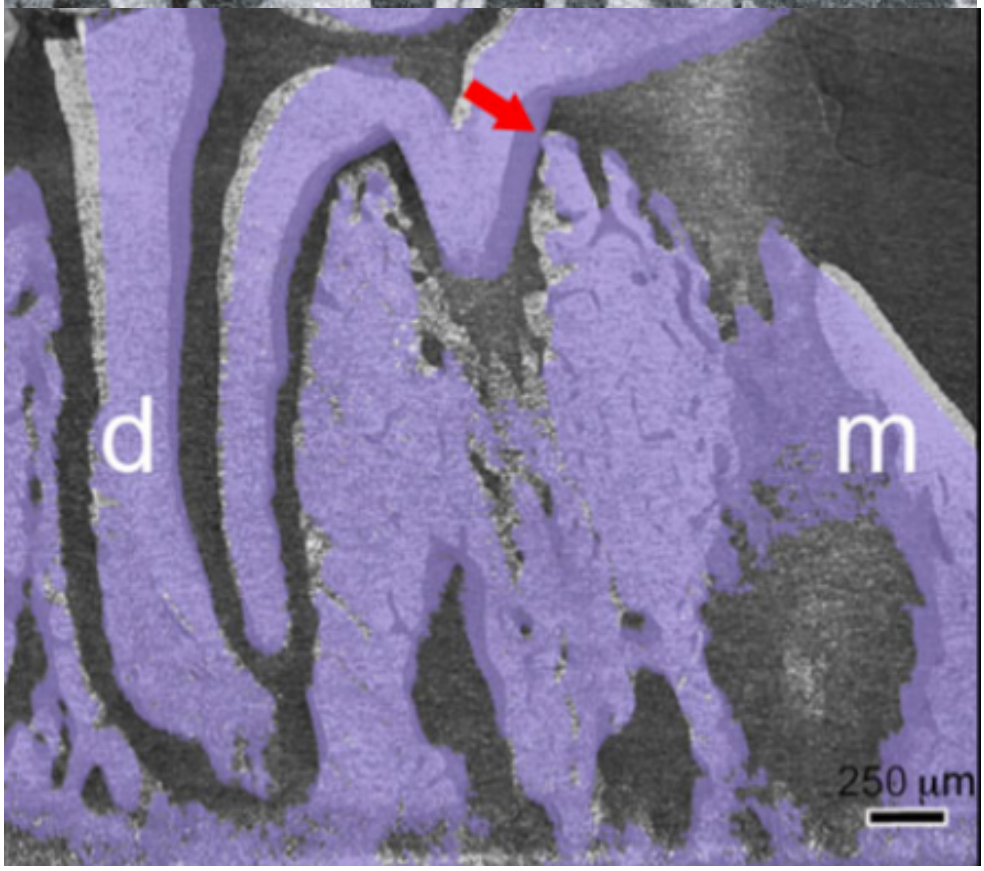

Figure 1-4: µCT of a rat molar tooth under mesial orthodontic force.

Legend for Figure 1-4: 2D micro CT image of a rat molar tooth during mesial orthodontic forces. (A) white arrow shows the mesial direction of the force. Distal and mesial portions of the tooth are marked with D and M, and b is the alveolar bone. The black arrowhead is the contact point between the tooth and the alveolar bone in the furcation area. (B) 2D overlapping of the gray (before movement) and purple (after mesial movement) of the tooth. The red arrow shows direct contact between the alveolar bone and the tooth in the furcation area. The larger PDL width on the distal aspects of the roots (tension) and narrow width on the mesial aspects of the roots (compression) are very clear. [Figure is from Naveh, 2015 [118]].

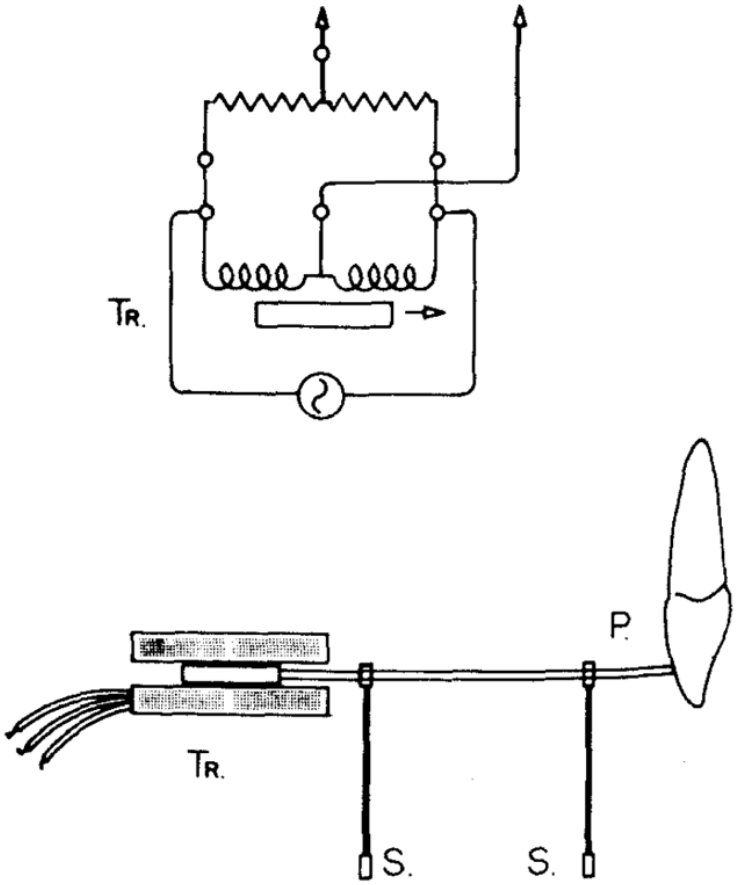

Figure 1-5: Transducer assembly used to measure tooth movement by Parfitt.

Legend for Figure 1-5: Circuit diagram and part of the transducer assembly. TR: Crescent engineering and research Type ZD subminiature rectilinear transducer, sensitivity 2.2 mv/v/0.001", impedance 800 ohms. P: probe. SS: cantilever springs carrying probe and core. [Figure from Parfitt, 1961[22]].

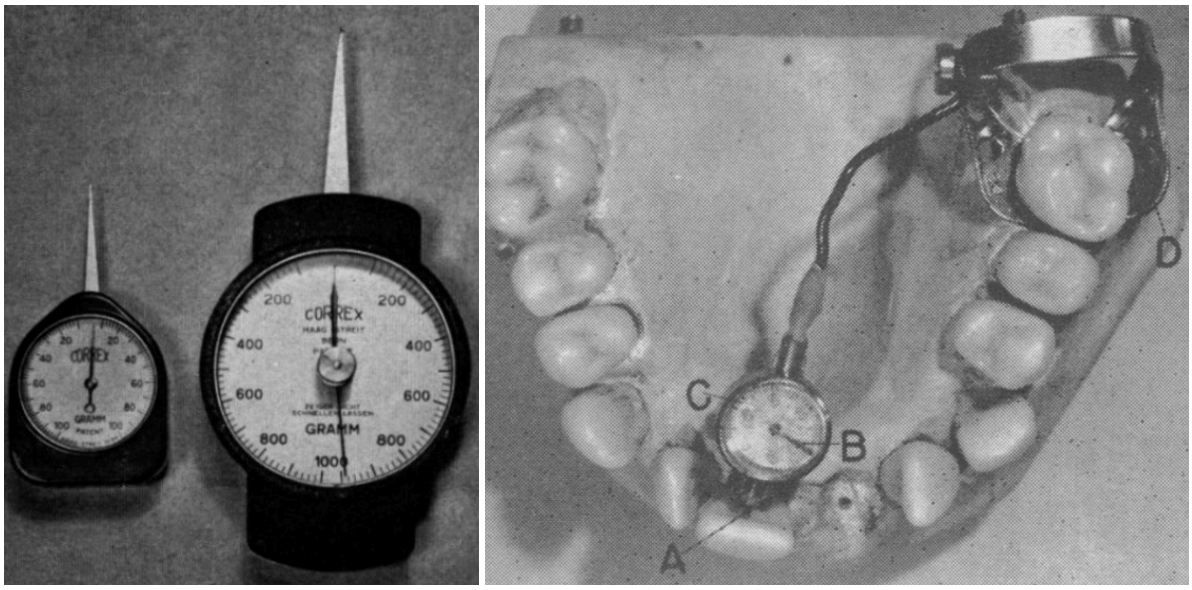

Figure 1-6: Dynamometer used by Muhlemann for application of known force to teeth crown.

Legend for Figure 1-6: A: dynamometers for the application of known forces to the crown. B: Microperiodontometer (A) contact point on the tooth crown, (B) hand, (C) dial markings, (D) rubber dam clamp as a device stabilizer. [Figure is from Mühlemann 1954 [15]].

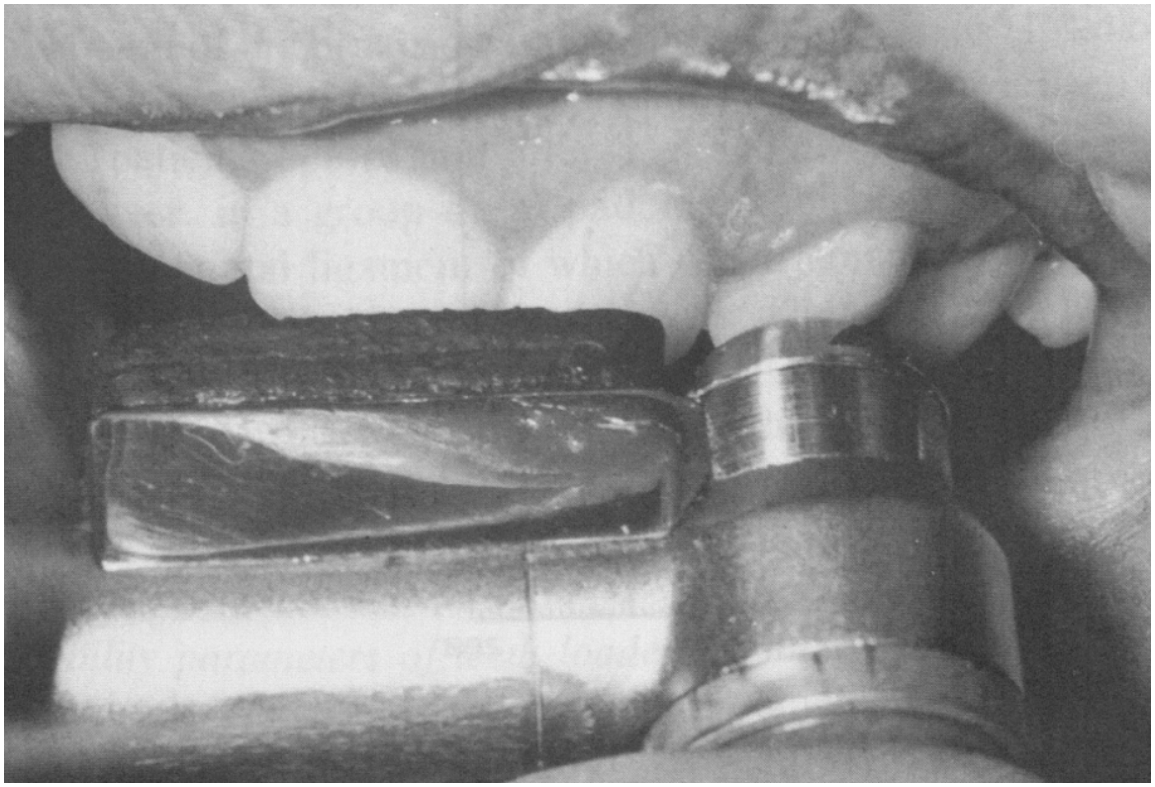

Figure 1-7: Desmodontometryused by Niedermeier.

Legend for Figure 1-7: Upper canine in contact with handpiece of Desmodontometry in the labio-palatal direction of force application and measurement. [Figure is from Niedermeier, 1993 [17]].

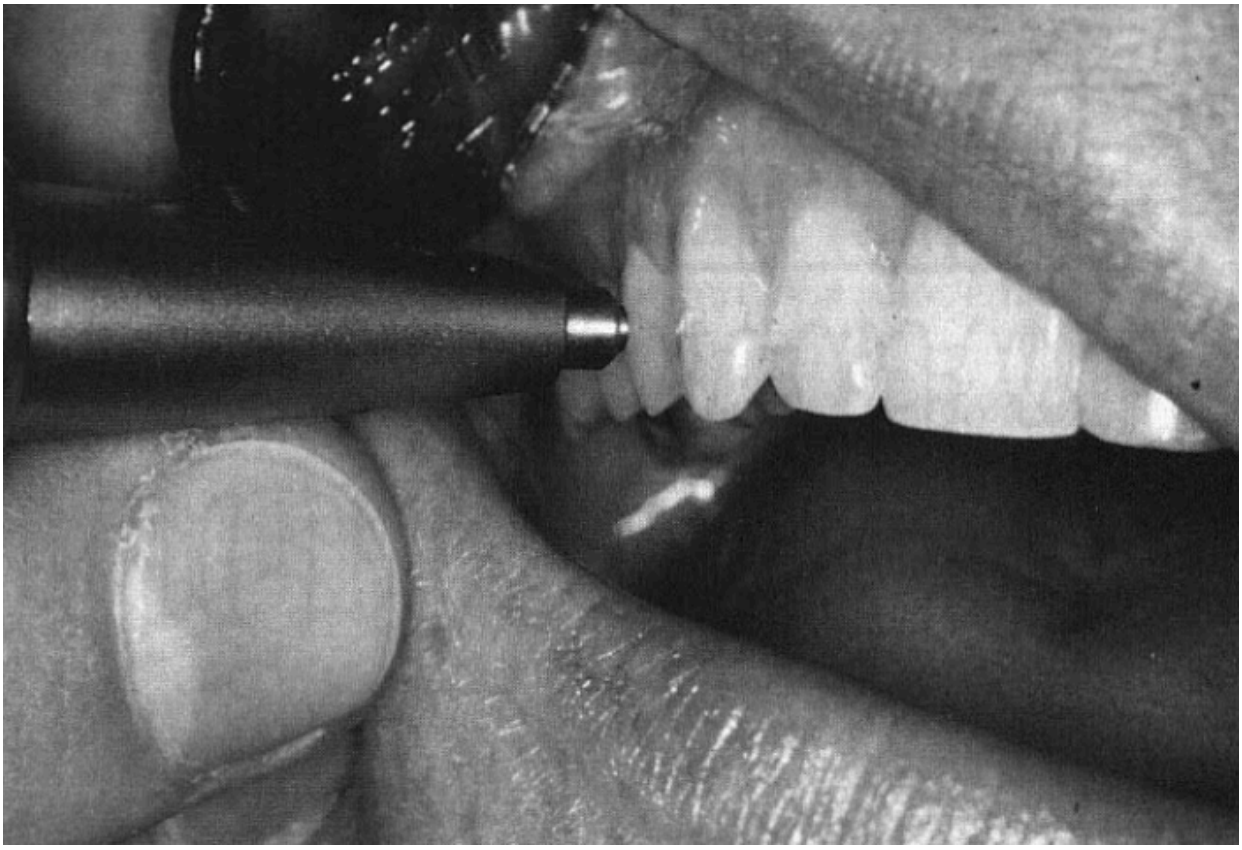

Figure 1-8: Periotest instrument by Schulte.

Legend for Figure 1-8: Periotest instrument held in the orthoradial position in the center of the anatomic crown. [Figure is from Schulte, 1988 [102]].

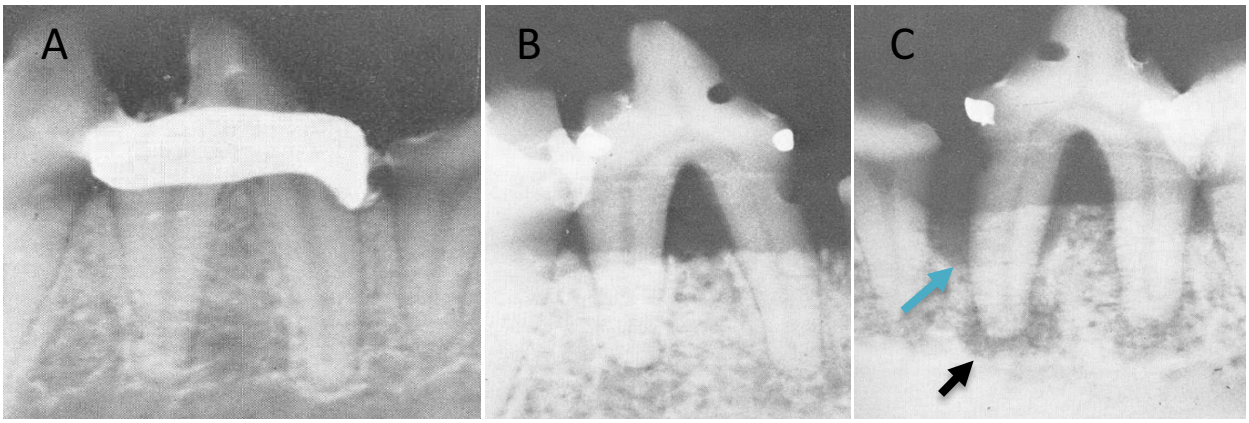

Figure 1-9: Advancement of periodontitis in mandibular premolar of a young dog.

Legend for Figure 1-9: Mandibular premolar (P_4) of a 3-year-old dog. A: beginning of the periodontal induction, copper band around the P_4. B: control P_4 at the end of the experiment showing the uniform horizontal alveolar bone loss (about 50%). C: the test P_4 at the end of the experimental period, showing the crestal bone loss (blue arrow) and the bone loss around the apex of the tooth (black arrow). (Figures modified from Lindhe and Svanberg, 1974) [180].

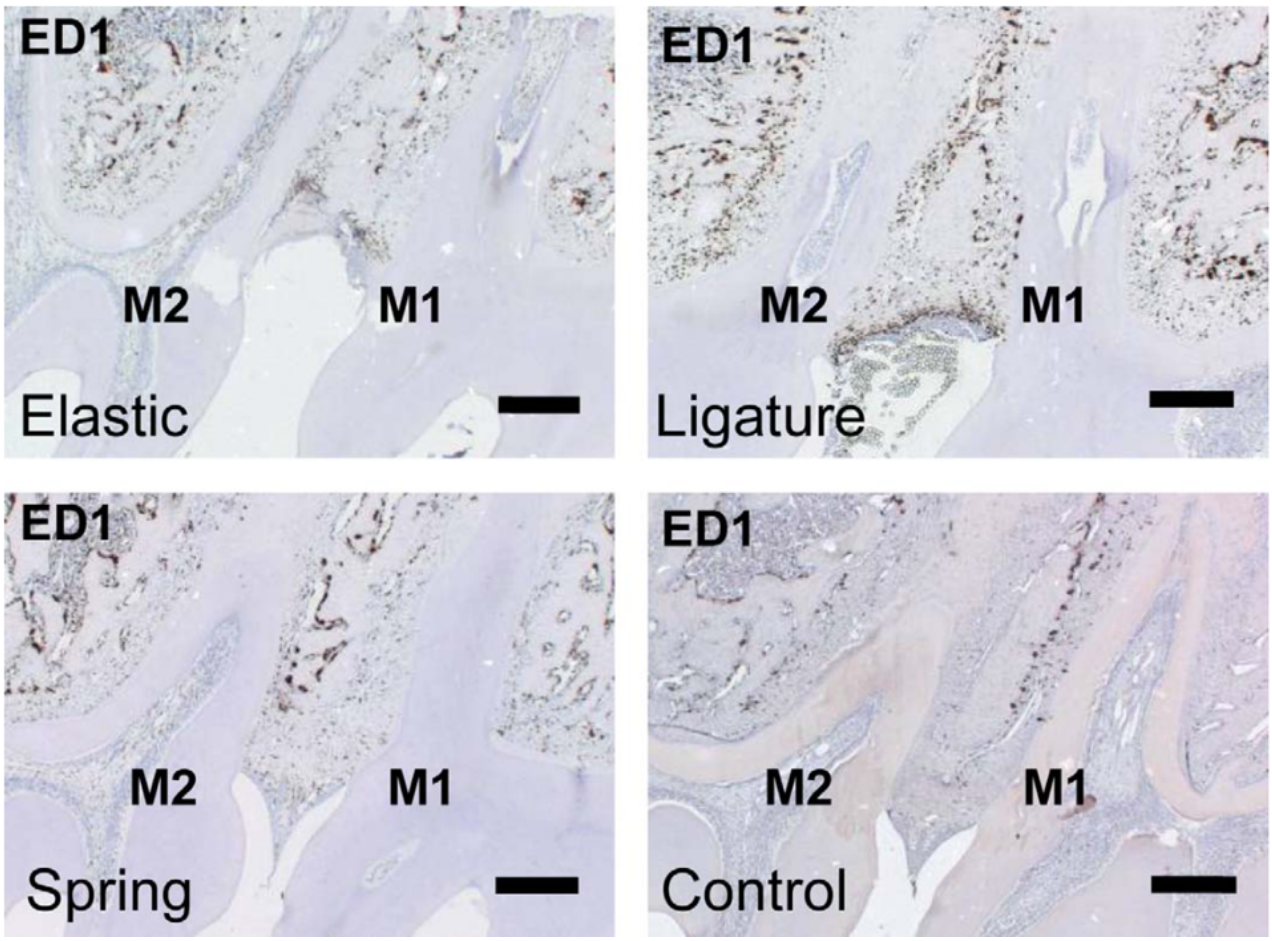

Figure 1-10: Inflammatory markers present around the ligated rat molars.

Legend for Figure 1-10: Staining for the ED1 (inflammatory marker) for three different ligature models and control groups after 1 day, between the first (M1) and second (M2) maxillary molar of the rat. Elastic and ligature model showed increased staining for ED1 (more brown stained cells) compared to the coil spring and the control rats. Scale bar is 250μm. (Figure is modified from Xie, et. al., 2011) [205].

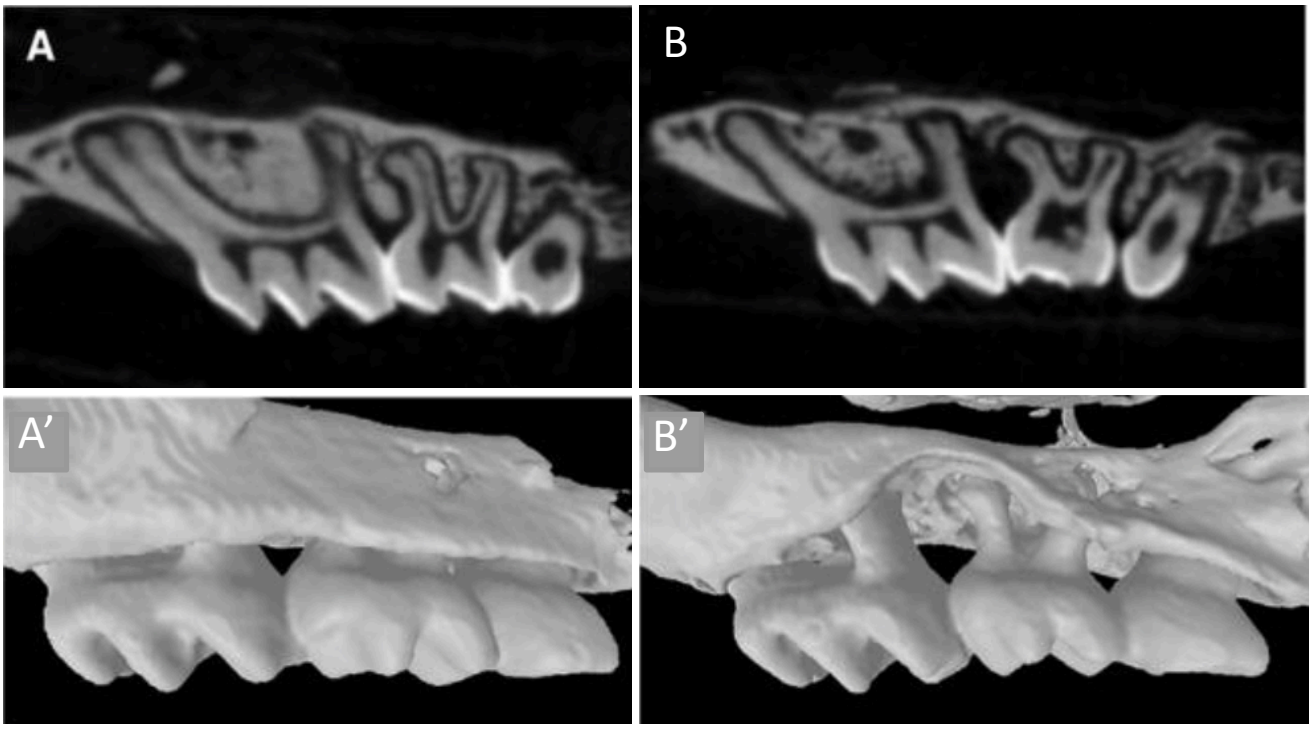

Figure 1-11: µCT images of control and ligated mouse maxillary molars and the associated bone destruction.

Legend for Figure 1-11: µCT images of control and ligated experimental periodontitis models after 30-day period in maxillary molar teeth of 8-week-old female mice. Figures A and B are 2D µCT images, and A' and B' are 3D sagittal views. A,A': control group. B, B': 6-0 nylon thread used as ligature and knotted mesio-buccally around the maxillary molars. The extent of interproximal alveolar bone loss is very significant in the ligature model, there is little loss of bone in the furcation or apical regions of the treated teeth. (Figure modified from Molon et. al., 2014) [209].

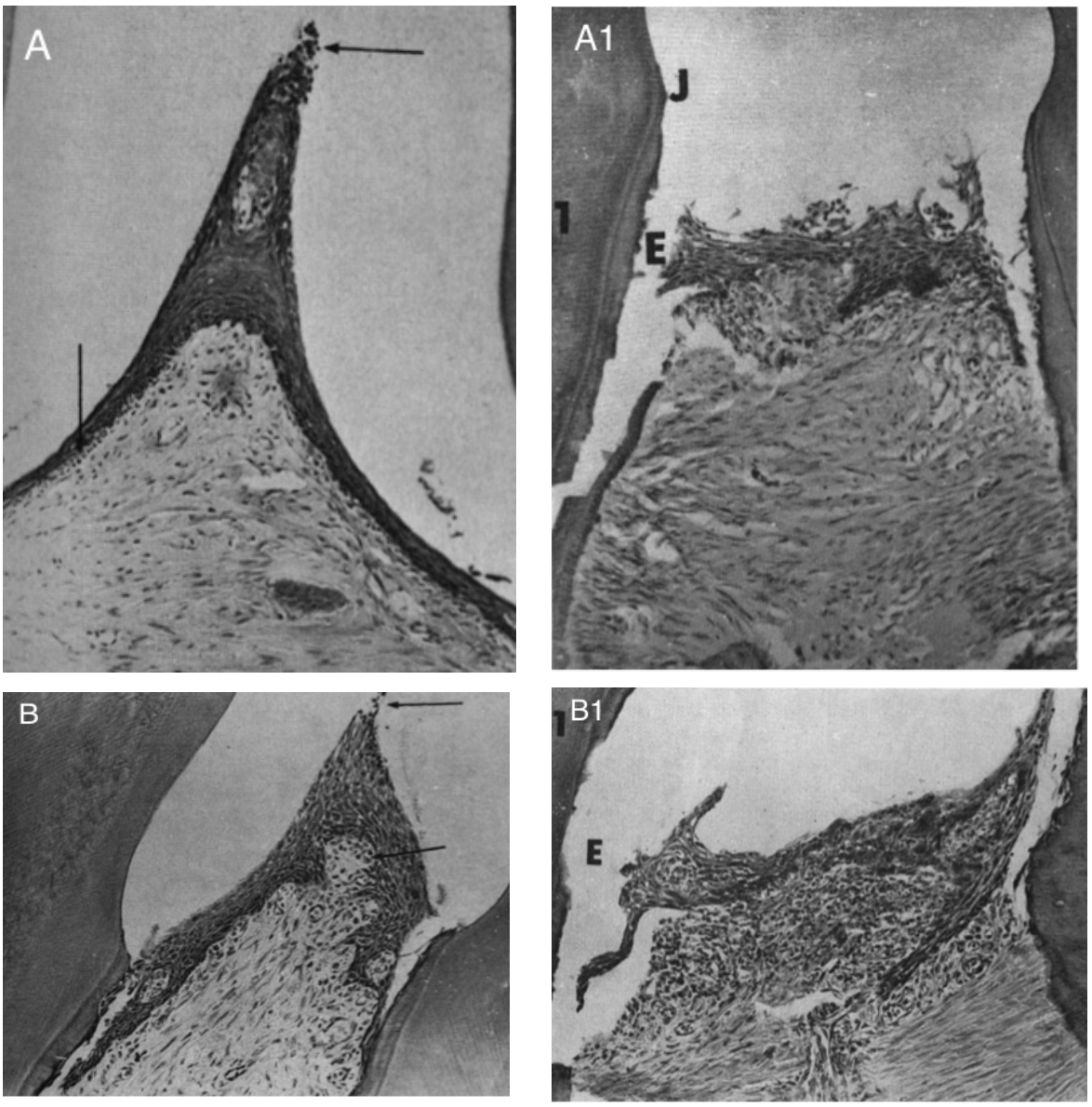

Figure 1-12: Neutrophils in the epithelial attachment of ligated molar of a germfree rat.

Legend for Figure 1-12: Interproximal view of a 26-week specimen. A: germfree control rat, arrows point to the location of polymorphonuclear neutrophils (PMNs), darker cells (magnification x120). A1: germfree ligated rat first molar (1) showing no increase in the inflammatory cells compared to the control. Epithelial attachment (E) is artificially torn away from the CEJ (J) (magnification x150). B: conventional control rat, arrows pointing to the location, which is similar to that of germfree control rat (magnification x150). B1: ligated conventional rat, increased inflammatory response (thicker band of dark stained inflammatory cells) compared to the control and ligated germfree (magnification x150). Figure is modified from Rovin et. al.,1966 [125].

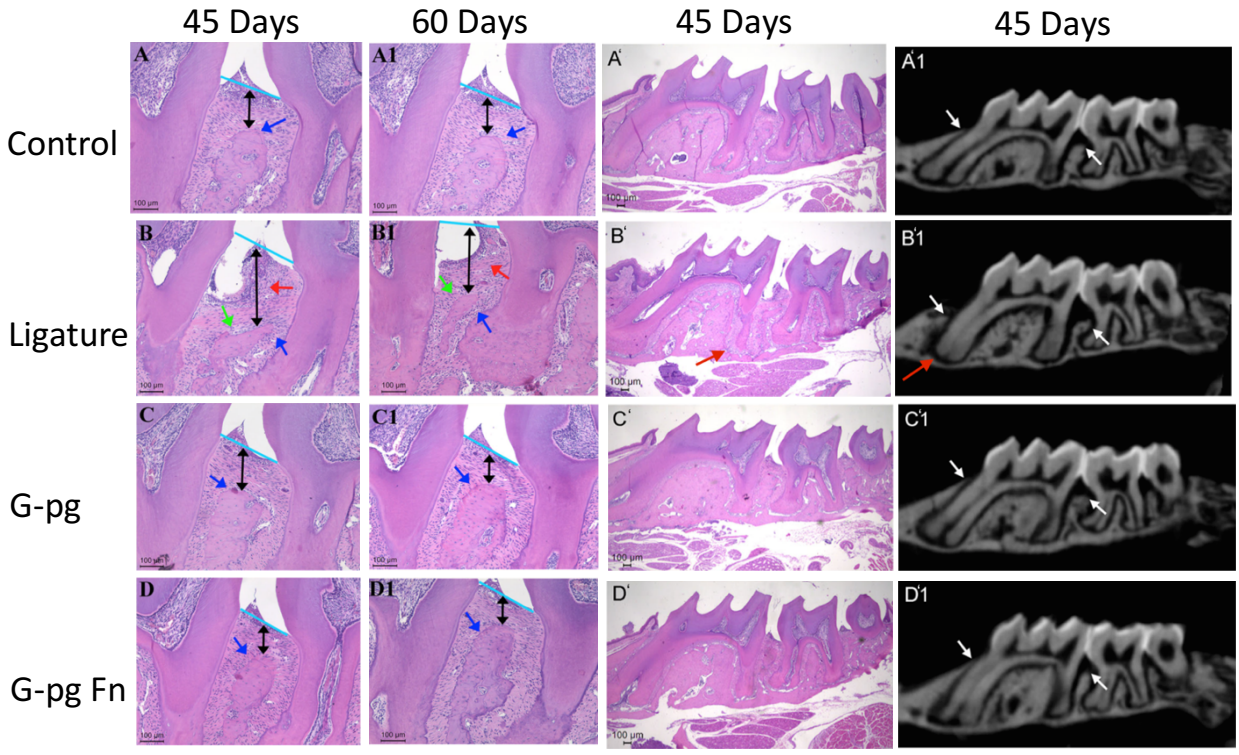

Figure 1-13: Histological and µCT evaluation of ligature, and oral gavage experimental periodontitis around mouse molars.

Legend for Figure 1-13: Histologic and micro-CT examination of the periodontal and alveolar bone of the interproximal of first (M^1) and second (M^2) maxillary molar, and the furcation area of the first molar in mice. Black double headed arrows show the distance from the CEJ to the alveolar bone crest (ABC). Blue arrows show the ABC. Red arrows point to the inflammation in B and B1. Red arrows in B' and B'1 point to the enlarged PDL space and it seems as if there are inflammatory markers in the enlarged space. White arrows in the μCT images point to the ABC in the interproximal and mesial of the M^1 tooth. Panel A shows the control mice, panel B shows the mice treated with ligatures for either 45 or 60 days, Panel C is mice treated with oral gavage using just P. gingivalis, and Panel D is treatment with oral gavage using combination of P. gingivalis and F. nucleatum. Figure is modified from Molon et. al., 2015 [142].

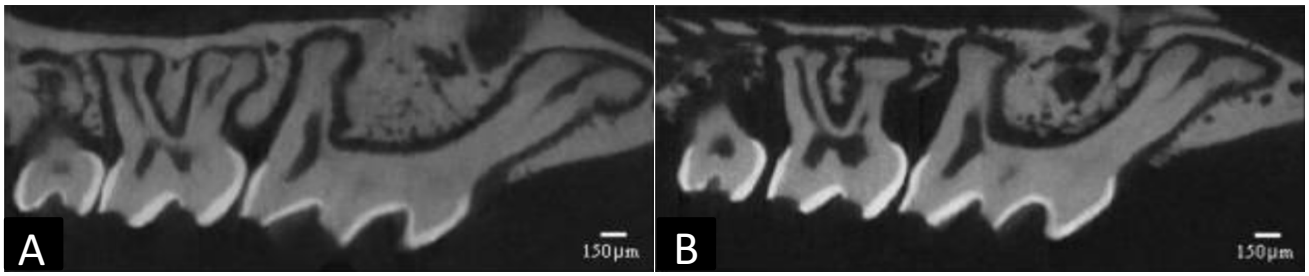

Figure 1-14: µCT evaluation of mouse experimental periodontitis after 10 days using ligature with *P.gingivalis*.

Legend for Figure 1-14: µCT image of control and ligature/P. gingivalis periodontal model of mouse maxillary molar tooth. A is control mouse B is after 10 days of treatment with ligature soaked in P. gingivalis. B: µCT image showing the interproximal, furcation and apical bone loss and increased PDL width (Figure is modified from Li and Amar, 2007) [166].

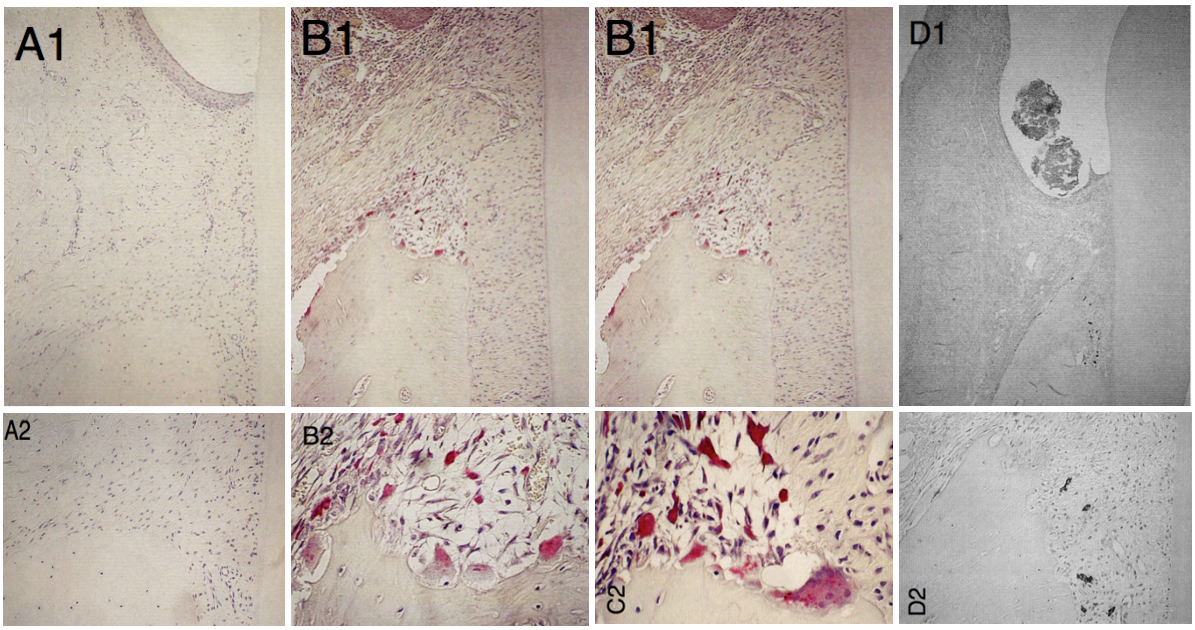

Figure 1-15: Inflammatory reaction around dog ligated molar.

Legend for Figure 1-15: Periodontal tissue of a dog molar stained with TRAP and hematoxylin. A1, A2: non-ligated control molar. B1, B2: 3-days after ligature placement, TRAP+ osteoclasts are seen on the alveolar bone ridge. Increased number of inflammatory cells in the connective tissue near the pocket epithelium. C1, C2: 7-days after placement of the ligature, inflammatory cells and blood vessels are further increased and TRAP+ osteoclasts remain active in resorption of the alveolar bone. D1, D2: 21-days after placement of the ligature, TRAP+ osteoclasts are no longer obvious and there are fewer inflammatory cells present. Osteoclast lacunae seem to be in the process of repair by osteoblasts, and the PDL is more fibrous and less cellular. (Figure modified from Shibutani et. al., 1997) [206].

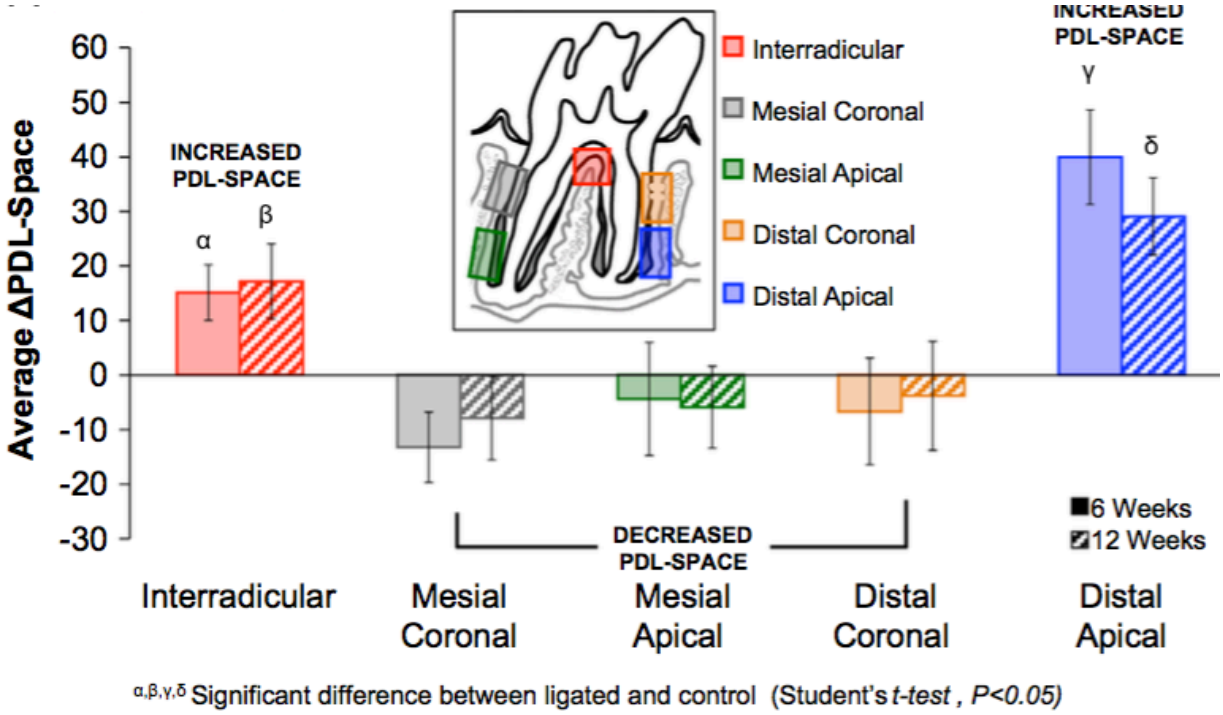

Figure 1-16: Proposed model for PDL space of 6- and 12-week ligated rat molars.

Legend for Figure 1-16: Average PDL space measurement difference between the control and at 6- and 12-weeks ligated samples (ligated PDL space – control PDL space). Positive values reflect increases in the PDL space in the ligated samples compared to the controls. (Figure modified from Lin et. al., 2014) [226].

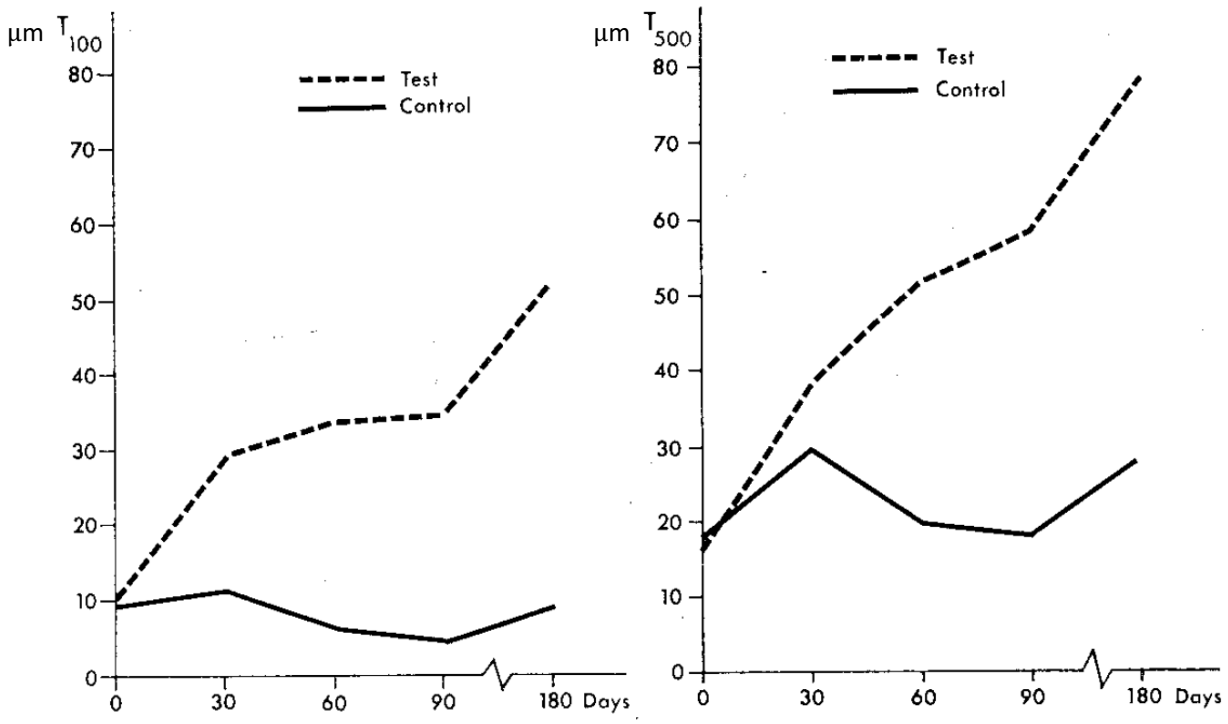

Figure 1-17: Tooth mobility measures after force application in dog experimental periodontitis model.

Legend for Figure 1-17: Mobility measurements of P_4 using 100g and 500g of force in 6 dogs over 180 days of combined experimental periodontitis and occlusal trauma. The forces applied to the teeth were in the buccal lingual directions (Figures modified from Lindhe and Svanberg, 1974) [180].

1.6 TABLES

Legend for Table 1-1: Effect of different diets on the PDL space, alveolar bone surface (AS), and root surface (RS) thicknesses at the cervical, mid-root, and apical levels of the maxillary molar tooth of 26 rats. "superscript letters denote statistically significant differences at $p<0.05$ for comparisons between levels: a: cervical to mid-root, b: cervical to apical, and c: mid-root to apical". [Data from Denes 2013 [64]].

Table 1-1: Effect of soft and hard diet food on PDL space, alveolar bone surface, and root surface of rats.

Variable	Tooth level	Hard diet		Soft diet		*P*-value
		Mean	SD	Mean	SD	
PDL thickness (μm)	Cervical	144.1	9.9	134.2[a,b]	8.3	**0.011**
	Mid-root	144.6	12.2	131.1	8.8	**0.004**
	Apical	146.5	14.2	129.6	7.8	**0.001**
	Average	145.1	11.3	131.6	7.9	**0.002**
AS (10^3 μm^2)	Cervical	688.9[a,b]	47.5	643.2[a,b]	62.2	**0.046**
	Mid-root	620.9[c]	61.4	563.0[c]	63.7	**0.027**
	Apical	556.0	70.9	492.3	65.3	**0.025**
	Average	621.9	56.1	566.2	62.9	**0.025**
RS (10^3 μm^2)	Cervical	341.0[a,b]	31.3	326.7[a,b]	31.2	0.253
	Mid-root	292.5[c]	38.3	275.4[c]	32.5	0.232
	Apical	245.1	43.9	229.2	33.3	0.306
	Average	292.9	34.6	277.1	31.5	0.236

Table 1-2 Legend: PDL width of functioning and functionless teeth of a 38 year old male [data from Kronfeld,1931 [57]].

Table 1-2: PDL space measurements in hypo- and hyperfunctional teeth of one human.

	HEAVY FUNCTION MAX. 2ND PM (MM)	**LIGHT FUNCTION** MAND. 1ST PM (MM)	**FUNCTIONLESS** MAX. 3RD M (MM)
AVE. PDL WIDTH: **CERVICAL**	0.35	0.14	0.10
AVE. PDL WIDTH: **MID-ROOT**	0.28	0.10	0.06
AVE. PDL WIDTH: **APICAL**	0.30	0.12	0.06

Table 1-3 Legend: Miller Mobility Index classifications.

Table 1-3: Miller Mobility Index (MMI) classifications.

MILLER MOBILITY INDEX	MOVEMENT	DIRECTION
MMI 1	less than 1 mm	Buccal, lingual
MMI 2	about 1 mm	Buccal, lingual
MMI 3	more than 1 mm	Buccal, lingual, apical

Table 1-4: Approaches in tooth mobility research.

Table 1-4: Review of literature on approaches for measuring tooth mobility.

Reference	Year	Species	Tooth type	Experimental Design	Method	Force	Tooth movement
[242] Elbrecht	1939	Human	Max. Incisors	Large dial indicator	In vivo	Digital pressure labio-lingually	Measured movement>7 50µm
[243] Werner	1942	Human	Incisors	oscillometer	In vivo	700g	Measured movement>2 50µm
[93] Miller	1950	Human	All teeth	Mirror handle	In vivo	Finger force	Class I-III
[2] Mühlemann	1951	Human	Max. incisor	Periodontometry dial indicator	In vivo	100-500g	0-500µm
[244] Manly	1951	Teeth in stone	Man. Incisors Man. C + PM Man. Molar	Vibration method, mobilometer	In vitro Labio-lingual	1000 cycle oscillator vibration	Class I-III Class I-III Class I-II
[15] Mühlemann	1954	Monkey	Different teeth	Micro-dial indicator	In vivo	50-500g labio-lingually	0-100µm
[21][22] Parfitt	1960	Human	1 max. incisor	Rectilinear transducer	In vivo	100-500g axial mastication	0-30µm 52µm
[245] Picton	1962	Human	Incisors, Max. M	Resistance-wire strain gauge, and dynamometer, btwn opposing teeth	In vivo	2kg 5kg axial force	10µm-100µm
[18] Picton	1963	Human	Mandibular PM, maxillary M	transducer of movement with High compliance wire strain gauge	In vivo	0-2kg	Vertical mobility, 2 phases of movement, 24-34µm
[20] Picton	1964	Human	1st Molar incisor	Electric stain gauge dynamometer	In vivo	Mastication force 1kg-bucolingual	100µm
[246] Lewin	1970	Human	Extracted Molar	Omnidirectional transducer (resistance strain gauge)	In vitro	Applied force axial direction	No data
[19] Korber	1971	Human	Max. Incisor	Parfitt's method, non-contact electronic registration	In vivo	Various forces, 5g labial force 5g palatal force pulsation force	Various 10µm 8µm 0.45µm
[9] Lear	1972	Human	Max. PM	Intraoral splints, miniature solenoid and displacement	In vivo	0.9-2.5 g labio-lingual direction	0.25-90µm
[16] Svanberg	1973	Dog	Mandibular PM	Mühlemann dial indicator, Periodontometry health and perio	In vivo Labio – lingual	100lbs 500lbs	Perio:80µm, health:15µm, perio:130µm health:40µm

Reference	Year	Species	Tooth type	Experimental Design	Method	Force	Tooth movement
[101] [102][99] Schulte	1983	Human	Max. Incisor	Periotest	In vivo	Measurement of PDL dampening characteristic, dynamic force of short durations	PTV:0-100, responding to 3 grades of TM
[17] Niedermeier	1993	Human	Incisor, canine, PM, M	Desmodontometry	In vivo	1.5N	20-400µm
[14], [40] Ioi	2002	Human	Max. Incisor	Amorphous sensor and a small magnet	In vivo	Periodontal pulsation	0.59µm
[115] Ziegler	2005	Minipig	Mand. M	Optoelectronic measurement	In vitro	0-6 N	0-800µm/ rotation
[107] Zaslansky	2006	Human	Mand. PM	ESPI	In vitro	0-100N	1-2µm move in cusp of PM
[247] Yaman	2008	Tooth model	Experimental tooth model	Electromagnetic vibration device, 1mm away from tooth	In vitro	$2*10^3$ Hz - $1.76*10^3$ Hz	More accurate than contact vibration devices. 500-5000µm
[58] Gonzales	2009	Rat	Maxillary Molars	µCT, FEM	In vivo	10-100g mesial tension	Mesial tipping, Palatal inclination 100-240µm
[248] Naveh	2012	Rat	Mandibular M	Load cell, µCT	Ex vivo-hemi mandible	0-100N axial compression	0-150µm
[4][108] Goellner	2013	Human	Central Incisor Lateral Incisor Canine	Photogrammetric measurement	In vivo bite load cell	3N intervals 3-30N	50-150µm 100-200µm 70-120µm
[88], [122] Lin	2013	Rat	Mand. M	µCT, DIC	In vitro	5-20N	35-50µm
[55] Chang	2014	Pig	Mand. PM	µCT	In vitro	0-80 N	100-300µm

CHAPTER 2

Establishing a Pig Animal Model for Periodontal Disease

2.1 INTRODUCTION

Periodontal disease, or periodontitis, by definition is a complex multifactorial chronic immunoinflammatory disease of the periodontium, initiated by subgingival biofilms and a shift from gram-positive aerobic bacteria to gram-negative anaerobic bacteria [123], [124], [132]. In the state of periodontal health there is a balance among the many species of commensal bacteria that reside in the oral cavity. The bacteria associated with periodontal health are mostly gram-positive, facultative anaerobes, cocci, and primarily non-motile [137], [138]. Most of these commensal bacteria are members of the *Streptococcus* and *Actinomyces* genera. However, as the gingival inflammation progresses, other gram-negative species, such as *F. nucleatem,* come into play.

As stated in Chapter 1, the main animal model for my thesis work is pig. While there is extensive literature about various methods for induction of experimental periodontitis in rodent models [151], [153], [160], [163]–[167], [249], [250], there are notably fewer papers on induction and characterization of periodontal disease in pigs. Almost all the existing literature concerning pig experimental periodontitis involves induction of the disease by mechanical reduction of alveolar bone with or without the use of ligatures associated with pathogenic periodontal bacteria [191], [192], [199]–[201].

In order to mimic the multi-species biofilm model present during the chronic moderate periodontal disease, in this study I have used a combination of four bacteria to induce

periodontitis in young pigs, namely *P. gingivalis*, *S. gordonii*, *A. actinomycetemcomitans*, and *F. nucleatum* [251] in conjunction with ligatures. Wang *et al.* have shown that such treatment in juvenile pigs results in periodontitis within 4-8 weeks [170], [193]. This reference, with some modifications, forms the basis of the proposed study for this chapter. These bacteria were selected due to the effect they have on induction and progression of periodontal disease (Figure 2-1) [136]. *S. gordonii* is an early colonizer that attaches to the acquired pellicle on the tooth surface and therefore provides a scaffold for other bacteria to attach to and form a biofilm community [157], [252]. *F. nucleatum* is a bridging organism between early and late colonizers, and is found in both periodontal health and disease [137], [138], [143], [144], [251]. During periodontal health, *F. nucleatum* increases transcription of many protease inhibitors, which when translated will result in inhibition of tissue damage caused by proteases released by neutrophils [253]. During periodontal disease, however, *F. nucleatum* co-aggregates with various other bacteria, especially with *P. gingivalis,* to elicit inflammation and result in alveolar bone destruction [140]–[142], [249], [253]. *P. gingivalis* is a member of the "red" complex of oral biofilm that has been named a 'keystone' periopathogen, since in low numbers, it can lead to progression of the periodontal disease [149], [153]. *A. actinomycetemcomitans* is another gram-negative potent periopathogen that is a late colonizer of the oral microbiome and indigenous to the oral cavity [254]. *A. actinomycetemcomitans* has been shown to be one of the main pathogens in localized aggressive periodontitis in humans, and it has been shown to increase the inflammatory polymorphonuclear neutrophil (PMN) response and osteoclastic response in a periodontal rat model [255].

A pig periodontitis model is necessary to be able to study the influence of the natural course of periodontitis on tooth mobility in a larger animal model and hence this study was undertaken.

Expectation: To produce 2-4 mm of alveolar bone loss and 4-6 mm of periodontal pocket depth (consistent with moderate periodontitis) around the last maxillary deciduous molar (Dm3) [193], [256] after 4-8 weeks of ligation with bacterial inoculation.

Periodontitis in young pigs was induced in 8 weeks using ligatures inoculated with bacteria. In addition to the species used by other workers [170], I used *F. nucleatum,* because it dramatically increases the efficiency of inducing periodontitis in other animal models.

2.2 Material and Methods

Eight three-month-old female farm pigs (Progressive Farm, Quincy, WA) with body weights ranging from 20-23 kg were used for this study. The experimental protocol was approved by the Institutional Animal Care and Use Committee (IACUC) of the University of Washington. Animals had no food restriction and were given regular pig chow with fresh apples as enrichment and water ad libitum. Prior to each procedure requiring anesthesia (discussed below), animals were deprived of food for 12 hours. The animals were sedated by combination of intramuscular injection of Butorphanol (0.3mg/kg) and xylazine (3mg/kg) +/- midazolam (0.5mg/kg). This was followed by induction of general anesthesia by 5% isoflurane by mask, and 2% isoflurane maintenance during the session via intubation. All administration and monitoring of anesthesia was performed by the University of Washington Veterinary Services, Department

of Comparative Medicine.

General anesthesia was used prior to placement of overhang markers and ligatures, refreshment of ligatures with bacteria, measures of Miller's Mobility Index (MMI), plaque index (PI), bleeding on probing (BoP), periodontal pocket depths (PPD), clinical attachment loss (CAL), periapical (PA) radiographs, the baseline Cone Beam Computed Tomography (CBCT) imaging, and the intraperitoneal injection of bone vital labeling markers (calcein and alizarin) 7 and 2 days prior to euthanasia. Note that the use of bone vital labeling to study the mineral apposition rate of the alveolar bone for the periodontally diseased pigs is part of a future follow-up study and the details are not included in this chapter. For each pig, a careful visual examination of the teeth and gums at baseline (defined as the day of the first general anesthesia) revealed healthy non-carious teeth and firm pink gingiva.

2.2.1 Placement of overhang markers and ligatures

In order to record the initial height of the gingiva in relation to the alveolar bone crest, and also to serve as an overhang for plaque accumulation and ligature retention, buccal amalgam fillings were planned. To do this, after the animals were anesthetized, a #2 carbide round bur in a high speed dental handpiece was used to prepare two buccal preparations in Dm3 with a depth of 2mm into the enamel at the level of the gingiva. After rinsing and drying the preparation, amalgam (Ivoclar Vivadent Inc., Amherst, NY, USA) was triturated in an amalgamator (VARI-MIX® III, Caulk-Dentsply, York, PA, USA) and placed in the preparations.

However, the pilot study showed that the amalgam markers were not adequate to hold the silk ligatures in place. Therefore, composite overhangs were placed on the pilot pigs at week 3 and on the rest of the pigs at baseline. To do this, both the buccal and palatal enamel surfaces

were rinsed and dried, 35% phosphoric acid Ultra-Etch (Ultradent Products, INC., UT, USA) was placed for 30 seconds on the enamel surface and then rinsed and dried. Finally, a line of flowable composite (Filtek™ Supreme Ultra, 3M ESPE, ST. Paul, MN) was placed on the buccal and palatal enamel surfaces above the gingival margin and cured for 40 seconds with a visible light curing unit (Ortholux™ XT, 3M Unitek™, 3M Dental Products). The integrity of the composite overhangs was tested and the overhangs were replaced if indicated. The ligatures were then placed around the Dm3 and knotted using a surgeon's square knot on the mesio-palatal side of the Dm3.

2.2.2 Bacteria culture conditions and inoculations

Four different bacteria from the periodontal microbial community, the early colonizer *Streptococcus gordonii* ATCC 51656 (Sg), the bridging organism *Fusobacterium nucleatum* 12230 (Fn), and the late-colonizing pathogens *Porphyromonas gingivalis* 381 (*Pg)* and *Aggregatibacter actinomycetemcomitans* ATCC 29522 (Aa) [20], were obtained from frozen glycerol stocks and were separately streaked on blood agar plates. Sg, Fn, Pg, and Aa cultures were grown anaerobically at 37°C in a Coy anaerobic chamber for three days under an atmosphere of 86% nitrogen, 10% carbon dioxide, and 4% hydrogen. Twenty-four hours prior to each ligature refreshing application, each of the bacteria were inoculated into 5 mL of trypticase soy broth (40 mg/mL) supplemented with yeast extract (5 mg/mL), vitamin K (1 μg/mL), and hemin (5 ug/mL), and then cultured to mid-log phase. Prior to harvesting bacterial cells for soaking of the ligatures, bacterial numbers were spectrophotometrically determined at optical density of 600nm and were adjusted to approximately 10^9 colony-forming units (CFU) [23]. The

bacterial cells were then centrifuged and re-dispensed in carboxymethyl cellulose (CMC) to make a thick slurry for better retention of the bacteria to the silk ligature [174].

The ligatures were placed while the pigs were under general anesthesia and were refreshed twice a week. The bacteria were painted on the designated teeth and the adjacent teeth to ensure adequate bacterial titer [199]. ligatures were refreshed twice per week with fresh bacteria. Co-contamination was judged to be of minimal importance since identifying the site with the most bone destruction and gingival inflammation was the goal. Furthermore, studies in non-human primates have shown no histological inflammatory changes in non-ligated sites in the presence of ligated teeth after 8 weeks [182], [186]. Once the animals were recovered from anesthesia, about 10-20 min after ligature refreshing, food was offered to them.

2.2.3 Clinical assessment of the disease progression

In addition to the baseline measurements taken during the first week, on weeks 2, 4, 6, and 8 pigs were anesthetized again and the measurements were retaken for comparison and evaluation of the progression of periodontal disease. Data for baseline, week 4 and terminal day (week 8 for pigs # 13, 16, 17, 18, 19, and week 7 for pigs # 14, 15) for the ligated Dm3, its adjacent Dm2, and for the non-ligated side Dm3 (to assess spread of disease) are reported here. The reason for different terminal time points for some of the pigs was due to schedule conflicts with the veterinarians for running the anesthesia. All the measurements were taken by one examiner, AS.

Miller Mobility Index was assessed by using the handles of two mirrors, one on the buccal and one on the palatal surfaces of the tooth. Movements of less than 1 mm in either the buccal or palatal direction were classified as MMI 1, MMI 2 was defined as movements of about

1 mm in either the buccal or palatal direction, and MMI 3 was any movement of more than 1 mm in the buccal or palatal direction with apical depression of the tooth [93].

Plaque index was assessed qualitatively and by visual examination on the surfaces of the teeth. If no or slight plaque was present (-) was assigned, minimal plaque (+) was when less than 1/3 of the clinical crown was covered by plaque, moderate plaque (++) was when more than 1/3 of the tooth crown was covered by plaque, and significant plaque (+++) was defined when more than 2/3 of the clinical crown was covered by plaque.

Bleeding on probing was assessed visually during clinical examination. If no bleeding occurred on any of the probing spots around the tooth (-) was given. Slight bleeding upon probing on less than two of the six probing spots was considered minimal (+). Moderate bleeding (++) was when more than two probing spots had bleeding, but it stopped quickly. Severe bleeding (+++) was scored if bleeding occurred at all the probing spots.

Periodontal pocket depths were measured by inserting a dental probe with a millimeter reading vertically in 6 spots around each tooth: the mesial, middle, and distal points of the buccal and palatal surfaces. Depth of the periodontal pocket was recorded for each spot and reported as a minimum to maximum range.

Clinical attachment loss was assessed by inserting the probe vertically, using the composite overhang marker on the buccal enamel of Dm3 as a reference point. However, the measurements were proved to be unreliable in pigs and thus results are not reported here.

2.2.4 Radiographic assessment for alveolar bone loss

PA radiographs were taken using #2 phosphor plates (Air-Techniques®, Inc., Melville, New York, USA) and an Oralix 50 X-ray machine (Philips Medical Systems Inc., Shelton, Conn,

USA) at 50 kVP,7.5 mA, and 1.25 seconds of exposure time. The images were scanned with an Air Techniques® scanner, and MiPACS® viewing software (Charlotte, NC, USA) was used to visualize the images. However, the measurement of bone loss from the PA images were unreliable due to distorted images, and thus only the measurements obtained from CBCT images are reported here.

CBCT radiographs were taken at the baseline and terminal time points. At baseline the anesthetized pigs were situated in the CBCT chair using a commercial car seat and were secured to the seat using belts (Figure 2-2e). The terminal CBCT images were taken after the animals were euthanized. A Morita Accuitomo 170 CBCT machine was used (Kyoto, Japan) with settings 90 kV, 5.0 mA, and a voxel resolution of 270 μm. To visualize the alveolar bone level for the ligated Dm3, non-ligated Dm3, and the Dm2 adjacent to the ligated Dm3 i-Dixel software (Morita, Kyoto, Japan) was used to reconstruct coronal CBCT images of sections showing the mesial roots of each tooth of intent. The distance from cementoenamel junction (CEJ) to alveolar bone crest (ABC) measured from the terminal CBCT was subtracted from that of baseline CBCT image for the buccal and palatal surfaces of the teeth.

2.2.5 Influence of periodontal disease on mastication

To ensure that the placement of ligatures and progression of the periodontal disease was not causing any discomfort for the pigs and affecting their eating pattern, surface EMG was done on a bi-weekly basis to monitor the masticatory pattern. Pigs were brought to the laboratory for feeding every two weeks. The facial hair was shaved off the skin overlying the masseter muscles, surface EMG electrodes were adhered to the skin, and the wires were connected to AC amplifiers (detailed description of the methods is provided in Chapter III, section 3.2.2). As the pigs

masticated their food, the signals were recorded. The recordings were then analyzed for the alternating right and left pattern that typifies pig mastication (Figure 2-3). Side of chewing was determined by relative amplitude of right and left EMG bursts, and chewing rate was determined by counting the number of chewing cycles per second. Furthermore, the animals were weighed on a weekly basis to ensure they were eating well and gaining weight.

2.2.6 Pilot study

Two animals were used in a pilot study and the remaining six were given the protocol that was most effective in producing periodontal disease in the pilot study (Table 2-1). In the pilot study a split mouth technique was used to compare four different methods:

Method # 1: no ligature treatment, only a buccal amalgam and composite overhang marker (Pig 12, right side)

Method # 2: amalgam and composite overhang markers and 3-0 black silk braided ligature (Pig 12, left side)

Method # 3: amalgam and composite overhang markers and ligature inoculated with *P. gingivalis* (Pig 13, left side)

Method # 4: amalgam and composite overhang markers and ligature inoculated with *P. gingivalis*, *A. actinomycetemcomitans, S. gordonii,* and *F. nucleatum* (Pig 13, right side). This mix of bacteria was selected to resemble the polymicrobial nature of the biofilm present in chronic periodontitis [251], [253], [257].

All the ligatures were knotted in the mesio-palatal line angle of the teeth. Each of the molars used in the pilot study initially received 2 buccal amalgam fillings as markers (Fig. 2-2b).

However, as mentioned above, the amalgam did not hold the ligatures in place, and, composite dental material was then bonded to the buccal and palatal enamel overhanging the ligature (Fig. 2-2c).

2.2.7 Histological evaluation of periodontal disease

In order to assess the inflammatory aspect of periodontal disease, immunohistochemistry (IHC) was used to stain for neutrophil markers. After euthanasia and collection of the bilateral blocks containing the Dm3 teeth (refer to Chapter III, section 3.2.4) tissues were further fixed in Prefer (Anatech, LTD., Battle Creek, MI, USA) for 1 week, washed in 70% ethanol, and decalcified in formic acid bone decalcifier (Immunocal®, Decal Chemical Corp, Tallman, NY, USA) for 6-8 months on a rocking platform at room temperature. The decalcifying solution was changed on regular basis. When decalcified, tissues were processed for paraffin embedding (Tissue-Tek VIP tissue processor, Miles Scientific, USA) according to standard histological protocols. Blocks were serially sectioned (Leica Biosystems microtome, Richmond, IL, USA) in the coronal plane at 7-10µm. The paraffin sections were mounted on charged glass slides (VWR VistaVision™ UniMark®, VWR International LLC, Radnor, PA, USA) and pre-heated on a heating block prior to the IHC staining. The protocol followed Greer *et. al.*, [258], modified by using monoclonal antibody to porcine neutrophils (BMA Biomedicals, product number T-3503, Rheinstrasse, Augst, Switzerland) and Vectastain Elite ABC kit (Rat IgG: PK-6104 Vector Laboratories Inc, Burlingam, CA, USA).

Specifically, the sections were deparaffinized by 3 Clearene® (Surgipath®, Leica Biosystems, Richmond, IL, USA) washes, rehydration in a decreasing graded dilutions of ethanol (100%, 95%, 70%), and blocking non-specific staining by incubation in 1.5% hydrogen

peroxide (H_2O_2) in methanol for 30 minutes. The slides were then incubated for 1 hour with the primary antibody (mouse monocolonal IgG1, and clone PM1 anti porcine antibody, BMA Biomedicals). The secondary antibody was biotinylated anti-mouse and the slides were developed using a DAB in peroxidase substrate kit (Vector Laboratories Inc, Burlingam, CA, USA) for 1 minute and 20 seconds. Negative controls did not receive the primary antibody. The epitope for this antibody has not been characterized, but the immunogen is reported to be from porcine lung extract and to be found in neutrophils in porcine soft tissues including blood and the red pulp of spleen. Therefore, positive controls were selected from 5 different soft tissue organs, namely lung, liver, spleen, kidney, and palatal gingiva. The stained slides were imaged under a Nikon light microscope (Nikon Eclipse E400, Nikon Corporation Instruments Company, Tokyo, Japan) and were examined for the presence of brown stained neutrophils, especially in the junctional epithelium (JE), furcation area of the tooth, and the apical region of the roots.

2.3 RESULTS

2.3.1 Pilot study

In the first pilot pig (pig #12) which had no bacteria added, no significant amount of bone reduction or increased pocket depth was observed in 8 weeks, although the use of ligature by itself appeared to increase the probing depth slightly (Table 2-1, Pig 12- L). This pig was therefore added to the control group in the tooth mobility study (Chapter III). The second pilot pig (pig #13) showed mild disease on the side with *P. gingivalis* (Table 2-1, Pig 13- L) as the only bacterium, and acute disease on the R side, with periapical abscesses and alveolar bone loss, with combination of the bacteria (Table 2-1). On the basis of these results, the method of ligature

with a combination of bacteria was adopted for the remainder of the periodontal disease study. The right side of pig #13 was included in the main study, along with 6 additional pigs. Four of these were treated unilaterally and the other 2 bilaterally.

2.3.2 Clinical assessment results for disease progression

All the 9 ligated teeth from the seven animals in the main experimental periodontitis disease study reached the criteria of at least 4 mm of probing depth and 2 mm of bone loss, and thus the protocol was successful in producing periodontal disease in young pigs. Most animals reached this threshold by 4 weeks, while other indications of disease continued to increase with time. Non-ligated Dm2s and Dm3s showed little or no evidence of periodontal disease at any time period. Data for each pig are given in Table 2-2, which includes baseline, week 4, and final (usually week 8) readings for each ligated Dm3, and also the probing depth and alveolar bone measure range for the adjacent but non-ligated Dm2, and the non-ligated Dm3 (if there was one).

Miller Mobility Index (MMI): Teeth that had the ligature with the combination of bacteria tended to show slightly more mobility than at baseline, but none of the teeth moved as far as 1 mm and hence all teeth scored as MMI1.

Plaque index (PI): All ligated teeth had increased levels of plaque accumulation compared to the non-ligated teeth.

Bleeding on probing (BoP): Upon probing, increased bleeding was seen around all of the ligature treated teeth, especially on the mesial side where the knot had been placed, where pus discharge was sometimes seen (Figure 2-2e). The peak in bleeding and pus discharge for most pigs was around week 5-6, after which there was no more pus discharge and the bleeding was reduced.

Probing pocket depth (PPD): Pocket depth varied within and among the pigs, which was expected due to individual variation in the development of the disease. The second pilot pig (pig #13- Table 2-2) may have had some pre-existing disease, as pocket depths were relatively great at baseline and in non-ligated teeth. However, pig #13 and all other pigs showed a clear increase in the probing depth on the experimental teeth when compared to other teeth (Table 2-2). In many cases, probing depths continued to increase until the terminal week. It is important to keep in mind that tissue swelling and inflammation and gingival recession in periodontal disease could have affected the PPD measurement.

2.3.3 Radiographic assessment results for alveolar bone loss

Radiographic analysis showed that in all the 9 treated Dm3s, the criterion of 2-4 mm of bone loss was met (Table 2-2). For some pigs the bone loss was very significant and involved the furcation area. However, the greatest amount of alveolar bone loss was seen on the buccal and palatal bone crests, where the range of loss was of 2.7 mm to 6.3 mm when measured from the CEJ to the alveolar bone crest. Non-ligated teeth showed a maximum bone loss of only 1.5mm.

2.3.4 Assessment of masticatory pattern for the periodontally diseased pigs

No noticeable difference in the pattern of mastication was seen from in the 7 pigs that were used for experimental periodontitis. All pigs chewed on both the right and the left sides, and the alternate side of chewing was evident on all the EMG recordings, including the pigs that only received ligature on one side. Figure 2-3 shows examples of mastication pattern for a pig (#15) that received ligatures bilaterally and for one (#19) that received a unilateral ligature on the left Dm3. The chewing rate also remained consistent throughout the experiment (Figure 2-4).

The non-significant and slight decline in the chewing rate that is observed from week 1 to week 6 and week 8 is most likely an aging effect, since it has been shown that older pigs have lower chewing rate compared to younger pigs [259]. Furthermore, Figure 2-4 shows that the chewing rate was not affected by the surgical implantation of the crystals (introduced in Chapter 3), since there is no significant change between the chewing rate at week 6 (2 weeks prior to the crystal implantation) and chewing rate at week 8 (chewing rate immediately after surgical implantation of the crystals). Furthermore, the percentage of time that the pigs preferred to chew on the ligated side did not differ significantly from the non-ligated side (Figure 2-5). These data as well as the steady weight gain (Figure 2-6) provide evidence that the ligatures did not hinder normal feeding behavior.

2.3.5 Histological assessment of periodontally diseased pigs

Neutrophils were readily detected in all positive controls from spleen, lung, liver, and kidney; positive reaction was indicated by brown stained cells (Figure 2-7). Therefore, the chosen antibody worked in pigs, although according to the manufacturer it was not well characterized for all pig tissues. Positive reaction was also seen in the junctional epithelium and apex of ligated Dm3 from pig #13 and #14, the only pigs available as of yet (Figure 2-8 A' and B'). Comparable tissues from the healthy animals (See Chapter 3) were negative for neutrophil antibody, however (Figure 2-8 A and B). Furthermore, there was no detection of neutrophils in the furcation of neither healthy nor diseased pigs (Figure 2-8 C, C').

In order to investigate the events that are occurring at the apex of the root of the ligated Dm3s compared to the apex of the non-ligated Dm3s, I looked at neutrophil activity and distribution from available tissues (n=2, P13 R and P14 R). Neutrophils were found in the

junctional epithelium and at the apex of the ligated teeth but no neutrophil was found at the furcation of the ligated nor non-ligated teeth. The rationale for antibody staining against neutrophils was to identify if the enlarged PDL space (as seen in Chapter 4) is in fact due to the inflammatory bone loss or frank abscess from the periodontal disease, or if the enlarged space is seen in both the ligated and non-ligated Dm3s and thus is associated with other factors such as the events linked to tooth eruption and aging.

2.4 DISCUSSION

Despite the existence of ample literature for inducing periodontitis in rodents, there is little information on inducing periodontitis in pigs. In this study, four different pilot methods were explored, and one was found to induce periodontitis efficiently and effectively. The variation in individual pigs made it possible to view a range of responses to the same treatment method, nevertheless, all developed clinical disease that met the criteria for this study.

2.4.1 Limitations

Several problems were encountered. First, *S. gordonii* and *A. actinomycetemcomitans*, did not initially grow well, but this problem was solved by using a candle jar under microaerophilic conditions. Second, initially, food was offered to the pigs immediately upon waking from general anesthesia. This however, probably created mechanical damage to the not-yet established biofilm, as bacteria would not have had adequate time to stick to a surface and grow. As a modification to resolve this problem, an extra 15 minutes of anesthetic maintenance was added after refreshing the bacterial cocktail of ligatures. This did not seem to be of much

significance however, since the later pigs (Pigs # 16-19, Table 2-2) for which the extra 15 minutes under general anesthesia was given, did not have deeper pockets compared to earlier pigs (Pigs #13-15, Table 2-2). Third, measurement of the clinical attachment loss was difficult and unreliable due to distorted PA images, and moreover it has not been proven to be a reliable measure of periodontal disease advancement in non-human species [182]. This measure was therefore abandoned.

2.4.2 Clinical assessment of disease progression

Use of ligatures with a combination of four different bacteria (*P. gingivalis*, *S. gordonii*, *A. actinomycetemcomitans*, *F. nucleatum*) was reliably successful in inducing periodontitis in all the 9 ligated teeth in 7 pigs with pronounced gingival inflammation and significant periodontal pocket depth formation. This perhaps could be explained by the protective effect of the multi-species biofilm formed. Biofilms shield bacteria against mechanical and immune system attacks [251], [257], [260]. During the experimental period, I ensured that the ligatures stayed in a subgingival position so the bacteria could adhere to them and grow, in order for periodontitis to progress. Over time, an increase in the probing depth was associated with an increase in plaque accumulation and bleeding, which are contributing factors to increased inflammation [37], further indicating the success of the method.

2.4.3 Radiographic assessment of disease progression

Radiographically there was significant amount of crestal bone loss on the buccal and palatal alveolar sides of the ligated Dm3 tooth. The bone loss probably involved inflammatory and osteoclastic processes introduced during the mechanical trauma from placement and re-

placement of the ligatures, as well as the presence of periodontal pathogens that further aggravated the inflammatory reaction locally [162], [261]. The loss of alveolar bone is one of the hallmarks of periodontal disease and has been seen in other species as well as humans [168], [188], [189], [224], [262].

2.4.4 Histological assessment of disease progression

To the best of my knowledge this is the first study to characterize the neutrophil abundance in junctional epithelium and periodontium of young pigs. Neutrophils are part of the first line of oral mucosal defense, and they have been found in the junctional epithelium of germ free mice and in human gingival epithelium before the clinical signs of gingivitis are detectable [263]–[266]. Thus, my expectation was that they should also exist, albite in low numbers, in junctional epithelium of periodontally healthy pigs.

The lack of detection of any neutrophils in the periodontally healthy pigs may be a technical problem, as stated above, the neutrophil antibody that was used in this study is not well documented, so it may bind poorly to the antigens in the gingival tissue from the healthy periodontium of young pigs. However, this explanation implies that neutrophils in healthy tissue differ from those of periodontally diseased tissue, since there were plenty of neutrophils detected in the ligated specimen analyzed (P13 R and P14 R). Another explanation with a similar problem is that due to the long decalcification time, as well as the radiation and associated desiccation, the antigens are damaged. Again, however, this explanation does not account for the many positive cells in the diseased specimen.

A third and more likely explanation involves the thickness of the sections that was 10µm for the tissues from the healthy periodontal pigs and 7µm for the tissues from the periodontally

diseased pigs. The thicker sections adhered poorly to the glass slide, and it is possible that damage to the section itself prevented the identification of neutrophils, especially if there were only a few to begin with A much greater number of neutrophils in periodontally diseased pigs would make these positive cells much easier to find.

2.4.5 Effect of the biological processes

One final pertinent observation is that eruption of permanent teeth might have altered progression of periodontal disease. In some of the pigs, the first permanent molar (M1) was erupting by the 6th week of the experiment. These same pigs (pigs #15-19, Table 2-2) showed a tendency for pocket depths to decrease (Table 2-2). The eruption of the permanent first molar could be stimulating the innate immune response, and thus act to decrease the level of damage of the periodontal pathogens. Alternatively, the events might be unrelated, and the periodontal improvement due to disease stabilization, as reported in non-human primates [160], [182], [183], [188], [189] and dogs [206], [267] after first seven weeks of the disease. The implication is that the acute phase of the disease, which usually occurs in the first few weeks, is gone, and therefore, the immune system has come into balance with stable chronic periodontal conditions [160], [182], [183], [188], [189], [267].

2.5 CONCLUSION

A pig periodontal model can be established in 4-8 weeks with the use of silk ligatures and periodic refreshment with a 4 bacteria cocktail, namely *P. gingivalis*, *S. gordonii*, *A. actinomycetemcomitans*, and *F. nucleatum*. All the pigs demonstrated more than 2-4 mm of

alveolar bone loss and 4-11mm of periodontal pocket depth, in addition to the gingival inflammation.

2.6 ACKNOWLEDGMENT

The funding that made it possible for me to form and carry out this part of my PhD project, for purchase and husbandry and CBCT imaging of the eight pigs used in this chapter, and also the follow-up future projects using the periodontal pigs from this method, was provided by the University of Washington SunStar Preventative Dentistry Award that was granted to me on November of 2014. I would also like to thank Dr. Richard Darveau for providing the antibody for neutrophil staining and his lab members for helping me in learning the IHC technique. Special thanks to Dr. Johan Aps and the UW Department of Comparative medicine for making CBCT imaging possible. Special thanks to members of Herring, Liu, and Rafferty labs and Dr. Qin Bai for their help along the way.

2.7 FIGURES

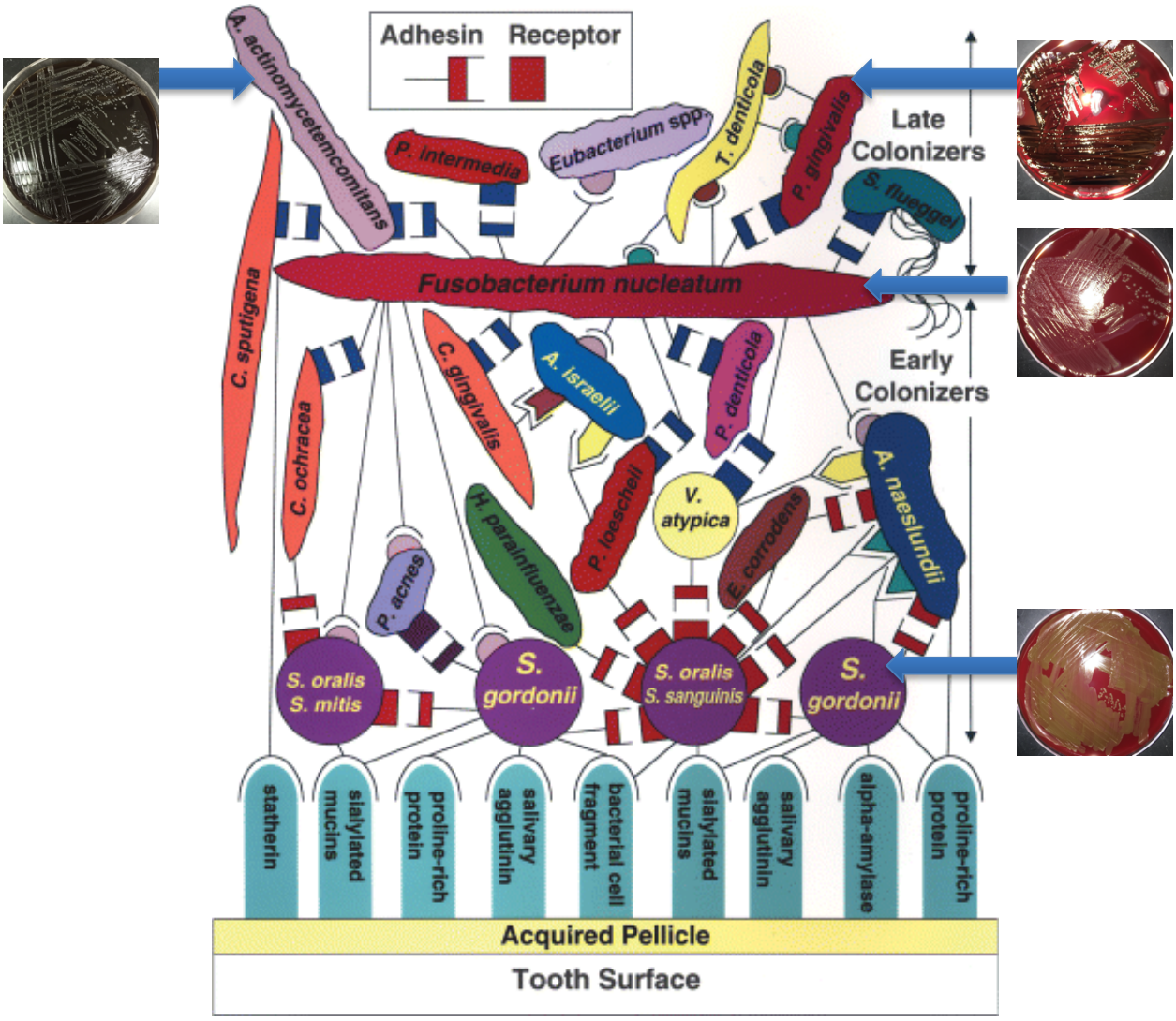

Figure 2-1: Bacteria selection for experimental periodontitis..

Legend for Figure 2-1: Bacterial interaction and plaque biofilm formation. Blue arrows point to the four different bacteria chosen to induce periodontitis in this project, grown on blood agar plates. [Figure is modified from Kolenbrander, et. al., 2006 [136]].

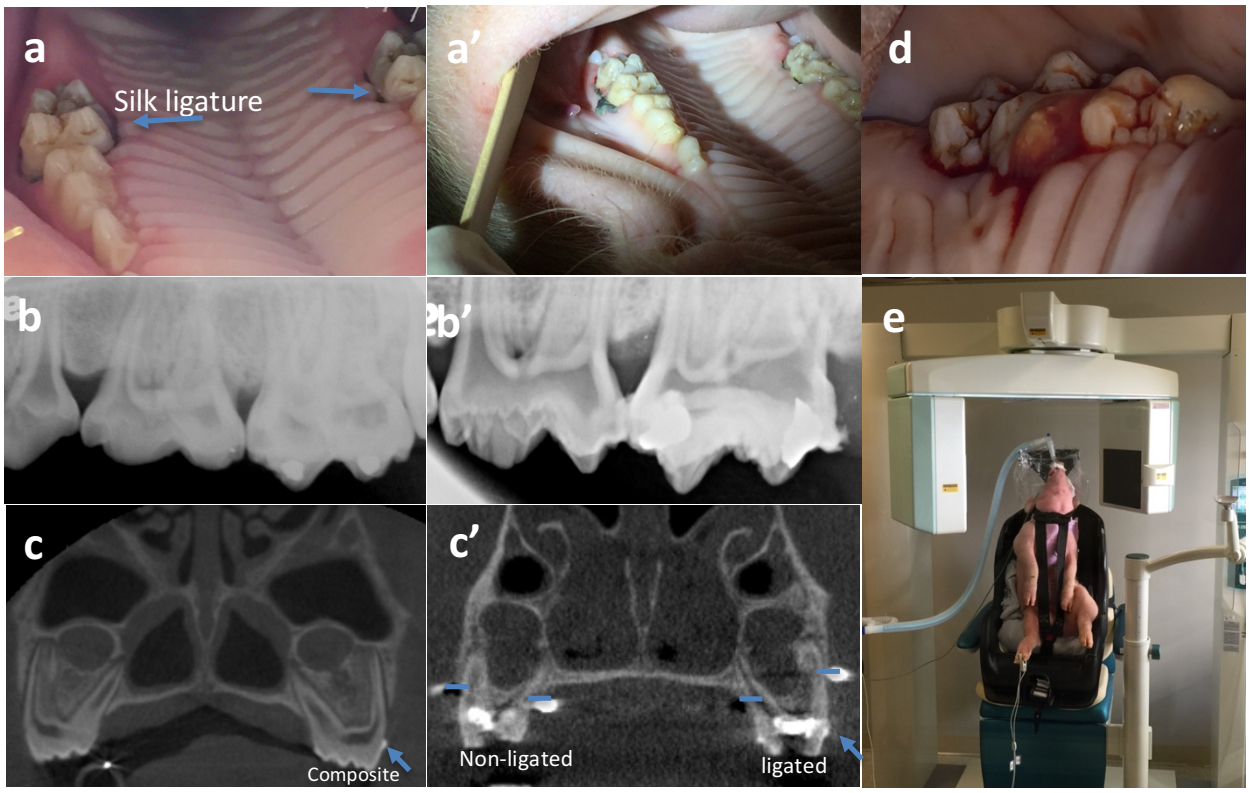

Figure 2-2: Experimental periodontitis method.

LEGEND FOR FIGURE 2-2: Experimental periodontitis method. a: shows bilateral placement of the silk ligature at baseline. The blue arrows are pointing to the silk ligatures wrapped around the last maxillary deciduous molar (Dm3). a': shows the accumulation of plaque and inflammation around the ligated teeth 6 weeks after placement of the ligatures. b: shows the baseline PA x-ray. The white dots on the Dm3 are the radiopaque amalgam markers. b': PA x-ray at 6 weeks showing vertical bone loss around the Dm3. c: baseline CBCT image. The blue arrow is pointing to the composite marker at the level of the CEJ. c': CBCT image at 8 weeks post ligation of the right Dm3. The blue arrows mark the composite marker. The round radiopaque dots are the ultrasound crystals to be discussed in chapter 3. Notice the significant reduction of buccal and palatal alveolar bone on the ligated Dm3 compare to the non-ligated side (blue horizontal lines). d: 8 weeks post ligation, showing extent of bleeding on probing and pus

exudate discharge from the mesio-palatal pocket, where the ligature knot was placed subgingivally. e: positioning of the pig in the CBCT machine, secured in a car seat, and under isoflurane general anesthesia.

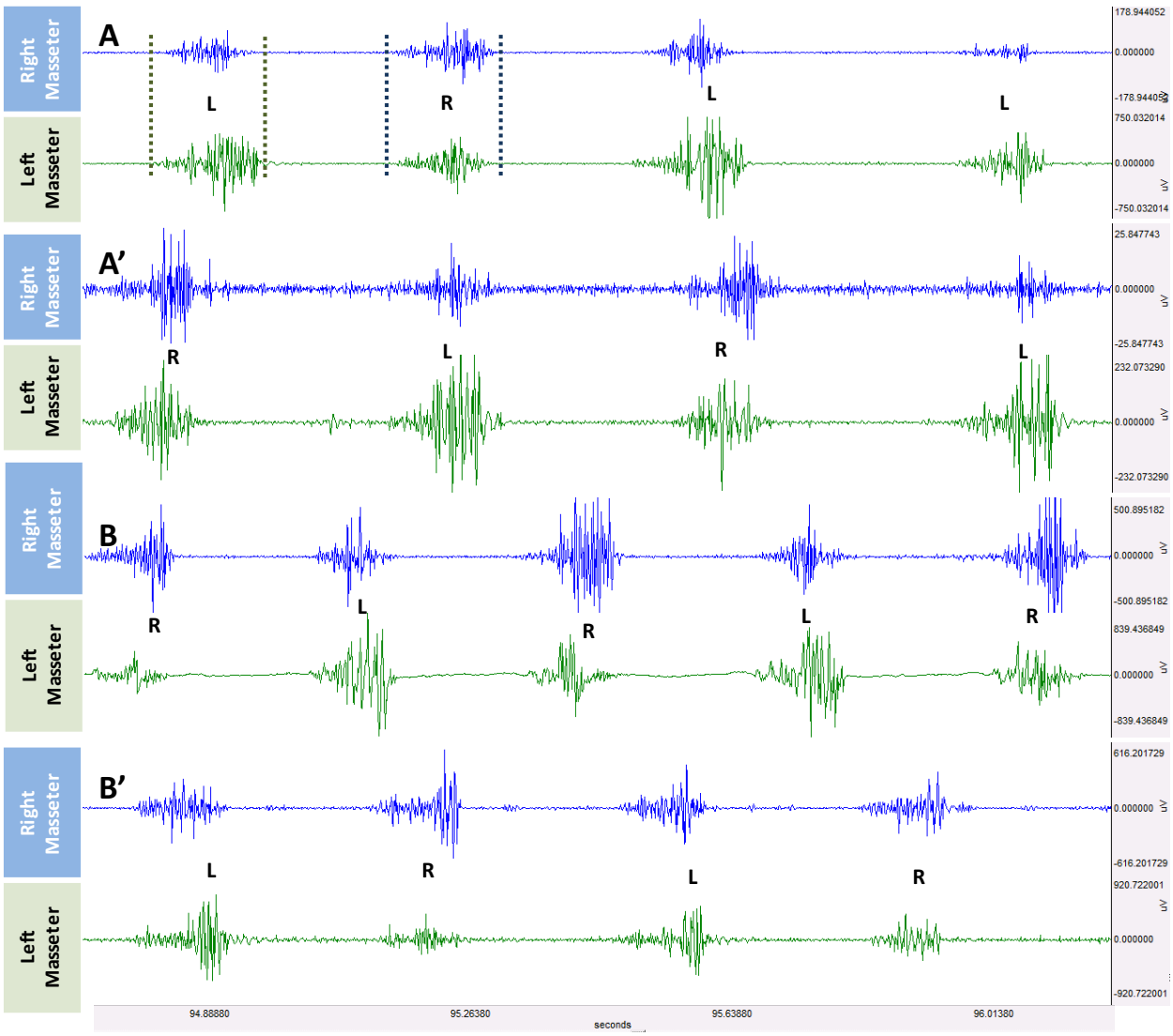

Figure 2-3: Pig muscle activity during mastication.

Legend for Figure 2-3: Alternating chewing side pattern is shown in 2 example pairs of EMG recordings during mastication. A: Baseline EMG recording after placement of ligatures bilaterally on pig#15 at week 1. A': EMG of the same pig after 8 weeks on the terminal day. B: Baseline EMG recording after placement of unilateral ligature around the left side Dm3 on pig#19 at week 1. B': EMG recording of the same pig after 8 weeks of left Dm3 ligation on terminal day. Although only the left tooth was ligated, chewing side continues to alternate between right and left sides.

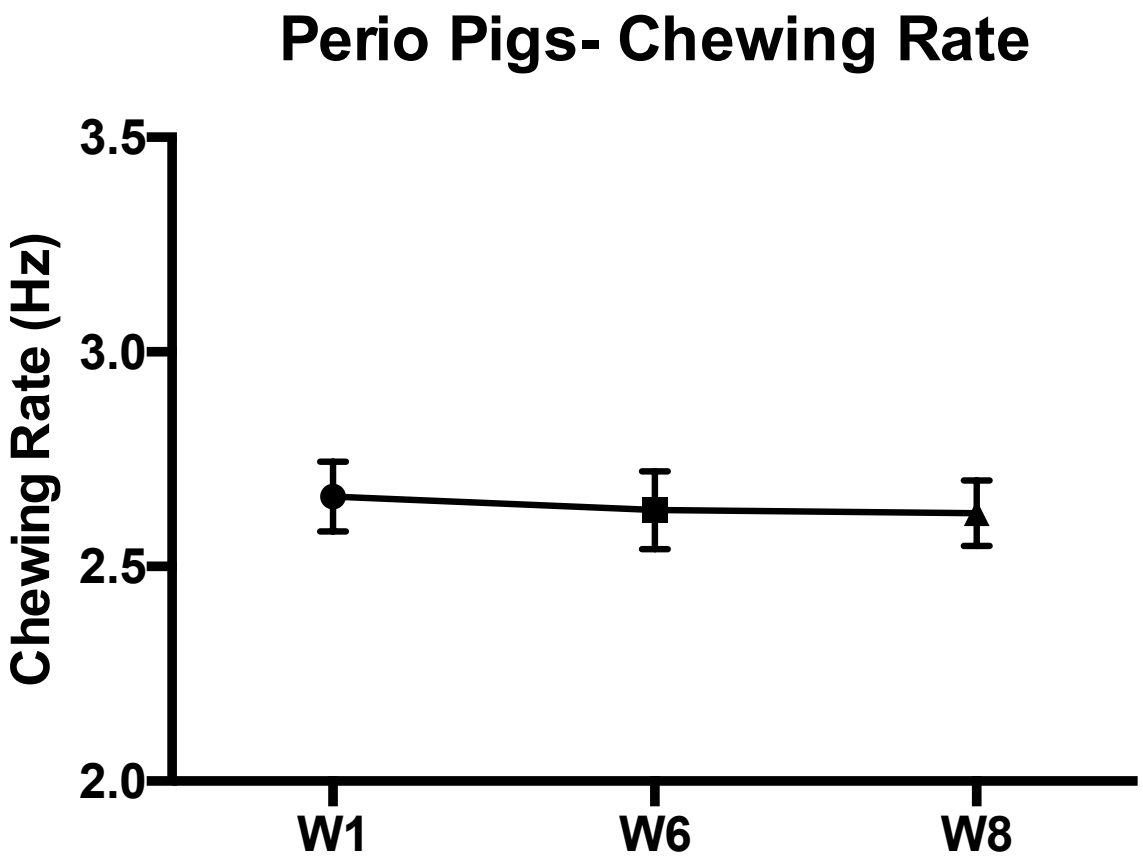

Figure 2-4: Chewing rate of pigs.

Legend for Figure 2-4: Chewing rate did not change during the the course of periodontal disease progression in young pigs. Raw data is presented in Table 2-3. N=7, error bars represent the standard error of the mean.

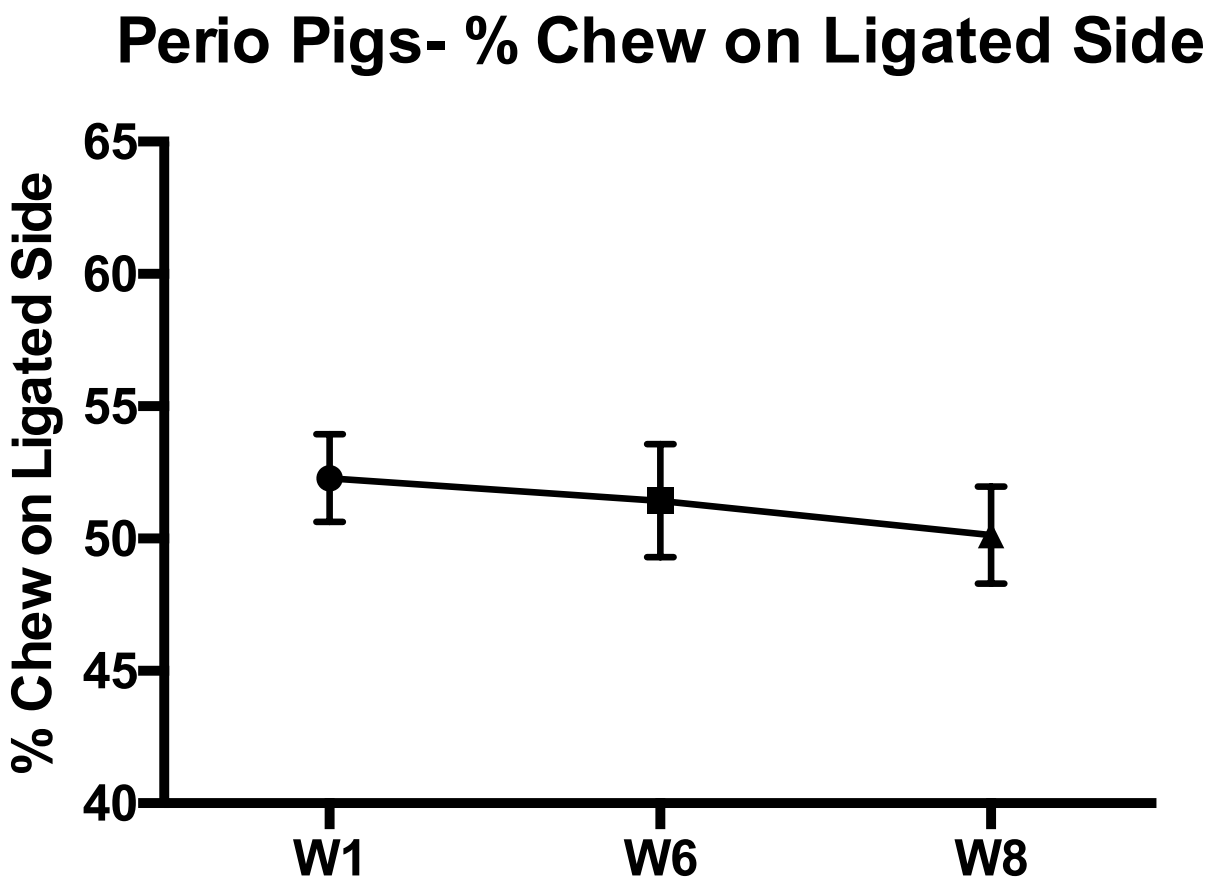

Figure 2-5: Frequency of chews on the ligated tooth (%).

Figure 2-5 legend: placement of ligatures did not seem to affect the frequency of chewing on the ligated *vs.* non-ligated sides significantly and pigs appeared to chew relatively equally on both the right and left side. Raw data is presented in Table 2-4. N=7, error bars represent the standard error of the mean.

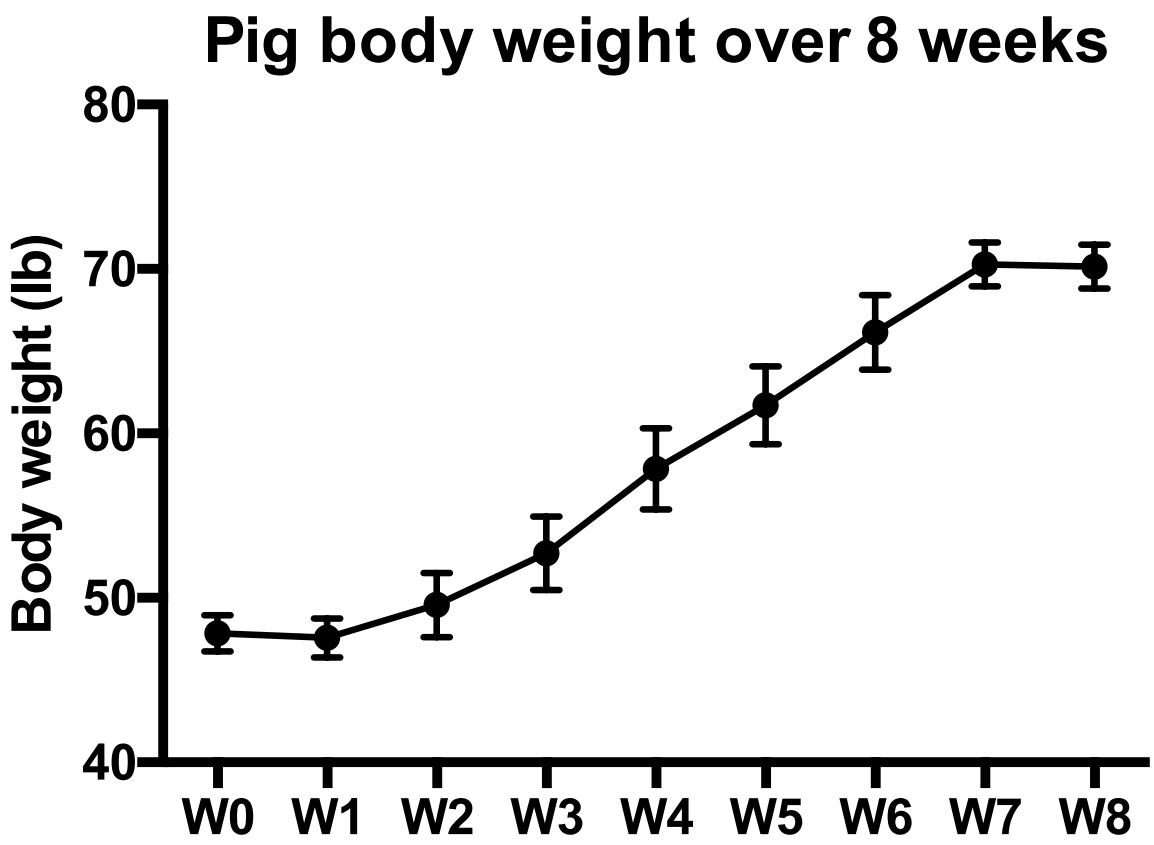

Figure 2-6: Weight gain in experimental Periodontitis Pigs.

Figure 2-6 legend: Body weight gain of pigs during the 8 weeks of experimental periodontitis (n=7). The pigs had a steady weight gain throughout the experiment, which suggests that the ligated teeth did not interfere with their chewing ability. Error bars represent the standard error of the mean in the sample.

Figure 2-7: Neutrophil detection in positive controls from spleen and lung.

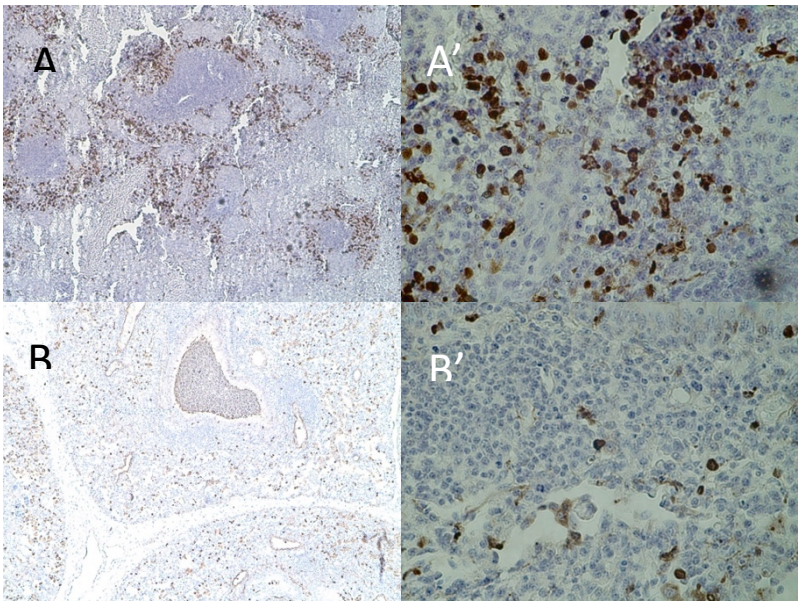

Legend for Figure 2-7: Neutrophil detection in positive controls from young pig tissues. A: 10X magnification of healthy young pig spleen tissue. Brown stained cells shown are neutrophils. A': 60X magnification of spleen tissue shown in A. B: 10X magnification of healthy young pig lung tissue. Brown stained cells shown are neutrophils. B': 60X magnification of lung tissue shown in B.

Figure 2-8: Neutrophil detection in periodontally healthy and diseased pigs.

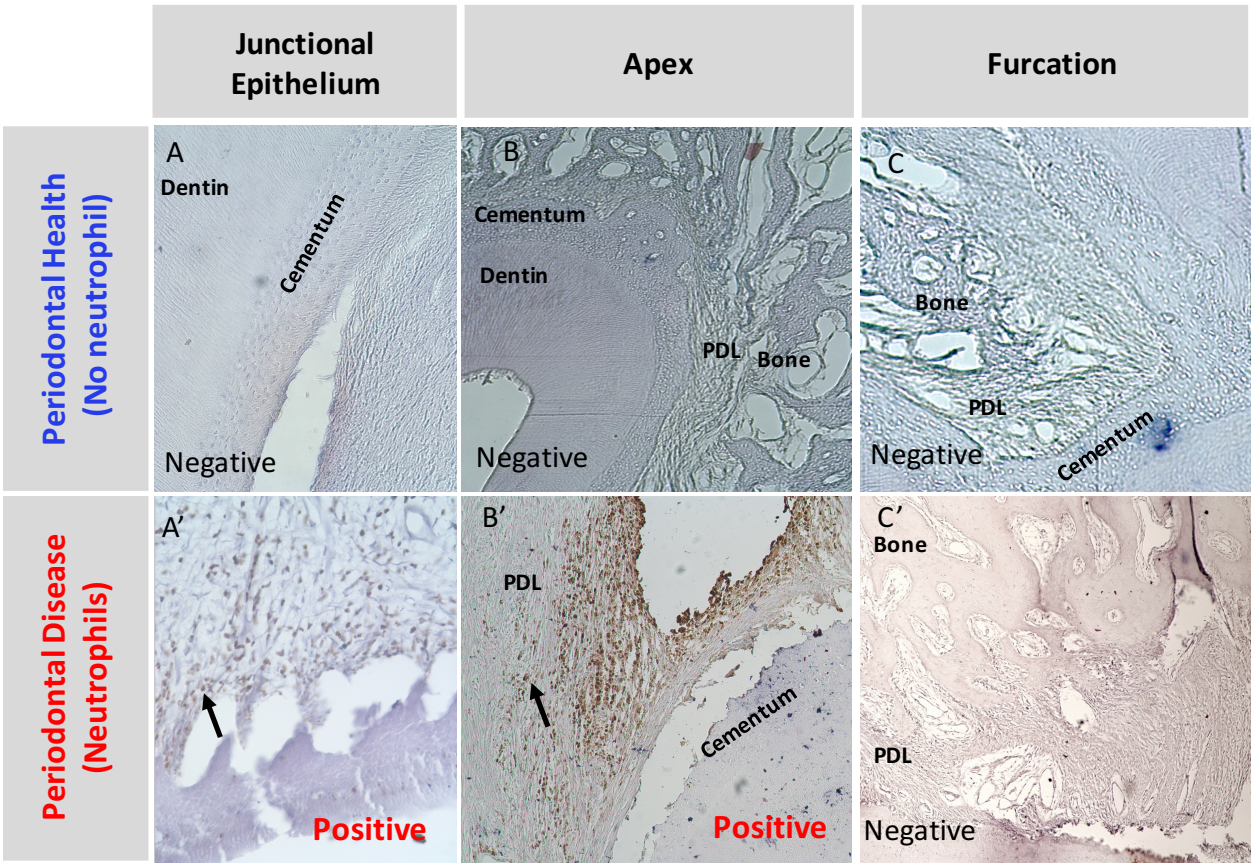

Legend for Figure 2-8: Neutrophil detection in young pig tissues. A: negative neutrophil detection in the junctional epithelium from healthy pigs. A': positive detection of neutrophils in the junctional epithelium of periodontally diseased pigs. Brown stained cells shown are neutrophils. B: 10X magnification of Dm3 root apex of a periodontally healthy pig. Again, the section is negative for the antibody. B': positive detection of neutrophils in the apex of the Dm3 from a periodontally diseased pig (pig#13). C: negative neutrophil detection in the furcation region of healthy Dm3. C': negative neutrophil detection in the furcation region of periodontally diseased Dm3.

2.8 TABLES

Table 2-1: Periodontal measurements for pilot pigs.

Animal	Treatment	Buccal PPD	Palatal PPD	MMI	BoP
Pig 12- R	Control	2,1,2	2,2,2	Non visible	Firm pink gums
Pig 12- L	Ligature (Lig)	4,4,3	4,4,6	Non visible	Slight bleeding
Pig 13- R	**Lig+Pg,Sg,Aa,Fn**	**6,11,7**	**6,11,9**	**<1mm**	**Very inflamed**
Pig13- L	Lig+Pg	7,4,6	6,4,6	<1mm	Inflamed

TABLE 2-1 LEGEND: Measurements of probing depths, MMI, and BI for the pilot pigs at 8th week end-point.

Table 2-2: Periodontal measurements for experimental periodontitis pigs.

TABLE 2-2 LEGEND: Summary of data on the experimental periodontal disease pig model. BoP: Bleeding on probing. PI: Plaque index.

Reading	Pig#	Lig side	BoP	PI	Periodontal probing depth (mm) [Range of 6 measurements per tooth]			CBCT analysis-Bone Loss (mm)		
					Dm2 - Ligated Side	**Dm3 - Ligated Side**	Dm3 - Non-ligated Side	Dm2-Lig	**Dm3-Lig**	Dm3-Non-lig
Baseline	**Pig 13 (Pilot)**	R	_	+	2-4	**3-4**	3-4	1-1.5	**4.0-5.9**	2.41-4.36
4 weeks			+	+	2-5	**3-6**	4-5			
8 weeks			+++	+++	1-4	**6-11**	4-7			
Baseline	**Pig 14**	R	_	+	1-3	**1-3**	-	0.1-0.6	**3.6-3.7**	-
4 weeks			++	+	2-4	**2-5**	-			
8 weeks			+++	+++	1-3	**4-6**	-			
Baseline	**Pig 14**	L	_	+	1-2	**2-3**	-	0.3-0.9	**3.8-5.9**	-
4 weeks			++	+	2-3	**3-5**	-			
8 weeks			+++	+++	1-5	**4-7**	-			
Baseline	**Pig 15**	L	_	+	1-3	**2-3**	-	0.5-1.5	**4.0-4.1**	-
4 weeks			++	++	1-3	**3-6**	-			
8 weeks			+++	+++	1-4	**4-6**	-			
Baseline	**Pig 15**	R	_	+	1-3	**2-3**	-	0.1-0.2	**3.5-6.3**	-
4 weeks			++	++	2-4	**3-5**	-			
8 weeks			+++	+++	1-4	**4-6**	-			
Baseline	**Pig 16**	L	_	+	1-3	**1-3**	2-3	0.9-1.0	**4.6-4.7**	0.9-1.0
4 weeks			++	+	1-4	**4-5**	1-3			
8 weeks			+++	+++	1-3	**4-6**	1-3			
Baseline	**Pig 17**	R	_	+	1-3	**2-4**	2-3	0.4-0.9	**3.4-3.6**	0.1-1.0
4 weeks			++	+	1-6	**3-12**	2-3			
8 weeks			+++	+++	1-6	**5-9**	2-3			
Baseline	**Pig 18**	R	_	+	1-3	**1-2**	1-2	0-0.1	**3.4-5.6**	0.3-1.1
4 weeks			++	++	1-4	**4-9**	2-3			
8 weeks			+++	+++	1-4	**4-6**	2-3			
Baseline	**Pig 19**	L	_	+	1-3	**2-3**	1-2	0.4-1.0	**2.7-3.2**	0.2-1.3
4 weeks			+	+	2-5	**5-7**	2-3			
8 weeks			+++	+++	1-5	**5-6**	2-4			

Table 2-3: Chewing rate of pigs (Hz).

Pig #	Week 1	Week 6	Week 8
13	3.00	2.64	2.71
14	2.59	2.82	2.60
15	2.60	2.83	3.00
16	2.71	2.50	2.63
17	2.55	2.67	2.37
18	2.34	2.80	2.60
19	2.85	2.16	2.46
average	***2.66***	***2.63***	***2.62***
stdev	***0.21***	***0.24***	***0.20***

Table 2-3 Legend: Each data point is the mean of 3 repeated measurements that were selected randomly and had different durations ranging from 5-40 seconds. Week 1 represents the chewing rate of pigs at baseline before placement of any ligatures. Week 6 represents the final EMG recording prior to implantation surgery for placement of SONO crystals (Chapter 3). Week 8 represents the final EMG recording after invasive surgery for implantation of the crystal. As shown, the placement of ligatures does not seem to affect the chewing rate from baseline to week 6 and even to week 8 after recovering from implantation surgery.

Table 2-4: Frequency of mastication on the ligated Dm3.

Pig #	Week 1			Week 6		Week 8	
	second	R	L	R	L	R	L
13	10 sec	20	15	10	12	13	14
14	10 sec	9	11	15	17	14	18
15	10 sec	13	14	16	17	14	18
16	10 sec	9	10	11	14	11	9
17	10 sec	12	12	13	15	14	13
18	10 sec	11	8	9	6	14	11
19	10 sec	17	18	11	13	7	7
average		***13***	***13***	***12***	***13***	***12***	***13***
stdev		***4.1***	***3.4***	***2.6***	***3.8***	***2.6***	***4.2***
%		***51***	***49***	***47***	***53***	***49***	***51***

Table 2-4 legend: Number of chews on right and left side was counted for each pig in a randomly chosen 10 second window of chewing EMG. Red numbers indicate the ligated tooth. Week 1 represents the baseline measurement before placement of any ligatures. Week 6 represents the final measurement prior to implantation surgery for placement of SONO crystals (Chapter 3). Week 8 represents the measurements from the final EMG recording after invasive surgery for implantation of the crystal. As shown, the placement of ligatures does not seem to have an effect on what side the pigs prefer to chew. The frequency of right and left side chews is relatively evenly distributed.

CHAPTER 3

Functional Tooth Mobility During Periodontal Health and Disease in Young Pigs

Specific Aim: **Determine range of movement of the mesiobuccal root of the last maxillary deciduous molar (Dm3) during mastication and masticatory muscle stimulation in periodontally healthy and experimental periodontitis pigs.**

Expectation: I expected that owing to the buccal-to-palatal excursion of the lower molars across the upper molars during chewing, and the apical pressure during power stroke of mastication [268], the teeth would displace three dimensionally with the coronal part of the tooth moving in the buccal to palatal and apical directions. Furthermore, I expected the tooth mobility to be increased in the experimental periodontitis Dm3, relative to the healthy control Dm3.

Strategies: Ultrasound crystals were used to measure the magnitude and direction of movement during natural chewing and stimulation of masticatory muscles, particularly the masseter.

3.1 INTRODUCTION

Understanding the movement of the teeth under various conditions has been a topic of interest for more than a century [1]. As reviewed in chapter 1, under occlusal forces, teeth move within their sockets. It was also reviewed that various aspects of the periodontium, such as the

height and health of the gingiva and alveolar bone, arrangement of the PDL fibers, and the fluid content of the periodontium regulate and limit the displacement of the tooth within its bony socket [24], [25], [78]. It was reviewed that periodontal inflammation and occlusal trauma are among the factors that increase tooth mobility [75], [93], and that increased tooth mobility is thought to be associated with increased periodontal breakdown [5]. Furthermore, various methods and technologies that have been used to quantify and characterize the movement of the tooth under *in vivo* and *in vitro* conditions during physiologic and orthodontic forces were reviewed [4], [6], [15], [75], [93], [104]–[108], [110].

Most of the existing studies focused on incisors and looked at the movement of these single rooted teeth in response to external forces that are supposed to mimic functional loads [4], [22], [105], [108]. However, it is important to acknowledge that although the mobility of incisors sheds some light on the range of tooth movement during mastication, these single rooted teeth are mainly involved in incising the food, and rarely do they undergo the forces of mastication or clenching, which can get quite high. Therefore, their pattern of tooth movement could be very different than molariform teeth, which are often exposed to high masticatory forces. Furthermore, the complexity of the multiple roots *vs.* single roots, makes the teeth behave differently under occlusal loads. The direction and extent of displacement of molar teeth under functional loads, such as clenching and chewing, and under disuse conditions, are unknown for both periodontal health and disease. To understand the quantity and quality of molar tooth movement under functional loads, the pig is a suitable animal model, because of its similar masticatory pattern to humans [193], [236], [268].

3.1.1 *Sonomicrometric crystals*

In order to investigate the magnitude and pattern of tooth mobility during mastication and masticatory muscle stimulation, 2mm round Sonomicrometic ultrasound crystals (SONO crystals) were utilized. SONO crystals are small piezoelectric transducers that are omnidirectional, meaning they can transmit and receive multiple ultrasonic pulses at the same time. The difference in time from transmission of sound waves from one crystal and their receipt by another is calculated and derived as distance between the two crystals.

3.1.2 *Electromyography (EMG) and muscle stimulation*

The major force produced during power stoke of pig mastication has been shown to come from the masseter muscles [269]–[272]. Although the best way to study physiologic tooth movement is under natural masticatory forces, it is important to note that there are many other variables that could contribute to tooth movement during chewing, such as the moving tongue, the cheeks, and the swallowing process. Therefore, individually stimulating the masticatory muscles, such as masseter, and studying the extent and direction of tooth movement produced in isolation is important.

EMG is a technique in which the electrical potential of a muscle is measured and reported in voltage [273]. Surface EMG records the summed motor unit activity of the musculature underlying the recording electrodes, which are located on the skin. This technique is useful for reading the masticatory activity of the masseter muscles, since they are large and subcutaneous. A recording of the two masseter muscles is sufficient for identifying the side of chewing in pigs, which often is fast, reaching 3 cycles/sec [268].

The objective of this Chapter is to provide new information on how much mastication and masticatory muscle contraction displace teeth during healthy conditions and under periodontal disease inflammation. In the next chapter these displacements will be related to the physical space of periodontal ligament (PDL). Pigs have similar mastication pattern and dental anatomy to humans [24], [111], [193] and are the most accepted and well-described non-primate model for human craniofacial function and growth [193], [235], [237], [238], [274]. Their multi-rooted posterior teeth are generally similar to those of humans [236], [239] except that they can have up to six roots and a much more complex root morphology than humans [193]. Although *ex vivo* studies have been performed [226], [248] the present study is the first to examine *in vivo* tooth mobility of pig molars during function.

3.2 Materials and Methods

3.2.1 *Animals*

Nineteen three-month-old female farm pigs (Progressive Farm, Quincy, WA, USA) with baseline body weights ranging from 20-23 kg were used for this study. Twelve pigs were used shortly after arrival as periodontally healthy controls, and seven pigs were kept for an additional two months as they developed ligature induced experimental periodontitis. These pigs constituted the sample studied in Chapter 2, where rationale and methods are described. The experimental protocol was approved by the Institutional Animal Care and Use Committee (IACUC) of the University of Washington. For acclimatization, the pigs were fed five times per week in the laboratory environment. Animals were given a standard pelleted pig chow diet and water ad libitum. Prior to each procedure they were deprived of food for 12 hours [271], [275].

3.2.2 *Baseline recordings of EMG*

Surface electromyography, sEMG, was performed to evaluate muscle motor function at baseline three days after animals had arrived. After 12-hour food deprivation, the pigs were fed in the laboratory. While the pigs ate, the skin overlying the bilateral masseter muscles was shaved and cleaned with alcohol wipes. A pair of sEMG electrodes were placed on the skin overlying each muscle aligned with fiber direction, and connected to leads which were then linked to AC amplifiers (MEC 100, BioPac Inc., Camino Goleta, CA, USA). EMG signals were recorded at a sampling frequency of 1000 Hz on a computer running AcKnowledge (Ver. 3.9, BioPac Inc. CA, USA) for 10-20 min. The electrodes were then removed gently and the animals were taken back to their pen.

The same procedure was carried out for the ligature-induced periodontal disease pigs, and additional sEMG recording sessions were performed every other week until the terminal week as described in Chapter 2. These extra sEMG recordings were intended to monitor the chewing ability and comfort level of the pigs to ensure that presence of ligature was not affecting the mastication and food intake. Body weight gain was also monitored (Figure 2-5).

3.2.3 *Cone-beam CT (CBCT) scans*

A baseline CBCT of all the pigs was taken in the first week after the pigs arrived. This was two days before the terminal experiment for the control (periodontally healthy) pigs and served to visualize the morphology of the upper molars for the implantation of the SONO crystals (see 3.2.4). In addition, for the ligature-induced periodontally diseased pigs a post-mortem CBCT was taken after the development of periodontal disease and the final measures of

the tooth mobility. This second CBCT served to show the location of the SONO crystals in the tooth and on the alveolar bone.

The anesthetized pigs were situated in the CBCT chair using a commercial car seat, and were secured to the seat using custom made belts (Figure 3- 1). A Morita Accuitomo 170 CBCT machine (Kyoto, Japan) was used with settings 90 kV, 5.0 mA, and a voxel resolution of 270 μm. i-Dixel software (Morita, Kyoto, Japan) was used to visualize the molar anatomy and to visualize the location of the SONO crystals (discussed in section 3.2.4) inside the tooth and their relation to the crystals attached to the surface of the alveolar bone post-operatively.

3.2.4 *In vivo tooth mobility experiment*

Measurement of mobility was the final *in vivo* procedure and was performed 7 days after arrival of the control pigs and about 8 weeks after arrival of the pigs in the experimental periodontitis group. The pigs were anesthetized (see Chapter 2 for procedures) for crystal placement. By referring to the CBCT 3D images of the target teeth, three ultrasound transducers (2mm diameter SONO crystals, Sonometrics, London, Ontario, Canada) were implanted in and adjacent to the last maxillary deciduous molar, Dm3, the largest and most molariform tooth in these young pigs.

Using a diamond dental bur and high-speed dental hand-piece, the mesial aspect of the pulp chamber was accessed through occlusal preparation. Pulpotomy was performed and a SONO crystal was placed in the pulp chamber of each prepared tooth close to the mesial occlusal pit over the orifice of the mesiobuccal root canal. Ultrasound transmission gel (Aquasonic 100, Parker CE Laboratories, Inc., Fairfield, NJ, USA) was injected around the crystal. The

preparations were obturated using Cavit™ temporary filling material (3M ESPE Dental, St. Paul, MN, USA) to restore normal occlusal contacts of the tooth.

Each side of the Dm3 tooth then received a SONO crystal placed on alveolar bone. First, buccal and palatal mucosal flaps were reflected. The buccal and palatal alveolar ridges were cleaned and dried, and one crystal was bonded to each alveolar ridge surface using commercial super glue. These alveolar crystals were located in line with the pulp chamber crystal, but 2-3 mm apical to it in the control pigs (Figure 3-2). In the experimental periodontitis pigs, the location of the buccal and palatal alveolar bone crystals was further apical due to crestal bone loss, and the amount depended on the extent of periodontal alveolar bone resorption. Ultrasound conducting gel was then injected around these alveolar SONO crystals and the gingival flaps were sutured back using 3-0 black silk-braided sutures (Reli™ Sutures, MYCO Medical, Cary, NC, USA).

To prevent post-operative discomfort, local anesthetic was administered (2% lidocaine with 1:100,000 epinephrine) through trans-mucosal infiltration. An analgesic, ketorolac (1 mg/kg) was administered intramuscularly (IM), 1 hour prior to waking up the animals. Then sEMG electrodes were placed and connected as for baseline recording (See 3.2.2). The SONO crystal leads were sutured onto the adjacent soft tissue (Figure 3-2b) and led out of the oral cavity and sutured to the skin to minimize their damage during mastication. The crystal leads were then connected to the sonomicrometer (TR-USB Series 8, SonoSoft, SonoLabDS3, Version 3.4.60 RC1, Sonometrics Co.) with the following settings: sampling rate: 178 Hz; transmit pulse: 343 ns; inhibit delay (set to less than the shortest anticipated distance of any crystal pair): 4mm, and speed of sound: 4080 m/sec (an adjustment because the signals had to travel through mineralized tissues of bone and tooth).

After these procedures, the anesthetic intubation was removed and the pigs were allowed to regain consciousness. This usually took a few minutes. Pigs were fed their regular pellets while the signals from SONO crystals and sEMG were recorded. The EMG recording served to identify the side of chewing and to relate power stroke of mastication to tooth movement (Figure 3-3). In addition to AcKnowledge recording, signals were monitored on an oscilloscope (Tektronix, TDS224, Beaverton, OR, USA) and recorded digitally using SonoLabDS3 (Version 1.0.0.67, Sonometrics Co.). The outputs of the EMG signals from BioPac system and the crystal signals from Sonometrics system were input into Sonometrics and BioPac systems, respectively. In addition, 4 channels of EMG were input into the Sonometrics digital ultrasound measurement system (TR-USB series 8) in order to synchronize the two systems.

After 15-20-minutes of masticatory recording, pigs were re-anesthetized via isoflurane mask and placed on their chest with the mandible at the rest position. In order to simulate the masseter muscle to simulate masticatory forces, indwelling wire electrodes were inserted through the skin with hypodermic needles [273]. The wire electrodes were constructed from insulated nickel-chromium, 0.05 mm wire, with 1 mm bared tips, and 2 mm separation between paired tips [273], [275]. The bipolar electrodes were placed bilaterally into the lower 1/3 of the superficial masseter muscles through direct skin penetration with 25G needles [276]. The needles were then withdrawn, leaving only the flexible painless wires in the muscle [273]. The electrodes were connected to a stimulator (Astro-Med, Inc., Grass Instrument, Model S48 Grass stimulator, W. Warwick, RI, USA). Muscles were stimulated to serial tetani with 600-ms trains of 5-ms pulses delivered at 50-60 pulses/s. The stimulation voltage was ramped up to produce as large a contraction as possible without spreading to adjacent muscles. The final stimulation voltages were typically 20-30V for unilateral and 40-50V for bilateral stimulations. Each stimulation

voltage was repeated three times at 0.5 trains/s. The settings used were thought to be sufficient to trigger both nerve and muscle action potentials. Stimulation of the masseter of the same side as the instrumented tooth was defined as ipsilateral masseter stimulation. Stimulation of the masseter opposite to the instrumented tooth was defined as contralateral. A bilateral stimulation of both muscles was considered the closest mimic of the forces of occlusion while avoiding motion to the extent possible.

After all recordings were completed, the pigs were euthanized through IV injection of euthasol (pentobarbital sodium and phenytoin sodium) at the dosage of 0.1ml/Kg, along with heparin. Once it was confirmed that the heartbeat had stopped, the thoracic cavity was opened and the pericardium was reflected to expose the heart. A trimmed spinal needle attached to silicon tubing was placed in the apex of the heart through the left ventricle and into the ascending aorta (where a clamp was placed around the needle). The descending aorta was then clamped off and perfusion was started with saline mixed with heparin, and an opening was made into the auricle of the right atrium so that blood and saline going through the head could be drained. About 4 liters of saline was used until the drainage out of the right atrium was clear, followed by about 4 liters of Prefer (Anatech, Ltd., Battle Creek, MI). The head was removed. A block of maxilla containing all posterior teeth was cut from the removed head on each side using an electric saw and stored in the Prefer solution for later μCT scanning (see Chapter 4).

3.2.5 *Analysis of tooth mobility*

Due to the fragility of the crystals and instrumentation and the vigor of pigs only some recordings of tooth mobility and muscle activity were successful. The noise level from the crystals was reduced by adjusting for the speed of sound in mineralized tissues (4080 mm/sec).

When the EMG signals from both masseter muscles were available, the chewing side was determined by looking at the amplitude and timing. The chewing side usually shows higher amplitude and longer lasting activity than the contralateral masseter, whereas the contralateral masseter usually starts its activity slightly earlier than the active masseter [268]. Consecutive chewing cycles, ideally with 5-15 cycles, were selected from SonoVIEW (Version 3.4.60 RC1, Sonometrics Co.). The distance change between baseline and masseter peak for each pair of SONO crystals was measured for each cycle and averaged (Figure 3-3A, P9). In addition to assessing the influence of terminal procedures on masticatory function, the major purpose of synchronized EMG recording was for the identification of the chewing side [275], [277], but unfortunately, EMG failed in a number of cases, so determination of chewing side was not often possible.

For the stimulation recording, the three consecutive tetani that showed the largest distance changes between baseline and tetanic peak were measured for each crystal pair and averaged (Figure 3-3B, P17 left masseter stimulation).

Increasing distances between the pulpal crystal and buccal crystal were scored as movement of the tooth (pulpal crystal) toward the palatal alveolar bone (*i.e*., away from the buccal bone). Decreasing distances between the pulpal crystal and the buccal crystal were scored as a move toward the buccal alveolar bone (*i.e.,* away from the palatal bone). Similarly, increasing distances between the pulpal and palatal crystals were scored as “toward buccal” and decreasing distances as “toward palatal”. However, it should be noted that such changes need not imply that the tooth is moving or tipping buccally or palatally, because extrusion and intrusion could also cause the distance to change in a similar fashion. The existence of extrusive or

intrusive movements could only be evaluated when both buccal and palatal distances were recorded simultaneously, which was usually not the case.

3.2.6 *Statistics*

Data from Sonometrics were analyzed using GraphPad Prism Software (version 6.0g, GraphPad Software, Inc., La Jolla, CA, USA) and Excel (Microsoft Co., Redmond, WA, USA). Descriptive statistics were calculated (means and standard deviations). In order to quantify the extent of tooth mobility, the distance changes were converted to absolute values, and were grouped to either buccal or palatal movement. Two-way ANOVA was performed to determine differences between the healthy and diseased teeth and between natural mastication and masseter stimulation. Results were considered statistically significantly different at $P \leq 0.05$.

3.3 RESULTS

3.2.7 *Tooth mobility during natural mastication*

Instrument failure resulted in collection of functional tooth mobility data from only 6 of the 11 control pigs plus the non-ligated side of the first pilot pig (P12). Data were obtained from all 7 of the experimental periodontitis pigs, although not always from both ligated and non-ligated Dm3s. Even for these "increases", however, not all crystal pairs gave measurable signals simultaneously, which made it impossible to derive tooth movement patterns for many pigs (Tables 3-1 to 3-4).

For the control pigs, the range of magnitude of tooth mobility during mastication was 63-322μm with an overall average of 192 ± 95 μm (Table 3-1, Figure 3-4 A). There was no statistically significant difference for the magnitude of tooth mobility in buccal and palatal directions.

Three teeth from the 7 control pigs had simultaneous buccal and palatal data. In one case with both palatal and buccal data (P9 Right side, Tables 3-1 and 3-3), the pulpal crystal moved both palatally (palatal distance shortened by 84μm) and buccally (buccal distance shortened by 175μm). The fact that both distances were reduced implies intrusion, and the greater reduction on the buccal side implies a simultaneous buccal tipping. The second case of simultaneous data (P7 Left side, Table 3-1) showed a similar intrusive pattern, but with palatal movement, because the distance between the pulpal crystal and the palatal crystal decreased more (310μm) than did the distance between the pulpal and buccal crystal (252μm). These two cases are indicated by the dashed lines in Figure 3-4 A. The third control pig with simultaneous buccal and palatal measurements, (P8 Right side, Table 3-3), showed very slight tipping toward the buccal bone, based on a palatal distance that increased 60μm and a buccal distance that decreased a similar amount (69μm). Of the teeth that had only one working crystal pair, two (P9 Left side, and P12 Left side) showed a decreasing pattern indicating intrusion or buccal tipping, and 3 showed a pattern that could have been either extrusion or tipping (P3 Right side and P10 Left side toward palatal and P4 Right side toward buccal) (Tables 3-3 and 3-5).

The tooth displacement data during mastication from the 7 experimental periodontitis pigs (7 ligated teeth and 5 non-ligated teeth) showed a comparable magnitude of movement ranging from 36-304μm for the ligated Dm3s, with an overall average of 170 ± 85μm, and 96-199μm for the non-ligated Dm3s, and an overall average of 140 ± 39 μm (Table 3-1, Figure 3-4

B). This was not statistically significantly different from the magnitude of movement during mastication in the control pigs. Three ligated teeth (from pigs P15, P17, P18) had data from both crystal pairs (buccal and palatal) on the same side (red in Table 3-1 and dashed lines in Figure 3-4B). These showed simultaneous decreases in the distance between the pulpal crystal and both the buccal and palatal crystals and thus the same pattern of displacement along the vertical axis (intrusive), as observed in two of the control pigs. All three pigs also showed inclination toward the palatal crystal.

3.2.8 *Subjective observations during mastication*

As shown in Chapter 2, although as expected, chewing sides alternate from left to right (Figure 2-5), in all cases where measurements were obtained (n=7 for control pigs, and n=7 for diseased pigs), tooth movements within a sequence were relatively consistent in both magnitude and direction. Thus for the most part, if tipping occurred it was always in the same direction regardless of chewing side (Figure 3-3A, Figure 3-5).

There were, however, 3 exceptions (P8, P13, and P15). In the case of P8 and P13 baseline shifts were seen during the recording. Figure 3-5 A shows an illustration of this for P13, however, note that the directionality of the signals did not change and had little to do with which side the pig was chewing on. Both before and after the baseline changes, the left Dm3 moved toward palatal during each masseter contraction (the distance between left buccal crystals increased) while at the same time the right Dm3 moved toward buccal bone (shortening of the right buccal crystal pair distance). In P15, there was an apparent effect of chewing side on the magnitude of movement (blue and red arrows on Figure 3-5 B) but again directionality of the movement was not affected. Note that P15 was one of the pigs that had no EMG recordings

available on the Sonometrics recording system, but the regular alteration of pattern implies it was caused by chewing side.

3.2.9 *Tooth mobility produced by stimulation of masseter muscles*

Masseter stimulation was performed on anesthetized animals to eliminate the effects of jaw opening and soft tissue movement. Figure 3-3B shows the displacement of the tooth (buccal and palatal crystal pairs) during right masseter muscle stimulation. Of the 12 control pigs, tooth mobility data on masticatory muscle stimulation were obtained from 7. Note that, as mentioned earlier, P12 was one of the pilot study pigs in Chapter 2, and the non-ligated side of it was counted as a control tooth since no signs of disease were apparent. Of the 7 experimental periodontitis pigs, data were obtained from 6. The stimulated masseter muscles were (1) the muscle ipsilateral to the targeted tooth, (2) the muscle on the contralateral side, and (3) bilateral. However, the sample size in each of these categories varied. Table 3-2 summarizes the absolute values of distance changes; the data are found in Table 3-4. The magnitude of tooth movement during masseter stimulation was from 20-302μm during masseter muscle stimulation in healthy controls, which is similar to the range of tooth displacement during mastication (63-322μm), but the overall average was smaller (113 ± 89 μm compared to overall average of 192 ± 95 μm during mastication).

For the experimental periodontitis pigs, the range of tooth displacement during masseter stimulation was 34-545μm in ligated Dm3s (overall average of 116 ± 147 μm). The right buccal crystal pair of P15 had an unusually high value (545μm) during bilateral masseter stimulation, and is an outliner. Without P15 the range of masseter stimulation for ligated teeth was 34-158μm with an overall average of 73 ± 39 μm. The movement of non-ligated teeth under masseter

stimulation ranged from 24-139μm with an overall average of 74 ± 47 μm, which also recalls the mastication results (36-304μm for ligated Dm3s, and 96-199μm for non-ligated Dm3s), but is lower overall. Again, however, there was no statistically significant difference in movement magnitude between the control and experimental periodontitis pigs during masseter muscle stimulation.

Also as for mastication, whenever, data from both buccal and palatal crystal pairs on a given side were available simultaneously, the movement pattern most often (4 teeth) suggested intrusive movement plus a lateral movement toward either buccal or palatal (Tables 3-4 and 3-5). Interestingly, the ligated right Dm3 of P14 moved palatally (in addition to intruding) when the ipsilateral masseter was stimulated, but buccally for bilateral contraction. Two teeth showed tipping only (P9 R to palatal and P8 L to buccal). Surprisingly, one control tooth showed extrusion (P7 R). Whereas control teeth did not seem to have a preferred lateral movement, most ligated teeth appeared to move buccally during masseter stimulations (Table 3-5).

In theory, a comparison of ipsilateral and contralateral masseter stimulation could show whether direction of mandibular movement determined the direction of lateral tooth movement. The ipsilateral masseter causes the mandible to move from buccal to palatal, whereas the contralateral muscle has the opposite effect. Unfortunately, only two teeth had data for both ipsilateral and contralateral stimulations, and they gave different results. P8 R changed direction of movement but P7 R did not (Table 3-4).

3.4 DISCUSSION

The intensity of the forces produced by functional and para-functional muscular loading, although reflected qualitatively on EMG recordings [278], and shown to affect alveolar bone biomechanics and bending [269], [270], [272], [279], [280], have yet to be studied for their effect on magnitude and pattern of molar tooth movement. With the current technological advancements, we attempted to tackle this area of long time interest by implanting piezoelectric ultrasound crystals in and around a tooth to get a better understanding of how molar teeth move under functional loads.

Sonomicrometery has not been used before to capture information on magnitude and direction of tooth movement. This technique is mainly applied in soft solids and liquids (such as muscle and blood), however, here we have shown that this technology can also be used to study the magnitude of movement of teeth during *in vivo* mastication when adjusting for the speed of sound through mineralized tissues.

To the best of our knowledge, this work is the first to shed light on the magnitude and direction of maxillary molar tooth displacement during actual mastication. The choice of pigs was intended to mimic the human condition as closely as possible, and normal animals were compared to those with periodontal disease to provide further clinical relevance.

3.2.10 *Limitations*

Theoretically, with crystals implanted in multiple locations and all distances reported, accurate tooth movements could be tracked in 3D and a map of movement could be created. However, even though theoretically this seems possible, it is not practical, due to the size of the

crystals available and the difficulty of sending ultrasound signals through mineralized tissues. In this study, after several attempts with additional crystal implantations, I assessed functional tooth movement during feeding using only 3 crystals, which at best can only give the pattern of movement in the coronal plane. I assumed that there was very minimal mesial or distal movement, if any, due to the tight proximal contact with the adjacent teeth, and to reduce the noise between crystals, I chose to not assess the movement in these directions.

Even with the simplified methodology, however, there were several technical problems. First, due to the complexities associated with functional *in vivo* tooth displacement measurements in pigs, the sample size from which data were obtained was very small, and even then data were seldom available from all crystal pairs. The incomplete data set hampered my ability to define an exact pattern of tooth movement. Second, it was impossible to implant all the crystals exactly co-linearly during the implantation surgery, and the orientation of the crystals relative to each other could only be learned from the CBCT images that were obtained post-mortem. However, such images were not routinely taken for the control pigs, and sometimes crystals were no longer intact. In 5 of the control pigs, there were no data available due to either breakage of the tooth cusp during mastication and loss of the pulpal crystal, or loss of the palatal or buccal crystals as the pig chewed on the wires. Third, the SONO signals were frequently noisy, even with only 3 crystals per side. This made the interpretation of the data more complex. Fourth, synchronization of masseter EMG and the SONO tooth mobility data often failed because EMG and crystal signals were not working simultaneously. Thus it was impossible at times to distinguish the working and non-working sides. However, because pigs chew alternately [269], [271] on the left and the right side, the 5-15 consecutive chewing cycles

should include roughly equal numbers of cycles from both the working and non-working sides. The final major limitation of the method used in this study is that due to the invasive nature of the crystals, it cannot be used in human vital teeth.

3.2.11 *The pig as a model for tooth mobility*

Despite the anatomical differences that exists between pigs and humans in the number and morphology of roots in maxillary molars [193] the Dm3 is more similar to human teeth than that of the other animal models discussed in Chapter 1, except for the squirrel monkey [185], [188] and was large enough to accommodate the size of the SONO crystals. It was advantageous to use young farm pigs with deciduous molars to investigate functional tooth mobility, because of their relatively greater availability and greater ease of handling compared to other larger animals. Although the pigs were young, the deciduous molars were firmly positioned in the alveolar bone, with completed apices and no evidence of resorption of deciduous roots. Another advantage was to ensure that the healthy control teeth had adequate amount of bone support around them since in pigs, periodontitis naturally occurs as the animals age [170]. However, in humans, with the progression of periodontal disease and significant bone loss, mobility of teeth increases often significantly. Although the increased bone loss associated with the periodontal disease was seen in pigs, there was no significant increase in the movement of the ligated Dm3. The surprising stability of the pig Dm3 may relate to the complexity of the roots, coupled with their varied orientation in the alveolar bone (see Chapter 4). However, this tooth may not be the best model for studying increased tooth mobility during periodontal disease.

3.2.12 *Magnitude of tooth mobility*

The results from this investigation indicate that periodontal disease with up to 6mm of crestal bone loss did not affect tooth mobility in pig Dm3s, perhaps because of the multiplicity and complicated curvatures of the roots. Healthy and diseased pigs showed similar ranges of movement of their Dm3 during both mastication and masticatory muscle stimulation. This thus disagrees with my original hypothesis that the mobility of Dm3 in pigs would be increased during periodontal disease. Tooth mobility may not be dependent on crestal bone height in pigs. Existing *in vivo* data in dog mandibular premolars show that the tooth movement increased from 15-40µm during health to 80-130µm during periodontal disease when using 100-500lbs of force labio-lingually [16]. This perhaps is due to the relatively simpler root morphology in a two-rooted mandibular premolar tooth of a dog (Figure 1-9) and the extensive destruction of the alveolar bone affecting the furcation of roots in this study.

The available data from this chapter showed that the displacement of the Dm3, regardless of whether the periodontium was healthy or inflamed with bone loss, and whether it was exposed to natural forces of mastication or simply masseter muscle stimulation, and regardless of the age of the animals, ranged from 20-545µm or 20-322 if the outlier (P15, bilateral masseter stimulation) is omitted (Tables 3-3, 3-4). This is very similar to the range of movement reported for other animal models, although most are *ex vivo* (Table 1-4). In rat when 10-100 grams of mesial tension was applied, the maxillary molars showed 100-240µm of movement in the direction of mesial tipping and palatal inclination [58]. In monkeys, 50-500 grams of force was placed in the labiolingual direction, and the movement range was reported

as 0-100µm [15]. Picton in 1964, applied 1Kg of force in the buccolingual direction to the human molar and reported 100µm of movement [20]. In a later study the movement of human molar teeth under forces of 1.5 N was reported in the range of 20-400µm [17]. *In vitro* studies using pig mandibular molariform teeth, reported 0-800µm of movement under 0-6 N force [115] and 100-300µm of movement when 0-80N force was used [55]. This similarity of the range of movement in the various animal models could be interpreted as an evidence that no matter how big or small the tooth, the range of tooth movement is conserved among species to some degree and thus studying it in any animal model could be relevant to humans.

3.2.13 *Direction of tooth movement*

From the limited cases in which signals from both the buccal and palatal crystal pairs for the same tooth were available, it appears that the pig's Dm3 moves mainly in the occluso-apical direction with lateral components. Clear extrusion was never observed in this study with the exception of P7 R during stimulation, and even this tooth intruded during natural mastication. This seems logical, since the measured peaks and valleys coincide with the masseter muscle activity that occurs during power stroke of mastication when teeth are expected to intrude [268], [275], [277]. In his *in vivo* studies Picton also reported a vertical mobility of the teeth that occurred in 2 phases [281]. A primary intrusive movement would also explain why there was no apparent difference between working side chews (when palatal tipping was expected) or balancing side chews (when buccal tipping might have occurred). Mastication in pigs involves opening, closing, and transverse (buccal to palatal movement on the working side and if there is balancing side contact, tooth movement would be palatal to buccal) movements of the lower teeth against the upper teeth [268]. At least one tooth showed tipping without intrusion (P8 on

the right side). The closing muscles involved in the power stroke or bite force, masseter and medial pterygoid [276], not only have the primary influence on the intrusive movement of the molar but also are involved in transverse excursion of the jaw, and therefore encourage the buccal and palatal movement of the molar as well. Most of the displacements observed did involve such movements, lending a three dimensional complexity to tooth mobility. However, the expected directionality of buccal and palatal movement was not observed. Teeth generally moved in only one direction, either buccal or palatal, regardless of chewing side or muscle stimulated. One possible explanation is that the exact location of each of the buccal and palatal alveolar crystals varied in relation to the pulpal crystal. It is also possible that animals had individual differences in the way their teeth occluded or in their chewing movements.

3.2.14 *Proposed model of Dm3 movement under loading*

Tooth movement studies in rats have shown that under *ex vivo* conditions the mandibular molar has a 3D movement when under loading and often shows a see-saw pattern of movement [226], [122]. Assuming a similar pattern of movement for pigs, the tooth must have a complex 3D displacement pattern and interaction within its PDL space, and based on the available evidence I am suggesting that this movement for pig Dm3 is a combination of intrusive and lateral movements. My proposed movement for the pig Dm3 starts with apical movement, and continues in the buccal or palatal direction. Future studies are needed to verify and refine this model and clarify the displacement in the mesio-distal direction, which was not considered in my study and might have been responsible for the apparent extrusion of P7 R during master stimulation. Additionally, for future studies the use of the pig mandibular molar might prove to

be both easier and more applicable to what might be happening in humans, due to higher similarity between the mandibular molars of pigs and humans.

3.5 CONCLUSIONS

In summary, using SONO crystals to capture the pattern and range of displacement of the last maxillary deciduous molar (Dm3) of the pig during mastication and masseter muscle stimulation appears to be feasible. The Dm3 showed a combination of intrusion (occluso-apical) and buccal or palatal (lateral) displacements during mastication. The magnitude and pattern of displacement were similar regardless of the side of chewing and under both periodontal health and periodontal disease states.

3.6 FIGURES

Figure 3-1: CBCT imaging of live pig head.

Figure 3-1 legend: CBCT in vivo imaging of the pig head. The scanning took approximately 9 seconds with 1 min of image reconstruction. Pigs were maintained under 3% isofluorane general anesthesia via intubation and vital signs were monitored by on-site veterinarians.

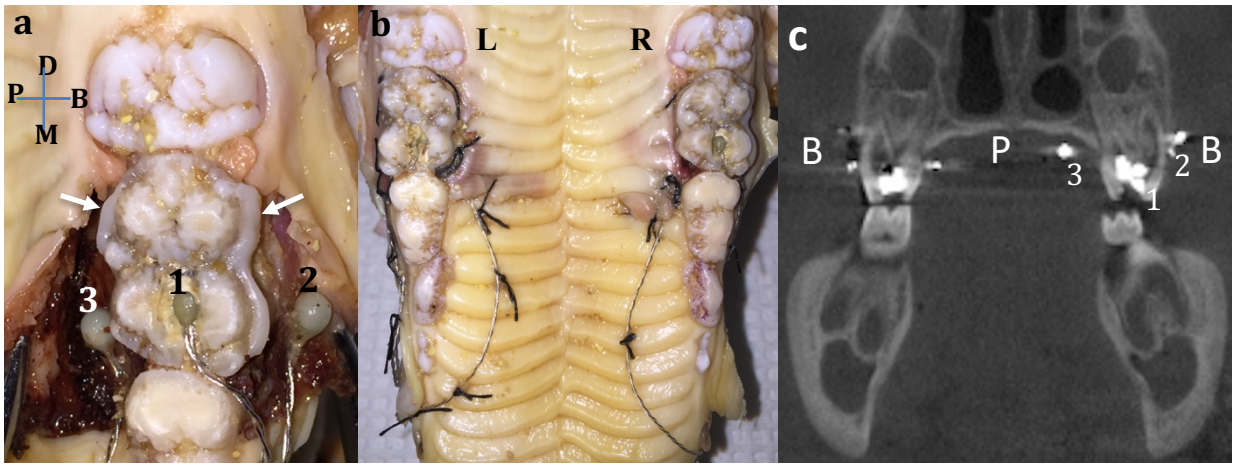

Figure 3-2: SONO crystal placement around Dm3.

Figure 3-2 legend: Illustration of SONO crystal placement on the pig's maxillary last deciduous molar (Dm3). (a) Placement of crystals: crystal 1 is intradental, over the mesiobuccal root canal, crystal 2 is on the buccal alveolar bone, and crystal 3 on the palatal alveolar bone. White arrows point to the location of the buccal and palatal composite overhangs. (b) Crystals were placed bilaterally and the wires led out of the mouth away from the teeth, (c) CBCT image confirming the location of the crystals post-mortem. Note bone crystals are slightly apical relative to pulp chamber crystal 1. B: buccal, P: palatal, D: distal, M: mesial, R: right, L: left.

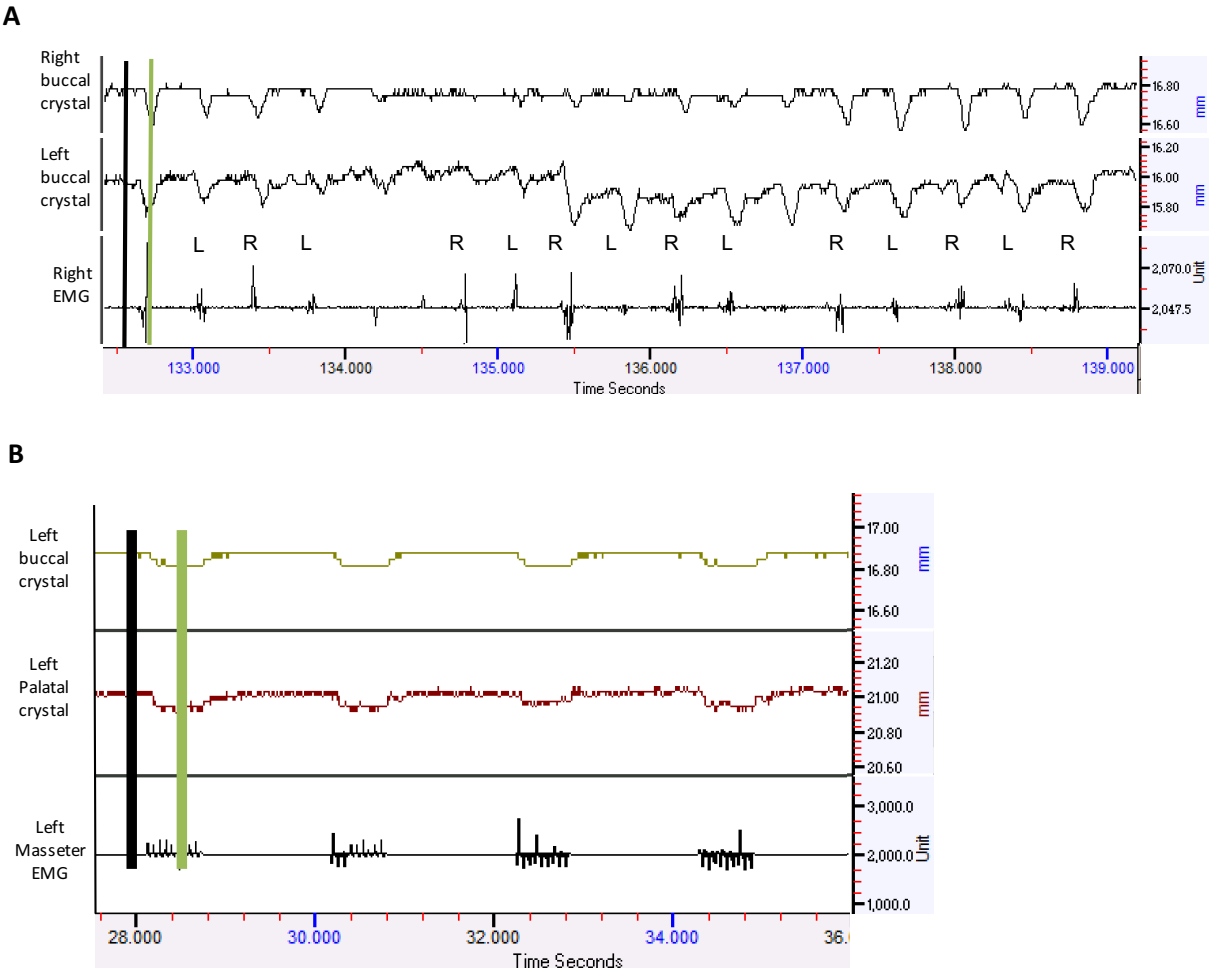

Figure 3-3:Example SONO recording of mastication and masseter stimulation.

Figure 3-3 legend: Example of tooth displacement recordings in SONO. (A) Sonometric recording of mastication for 6 seconds. The upper traces show the changing distances (mm) between the MB pulp chamber crystal and the buccal alveolar bone crystal on the right side and left side. The third trace is EMG activity in the right masseter and the alternating side of chewing (L, R) deduced from that activity. Alternate side chewing is normal for pigs [268]. Black line: baseline measurement (no muscle activity), Green line: peak measurement (Right masseter

muscle contraction). Note that both teeth show shortening of the distance to the buccal bone of about 0.2mm during each cycle. A: Distance change between left molar crystal and buccal and palatal crystals of P9. B: Tetanic left masseter stimulation (P17). Vertical lines show where baseline (black line) and tetanus (green line) distances were measured. Note that in the example the distance of the tooth from both buccal and palatal crystals decreases by about 0.2 mm during each tetanus.

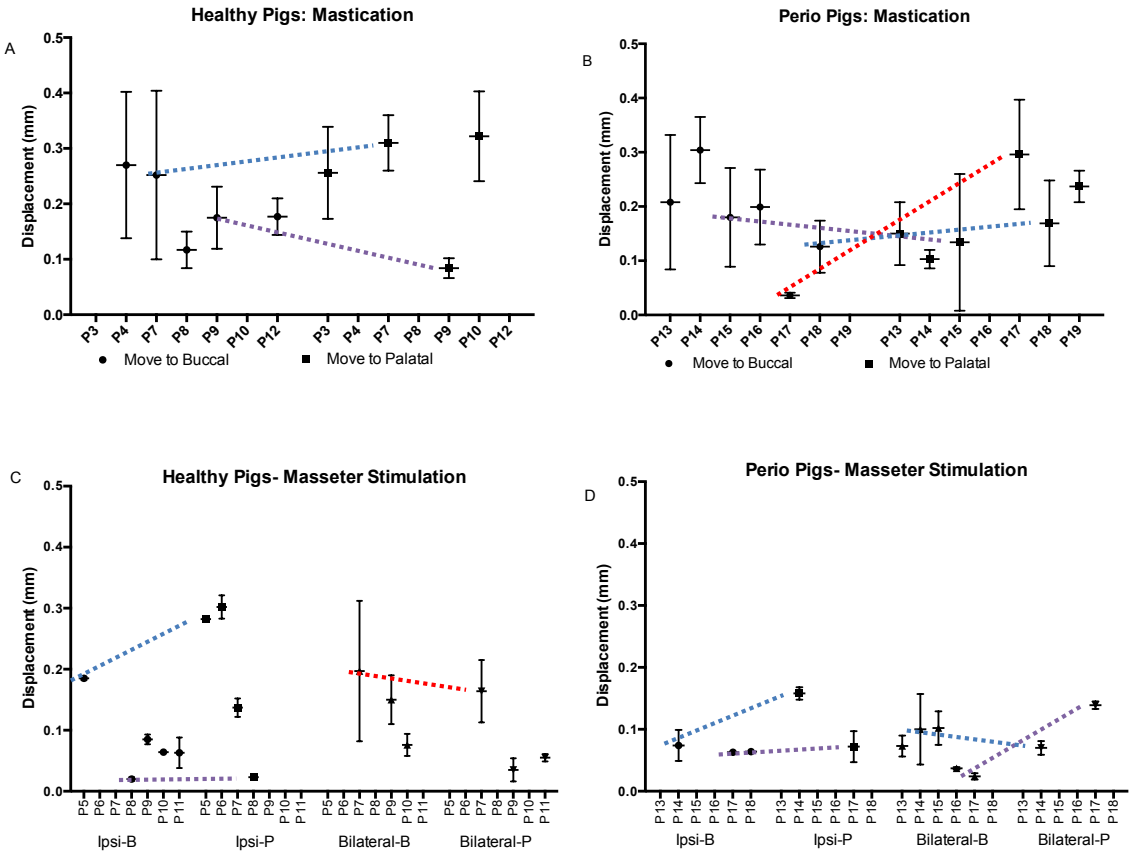

Figure 3-4: Graphic illustration of mastication and masseter stimulation data for healthy and diseased pigs.

Figure 3-4 legend: Graphic illustration of data presented in Table 3-1 and Table 3-2. Dotted lines connect the data from the same side buccal and palatal crystal pairs. Error bars represent the standard error of the mean. For each pig 5-15 masticatory cycles were measured.

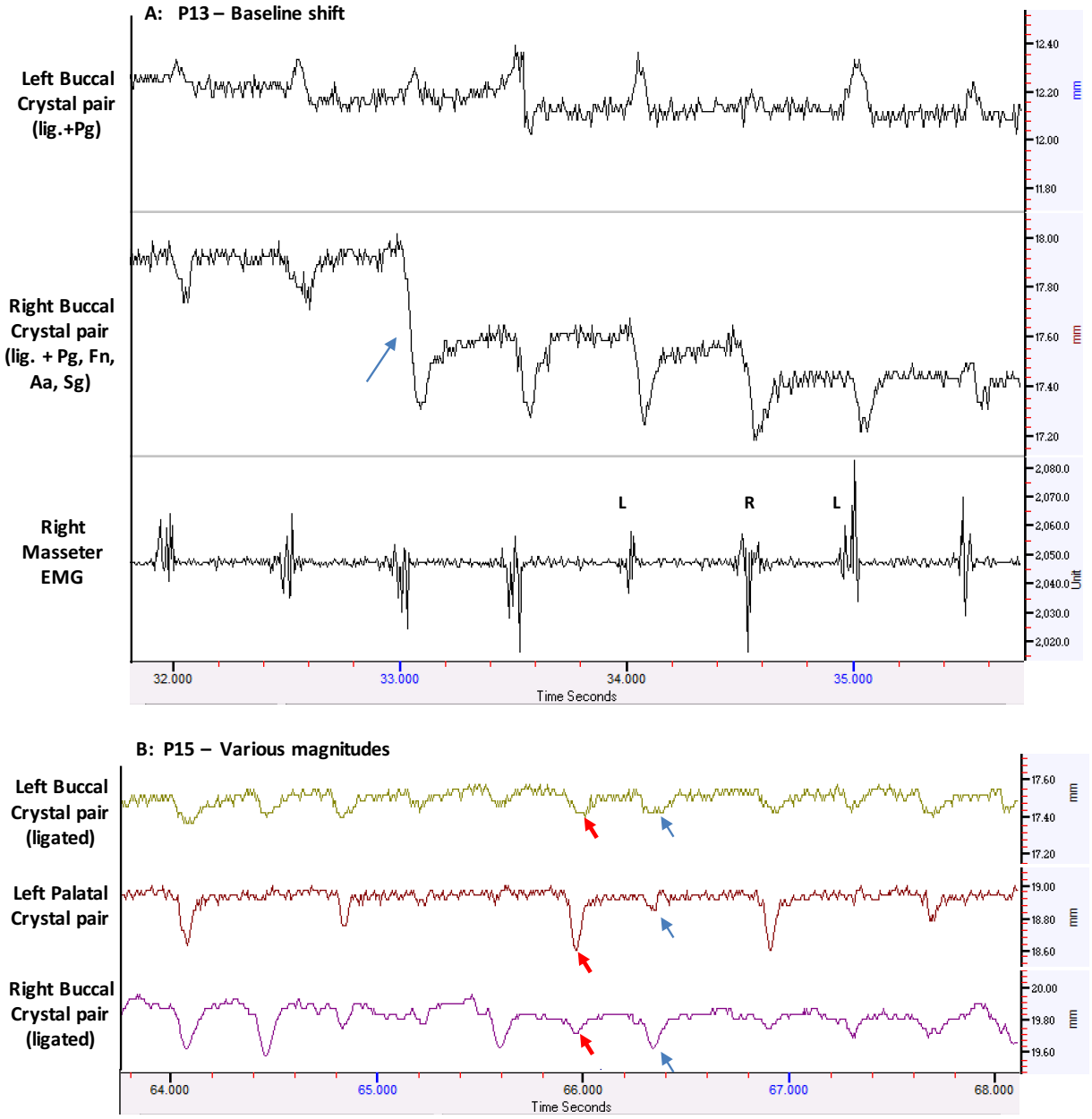

Figure 3-5: Examples of unusual patterns in SONO recordings during mastication.

Figure 3-5 legend: Among the unusual patterns seen in SONO recordings during mastication were A: baseline shift shown by blue arrow (P13), and B: various magnitudes that seemed to correspond to the side of chewing, although EMG signals were not available (P15).

3.7 TABLES

Table 3-1: Masticatory tooth movement in healthy control and periodontally diseased pigs.

Table 3-1 legend: Data are reported as mean (SD) of the movement of the pulpal crystal (μm) obtained from 5-15 consecutive masticatory cycles. When data were not available (-) is placed. P7, P9 (control) and P15, P17, and P18 (diseased) had simultaneous data from same side buccal and palatal crystal pairs and are highlighted in ***red***. The **bold** numbers indicate the data from the ligated Dm3s. * indicates the data from the Dm3 of a pilot pig that was ligated with only *Pg* (refer to Chapter 2 for more details).

Masseter Stim. and SONO Crystal Side		Pulpal Crystal Move Toward	P5	P6	P7	P8	P9	P10	P11
Periodontal Health (Control)	Ipsilateral	Buccal	***185 (3)***	-	-	***20 (3)***	85 (8)	64 (0)	63 (25)
		Palatal	***282 (2)***	302 (19)	137 (15)	243 (29) ***23 (3)***	-	-	-
	Contralateral	Buccal	-	-	-	35 (2)	-	-	-
		Palatal	-	-	77 (30)	-	-	-	-
	Bilateral	Buccal	-	-	***197 (115)*** 153 (52)	-	32 (0)	76 (18)	-
		Palatal	-	-	***164 (51)***	-	35 (19)	-	55 (6) 33 (1)
Masseter Stim. and SONO Crystal Side		**Pulpal Crystal Move Toward**	**P13**	**P14**	**P15**	**P16**	**P17**	**P18**	**P19**
Periodontal Disease	Ipsilateral	Buccal	-	***74 (25)***	-	-	***63 (1)***	**64 (0)**	-
		Palatal	-	***158 (10)***	-	-	***72 (25)***	-	-
	Contralateral	Buccal	-	-	-	-	-	-	-
		Palatal	-	-	-	-	-	-	-
	Bilateral	Buccal	**73 (17)**	***100 (57)***	**102 (27)** 545 (363)	37 (2)	***24 (5)*** 23 (10)	-	-
		Palatal	-	***70 (11)*** 34 (4)	-	-	***139 (6)***	-	-

Periodontal Health (Control)	Pulpal Crystal Move Toward	P3	P4	P7		P8		P9		P10		P12			
	Buccal	-	270 (132)	***252*** ***(152)***		***69*** ***(38)***	63 (39)	***175*** ***(56)***	141 (33)	-		177 (33)			
	Palatal	256 (83)	-	***310*** ***(50)***		-		***84*** ***(18)***		322 (81)		-			
Periodontal Disease	Pulpal Crystal Move Toward	P13	P14	P15		P16		P17		P18		P19			
	Buccal	**208** **(124)**	**304** **(61)**	***85*** ***(59)***	180 (91)	199 (69)	96 (43)	***36*** ***(5)***		***126*** ***(48)***		-			
	Palatal	*150 (58)	**103** **(17)**	***134*** ***(126)***		-		***296*** ***(101)***	116 (27)	***169*** ***(79)***	139 (41)	**237** **(29)**			

Table 3-2: Tooth mobility caused by masseter muscle stimulation in periodontally healthy pigs and periodontally diseased pigs.

Table 3-2 legend: Data are reported as mean (SD) of the movement of the pulpal crystal (µm) relative to the buccal and palatal crystals placed on the bone (absolute values). The measurements are obtained from 3 consecutive masseter muscle tetani. Ipsilateral refers to same side masseter stimulation and tooth movement. Contralateral refers to contraction of the masseter opposite to the instrumented tooth. Bilateral refers to right and left masseter co-stimulation and either the left or the right Dm3. When data were not available (-) is placed. The ***red*** numbers, indicate simultaneous data from buccal and palatal crystals placed around the same tooth. The **bold** numbers, indicate the data from the ligated Dm3s.

Masseter Stim. and SONO Crystal Side		Pulpal Crystal Move Toward	P5	P6	P7	P8	P9	P10	P11
Periodontal Health (Control)	Ipsilateral	Buccal	*185 (3)*	-	-	*20 (3)*	85 (8)	64 (0)	63 (25)
		Palatal	*282 (2)*	302 (19)	137 (15)	*243 (29)*	-	-	-
	Contralateral	Buccal	-	-	-	35 (2)	-	-	-
		Palatal	-	-	77 (30)	-	-	-	-
	Bilateral	Buccal	-	-	*197 (115)*	-	32 (0)	76 (18)	-
		Palatal	-	-	*164 (51)*	-	35 (19)	-	55 (6)
Masseter Stim. and SONO Crystal Side		**Pulpal Crystal Move Toward**	**P13**	**P14**	**P15**	**P16**	**P17**	**P18**	**P19**
Periodontal Disease	Ipsilateral	Buccal	-	*74 (25)*	-	-	*63 (1)*	**64 (0)**	-
		Palatal	-	*158 (10)*	-	-	*72 (25)*	-	-
	Contralateral	Buccal	-	-	-	-	-	-	-
		Palatal	-	-	-	-	-	-	-
	Bilateral	Buccal	**73 (17)**	*100 (57)*	**102 (27)**	37 (2)	*24 (5)*	-	-
		Palatal	-	*70 (11)*	-	-	*139 (6)*	-	-

Table 3-3: Mean distance change between the SONO crystal during mastication in health and periodontitis.

Table 3-3 legend: Data are reported as mean (SD), of the movement (µm) of the pulpal crystal relative to the buccal and palatal crystals placed on the bone. When data were not available (-) is placed. * indicates the data from the Dm3 of a pilot pig that was ligated with only *Pg* (refer to Chapter 2 for more details). The **bold** numbers, indicate the data from the ligated Dm3s.

Pig#	Left Buccal Crystal pair	Left Palatal Crystal Pair	Right Buccal Crystal Pair	Right Palatal Crystal Pair
P1	-	-	-	-
P2	-	-	-	-
P3	+256 (83)	-	-	-
P4	-	+270 (132)	-	-
P5	-	-	-	-
P6	-	-	-	-
P7	-	-	-252 (152)	-310 (50)
P8	-69 (38)	+63 (39)	-	-
P9	-141 (33)	-	-175 (56)	-84 (18)
P10	-	-	+322 (81)	-
P11	-	-	-	-
P12	-	-	-177 (33)	-
P13	*+150 (58)	-	**-208** (124)	-
P14	**+103** (17)	-	-	**+304** (61)
P15	**-85** (59)	**-134** (126)	**-180** (91)	-
P16	-199 (69)	+96 (43)	-	-
P17	+116 (27)	-	**-36** (5)	**-296** (101)
P18	-	-139 (41)	**-126** (48)	**-169** (79)
P19	**+237** (29)	-	-	-

Table 3-4:Mean distance change between the SONO crystal during masseter stimulation in health and periodontitis.

Table 3-4 legend: Data are reported as mean (SD) of the movement (μm) of the pulpal crystal relative to the buccal and palatal crystals placed on the bone during tetani stimulation of the

unilateral or bilateral masseter muscle. When data were not available (-) is placed. The **bold** numbers indicate the data from the ligated Dm3s.

Pig#	Right Buccal Crystal pair			Right Palatal Crystal Pair			Left Buccal Crystal Pair			Left Palatal Crystal Pair		
Masseter stimulated	R	L	R+L	R	L	R+L	R	L	R+L	R	L	R+L
P1	-	-	-	-	-	-	-	-	-	-	-	-
P2	-	-	-	-	-	-	-	-	-	-	-	-
P3	-	-	-	-	-	-	-	-	-	-	-	-
P4	-	-	-	-	-	-	-	-	-	-	-	-
P5	-185 (3)	-	-	-282 (2)	-	-	-	-	-	-	-	-
P6	-	-	-	-	-	-	-	-	+302 (19)	-	-	-
P7	+137 (15)	+77 (30)	+164 (51)	-	-	+197 (115)	-	-	-153 (52)	-	-	-
P8	+243 (29)	-35 (2)	-	-	-	-	-	-20 (3)	-	-	+23 (3)	-
P9	-85 (8)	-	+35 (19)	-	-	-32 (0)	-	-	-	-	-	-
P10	-64 (0)	-	-76 (18)	-	-	-	-	-	-	-	-	-
P11	-	-	-	-	-	-55 (6)	-	-63 (25)	+33 (1)	-	-	-
P12	-	-	-	-	-	-	-	-	-	-	-	-
P13	-	-	**-73** (17)	-	-	-	-	-	-	-	-	-
P14	**-74** (25)	-	**-100** (57)	**-158** (10)	-	**-70** (11)	-	-	**-34** (4)	-	-	-
P15	-	-	**-545** (363)	-	-	-	-	-	**-102** (27)	-	-	-
P16	-	-	-	-	-	-	-	-	**-37** (2)	-	-	-
P17	-	-	**-23** (10)	-	-	-	-	-63 (1)	-24 (5)	-	-72 (25)	-139 (6)
P18	**-64** (0)	-	-	-	-	-	-	-	-	-	-	-
P19	-	-	-	-	-	-	-	-	-	-	-	-

Table 3-5: Direction of Dm3 movement during mastication and masseter stimulation.

Table 3-5 legend: Direction of movement of the healthy and periodontally diseased Dm3s were grouped by whether data was available from both the buccal and palatal crystal pairs (determinate) or just one pair of either buccal or palatal crystals (indeterminate). This table is based on the data in Tables 3-3 and 3-4. Where the distance between the two crystals was increasing, extrusion and/or the respective buccal or palatal movement was assumed. If the distance between the two crystals in a pair was decreasing, intrusion and/or the respective buccal or palatal movement was assumed. The **bold** numbers, indicate the data from the ligated Dm3s. Note that P13 (L) is from the Dm3 of a pilot pig that was ligated with only *Pg* and thus not included in the experimental periodontitis data (see Chapter 2).

	Chewing									
	1 crystal pair				2 crystal pairs					
	Extrusion and/or tipping		Intrusion and/or tipping		Extrusion and/or		Intrusion and		Tipping only	
	Palatal	Buccal	Palatal	Buccal	Palatal	Buccal	Palatal	Buccal	Palatal	Buccal
Control	P3 (L) P10 (R)	P4 (L)	-	P9 (L) P12 (R)	-	-	P7 (R)	P9 (R)		P8 (L)
Disease	P13 (L) **P14 (L)** P17 (L) **P19 (L)**	**P14 (R)**	P18 (L)	**P13 (R)** **P15 (R)**	-	-	**P15 (L)** **P17 (R)** **P18 (R)**	P16 (L)		
	Masseter Stimulation									
Control	P6 (L) P7 (R) P8 (R) P11 (L)	-	P11 (R)	P7 (L) P9 (R) P10 (R) P11 (L)	P9 (R)	P7 (R) P8 (L)	P5 (R)	-	P9 (R)	P8 (L)
Disease	-	-	-	**P13 (R)** **P14 (L)** **P15 (R)** **P15 (L)** **P16 (L)** **P17 (R)** **P18 (R)**	-	-	**P14 (R)** P17 (L)	**P14 (R)**		

Table 3-6: Comparison of tooth movement direction based on available data from either 1 crystal pair or bilateral crystal pair.

Table 3-6 Legend: Different presentation of the direction of Dm3 movement based on data available from the unilateral or bilateral crystal pairs. This table is based on the data in Tables 3-3 and 3-4. R: right crystal pair, L: left crystal pair. The **bold** numbers, indicate the data from the ligated Dm3s. Note that P13 (L) is from the Dm3 of a pilot pig that was ligated with only *Pg* and thus not included in the experimental periodontitis data (see Chapter 2).

CHAPTER 4

Morphological assessment the bone and PDL space by µCT and histology in periodontally healthy and diseased young pigs

4.1 INTRODUCTION

In order to better understand the behavior of teeth under loads, it is crucial to understand the morphology of the involved structures. As reviewed in Chapter 1, numerous tissues are involved in support of the tooth and regulation of its movement, many of which are affected by disease and aging [142], [226], [282]–[284].

In rats with increasing age the formation of new collagen reduces, and the new collagen is mainly produced at the cervical and apical thirds of the root, where the occlusal forces may be transmitted [283]. In older mice, the PDL space narrows and the PDL fibers are less organized in older mice [285]. Another change in the periodontium with aging is an increase in the apposition of apical cementum [284], [286]–[288]. The alveolar bone shows decreased in bone turnover in older rodents, and also in humans [282], [284], [287]. The number of osteoclasts in older rodents seems to be less than younger ones despite a net loss of bone [282], [286]. However, it is important to note that although there is a general trend for alveolar bone loss to occur with aging, in aged mice the distance from the CEJ to the alveolar bone crest is not changed compared to the younger mice [286], [289]. It has been reported that alveolar bone loss is not related to the inflammation in older mice [286]. Rather, the bone loss in older mice may be functionally related, perhaps to changes in occlusal force or wear [286].

On the other hand, the bone loss that is seen during periodontal disease is mostly due to a significant increase in the number of inflammatory cells and the resultant osteoclastic activity. The periodontal bone loss is often seen as an increase in distance between the CEJ and the alveolar bone crest accompanied by bone loss in the furcation region and interproximally [142], [147], [206], [209], [235], [288]. Furthermore, Lee *et. al.,* have shown that during ligature-induced periodontal disease in rats, the PDL space increases up to day 4, then decreases until day 8, and again increases by day 15 [288]. The authors also noted that changes in the PDL space were not consistent for different regions of the root [288]. The general organization of PDL fibers during ligature induced periodontitis is said to be more elongated, organized and sparse compared to control rats [226].

In this chapter I will be using two different methods, namely μCT scanning and histology, to assess the morphology of the tooth roots and the alterations that the alveolar bone, PDL fibers, and PDL space go through as periodontal disease develops in young pigs. Furthermore, due to the 8-week age difference between the control pigs and experimental periodontitis pigs, I will discuss the possible effect of growth and maturation in the morphology of the regions.

4.2 Materials and Methods

4.2.1 Animals

All the animals from which the samples were obtained and analyzed in this chapter are from the pigs discussed in Chapter 2 and Chapter 3. Bilateral maxillary blocks were obtained

from all 19 pigs after euthanasia and fixed as described in Chapter 3. As discussed previously, 11 pigs were periodontally healthy (controls) which were only kept for 1 week after arrival and their mean age was 3 months. For the remaining 8 pigs, the induction of periodontal disease took 8 weeks and thus the mean age for this group of pigs was 5 months. As described in Chapter 2, two of the 5-month-old pigs were used in the pilot study (P12, P13). One of these (P12) only received ligatures on its left Dm3 (this is shown by asterisk in Tables 4-1 to 4-7) and no treatment on its right side Dm3, and thus did not show signs of periodontal disease. However, only the non-ligated side (P12 R) is used for statistics. The second pilot pig (P13) received ligature soaked in *P. gingivalis* on its left side (P13 L) and on its right Dm3 (P13 R) it received ligature soaked in four bacteria for development of experimental periodontitis. Although both sides of P13 showed signs of disease, because the protocol for inducing experimental periodontitis was chosen based on the more severe damage seen when ligatures with a combination of bacteria were used, P13 L is marked with asterisk in Tables 4-1 to 4-7 and was not included in the calculations. Therefore, the diseased animals yield 9 ligated teeth and 5 non-ligated Dm3s for this project. Data were organized as control, non-ligated, and ligated Dm3s, in the 2 groups of pigs (periodontally healthy and periodontally diseased). The sample size varied and consisted of young control teeth (n=9 for μCT assessments, since 2 animals were decalcified without scanning), non-ligated teeth from periodontal diseased animals (n=5), and ligated teeth from the periodontal diseased animals (n=9, including 2 pigs with bilateral ligatures, P14 and P15).

4.2.2 Micro-CT imaging and measurements

After fixation in Prefer® and prior to decalcification, the maxillary alveolar segments containing Dm3 from the left side of 9 control pigs and from both the left and right side of experimental periodontitis pigs received μCT scans (Skyscan 1076, Bruker, Kontich, Belgium).

The μCT source was set to 59 kV, 169 μA, 0.5 mm Al filter, 120 ms, 34.4 μm pixel size, 0.6 degrees of rotation steps and 3 frame averaging. Scans were reconstructed using NRecon software (version 1.6.9.18; Skyscan) in all three spatial dimensions. The settings for reconstruction were as follows: ring artifact correction 10, beam-hardening correction 40%, and for contrast and brightness the dynamic range was set to 0.005-0.11. The reconstructed images were saved as BMP files and imported into Data Viewer (version 1.3.2; Skyscan) to be re-oriented as sagittal, coronal, and horizontal images. The saved horizontal and coronal images were then imported into CT-Analyser (CTAn, version 1.14.4.1; Skyscan) software to perform the measurements for the PDL space width, PDL space volume, root perimeter, and alveolar bone crestal height.

The measurements were obtained from 3 levels on the mesiobuccal (MB) and mesiopalatal (MP) roots (Figure 4-1A). For each root, the cervical region was defined as the level at which the entire perimeter of the root was first observed (Figure 4-1 A, blue line). The apical region was defined as the level at which the entire perimeter of the root was last visible (Figure 4-1 A, green line), and the middle region was the midpoint between the cervical and apical levels (Figure 4-1 A, red line). In each of the cervical, mid-root, and apical regions, 30 slices were measured and averaged. Note that the sample size for each of these measurements varied due to extent of bone loss for the 5-month-old pigs (Tables 4-1 to 4-7).

4.2.2.1 Root perimeter

For measurement of the MB and MP root perimeters, the horizontal images from CTAn were used. The perimeter was drawn manually with the ROI tool and the CTAn software calculated the value (Figure 4-1 B).

4.2.2.2 PDL space dimensions

The PDL space width was measured in 4 directions (mesial, distal, buccal, and palatal) for each root using the horizontal images of each level from CTAn. In addition, PDL height was measured at the furcation (inter-radicular space) and at the apex of each of the MB and MP roots using the coronal images from CTAn (Figure 4-1 A, yellow asterisks).

4.2.2.3 PDL space volume

As a supplementary measurement for the PDL space width (section 4.2.2.2) PDL space volume was measured at the same locations to look at the overall global change in the PDL space between the healthy and periodontally diseased pigs. The PDL space volume was measured by manually defining the alveolar bone surface as the outer limit, and the Dm3 root surface as the inner limit (Figure 4-1 C). This measurement was averaged for 30 slices in each of the cervical, mid-root, and apical levels. Because the vertical dimension was always the same (30 slices, about 1mm), this measurement reflects average periodontal space width for the ROI rather than volume *per se*.

4.2.2.4 Alveolar crestal bone height

Although the alveolar bone heights were measured in Chapter 2 using CBCT images, measurements were repeated using μCT to enable comparison of control and diseased pigs.

Measurements were performed as the linear vertical distance from either the buccal or palatal CEJ to the respective buccal or palatal alveolar bone crest. This is illustrated by the light green line on Figure 4-1 A.

4.2.2.5 % root coverage by alveolar bone

In order to compare the bone support of each of the mesial roots, the percent root coverage by alveolar bone was measured. For the MB root, this was done by first measuring the vertical linear distance from the buccal CEJ of Dm3 to the MB root apex (X), *i.e.* root length. Then the vertical linear distance from the buccal CEJ to the buccal alveolar bone crest was measured (Y), *i.e.* the uncovered part of the root. The same measurements were done for the MP root. The % root covered by alveolar bone was calculated as the difference between the two measurements (X and Y), divided by the root length (X), times 100 for each of the MB and MP roots separately. This is shown in the equation below.

$$\textbf{\% Root coverage} = (X - Y) / X * 100$$

Where X= root length, and Y=uncovered part of the root.

Measurements were performed separately for the buccal side of the MB root and the palatal side of the MP root (Table 4-7).

4.2.3 Histology

As described in Chapter 2, the maxillary blocks were decalcified, embedded in paraffin, and 7-10µm sections were obtained in the coronal direction. Standard protocols were used to perform hematoxylin and eosin (H&E) staining. Images were taken using an optical microscope

to look at the gross morphology of the PDL fibers along the Dm3 roots and especially the organization of the fibers in the furcation and apex of the roots. In addition, picrosirius red (PR) staining was performed to examine the collagen fiber organization in these areas. Picrosirius red stains the PDL collagen fibers either red, green, or yellow under polarized light against the black background, which makes visualization easy [290]. For the young control pigs and experimental periodontitis pigs with bilateral ligatures, the H&E and PR staining were done on the right Dm3s (n=11) and the left side was saved for future IHC staining. For the experimental periodontitis pigs that received unilateral ligatures, each Dm3 was cut in half. The mesial half was decalcified and embedded in paraffin and is to be used for H&E, PR, and neutrophil antibody staining, and the distal half was embedded in resin to be looked at in another study for alizarin and calcein bone markers. At this point not all the specimens are decalcified or prepared as slides, and sections from one control pig (P5) were of poor quality. Thus the sample size for control pigs includes 6 animals (P1-P7) and for the experimental periodontitis group 2 animal (P13 R and P14 R).

4.2.4 Statistics

Data from μCT were analyzed using GraphPad Prism Software (version 6.0h, GraphPad Software, Inc., La Jolla, CA) and Excel (Microsoft Co., Redmond, WA). Descriptive statistics were calculated, including mean, standard deviation, and standard error of the mean (SEM). Comparisons of PDL space width in different directions, PDL volume, root perimeter, alveolar bone height, and percent root coverage by bone between MB and MP roots and between control, non-ligated, and ligated Dm3s were carried out using two-way analysis of variance (ANOVA)

followed by post hoc Turkey's tests for multiple comparisons. Statistical significance was considered when $p<0.05$.

4.3 RESULTS

4.3.1 µCT results and general observations

Data for µCT can be found in Tables 4-1 to 4-7. In both the control pigs (3-month) and experimental periodontitis pigs (5-month) Dm3 root morphology was complex. The MB root always branched off the main root trunk earlier (Figure 4-11 a, a', and Figure 4-12 A, B) and it never showed any further branching. The MP root was always the second root that branched off the root trunk (Figure 4-11 b, b'). This root also did not show any further branching in any of the pigs studied. The disto-palatal (DP) root was always the third root that branched off the remaining root trunk, before the disto-buccal (DB) root trunk trifurcated into 3 smaller disto-buccal roots (Figure 4-11 c, c', roots # 4, 5, 6). All the 19 pigs showed 6 roots for the Dm3 tooth. Additionally, all the 9 teeth with experimental periodontitis showed evidence of increased PDL space at the apex of their roots (Figure 4-4). This increased space at the apex of the roots appeared similar to radiographic presentation of periodontal abscess on a volume rendered µCT image of P13 (Figure 4-13A). Furthermore, all the 5-month-old pigs showed formation of a permanent tooth in the space between the buccal and palatal roots as shown on the coronal images from µCT (Figure 4-13B).

4.3.1.1 Root perimeter

The MB root presented a much larger perimeter than the MP root at the cervical level, which could be because of its pattern in branching off the main trunk before other roots showed branching (See section 4.3.3). As expected, both the MB and MP roots showed conical morphology and tapered towards the apical region (Figure 4-2). There was no significant difference between the control, non-ligated, and ligated Dm3s at any of the cervical, midroot, and apical levels at alpha =0.05. Note that the significant difference seen between the control and non-ligated MB root of Dm3, was due to unusually bigger root MB root trunk of P18 and P19 which could be due to individual variations among animals. The larger values contributed by P18 and P19, were also seen for the MP roots.

The MB root perimeter was in the range of 8-17 mm for the control Dm3s, 8-36 mm for the non-ligated Dm3s, and 9-33 mm for the ligated Dm3s. For the MP root, perimeter ranged from 5-12 mm for the control Dm3s, 5-19 mm for the non-ligated Dm3s, and 4-19 mm for the ligated Dm3s.

4.3.1.2 PDL space volume

As expected from the smaller root, PDL volume was smaller in the MP root than the MB root. However, although often the PDL space volume was the greatest at the cervical region, there was no general decrease toward the apical end for either root (Figure 4-3). Despite many missing values at the cervical level in the ligated teeth (Table 4-3, 4-6) it was evident that the PDL space volume did not increase in the periodontally diseased pigs (Figure 4-3). Values for the MB root ranged from 3-11 mm^3 for the control group, 3-6 mm^3 for the non-ligated teeth, and 3-7 mm^3 for the ligated teeth. For the MP root the PDL volume was in the range of 2-6 mm^3 for the control group, 1-4 mm^3 for the non-ligated teeth and 1-4 mm^3 for the ligated teeth.

4.3.1.3 PDL space width

There were no consistent trends in buccal-palatal-mesial-distal width directions (Tables 4-1 to 4-6). Similarly, there were no consistent differences from cervical to apical in the PDL space width (Figure 4-4). Although the PDL space around the roots was not uniformly distributed, it didn't vary significantly for the MB and MP roots and among the control, non-ligated, and ligated Dm3s. PDL height at the furcation area was the smallest and ranged from 116-429 μm. PLD height at the root apex tended to be the largest and in the range of 334-1833 μm, compared to lateral widths in the overall range of less than 819μm (Tables 4-1 to 4-6, Figure 4-4). Furthermore, the PDL height at the apex of the roots for the ligated teeth was significantly larger than that of the control pigs for both roots and significantly larger than the non-ligated teeth for the MB root ($P \leq 0.0001$).

4.3.1.4 Effects of periodontal disease

Although there was a trend for increase of the PDL space width at the 3 levels for the ligated Dm3, this increase was not statistically significant for either of the MB or MP roots. However, for the PDL space height at the apex of the MB and MP roots, the ligated Dm3s showed notable increases ($P < 0.0001$). The non-ligated Dm3s' apical space heights were smaller but still increased compared to healthy Dm3s, although this increase was not statistically significant.

Interestingly the PDL space height at the furcation of the Dm3s did not increase in either ligated or non-ligated Dm3 of the diseased pigs and in fact showed a downward trend (Table 4-1 to 4-3 and Figure 4-4).

4.3.1.5 Alveolar crestal bone height

CEJ to alveolar crest distances were smallest in 3-month old control pigs, 1.4 - 4.9 mm (Figure 4-5 and Table 4-7). These distances were greater in non-ligated Dm3s of the 5-month-old periodontitis group (2.6 – 5.5 mm) and the greatest for the ligated teeth (3.5 – 5.8 mm). Both roots showed similar effects.

4.3.1.6 % root coverage by alveolar bone

Root length did not change significantly between the control (3-month) and older (5-month) pigs, but percent of the MB and MP roots that were covered by alveolar bone decreased (Figure 4-6, Table 4-7). Similar to the distance from CEJ to alveolar bone crest pattern, percent root coverage was low in both the ligated and non-ligated Dm3s. Although coverage was generally less on the ligated side, the difference between the two sides of the diseased pigs was not statistically significant for either root.

4.3.2 Histology

Descriptive data for examined H&E histology can be found in Table 4-8. In the young control pigs, the PDL collagen fibers along the roots had an acutely angled attachment to the root's cellular cementum on one side and insert into the alveolar bone on the other side. Under magnification, images showed that the fibers were very densely packed and highly organized along the middle third of the roots (Figure 4-7 and 4-8). In the apical region (Figure 4-9), and the furcation area (Figure 4-10), the fiber density appeared to be less dense, more unorganized and travelling in different directions (dotted enclosed outline on Figure 4-9), and sparser.

Note: At this point tissues have been examined for (n=7) control pigs, none of the non-ligated (n=0) specimen have been fully decalcified, and for the ligated Dm3 (n=1) samples from P14 (right side, M1 tooth) is examined. However, the sections from P14 are from the partially erupted first molar region, and thus don't show complete roots or closed apex.

Histologically a thick layer of cellular cementum was noted in all the examined sections (Figure 4-7 to 4-10). In control pigs, higher number of blood vessels were noted in the furcation and apical regions compared to the sides of the roots (Table 4-8 and Figures 4-9 an 4-10).

4.4 DISCUSSION

4.4.1 µCT analysis

Although for the most part the PDL space did not differ significantly in buccal, palatal, mesial, or distal width or furcation height among the control, non-ligated, and ligated Dm3 teeth, the periodontally diseased pigs showed a significant increase in PDL height at the apex of the MB and MP roots, particularly of the ligated teeth, which also showed increased cervical widths around the MB roots (Figure 4-4). Lack of significant change in the PDL space in the lateral directions of the roots has also been observed in other species subjected to ligation [291].

Despite a significant amount of crestal palatal alveolar bone loss occurring around the ligated Dm3s, the disease process did not affect the cervical width of the MP root's PDL space. This perhaps is due to the fact that the MP root separates from the main root trunk more apically than the MB root (Figure 4-12 D), and thus its supporting bone is not resorbed to result in increased PDL space around MP root.

The inconsistencies seen in the MB and MP root perimeter (P18 and P19), could be explained by the individual variations in the teeth and pigs (Table 4-2).

The significant increase in PDL height seen in the apex of both roots is surprising, but similar phenomena have been observed in other experimental periodontitis animal studies [142], [166], [180], [209], [226]. In the ligated teeth this increase in the PDL space at the apex of the roots may reflect bone destruction due to the development of periapical periodontal abscesses (Figure 4-12). An additional feature that can further highlight the role of periodontal disease as the primary culprit for the increased height of the PDL at the apex of the ligated Dm3s, is an increased presence of inflammatory cells in this region reported in Chapter 2. However, the fact that the non-ligated Dm3s of the periodontitis animals also showed increases in apical space, despite an absence of clinical symptoms, suggests that additional factors may be involved. The increased PDL space height could be due to transfer of bacteria from the ligated side to the non-ligated side, producing incipient disease with bone damage but no visible gingival inflammation or abscess formation. However no neutrophils were detected and unfortunately it is not yet known whether neutrophils were present around non-ligated teeth of diseased animals. As an alternative explanation, the increase in the apical space could also be due to tooth eruption and aging. These 5-month-old pigs were actively growing, and as the maxilla increases its vertical dimension alveolar apposition occurs [292] accompanied by further eruption of teeth already in occlusion as well as the emergence of the permanent molars. μCT images from all the experimental periodontitis pigs showed radiolucency that could have been due to formation of the 1st maxillary permanent molar (Figure 4-13B). In either case, as shown in mouse studies, the increase in the PDL space height and the intensity of damage was greater in the ligated teeth than

the non-ligated teeth, perhaps because of the irritating effect of the ligature in addition to the bacterial insult on the ligated side [142], [162], [166], [167], [188].

In order to address whether age or disease is primarily responsible for the increasing PDL height at the apex, data for the pilot pig (P12) in Table 4-2 (MB root) and Table 4-5 (MP root) can be referenced. Pig 12 was 5 months old and had ligatures on its left Dm3 and no treatment on its right Dm3. When comparing the height of the PDL at the apex of its mesial roots (596μm for the ligated MB and 689 μm for the non-ligated MB root, and 498 μm for the ligated MP, and 595 μm for the non-ligated MP root), the values seem to be very similar to that of 3-month-old control pigs (459-537 μm) and less similar to the values from the experimental periodontitis pigs (890-1168 μm) that developed periodontitis.

In a rat study, osteoclasts were detected as early as 4 days in the disease process, when the PDL space still was not enlarged, and after 4 weeks of disease progression, although the radiographic signs of alveolar bone resorption and widen PDL space was evident, the number of osteoclasts had decreased [288]. In this study we did not look at expression of osteoclasts. Thus, although similar to the rat study there is signs of enlarged PDL space, and the possible explanations could be osteoclastic bone resorption, aging or dental development might also be contributing factors. The lack of detection of osteoclasts at a later time point is not however a valid reason to reject them as a culprit for bone loss. This is because by the time the radiographic signs of bone destruction and widen PDL are detectable, the state of active inflammation and osteoclast activity might have already been brought to stable conditions.

For future studies, in order to better address this concern, it would be necessary to investigate the tissues histologically with tissues that are collected at different time points after

initiation of disease. The presence and abundance of osteoclasts (via TRAP staining) and neutrophils (via antibody staining for neutrophils) for ligated and non-ligated teeth can then be compared. In addition, a follow up study that can shed some light on the effect of aging and disease in pigs on bone deposition is being done currently, using the tissues generated Chapter 2 and the bone labeling markers [293].

4.4.2 Histological assessment

As is typical for healthy roots in other pig studies [24], in the middle of the Dm3 roots of the control pigs (n=7) fibers were densely packed and generally parallel in an oblique and longitudinal direction (Figure 4-8), whereas at the cervical third fibers were more horizontal, and at furcation and apex fibers showed more complex and cellular composition. This is in agreement with how the fibers would react during horizontal and vertical movement of teeth. The complex direction of fibers in the furcation resists lateral movement or tipping of the teeth. Whereas the oblique orientation of the fibers along the roots and the fibers at the apical third of the root resists intrusion (Figure 4-9, 4-10). In both the furcation and apex regions of all the samples examined thus far, a high number of blood vessels were noticed (Figures 4-9 and 4-10 black and yellow arrows) compared to the cervical and mid-root areas, which suggests an important role of fluid pressure in controlling dynamics of the tooth in these specific regions. For the middle third of the root, similar general patterns for the direct organization and density of the PDL collagen fibers have been reported in healthy molars of rats, mice, and minks [226], [291], and in healthy teeth of pigs [294]. However, those studies have not looked at the fiber orientation and density in the furcation areas of these multi-rooted teeth, which as suggested in chapter 3, might be an important area to study for better understanding the role of the PDL in regulating

tooth displacement. In the ligated teeth, tissue damage and abscess formation disrupted the fibers in the cervical and apical regions. This findings recalls earlier work on dogs, showing that the PDL fibers at the periapical region were extremely wide and the bony surface that they inserted into was undulated, representing possibly high osteoclastic activity [180].

Periodontal studies in non-human primates have looked at the histological findings of the non-ligated teeth in the presence of ligated teeth, and have noted that there were no significant clinical or histological changes associated with the non-ligated teeth, and they were comparable to control teeth [182]. However, given the osseous changes seen on the non-ligated teeth in the present study, I expect to find a different result. Unfortunately, the non-ligated samples are not decalcified yet to be included in the results and discussion for this chapter.

4.5 Conclusion

The mesial roots of the Dm3 tooth in pigs and their associated PDL space dimensions are stable between the ages of 2 to 5 months, even in the presence of periodontal disease, except at the apices of the roots. As apical space increases with age or disease, so does the CEJ-alveolar crest distance, and percent root coverage by bone. The use of bacteria with ligature to induce periodontitis further increases apical space height and CEJ-crest distance and creates significant changes in the cervical bone level. Histological assessment of the normal organization and orientation of the PDL collagen fibers from the H&E and PR stains appear to show densely packed organized fibers along the roots, but a less dense and less organized pattern at the apices of the roots and the furcation areas.

4.6 FIGURES

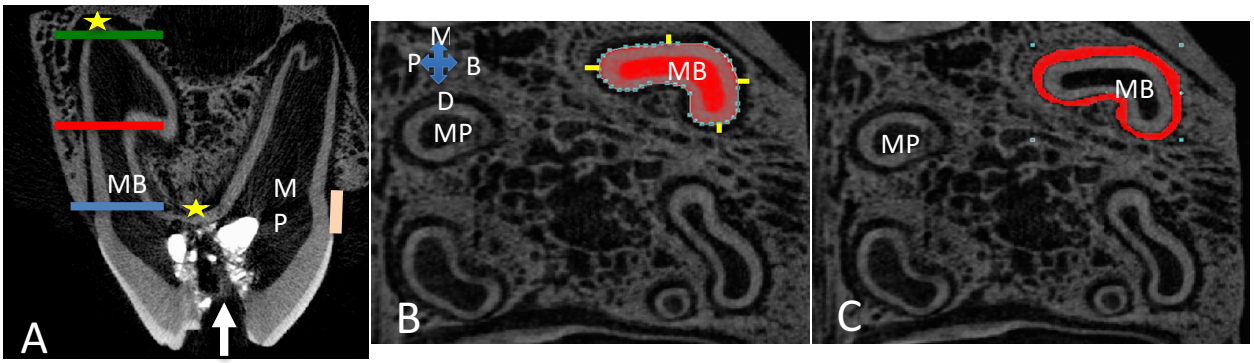

Figure 4-1: µCT image analysis of pig maxillary last deciduous molar (Dm3).

Legend for Figure 4-1: µCT images of Dm3 with measures of the mesiobuccal (MB) root. (A) shows a coronal view of the tooth morphology. Blue line: cervical level, Red line: mid-root level, Green line: apical level, light green: distance between the CEJ and ABC. Yellow stars: furcation PDL height and apical PDL height for the PDL space of the MB root. The white arrow shows the occlusal cavity where the crystal and the Cavit™ filling material was placed. (B) Horizontal view shows PDL space width of the MB root in the palatal, buccal, distal, and mesial directions (yellow lines) and the measurement of root perimeter (blue dots). (C) the ROI for measuring the PDL volume is shown in red for the MB root. MB: mesiobuccal root. MP: mesiopalatal root, B: buccal, P: palatal, M: mesial, D: distal. CEJ: cementoenamel junction. ABC: alveolar bone crest.

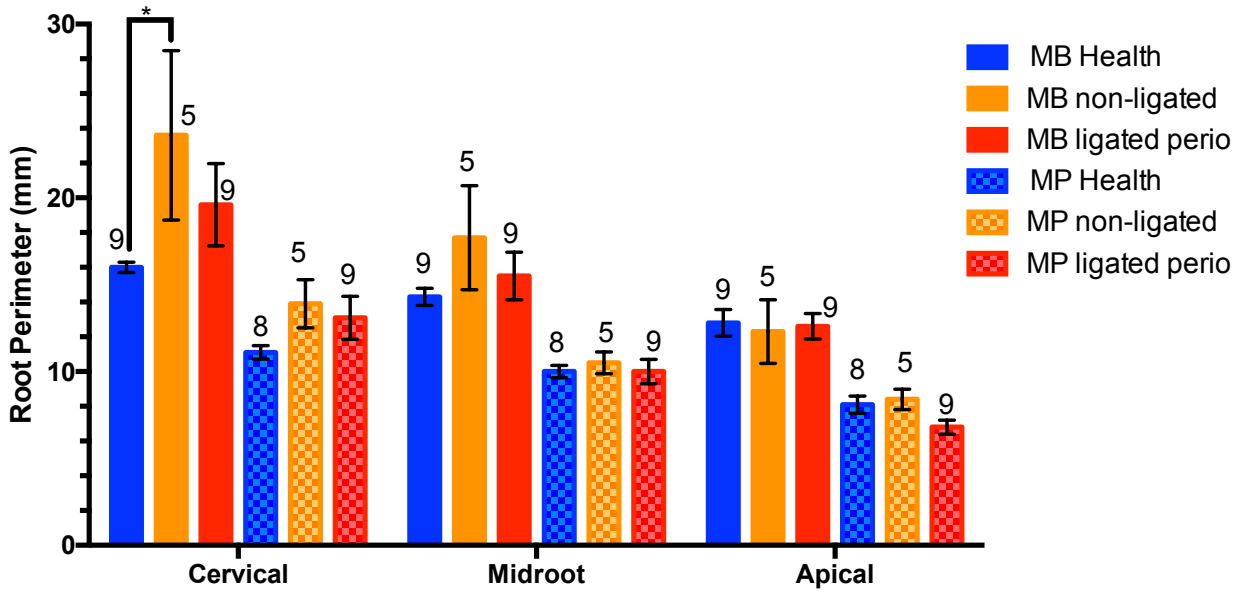

Figure 4-2: Root perimeter measurement of control, non-ligated, and ligated Dm3s.

Legend for Figure 4-2: The main MB root is consistently larger than the MP root. Both the MB and MP roots gradually taper towards the apical region. At alpha =0.05 there was no significant difference among the control, non-ligated, and ligated Dm3s at any of the cervical, midroot, and apical levels, except between the healthy and non-ligated samples of the MB root. The error bars represent the standard deviation. Sample size is marked on top of each bar. Data are shown in Tables 4-1 through 4-6. MB: mesiobuccal root. MP: mesiopalatal root.

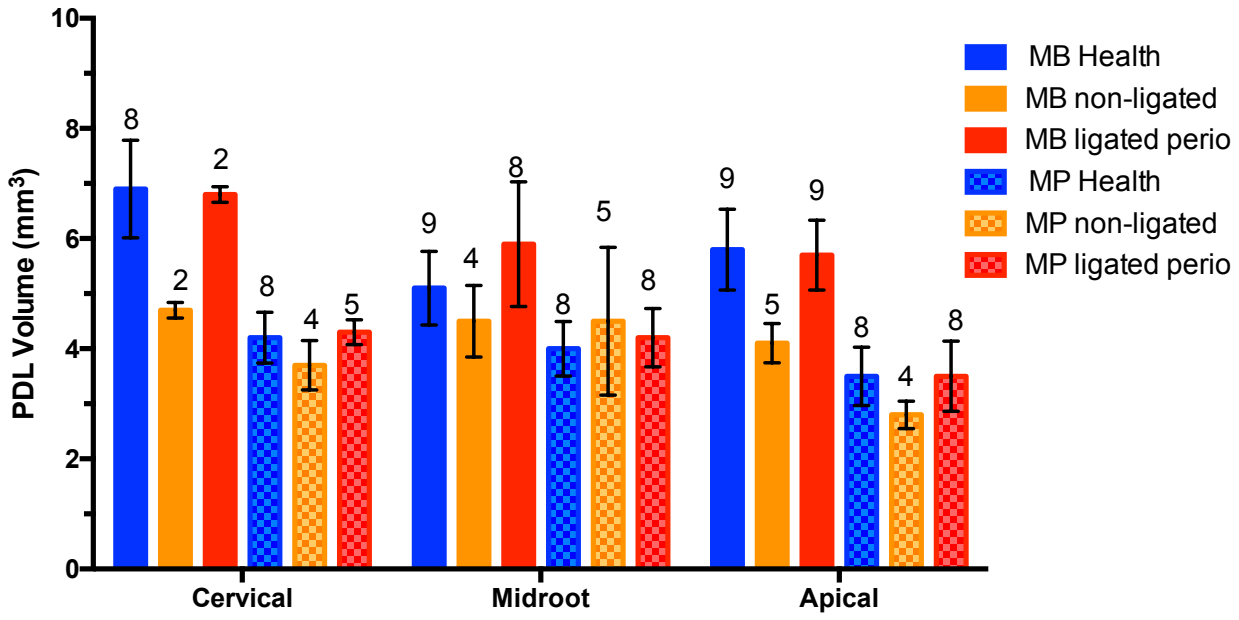

Figure 4-3: PDL volume measurements of control, non-ligated, and ligated Dm3s.

Legend for Figure 4-3: The PDL volume for MB root is larger than that around the MP root, but at alpha = 0.05 there is no significant difference in the PDL volume measurements around the control, non-ligated, and ligated roots. The error bars represent the standard deviation. Sample size is marked on top of each bar. Data are shown in Tables 4-1 through 4-6.

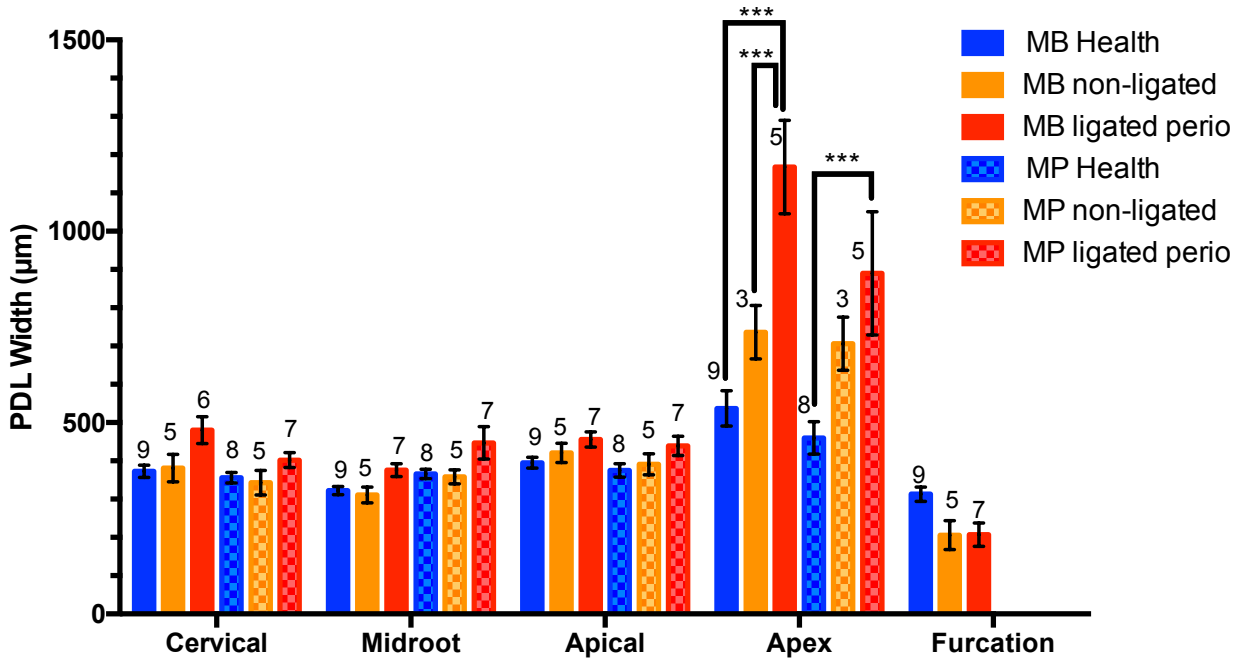

Figure 4-4: PDL space width measurements of the control, non-ligated, and ligated Dm3s.

Legend for Figure 4-4: MB and MP roots show similar patterns and dimensions. The PDL space dimensions in healthy controls were all similar, albite apical height is slightly greater and furcation height slightly lesser than the width measurements. Periodontal disease had little effect on space width in the cervical, midroot and apical thirds of the roots. PDL space height at the apex was increased on the non-ligated Dm3 for both the MB and MP roots and was further increased significantly on the ligated Dm3 ($P \leq 0.0001$). The furcation space height was usually the smallest dimension and showed a non-significant decrease ($P=2.206$) with periodontal disease. ***: $P \leq 0.0001$. The error bars represent the standard deviation. Sample size is marked on top of each bar. Data are shown in Tables 4-1 through 4-6. MB: mesiobuccal root. MP: mesiopalatal root.

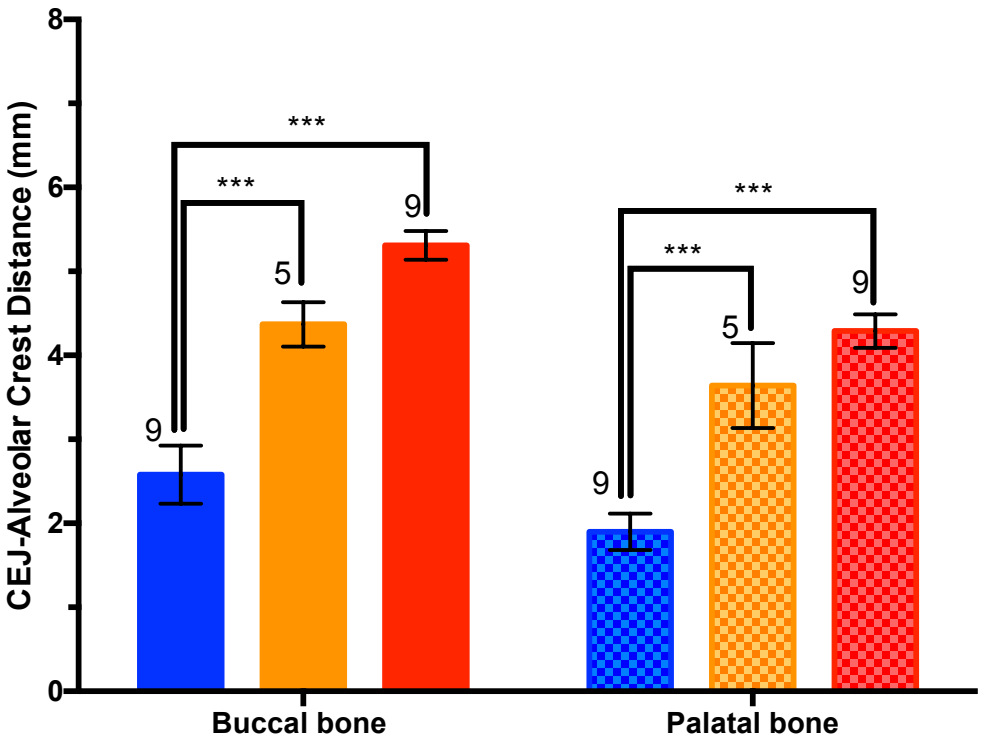

Figure 4-5: Distance between CEJ to alveolar bone crest from µCT for control, non-ligated, and ligated Dm3s.

Legend for Figure 4-5: Statistically significant increases in the distance from CEJ to the alveolar bone crest were seen around the control, non-ligated, and ligated Dm3s for both the MB and MP roots. ***: $P \leq 0.0001$. The error bars represent the standard deviation. Sample size is marked on top of each bar. Data are shown in Table 4-7.

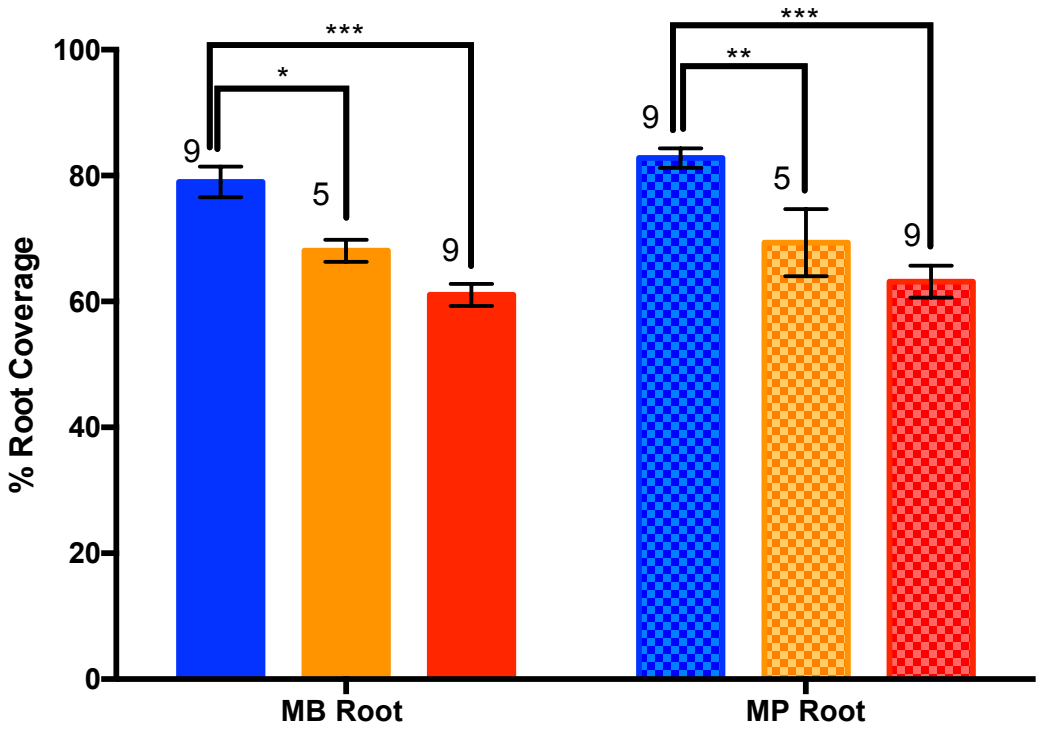

Figure 4-6: % root coverage for the control, non-ligated, and ligated Dm3s.

Legend for Figure 4-6: The percent of MB and MP roots that was covered by alveolar bone had a significant decrease compared with that of healthy control Dm3s (about 80% bone coverage) on both the non-ligated (about 70% bone coverage) and ligated Dm3s (about 60% bone coverage). *: $P < 0.05$. **: $P < 0.01$. ****: $P < 0.0001$. The error bars represent the standard deviation. Sample size is marked on top of each bar. Data are shown in Table 4-7. MB: mesiobuccal root. MP: mesiopalatal root.

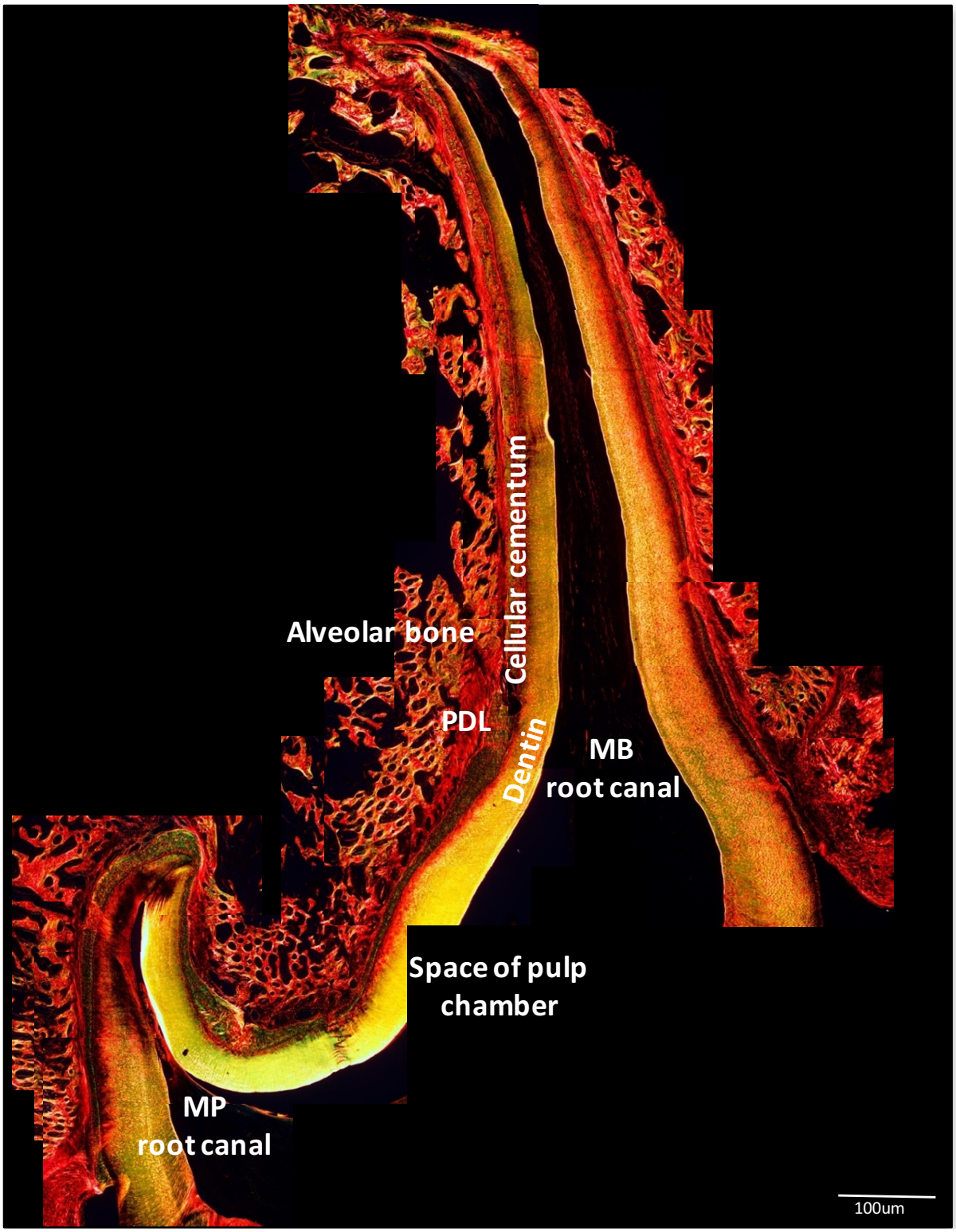

Figure 4-7:Picrosirius red (PR) stain of a control, non-ligated Dm3, showing the buccal and palatal roots with associated PDL fiber network.

Figure 4-7 legend: Coronal section through the MB and MP roots of Dm3 of a control pig (P1) stained for picrosirius red. The image is a composite of multiple images captured at 10X magnification.

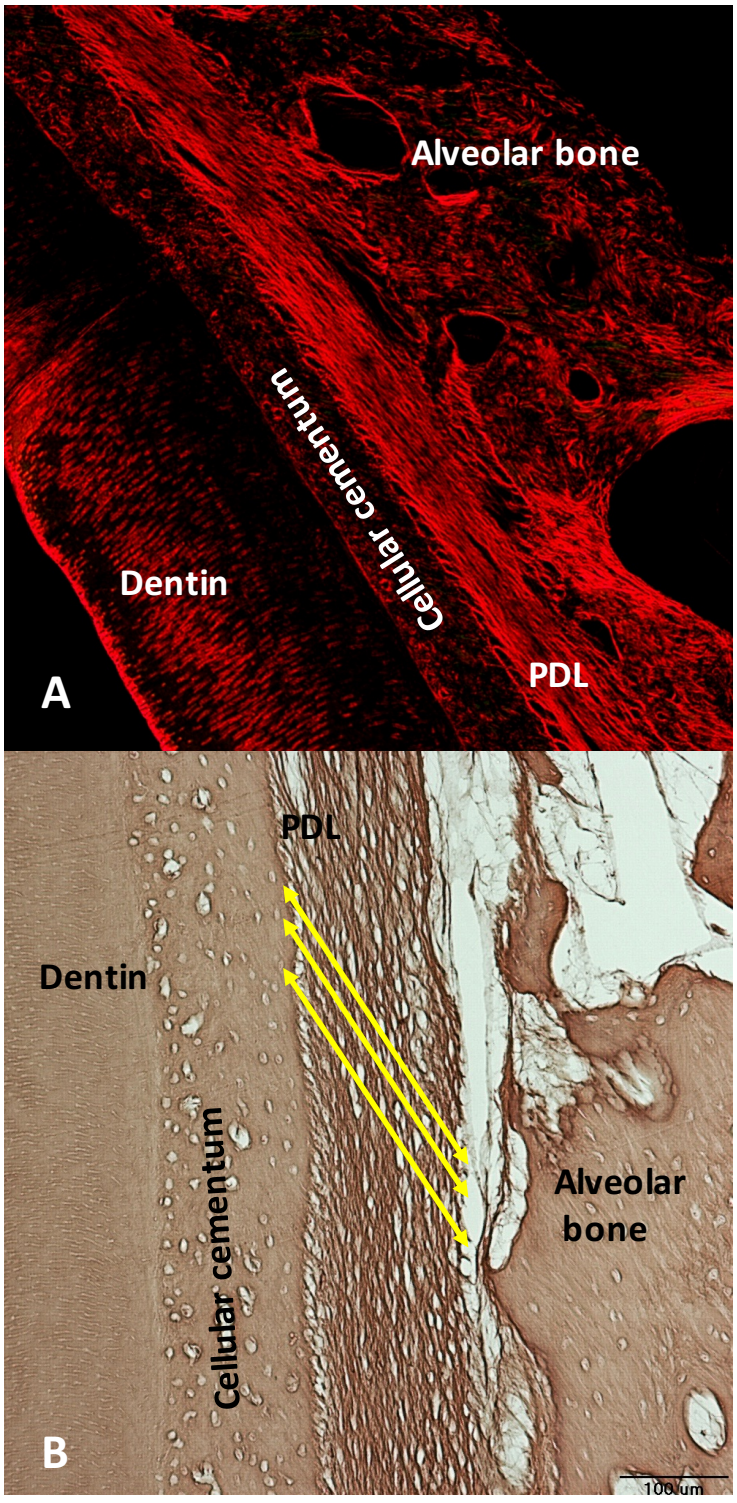

Figure 4-8: PDL fiber network along the root of a control Dm3 root.

Legend for Figure 4-8: The PDL collagen along the buccal aspect of the MB root of a control Dm3 root (P1). Both images show the densely packed, parallel fibers attached at a very acute angle. A: picrosirius red stain. B: H&E stain. For both images magnification is 10X.

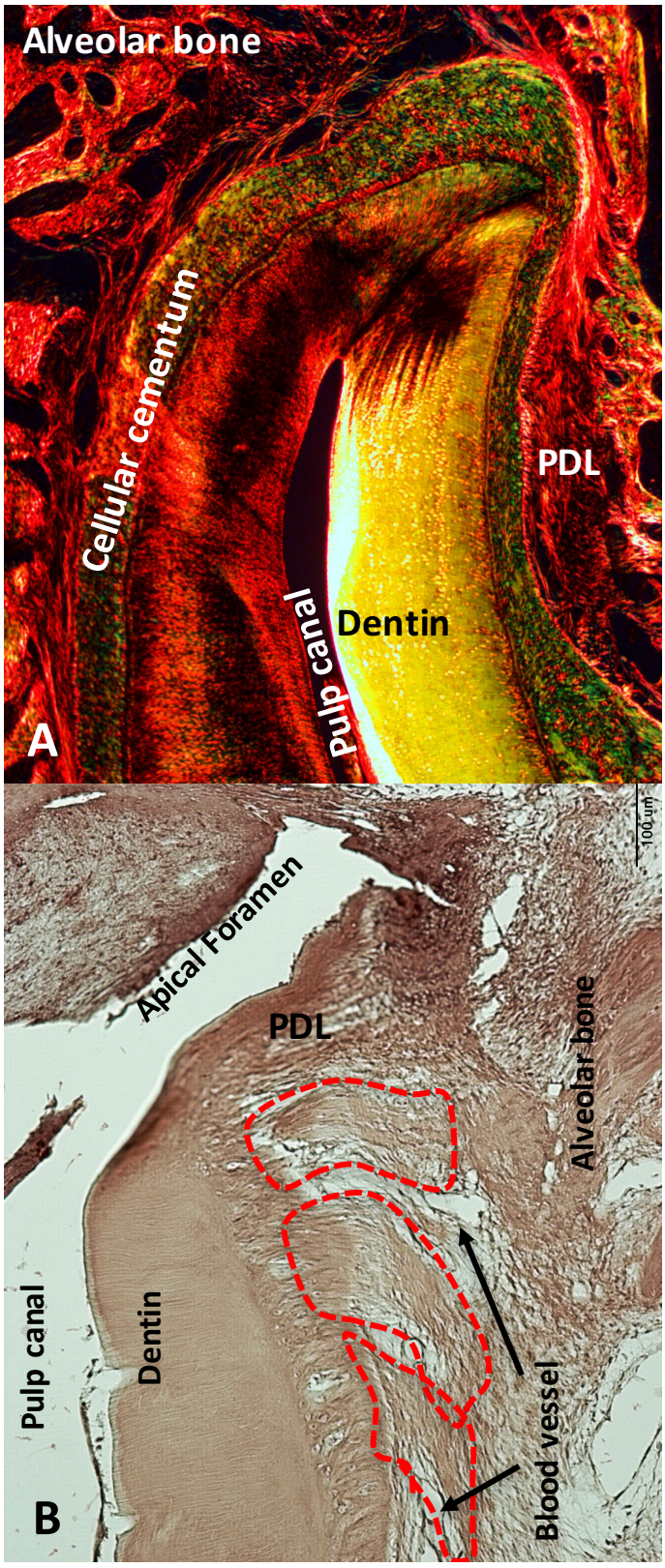

Figure 4-9: PDL fiber network at the apex of a control Dm3 root.

Legend for Figure 4-9: PDL collagen fiber network at the apical region of a control Dm3 root. Both images show patchy PDL fiber bundles that are organized different directions (dotted closed circles). Note the veins at the PDL at the apex (black arrows). A: Enlargement of Figure 4-7 picrosirius red stain (P1), magnification 10X. B: H&E stain (P4), magnification 4X.

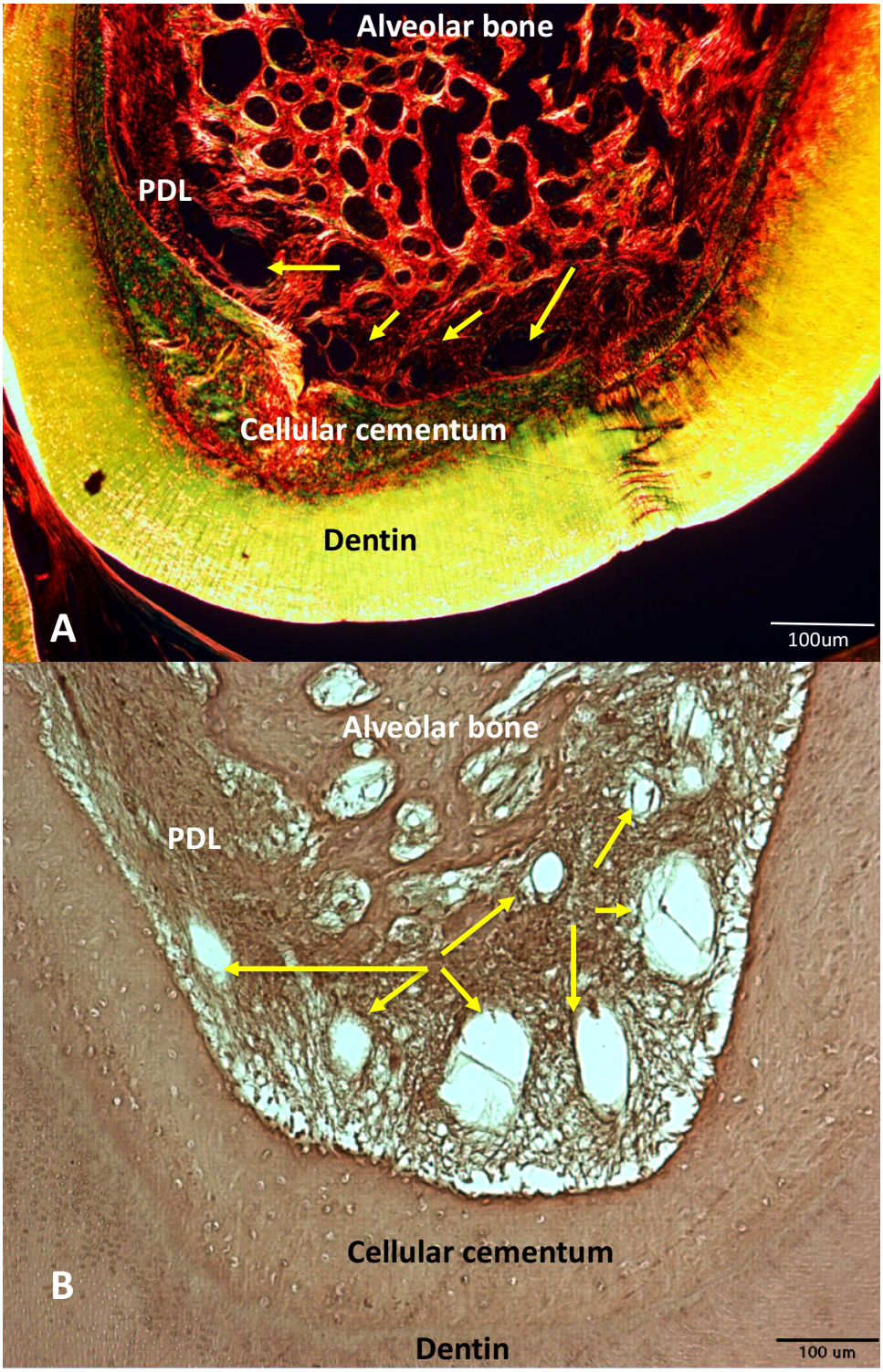

Figure 4-10: PDL fiber network at the furcation of a control Dm3.

Legend for Figure 4-10: PDL collagen fiber network at the MB-MP furcation of a control Dm3. The fibers are not parallel but form a mesh connecting the bone to the tooth as a network of crossed bundles. Yellow arrows indicate the presence of blood vessels within the PDL at the furcation region. A: Enlargement of Figure 4-7, picrosirius red stain (P1). B: H&E stain (P1).

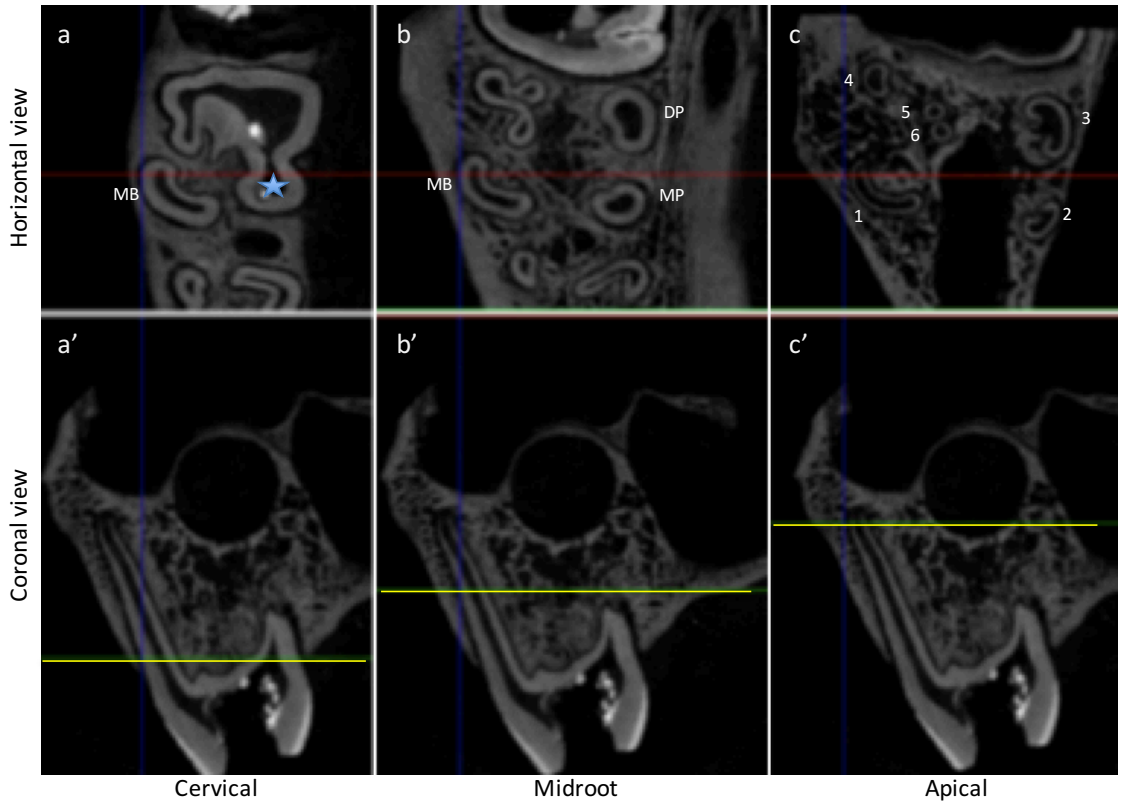

Figure 4-11: Coronal and horizontal µCT images at the cervical, midroot, and apical thirds of the MB root of a control Dm3.

Figure 4-11 legend: A control Dm3 of a 3-month-old farm pig (P3). a: Horizontal µCT images at the cervical level showing the early separation of the MB root from the main root trunk. The blue asterisk shows the MP root that is still part of the root trunk at the time that the MB root is separated from the main trunk. b: Horizontal view of Dm3 roots at the midroot level, showing the MB, MP, and DP roots completely separated from the main trunk. c: Horizontal view of Dm3 roots at the apical third of the MB root, showing the 6 roots of this tooth. a', b', c': Coronal views of the MB root of the Dm3 tooth at the cervical, midroot, and apical thirds of the root respectively (yellow line). MB: mesiobuccal. MP: mesiopalatal. DB: distobuccal.

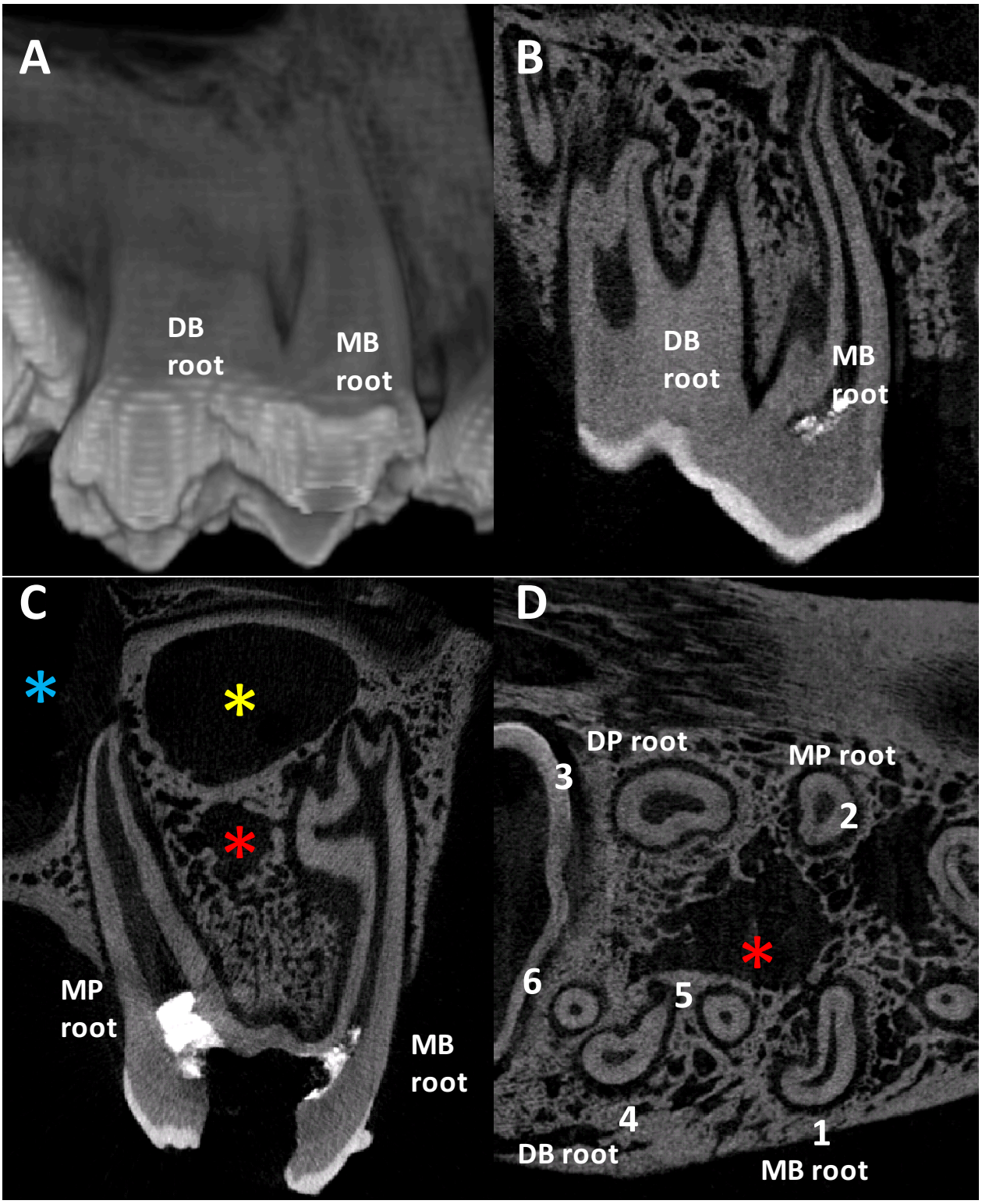

Figure 4-12: Morphology of pig Dm3.

Figure 4-12 legend: A Non-ligated Dm3 of a 5-month-old farm pig (P14). A: Scout scan showing the MB and DB roots and the thick DB root trunk that will further separate into smaller roots. B: Sagittal μCT scan showing the MB and DB main root trunks. C: Coronal μCT scan showing the MB and MP roots. Note the apical trifurcation of the MB root. Yellow star shows the maxillary sinus. Blue star shows the nasal cavity. Red star shows the potential space for permanent tooth formation. D: Horizontal μCT image of the Dm3 at the apical level showing the labeled 6 roots. The yellow star shows the space of developing permanent tooth. MB: mesiobuccal. MP: mesiopalatal. DB: distobuccal. DP: distopalatal.

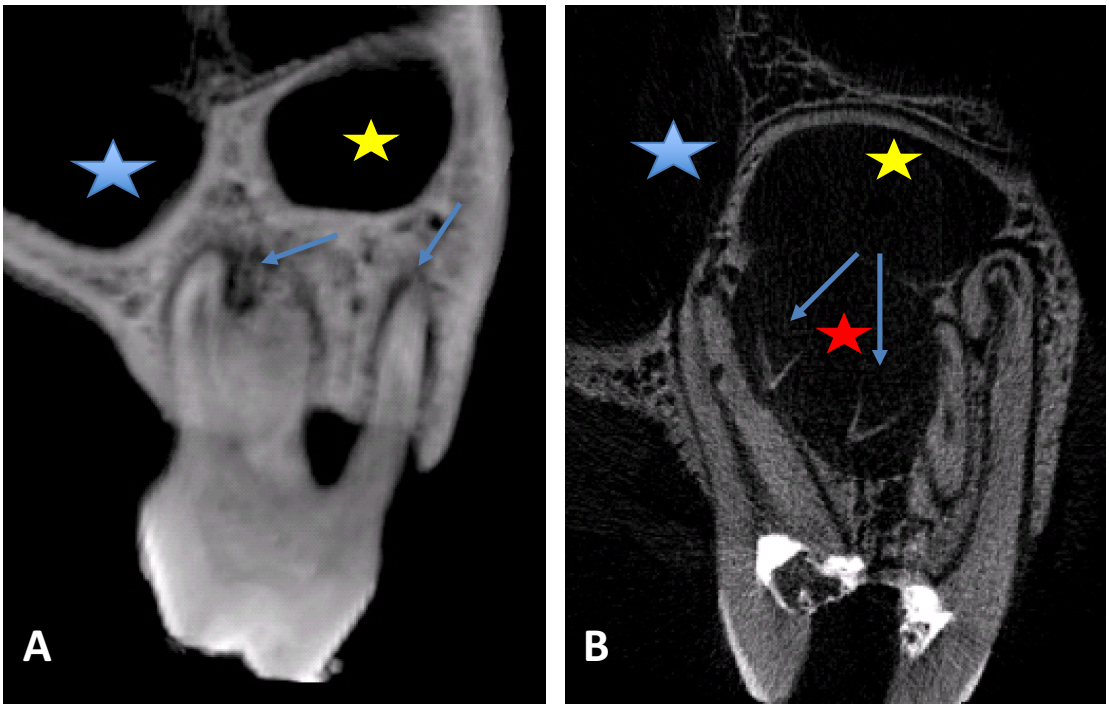

Figure 4-13: Subjective observations in the experimental periodontitis pigs.

Figure 4-13 legend: Coronal plane μCT images showing examples of observations in the experimental periodontitis pigs. A: Blue arrows are pointing to the apparent development of periodontal abscesses around the buccal and palatal roots of a ligated Dm3 (P13 L). B: Blue arrows are pointing to the development of the crowns of the permanent tooth (P17 R). Yellow star shows the maxillary sinus. Blue star shows the nasal cavity. Red star shows the space for permanent tooth formation.

4.7 TABLES

Table 4-1: µCT measurements of root perimeter, PDL space volume and PDL space width for MB roots of control Dm3s.

Pig #	Level	Root perimeter	PDL volume	Apical height	Furcation height	Mesial width	Distal width	Buccal Width	Palatal width
1		16.2	9.7	674.0	250.0	390.6	344.6	298.7	367.6
2		16.1	11.5	492.0	302.0	548.7	318.7	370.7	340.7
3		14.4	5.2	451.0	360.0	502.3	273.0	287.3	373.7
4	Cervical	16.4		561.0	318.0	390.6	277.0	400.2	448.0
5		16.2	4.7	608.0	318.0	331.7	280.7	299.7	280.7
7		16.9	5.3	334.0	426.0	423.3	302.3	447.3	320.3
9		14.8	5.6	376.0	238.0	525.3	328.3	267.7	465.5
10		17.2	7.7	764.0	287.0	698.7	421.3	450.3	287.7
11		16.0	5.7	575.0	314.0	469.3	299.3	307.7	291.0
Average		**16.0**	**6.9**	**537.2**	**312.6**	**475.6**	**316.1**	**347.7**	**352.8**
Stdev		**0.9**	**2.5**	**138.7**	**56.4**	**109.7**	**46.3**	**70.8**	**67.9**
n		**9**	**8**	**9**	**9**	**9**	**9**	**9**	**9**
1		14.9	7.7			298.7	183.8	137.9	298.7
2		14.8	8.7			377.7	323.3	328.0	399.7
3		11.6	3.4			351.7	373.7	236.7	201.0
4	Midroot	13.5	3.2			298.7	264.2	287.9	345.2
5		15.4	4.3			268.0	364.0	306.7	357.3
7		15.7	4.0			290.3	344.7	357.0	357.0
9		12.5	3.7			336.3	380.3	310.0	362.3
10		15.9	5.8			431.0	431.0	354.0	325.7
11		14.4	5.5			372.3	364.0	243.0	340.0
Average		**14.3**	**5.1**			**336.1**	**336.6**	**284.6**	**331.9**
Stdev		**1.5**	**2.0**			**52.2**	**72.9**	**69.5**	**56.3**
n		**9**	**9**			**9**	**9**	**9**	**9**
1		10.3	6.3			321.7	206.8	206.8	298.7
2		13.0	10.7			472.0	414.7	408.3	389.3
3		8.9	3.4			502.7	380.7	431.0	416.7
4	Apical	12.8	4.6			356.1	482.5	344.6	574.7
5		14.7	5.3			370.0	517.0	351.3	351.0
7		14.6	4.8			380.7	544.0	368.7	296.3
9		10.6	4.0			370.0	328.7	451.7	312.3
10		15.8	6.3			455.7	373.7	479.0	383.0
11		14.2	7.3			396.7	437.0	517.7	315.3
Average		**12.8**	**5.8**			**402.8**	**409.4**	**395.5**	**370.8**
Stdev		**2.3**	**2.2**			**60.2**	**103.4**	**91.8**	**87.9**
n		**9**	**9**			**9**	**9**	**9**	**9**

Legend for Table 4-1: The units of measurements are: root perimeter (mm), PDL volume (mm^3), and the PDL widths and heights (µm). Pig 11 is from the pilot study (Chapter 2). The results of the statistical analysis are reported in Figure 4-2 for root perimeter, Figure 4-3 for PDL volume, Figure 4-4 for PDL width.

Table 4-2: µCT measurements of root perimeter, PDL space volume and PDL space width for MB roots of non-ligated Dm3s.

Pig #	Level	Root perimeter	PDL volume	Apical height	Furcation height	Mesial width	Distal width	Buccal Width	Palatal width
***12 L**		16.7	6.5	596.0	299.0	469.7	396.3	260.7	500.7
***12 R**		14.8	4.9	689.0	284.0	391.3	326.7	295.3	302.7
***16 L**	Cervical	17.2		874.0	303.0		320.0		492.3
***17 R**		15.0	31.0	646.0	116.0	383.0	344.7	300.0	350.7
***18 L**		36.3	4.6		139.0	430.7	272.7	251.0	819.0
***19 R**		34.8			187.0		434.0		
***Average**		***23.6***	***13.5***	***736.3***	***205.8***	***401.7***	***339.6***	***282.1***	***491.2***
***Stdev**		***10.9***	***15.2***	***121.1***	***84.3***	***25.5***	***59.1***	***27.0***	***232.9***
***n**		***5***	***3***	***3***	***5***	***3***	***5***	***3***	***4***
***12 L**		16.5	4.7			302.7	386.0	271.3	323.3
***12 R**		12.9	3.5			268.3	299.0	230.0	260.7
***16 L**	Midroot	13.6	4.4			369.3	295.7	394.0	271.0
***17 R**		12.2				306.3	312.7	216.7	
***18 L**		26.6	3.8			294.3	273.0	165.3	215.5
***19 R**		23.3	6.4			485.0	478.7	312.3	466.3
***Average**		***17.7***	***4.5***			***344.7***	***331.8***	***263.7***	***303.4***
***Stdev**		***6.7***	***1.3***			***86.8***	***83.3***	***90.0***	***111.3***
***n**		***5***	***4***			***5***	***5***	***5***	***4***
***12 L**		13.9	4.6			302.7	428.0	302.3	334.0
***12 R**		8.3	2.9			375.3	673.7	383.0	528.3
***16 L**	Apical	14.0	4.8			328.3	385.7	443.0	467.7
***17 R**		8.0	3.9			370.3	440.7	383.0	383.3
***18 L**		17.7	3.9			280.0	294.3	309.0	294.3
***19 R**		13.4	4.9			524.0	581.3	359.0	610.3
***Average**		***12.3***	***4.1***			***375.6***	***475.1***	***375.4***	***456.8***
***Stdev**		***4.1***	***0.8***			***91.4***	***152.1***	***48.4***	***123.1***
***n**		***5***	***5***			***5***	***5***	***5***	***5***

Legend for Table 4-2: The units of measurements are: root perimeter (mm), PDL volume (mm^3), and PDL widths and heights (µm). Missing data are due to the absence of alveolar bone in any of the slices in the selected region, which made it impossible to have a PDL height measurement. The results of the statistical analysis are reported in Figure 4-2 for root perimeter, Figure 4-3 for PDL volume, Figure 4-4 for PDL width. * denotes the side that did not receive any ligatures and thus its values were not included in the calculations of average and standard deviations.

Table 4-3: µCT measurements of root perimeter, PDL space volume and PDL space width for MB roots of ligated Dm3s.

Pig #	Level	Root perimeter	PDL volume	Apical height	Furcation height	Mesial width	Distal width	Buccal Width	Palatal width
*13 L				1480.0	429.0				
13 R		18.6		1249.0	429.0				
14 L		16.4	6.7	1105.0	142.0	519.0	360.3	310.0	350.0
14 R		15.9	7.0	1038.0	195.0	510.7	427.7	325.3	542.3
15 L	Cervical	15.6		920.0	164.0	595.0	466.3	385.3	770.0
15 R		14.6		1173.0	164.0	943.5	558.0		648.0
16 R		16.7		1833.0	260.0		392.0		
17 L		14.9		859.0	156.0	398.7	276.0		322.0
18 R		30.3			147.0		350.7		635.0
19 L		33.6			208.0		476.5		
Average		**19.6**	**6.8**	**1168.1**	**207.2**	**593.4**	**413.4**	**340.2**	**544.6**
Stdev		**7.1**	**0.2**	**323.2**	**91.1**	**207.9**	**87.8**	**39.8**	**177.3**
n		**9**	**2**	**7**	**9**	**5**	**8**	**3**	**6**
*13 L		14.6	6.5			517.3	471.0	197.2	517.3
13 R		16.1	12.2			448.0		242.1	598.0
14 L		15.4	6.8			459.3	360.0	310.0	330.0
14 R		13.8	5.6			402.0	395.7	350.7	370.0
15 L	Midroot	13.0	5.3			358.0	405.3	311.0	392.0
15 R		11.7	0.4			451.0	468.0	459.0	198.0
16 R		13.5	5.9			493.3	331.3	425.7	263.5
17 L		11.7				337.3	314.3	214.7	
18 R		21.4	5.0			429.3	278.0	230.0	290.0
19 L		23.3	6.4			505.0	512.7	291.3	543.3
Average		**15.5**	**5.9**			**431.5**	**383.2**	**314.9**	**373.1**
Stdev		**4.1**	**3.2**			**56.8**	**79.0**	**84.8**	**137.0**
n		**9**	**8**			**9**	**8**	**9**	**8**
*13 L		15.1	9.4			706.9	879.1	431.6	743.8
13 R		15.4	9.8			333.1		322.3	448.0
14 L		12.8	6.7			440.0	559.7	489.7	519.7
14 R		12.2	5.2			417.0	451.7	324.7	568.0
15 L	Apical	11.0	5.0			398.7	405.3	425.7	453.0
15 R		10.6	4.6			358.0	459.0	501.0	369.5
16 R		12.6	7.4			821.7	451.0	795.3	530.0
17 L		9.6	3.6			437.0	391.0	474.7	306.7
18 R		16.3	4.6			445.0	366.3	474.0	345.0
19 L		12.8	4.8			391.0	467.3	375.7	643.3
Average		**12.6**	**5.7**			**449.0**	**443.9**	**464.8**	**464.8**
Stdev		**2.2**	**1.9**			**144.8**	**59.3**	**141.8**	**111.0**
n		**9**	**9**			**9**	**8**	**9**	**9**

Legend for Table 4-3: The units of measurements are: root perimeter (mm), PDL volume (mm^3), and PDL widths and heights (µm). Missing data are due to the absence of alveolar bone in any of the slices in the selected region which made it impossible to measure PDL height. The results of the statistical analysis are reported in Figure 4-2 for root perimeter, Figure 4-3 for PDL volume, Figure 4-4 for PDL width. * denotes the side that only received ligature and one bacterium and thus its values were not included in the calculations of average and standard deviations.

Table 4-4: µCT measurements of root perimeter, PDL space volume and PDL space width for MP roots of control Dm3s.

Pig #	Level	Root perimeter	PDL volume	Apical height	Mesial width	Distal width	Buccal Width	Palatal width
1								
2		10.3	6.1	505.0	402.0	293.3	338.3	363.7
3		10.1	2.8	478.0	402.0	165.0	287.3	366.0
4	**Cervical**	12.4	3.7	565.0	264.9	368.8	345.3	379.8
5		10.8	3.9	329.0	344.7	367.3	207.0	459.3
7		12.5	3.4	364.0	296.0	363.0	326.0	381.0
9		9.4	3.0	335.0	413.7	290.0	316.3	378.3
10		11.7	6.2	669.0	469.0	354.0	574.7	488.3
11		11.5	4.3	432.0	364.0	380.7	315.7	323.7
Average		***11.1***	***4.2***	***459.6***	***369.5***	***322.8***	***338.8***	***392.5***
Stdev		***1.1***	***1.3***	***119.4***	***66.5***	***72.6***	***104.8***	***54.0***
n		***8***	***8***	***8***	***8***	***8***	***8***	***8***
1								
2		9.2	7.1		389.3	319.0	414.7	357.7
3		11.1	2.6		395.0	430.7	280.0	287.3
4	**Midroot**	9.4	3.3		310.8	322.3	367.6	298.7
5		10.0	3.7		389.3	319.0	197.7	485.3
7		11.3	3.4		290.0	284.0	338.7	393.0
9		8.5	2.8		465.0	342.3	316.3	412.3
10		10.4	4.5		440.3	325.7	497.7	440.7
11		10.5	4.7		348.0	364.0	420.7	477.3
Average		***10.0***	***4.0***		***378.5***	***338.4***	***354.2***	***394.0***
Stdev		***1.0***	***1.4***		***60.0***	***43.6***	***93.0***	***75.2***
n		***8***	***8***		***8***	***8***	***8***	***8***
1								
2		7.9	6.8		459.3	344.7	498.0	459.7
3		5.7	2.3		423.3	423.3	423.7	215.3
4	**Apical**	6.9	2.6		402.1	528.7	620.6	290.9
5		9.2	3.0		421.3	293.3	166.0	332.0
7		8.6	3.1		320.7	356.7	356.7	266.0
9		7.1	2.1		403.7	377.0	333.0	298.7
10		9.6	3.8		388.7	354.0	584.0	344.3
11		9.6	4.5		315.3	258.7	429.0	324.0
Average		***8.1***	***3.5***		***391.8***	***367.1***	***426.4***	***316.4***
Stdev		***1.4***	***1.5***		***50.1***	***82.3***	***145.9***	***71.0***
n		***8***	***8***		***8***	***8***	***8***	***8***

Legend for Table 4-4: The units of measurements are: root perimeter (mm), PDL volume (mm^3), and PDL widths and heights (µm). The results of the statistical analysis are reported in Figure 4-2 for root perimeter, Figure 4-3 for PDL volume, Figure 4-4 for PDL width.

Table 4-5: µCT measurements of root perimeter, PDL space volume and PDL space width for MP roots of non-ligated Dm3s.

Pig #	Level	Root perimeter	PDL volume	Apical height	Mesial width	Distal width	Buccal Width	Palatal width
***12 L**		11.4	0.8	498.0	396.3	344.3	271.0	313.0
12 R		12.4	3.5	595.0	302.8	268.3	391.0	299.0
16 L	***Cervical***	12.6	5.0	833.0	344.7	287.3	591.0	287.0
17 R		11.2	3.6	690.0	299.7	364.0	274.3	204.3
18 L		14.4	2.8		330.7	222.3	287.0	172.3
19 R		19.1				603.0	644.7	
Average		***13.9***	***3.7***	***706.0***	***319.4***	***349.0***	***437.6***	***240.7***
Stdev		***3.1***	***0.9***	***119.8***	***21.8***	***150.9***	***171.7***	***62.0***
n		***5***	***4***	***3***	***4***	***5***	***5***	***4***
***12 L**		8.7	2.4		208.7	375.7	271.3	250.0
12 R		10.3	2.9		291.3	352.7	337.3	329.7
16 L	***Midroot***	10.1	9.7		295.3	344.7	406.0	418.3
17 R		9.0	2.7		299.7	312.7	325.5	204.0
18 L		10.4	2.4		352.0	316.0		366.3
19 R		12.9	4.9		408.7	497.7	568.0	376.7
Average		***10.5***	***4.5***		***329.4***	***364.7***	***409.2***	***339.0***
Stdev		***1.4***	***3.0***		***50.7***	***76.3***	***111.7***	***81.8***
n		***5***	***5***		***5***	***5***	***4***	***5***
***12 L**		5.2	1.6		260.7	334.0	323.3	365.3
12 R		7.4	2.3		191.7	406.0	322.0	352.7
16 L	***Apical***	8.5	2.8		377.3	352.7	590.5	459.3
17 R		7.2			274.3	312.7		268.0
18 L		10.4	2.9		502.7	258.3	617.3	395.0
19 R		8.4	3.4		530.0	447.0	491.3	274.3
Average		***8.4***	***2.8***		***375.2***	***355.3***	***505.3***	***349.9***
Stdev		***1.3***	***0.5***		***145.0***	***74.5***	***133.7***	***81.3***
n		***5***	***4***		***5***	***5***	***4***	***5***

Legend for Table 4-5: The units of measurements are: root perimeter (mm), PDL volume (mm^3), and PDL widths and heights (µm). The results of the statistical analysis are reported in Figure 4-2 for root perimeter, Figure 4-3 for PDL volume, Figure 4-4 for PDL width. * denotes the side that did not receive any ligatures and thus its values were not included in the calculations of average and standard deviations.

Table 4-6: µCT measurements of root perimeter, PDL space volume and PDL space width for MP roots of ligated Dm3s.

Pig #	Level	Root perimeter	PDL volume	Apical height	Mesial width	Distal width	Buccal Width	Palatal width
*13 L		11.0	4.8	1275.0	483.2	534.2	689.6	137.9
13 R				656.0	448.0	494.4	379.1	
14 L		11.4	4.4	705.0	390.0	250.0	430.0	
14 R		11.4	4.6	965.0	434.0	408.3	440.3	357.3
15 L	Cervical	10.3	3.4	667.0	398.3	372.0	317.3	250.0
15 R		10.6	4.5	854.0	443.0	443.5	492.5	189.5
16 R		12.1		1809.0		527.5	608.0	304.3
17 L		11.7		576.0	368.0	459.7	345.0	218.5
18 R		17.9	4.7		514.0	393.0	399.0	205.7
19 L		19.5				585.5	597.0	
Average		**13.1**	**4.3**	**890.3**	**427.9**	**437.1**	**445.4**	**254.2**
Stdev		**3.5**	**0.5**	**426.0**	**48.3**	**97.5**	**103.0**	**64.8**
n		**8**	**5**	**7**	**7**	**9**	**9**	**6**
*13 L		9.3	3.0		264.2	528.4	494.0	172.3
13 R		9.5	7.1		344.7	1690.0	448.6	242.4
14 L		9.2	3.2		350.0	330.0	350.0	250.0
14 R		8.9	3.2		293.3	383.0	485.3	376.7
15 L	Midroot	10.0	2.7		405.3	344.7	182.3	297.3
15 R		7.6	3.1		377.5	427.0		270.5
16 R		9.2			567.7	479.7		473.3
17 L		8.8	3.8		337.3	505.3	494.0	345.0
18 R		14.3	5.1		568.7	471.3	462.5	477.7
19 L		12.7	5.4		467.0	589.3	696.7	406.3
Average		**10.0**	**4.2**		**412.4**	**580.0**	**445.6**	**348.8**
Stdev		**2.1**	**1.5**		**100.7**	**424.2**	**155.8**	**90.9**
n		**9**	**8**		**9**	**9**	**7**	**9**
*13 L		7.7	3.5		345.9	449.0	529.3	368.1
13 R		7.8	6.4		356.7		436.6	391.2
14 L		8.1	3.6		290.0	340.0	301.3	360.0
14 R		5.7	2.5		325.3	389.3	510.7	261.7
15 L	Apical	5.4	1.8		278.0	387.0	369.0	368.7
15 R		5.0	1.9		509.5	435.0	410.5	262.5
16 R		7.1			526.7	648.7		473.3
17 L		6.5	2.2		406.3	429.0	329.7	245.3
18 R		7.7	6.0		683.0	777.3	674.3	788.3
19 L		8.2	3.5		543.7	490.3	612.3	329.7
Average		**6.8**	**3.5**		**435.5**	**487.1**	**455.5**	**386.7**
Stdev		**1.2**	**1.8**		**137.8**	**150.1**	**133.6**	**167.4**
n		**9**	**8**		**9**	**8**	**8**	**9**

Legend for Table 4-6: The units of measurements are: root perimeter (mm), PDL volume (mm^3), and PDL widths and heights (µm). Missing data are due to the absence of alveolar bone in any of the slices in the selected region which made it impossible to have a PDL height measurement. The results of the statistical analysis are reported in Figure 4-2 for root perimeter, Figure 4-3 for PDL volume, Figure 4-4 for PDL width. * denotes the side that only received ligature and one

bacterium and thus its values were not included in the calculations of average and standard deviations.

Table 4-7: : µCT measurements of buccal and palatal bone and percent root coverage for the control, non-ligated, and ligated Dm3s.

Pig #	Buccal CEJ-ABC (mm)	MB root length (mm)	% MB root coverage	Palatal CEJ-ABC (mm)	MP root length (mm)	% MP root coverage
1	1.94	8.68	77.71	1.87	8.77	78.65
2	1.59	13.10	87.88	1.86	11.27	83.49
3	2.64	8.79	69.93	1.53	12.36	87.66
4	4.88	14.88	67.17	3.56	13.25	73.16
5	3.11	14.36	78.36	1.51	9.69	84.47
7	2.29	13.72	83.35	1.42	12.32	88.46
9	2.41	12.83	81.25	1.54	9.44	83.67
10	2.96	12.51	76.30	1.86	11.37	83.60
11	1.38	12.46	88.96	1.94	10.79	81.99
Average	**2.58**	**12.37**	**78.99**	**1.90**	**11.03**	**82.79**
Stdev	**1.04**	**2.22**	**7.36**	**0.65**	**1.50**	**4.63**
N	**9.00**	**9.00**	**9.00**	**9.00**	**9.00**	**9.00**
*12 L	2.73	12.86	78.77	3.33	12.81	73.98
12 R	3.55	13.88	74.46	2.67	13.37	80.06
16 L	4.34	12.92	66.38	2.98	11.62	74.37
17 R	4.42	14.18	68.81	3.46	11.83	70.80
18 L	4.36	13.03	66.57	3.55	12.94	72.56
19 R	5.20	14.48	64.06	5.57	10.91	48.95
Average	**4.37**	**13.70**	**68.06**	**3.64**	**12.13**	**69.35**
Stdev	**0.59**	**0.69**	**3.96**	**1.13**	**1.00**	**11.92**
N	**5.00**	**5.00**	**5.00**	**5.00**	**5.00**	**5.00**
*13 L	4.12	10.81	61.88	3.51	10.47	66.44
13 R	5.65	12.61	55.17	4.04	11.62	65.25
14 L	5.82	12.71	54.21	4.07	11.86	65.69
14 R	4.97	14.80	66.40	3.75	14.17	73.57
15 L	5.34	14.46	63.06	4.44	12.56	64.63
15 R	5.24	13.38	60.86	4.29	11.86	63.83
16 R	4.23	14.24	70.32	3.96	11.04	64.15
17 L	5.20	12.99	59.98	4.18	12.26	65.94
18 R	5.88	13.76	57.23	4.07	10.24	60.26
19 L	5.48	14.50	62.20	5.78	10.53	45.10
Average	**5.31**	**13.72**	**61.05**	**4.29**	**11.79**	**63.16**
Stdev	**0.51**	**0.83**	**5.21**	**0.60**	**1.18**	**7.63**
N	**9.00**	**9.00**	**9.00**	**9.00**	**9.00**	**9.00**

Legend for Table 4-7: The units of measurements are mm. Note that 'buccal CEJ-ABC' refers to the distance from the buccal CEJ to the buccal alveolar bone crest (ABC), 'MB root length' refers to the linear vertical distance from the CEJ to the apex of the MB root, 'palatal CEJ-ABC refers to the distance of the palatal CEJ to the palatal alveolar bone crest (ABC), 'MP root length' refers to the linear vertical distance from the CEJ to the apex of the MP root. The results

of the statistical analysis are reported in Figure 4-5 for alveolar bone loss, and Figure 4-6 for % root coverage.

Table 4-8: PDL gross morphology along the roots of Dm3 of available H&E samples of control and diseased pigs.

Pig #	H&E Side	PDL Organization				
		Apex	Furcation	Cervical third	Mid-root third	Apical third
P1	R	BV, Bundles, Unorganized, patchy	BV, mesh network, lots of fibroblasts	Less obtuse angle than mid-root, Organized, Dense bundles	Dense, oblique	BV, dense, lots of fibroblasts
P2	R	Bundles, Unorganized, patchy	-	Less obtuse angle than mid-root, Organized, Dense bundles	Dense, oblique	BV, dense,
P3	R	Bundles, Different directions, Patchy	Lots of fibroblasts, Not good stain	Less obtuse angle than mid-root, Organized, Dense bundles	Oblique , Dense, Organized in bundles	BV, dense,
P4	R	Thick bundles, different directions, patchy, BV	-	Less obtuse angle than mid-root, Organized, Dense bundles	Dense, oblique	BV, dense,
P6	R	BV, Bundles, Different directions, Patchy	-	Less obtuse angle than mid-root, Organized, Dense bundles	Oblique , Dense, Organized in bundles	BV, Dense, Lots of fibroblasts, Bundles of fiber
P7	R	Unorganized fiber bundles in different directions	Network of fibers, BV, Patchy	Less obtuse angle than mid-root, Organized, Dense bundles	Oblique, Dense, Organized in bundles	BV, Dense, Lots of fibroblasts Bundles of fiber different directions
P14	R	Very large space, LOTS of fibroblasts, Lots of cells, LOTS of BV, Same general direction but patchy	-	-	Oblique , Dense, Organized in bundles	Lots of fibroblasts, Oblique fibers, Organized, Dense

Legend for Table 4-8: Description of PDL fiber bundle organization around the roots of the Dm3 (P1-P7, periodontal health) and M1 (P14, periodontal disease pig). BV: blood vessel.

Chapter 5

Changes in alveolar bone modeling in a rabbit disuse model

"..... the form of a bone being given, the bone elements place or displace themselves in the direction of functional forces and increase or decrease their mass to reflect the amount of functional forces." Wolff's law, 1892 [295].

There are various ways to study the effect of muscle loading on growth and architecture of bones. One of the methods is to make a disuse model, by paralyzing the muscle and studying its influence on the bones that it loads. In this chapter I will describe a disuse model that was created in rabbits by paralyzing the masseter muscle unilaterally by injection of *Clostridium botulinum* neurotoxin serotype A (BoNT/A), in order to investigate its effects on the alveolar bone.

Expectation: Unloading of the mandible, caused by temporarily paralyzing the masseter muscle with BoNT/A, will lead to reduction of relative bone density around the mandibular molars.

Rationale: The paralyzed masseter muscle will not be able to exert the same force on the alveolar bone as a normal masseter muscle does, and thus unloading should lead to disuse atrophy of the bone.

Note: Part of the results of this chapter, from group 1 (single-injection) have been published as part of a larger study [296].

5.1 INTRODUCTION

Studying the response of bone to various loading conditions, such as increased or decreased loading, has been a topic of interest for a long time. This translates to hyper-function or hypo-function of the muscles of mastication. In this chapter I will be focusing on effects of hypo-function of the masseter muscle on the alveolar bone. There are various techniques for creating a hypo-functional state of the muscle that results in its disuse atrophy.

In this study Botox® injection into masseter muscle was chosen to study the effect of masseter paralysis on morphology of the tooth-bearing bone. In using BoNT/A to create a disuse model, this study follows recent trends [297], [298]. In contrast to older methods such as compared to tooth extraction [299], use of occlusal bite appliances [300]–[302], and soft diet [303]–[305], which affect chewing and jaw muscles generally, BoNT/A can be targeted to individual muscles. Compared to other methods of inducing disuse atrophy of the masseter muscle such as nerve lesions [306], [307], and muscle resection [308], the injection of the toxin is much less invasive and less traumatic, and is far easier to carry out reliably. Further, the anatomical contacts between the nerve and the muscle remain intact [309].

5.1.1 *Botulinum neurotoxin and animal disuse models*

Botulinum neurotoxins (BoNT) are nature's most potent neurotoxins in the form of metalloproteases and are produced by gram-positive, spore-forming, anaerobic *Clostridium* bacterium [310], [311]. In the early 19th century, the clinical presentation of the motor and autonomic effects of botulism were first described by Justinus Kerner [312] along with speculations about the potential therapeutic uses of the toxin. There are seven different serologic botulinum neurotoxins with various isoforms that are denoted as BoNT/X, where X refers to one

of the seven immunological serotypes A-G and the isoform of the serotype is then denoted by a number after X [311], [313], [314]. Botulinum neurotoxin serotype A (BoNT/A) is one of the members of the botulinum family that has been put to good clinical and cosmetic use [310]. The first therapeutic use of the toxin was in the 1960s for treatment of strabismus in infants [312], [315]–[317]. BoNT/A is by far the most widely used form of the neurotoxin and it is manufactured under the name of Botox® (Allegran Inc. Irvine, CA, USA), Xeomin® (Merz Pharmaceuticals, Frankfurt/M, Germany), and Dysport® (Ipsen Ltd, Slough, Berks, UK) [309], [312].

5.1.2 *Mechanism of action of botulinum neurotoxins*

BoNT/A is a paralyzing agent of cholinergic junctions that acts by preventing exocytosis at the nerve terminals [311], [318], [319]. BoNT is composed of a heavy (100 kD) and a light (50 kD) amino acid chain, which are connected by a single disulfide bond [312], [319]. The structural organization of the neurotoxin allows it to intoxicate the neurons through four steps of 1) binding, 2) internalization, 3) translocation, and 4) enzymatic cleavage of the target protein [320]. When the BoNT is injected into a target muscle, it selectively binds to the cholinergic nerve terminals, and its light chain is internalized [320]. Once internalized different BoNT serotypes target different SNARE (**s**oluble **N**-ethylmaleimide-sensitive fusion **a**ttachment protein **re**ceptor) proteins which transport the acetylcholine vesicles from the intracellular space into the synaptic cleft [309], [320]. Type A toxin targets and cleaves SNAP-25 (synaptosome-associated protein of 25 kDa), a membrane-associated protein of the nerve terminal, but leaves residues 181-197, forming a stable but non-functional SNARE complex at the nerve endings [321]–[323]. While the cholinergic synapse at the neuromuscular junction is blocked by the neurotoxin, new

neuronal sprouts arise from the parent nerve and make new synapses [310], [319], [324]. However, it is now thought that these new neuronal sprouts are a temporary recovery mechanism, and the original blocked synapses regenerate with time while the sprouts are retracted [325]. This transient muscle paralysis and long-lasting synaptic blockade at the neuromuscular junction has been exploited to treat a variety of muscle hyperactivity and neuromuscular disorders [326].

5.1.3 *Therapeutic and cosmetic uses of Botox®*

Depending on the target tissue that the BoNT/A is injected into, either cholinergic neuromuscular transmission of skeletal muscles, or the cholinergic autonomic innervation to the sweat glands, salivary glands, tear glands, or smooth muscles is targeted and temporarily paralyzed. Therefore, the variety of the conditions that are being treated with injection of the neurotoxin includes but is not limited to muscle dystonia, tremor, spasticity, tics, anti-nociceptive action in treatment of osteoarticular pain and peripheral neuropathies, and hyperhidrosis, as well as the neurotoxin's extensive use in cosmetics to paralyze facial muscles for improvement of wrinkles and facial contour [310], [318], [327]–[334].

It is reported that botulinum neurotoxin, if used within the reported therapeutic and cosmetic range, is relatively safe, although dose dependent, since the effects are transient and last 4-6 months [310], [312], [319]. However, among the adverse effects is the possible spread of the neurotoxin through the blood stream to distant sites, which could result in unwanted inhibition of distant autonomic and motor nerve endings [312], [332], [335], [336]. Furthermore, the exact effect of the neurotoxin is not well understood, especially on the adjacent tissues, and thus the risk *vs.* benefit of receiving the toxin remains questionable for some cases.

BoNT/A is used in the head and neck muscles, including masticatory muscles, to reduce pain in TMJ disorders, to treat bruxism, trismus, masticatory myalgia, and migraine headaches, and to shrink hypertrophic masseter muscles to round the borders of the face [337]–[342]. Some reports indicate the use of BoNT/A to reduce loading on the alveolar bone for healing of dental implants, especially in patients who have history of bruxism [343]. The loading from the muscles of mastication, especially the masseter muscle, is important in maintaining homeostasis of the alveolar bone which supports the teeth and thus the chewing function. In order to understand the effects of loading on alveolar bone homeostasis, it is important to study it first in an animal disuse model.

5.1.4 *Bone quality in masticatory disuse model*

Alveolar bone, like other bones, relies on the mechanical stimulus that it receives from teeth, which in turn receive loads through muscle contraction [295], [302], [344], [345]. It has long been suggested that changes in the activity of the craniofacial neuromuscular structures strongly influence the underlying bones and their growth and remodeling patterns [306], [307]. The masseter muscle is an important source of loading for the alveolar bone, and most of the animal studies that have created disuse atrophy of the masseter muscle have shown changes in reduction of the density of the alveolar bone compared to control subjects [296], [297], [299], [301]–[303], [306], [307], [346]. In humans, the limited information available is contradictory. In one study, Chang *et.al.*, found no bony changes in the mandibular bone thickness, mandibular volume, and mandibular cortical thickness of adult humans who received Botox® to create atrophy of the lower third of their bilateral masseter muscles [347]. A second study used CBCT images to investigate the effect of BoNT/A injection of the masseter muscle on the density of the

condylar bone [348]. Despite a small sample size, this group showed reduction of trabecular bone density in the condyles of women who received BoNT/A injections in their masseter muscles for orofacial pain, consistent with our previous rabbit study [296].

5.2 Materials and Methods

The experimental methods are summarized in Figure 5-1 and the methods for the μCT scanning are given in Figure 5-2.

5.1.1 *Animals and experimental procedures*

The experiments and sample collection for this aim were completed previously and not by me. A total of 53 five-month-old female New Zealand white rabbits with body weights ranging from 3.8-5.1 kg were used in two studies, one involving a single BoNT/A injection and the other involved three repeated injections. The experimental protocols were approved by the Institutional Animal Care and Use Committee (IACUC) of the University of Washington.

Briefly, the disuse rabbit model was created by injections of BoNT/A, referred to as Botox® (Product of Allergan, Inc., Irvine, CA), into the superficial masseter muscle unilaterally *vs.* similar injection of 0.9% saline as a control (Figure 5-1). Rabbits were in 2 groups. Group 1 received a single injection and tissues were collected either at 4 weeks (n=7 for saline and n=9 for Botox® treatment groups) or at 12 weeks (n=9 for saline and n=10 for Botox® treatment groups). The experimental protocol for these 4 and 12 week rabbits is described in detail elsewhere [296]. Rabbits of group 2 received three repeated injections of either Botox® or saline into one masseter muscle at 12-week intervals. Thus the samples were collected 36 weeks after

the initial injection (n=5 for saline and n=13 for Botox® treatment groups). All the rabbits gained weight as expected, and Botox® had no observable effect on feeding ability. The objective was to analyze the effects of disuse on the mandibular alveolar bone density of adult animals. The mandibular molar region was removed by two vertical cuts through the mandibular body as shown in Figure 5-1, at the mesial and distal borders of the tooth row.

5.1.2 *μCT measurements of alveolar bone*

The analysis of the bone was done using μCT images of the mandibular bone specimens. However, the single injection group (Group 1) was scanned using a different machine [296] than the repeated injection animals in Group 2. I was not involved in scanning the single-injection groups, for which the technique is described elsewhere [296], although I performed the statistical analysis. The molar region was scanned with a Viva CT40 (Scanco, Brüttisellen, Switzerland) at 21μm voxel resolution. The teeth were excluded from the images. A total of 200 consecutive coronal images (4.2mm) at the midpoint of the tooth row were analyzed to obtain tissue volume (TV, mm^3), bone volume (BV, mm^3), and bone volume fraction (% BV/TV, which will be referred to as density for the rest of this chapter) using a threshold of 400. This threshold was determined during a pilot study as optimal for capturing the cortical and trabecular bone within the samples. I scanned the mandibles of Group 2 using a Skyscan 1076 micro CT scanner (resolution 9μm, 74kV, 129 μA, 0.5mm Al filter, 600 ms exposure, and frame averaging of 2). A phantom with appropriate density was scanned under the same conditions. NRecon software was used to reconstruct the scanned images and CTAn software was used to segment the region of interest (ROI) (Figure 5-2), the bone surrounding either the mandibular first molar (M1) or last premolar (P4). Teeth were excluded as before. The ROI was typically 3-5 mm in anterio-

posterior length. As with Group 1, TV, BV, and %TV/BV (density) were determined. I was blinded to treatment groups until measurements were completed.

5.1.3 *Statistics*

Statistical analysis was performed using GraphPad Prism (version 6.0g, GraphPad Software, Inc., La Jolla, CA, USA) and Excel (Microsoft Co., Redmond, WA, USA). Samples were divided into Botox® and saline injected groups and an independent samples t-test was run for bone density on these groups in GraphPad Prism software. Two-way ANOVA with Sidak's multiple comparisons tests were performed to compare the injected side and non-injected sides of rabbits treated with Botox® or with saline, and to compare the injected side of Botox® animals with the injected side of saline animals. Alpha was set to 0.05 and the results were considered statistically significantly different at $P \leq 0.05$.

5.3 RESULTS

The mandibular bone specimens for the 4-week and 12-week single injection rabbits were analyzed separately because the latter had time for recovery. The results are shown in Table 5-1 and examples are illustrated in Figure 5-3. Visual μCT examination suggested that the bone loss in the Botox® injected group was largely due to enlarged marrow cavities (Figure 4-3). At the 4-week end point of the Botox® animals, the tooth-bearing section of the mandibular body showed significant decreases in density from 60% in the saline controls to 54% on the injected side and 56% on the non-injected side ($p \leq 0.01$, Table 5-1). There was a trend for a greater reduction in

bone density on the injected side ($p = 0.04$) [296]. At the 12-week end point, the reductions were no longer statistically significant, although values were still low (Table 5-1).

The results for the 36-week multiply-injected specimens are also presented in Table 5-1. Because the method of μCT imaging was different for this group, the bone density measurements may not be fully comparable to those of the single injected group. Saline animals had values of 55-57%, slightly lower than the 60% value seen in Group 1 saline animals. Botox® animals were lower yet, 49-52%. Despite the very small sample for saline controls (n=5), there was a statistically significant difference in bone density between the injected sides of saline and Botox® rabbits ($P = 0.017$) (Figure 5-4). The non-injected side, although low, did not differ statistically from controls.

If it could be assumed that the difference in scanning methods used for the single injected group and repeated injected group is negligible, we can compare the values between the groups. Under this assumption, the repeated injected Botox® group, showed an even more significant in bone density reduction compared to the 4-week Botox® injected ($P = 0.0313$) and 12-week Botox® group ($P < 0.0001$). A comparison was also done for the saline non-injected groups to find out if the increased age of the 36-week rabbits had any effect on the reduced bone density in the older animals. The P-value suggested no statistically significant difference between the groups, but there was a trend for the 36-week rabbits to have lower density compared to the 4-week ($P = 0.0925$) and 12-week ($P = 0.0892$) animals (Table 5-1).

5.4 DISCUSSION

Due to limitations of analyzing tissues from patients who receive BoNT/A injections for therapeutic and cosmetic reasons, animal models are necessary. In this study rabbits were used as an animal model. Each half of the rabbit lower jaw bone houses the continuously erupting incisors and molars and therefore receives occlusal loading. The two halves are connected via a tight symphysis that occasionally fuses [349]. Although the continuously erupting teeth in rabbits may introduce unusual properties in the surrounding alveolus, reduction of muscle force should still have an effect on the structure of the tooth bearing jaw. The masseter muscle is known to be important in loading the mandibular alveolar bone and thus regulating its growth in rabbits[297]. Thus disuse atrophy of the masseter was expected to result in unwanted changes of the bone [56].

This study verifies that when Botox® is used to paralyze the masseter muscle and thus lower its ability to load the alveolar bone, the relative bone density (% BV/TV) significantly decreased within the first four weeks. Bone density tended towards recovery at 12 weeks, but with additional injections, recovery was less complete. There was a trend for the non-injected side of animals who received Botox® injection to have low bone density as well, although differences were statistically significant only at 4 weeks. This could be due to diffusion of the toxin to other areas, or to the decreased bite force on both sides of the jaw that would result from deactivating one masseter. In rats (which have a more movable symphysis than rabbits and hence less bilateral action of muscles) no effect was seen on the non-injected side [351], suggesting mechanics rather than diffusion for our results. In either case, the effect on the non-injected side was mild and not statistically significant after the recovery period.

In addition to the clear effects of the toxin, mandibular relative density may also show an age effect. The difference in age between the two groups may have played a role in the lower density associated with Group 2. However, we cannot be sure that the change of technique was not responsible for the apparent loss of bone density with age.

The pattern of enlarged marrow spaces leading to lower bone density was also seen in the rat study mentioned previously [351]. If alveolar bone loss also occurs in human alveolar bone on the Botox® injected side, then it would be alarming to use pre-implant Botox® treatment of the masseter. Currently some dentists recommend the use of Botox® injection into the masseter muscles to treat bruxism and also lower the loading of the alveolar bone for integration and increased success rate of immediate dental implants [343]. However, if the architecture of the human alveolar bone changes as does that of rabbits, it could mean that the prognosis of implants when using Botox® could be worse because of the loss of bony support. Besides proper patient education on the knowns and unknowns, more studies need to be done to find a balanced treatment option that would help the patients with bruxism have better success in retaining their immediate implants. The larger marrow spaces and decreased bone density seen in rabbits may be especially important for women, who on average have less dense bone than men and are more prone to osteoporosis. Furthermore, women receive more cosmetic injections of BoNT/A [334], [347]. Admittedly, clinical studies have not shown deleterious effects, for example, a recent study utilizing CT scans was used to evaluate the mandible 3 months after BoNT/A injection in square faced patients [347]. The authors found no significant changes in the thickness of the mandibular cortex, mandibular bone, and mandibular volume, while reporting that the bilateral masseter muscles showed 30% reduction in volume as desired [347]. One point to keep in mind however, is that the resolution of regular medical CT scans is not as good as detailed resolution

that can be obtained from μCT imaging [347]. Another point is that the study was conducted after a single treatment and a recovery period (as in my 12-week rabbits, which had normalized values). Multiple treatments, which are common clinically, might show different findings.

For this study several limitations were present. Because the first group was scanned using the Viva CT40 and the last group was scanned using the Skyscan 1076 micro CT scanner, thus the thresholds for the two groups were not the same and the results are not directly comparable. Among the technical problems that I encountered with Group 2 was that the mandibular bone specimens were not all the same length. Note that Group 1 was standardized to the length of 4.2mm. This was addressed by focusing on the P4/M1 area for data analysis. Another potential shortcoming of my method is that I worked with whole horizontal slices and did not distinguish between buccal and lingual bone, whereas in reality there might be a higher reduction of density on the buccal cortex, which appears to have more marrow spaces and nutrient canals than the lingual cortex of the rabbit jaw. However, a recent rat study has shown that the bone density of the buccal bone was affected to the same degree as that of the lingual bone [338].

5.5 CONCLUSION

Injection of BoNT/A into rabbit masseter muscle unilaterally decreased the alveolar bone density of the injected side from 60% to 53% (12% reduction) after 4 weeks, but as the muscle regains its strength the density returned toward normal (57%, a 5% reduction from saline by 12 weeks). After 3 repeated injections of the toxin into the muscle, there was greater reduction in bone volume even compared to the single injected 4-week samples (49%, a 14% reduction from saline), although a full 12-week recovery had been allowed after each injection. Therefore,

caution needs to be taken when injecting Botox® into the masseter muscle repeatedly especially for elective cosmetic reasons, since repeated injections may permanently affect alveolar bone quality and the main housing support of the dentition.

5.6 FIGURES

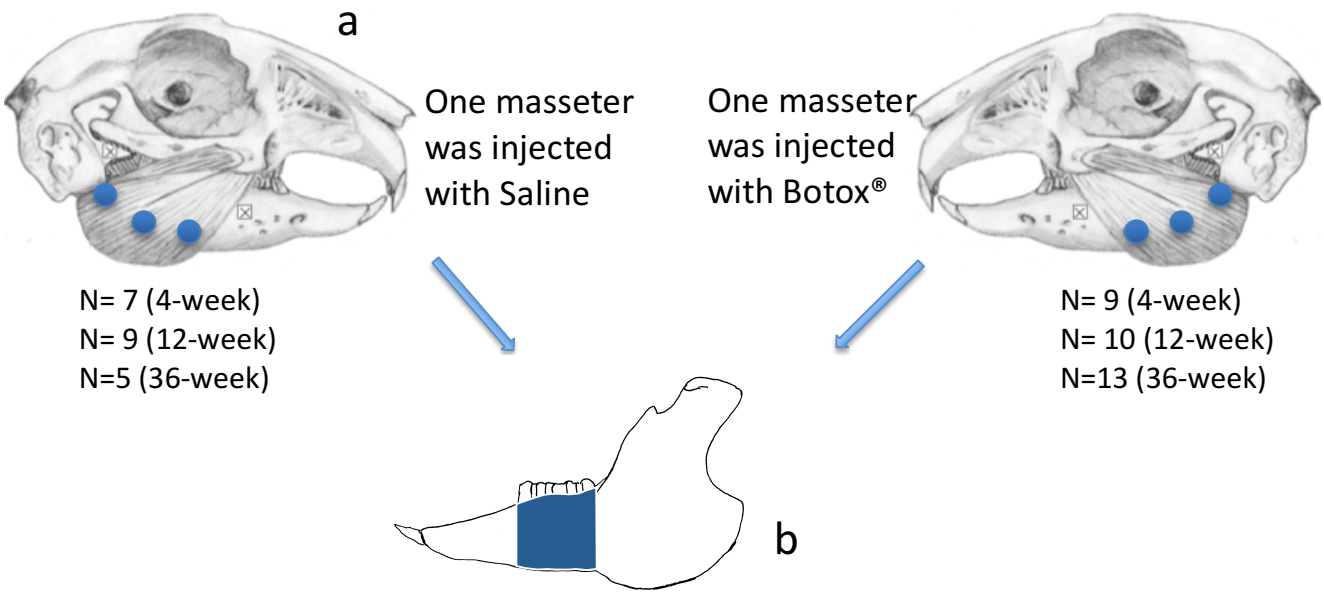

Figure 5-1: Experimental method.

Figure 5-1 legend: Experimental method: one masseter muscle of each rabbit was injected with either Botox® or saline. The 4-week and 12-week rabbits received single injections and allowed to recover for either 4 or 12 weeks. The 36-week rabbits were injected three times, with a 12-week recovery period after each injection. N represents the sample size for each treatment group. a: Shows the injection points of Botox® or saline into superficial masseter muscle (Blue circles). b: Shows the region of the mandible that was removed and scanned. (Picture from Dr. Herring).

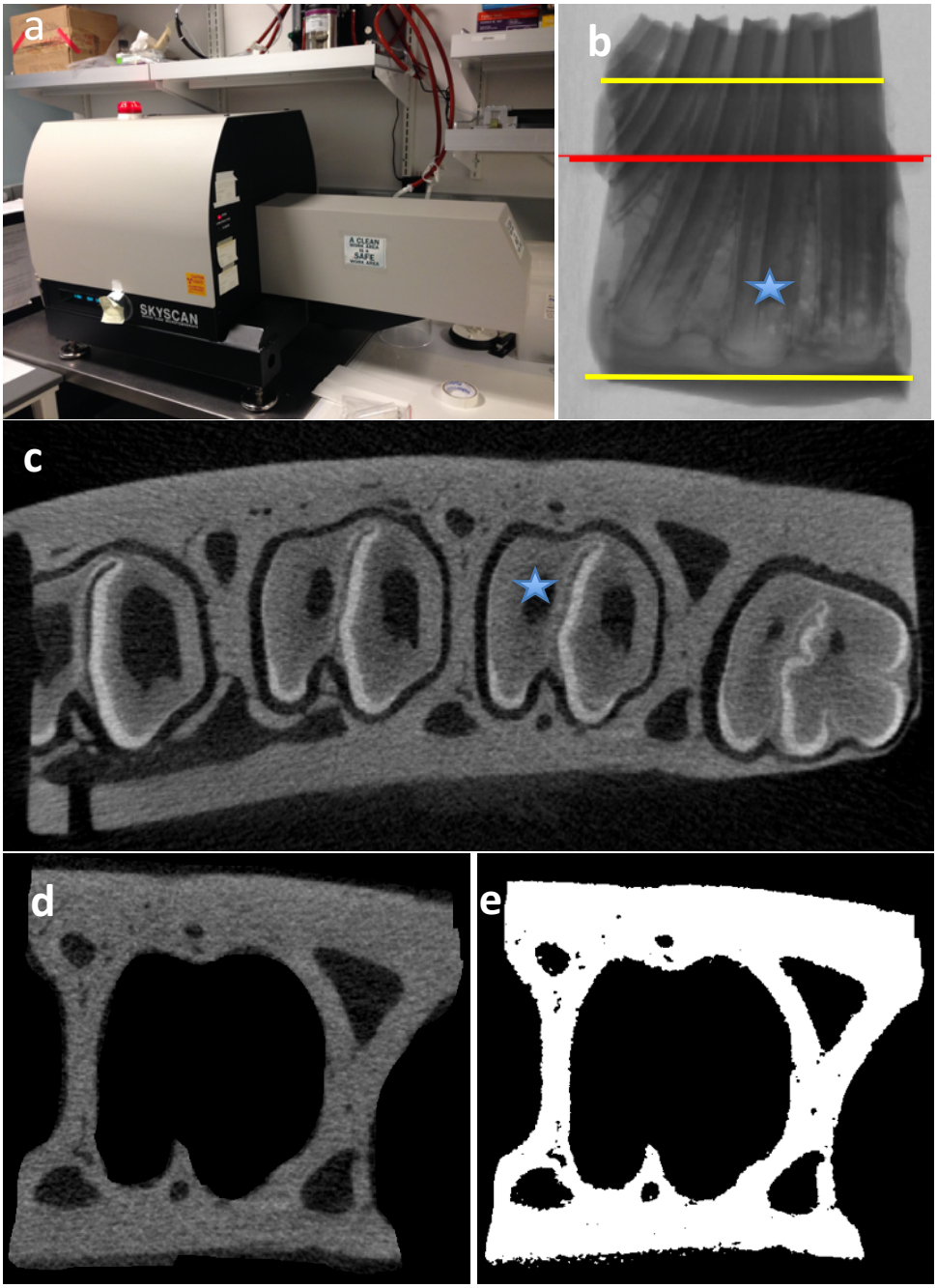

Figure 5-2: µCT method for mandibular density measurement.

Figure 5-2 legend: a: μCT scanner. b: Raw μCT scout image. the yellow lines indicate the cervical and apical limits of the measured tooth. Red horizontal line marks the level of the scout image for which the reconstruction and analysis is done and from which c, d, and e are taken. The blue asterisk shows the P4 tooth. c: Reconstructed μCT image segment containing the lower cheek teeth of the rabbit jaw. Blue asterisk points to the P4. d: Segment of alveolar bone surrounding the last premolar (P4), ready for analysis. e: Digitized image after removal of the tooth, thresholding and recoloring bone pixels to white.

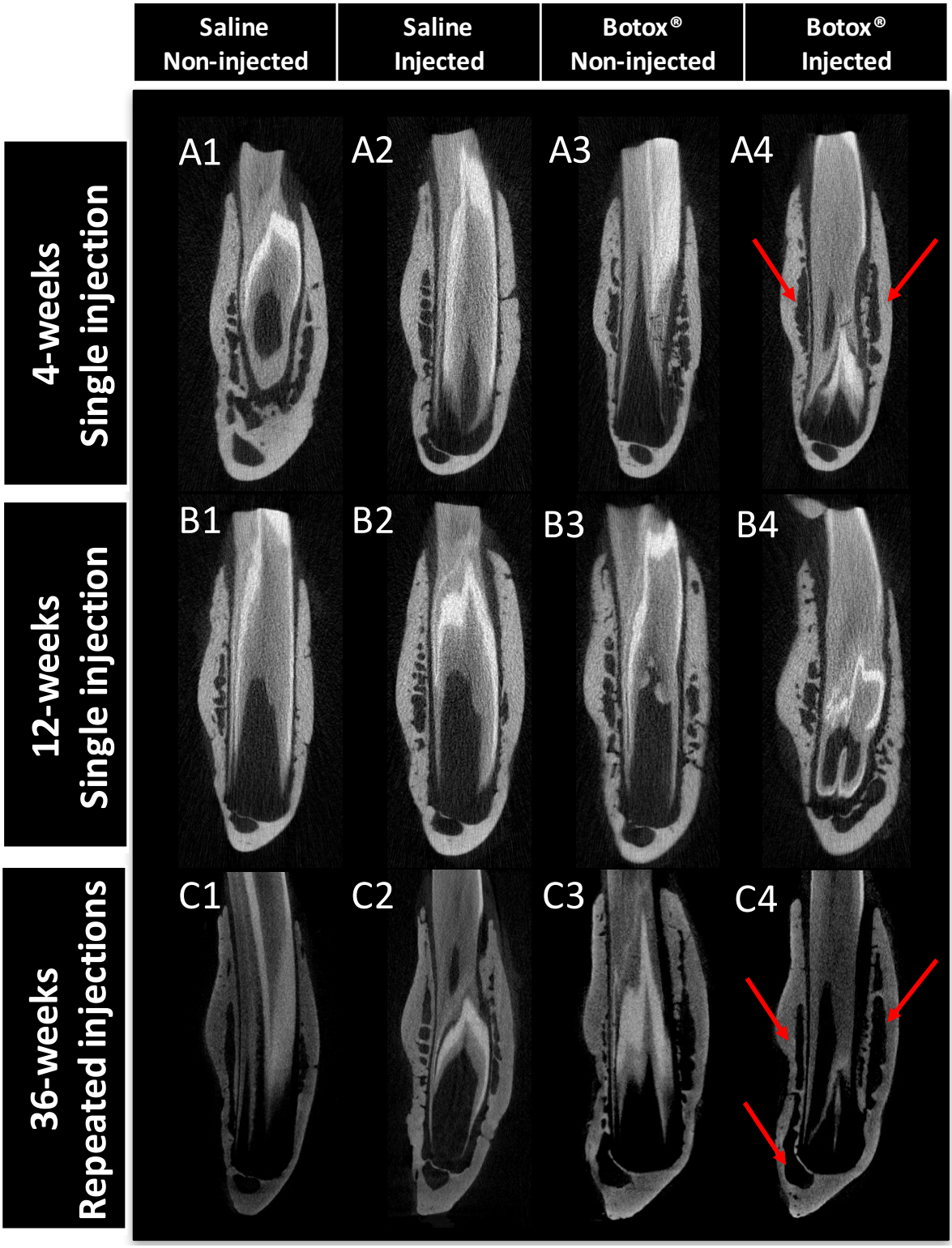

Figure 5-3: Coronal μCT images showing mandibular bone around P4 for the single and repeated saline and Botox® injected groups.

Figure 5-3 legend: Coronal plane μCT slices showing examples of the tooth-bearing region of the mandibular bone for the saline and Botox® injected and uninjected treatment groups at 4-weeks (A1-A4), 12-weeks (B1-B4), and 36-weeks (C1-C4). Red arrows show apparently enlarged marrow cavities on the injected side of Botox® animals.

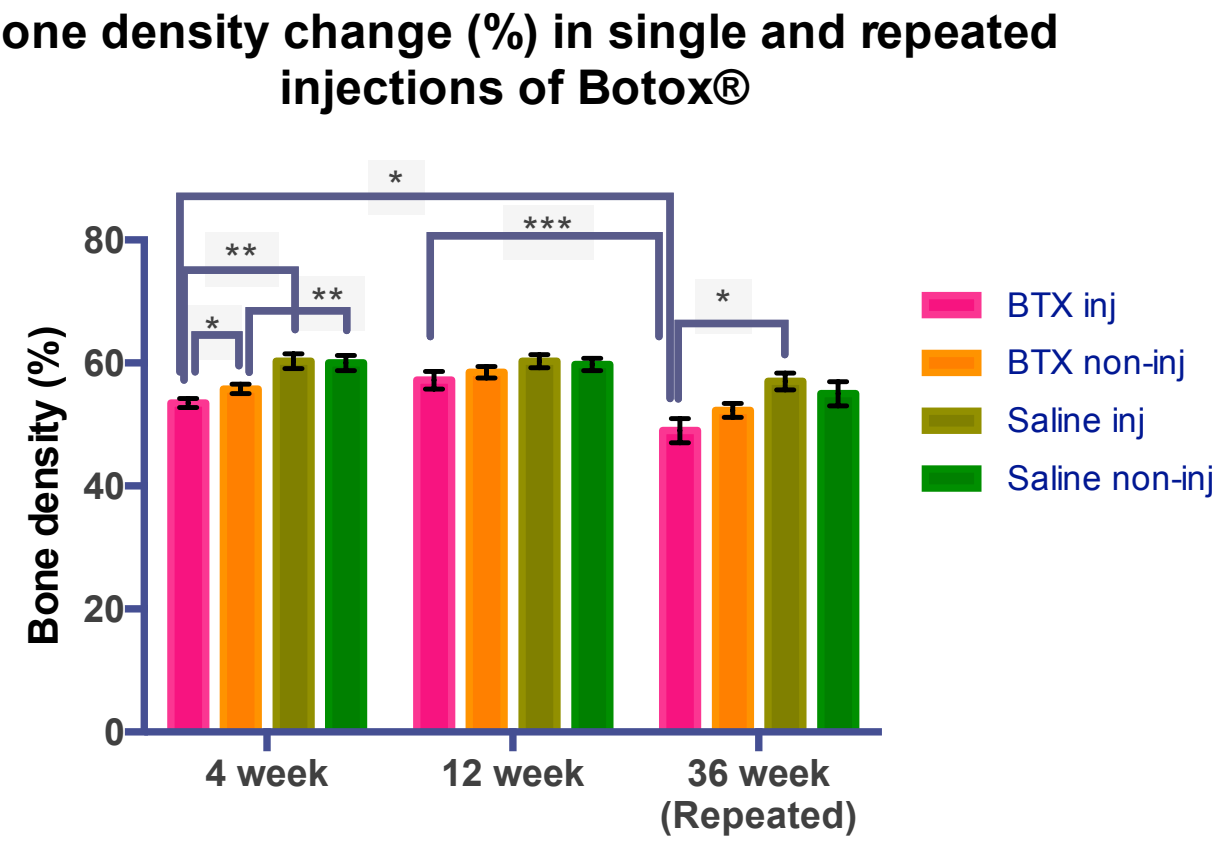

Figure 5-4:% relative bone density change in the mandibular bone bearing the P4.

Figure 5-4 legend: Change in % mandibular bone density is significant 4 weeks after single injection of Botox® and 12 weeks after multiple injections of Botox® compared to saline injected control rabbits. Data are presented as means and error bars are representing the standard error of the mean. * $P < 0.05$, and ** $P \leq 0.01$, *** $P \leq 0.0001$, see Table 5-1.

5.7 TABLES

Table 5-1: Mandibular bone density after unilateral masseter paralysis.

Table 5-1 Legend: Bone density (% BV/TV) measurements of single (4-weeks and 12-weeks group) and repeated (36-weeks group) injections of Botox® and saline into one masseter muscle. Data are reported as mean [standard deviation].

Group	Treatment	Injected side	Non-injected side	P- value
4-Weeks	Saline (n=7)	60.3 [3.1]	60.0 [3.2]	**NS**
	Botox® (n=9)	53.5 [2.1]	55.8 [2.4]	**0.04**
	P- value	**0.0001**	**0.01**	
12-Weeks	Saline (n=9)	60.3 [3.3]	59.8 [3.3]	**NS**
	Botox® (n=10)	57.2 [4.6]	58.5 [3.0]	**NS**
	P- value	**NS**	**NS**	
36-Weeks	Saline (n=5)	57.0 [3.9]	55.9 [4.4]	**NS**
	Botox® (n=13)	49.5 [7.9]	52.3 [4.1]	**NS**
	P- value	**0.017**	**NS**	
4-week *vs.* 12-week	**Saline**	**>0.99**	**0.99**	
4-week *vs.* 36-week	**Saline**	**0.34**	**0.09**	
12-week *vs.* 36-week	**Saline**	**0.31**	**0.08**	

5.8 APPENDIX

Table 5-2: Raw data from 36-weel repeated injection rabbits.

Legend for Table 5-2. The data from measured μCT images are included in the table below.

Rabbit ID	Inj side	Treatment	BV	TV	BV- non inj	TV- non inj
3866	R	Saline	0.515	1.004	0.507	1.046
3875	L	Saline	0.546	1.052	0.520	1.024
8002	L	Saline	0.586	1.042	0.612	1.054
8007	L	Saline	0.598	1.051	0.567	1.003
8008	R	Saline	0.606	1.011	0.589	1.001
3867	R	Botox®	0.484	0.999	0.494	1.043
3868	L	Botox®	0.538	1.059	0.517	1.051
3870	R	Botox®	0.497	1.016	0.508	1.024
3871	L	Botox®	0.509	1.052	0.490	1.000
3872	R	Botox®	0.251	0.807	0.522	1.018
3873	L	Botox®	0.544	1.049	0.540	1.000
3874	R	Botox®	0.501	1.003	0.508	1.015
7999	R	Botox®	0.569	1.004	0.584	1.008
8000	L	Botox®	0.555	1.030	0.599	1.034
8001	R	Botox®	0.507	1.009	0.570	1.048
8003	L	Botox®	0.464	0.993	0.471	0.966
8005	L	Botox®	0.511	1.028	0.534	1.012
8006	L	Botox®	0.504	0.992	0.466	0.994

CHAPTER 6

Summary, synthesis, and future directions

6.1 Design of Studies

The preceding chapters have shown the detailed methods, results, and discussions for the main five experimental methods that were utilized in this dissertation to 1) establish an experimental moderate periodontitis model in pigs, 2) characterize the magnitude and direction of tooth movement during periodontal health and disease in pigs, 3) compare the changes in PDL and the tooth-bearing alveolar bone during periodontal health and disease, and 4) characterize the quality of the tooth bearing alveolar bone in a disuse rabbit model. Although it would have been ideal to look at the relationship between the tooth and all of its supporting periodontium (alveolar bone, PDL, and gingiva) in health, disease and disuse in a single animal model, this was not feasible for the following reasons. The immunity of pigs to botulinum neurotoxin made it impossible to study the disuse atrophy of the masseter muscle as a result of BoNT/A injection in pigs [240]. Furthermore, the small size of rabbit molariform teeth made it impossible to use this model for implantation of the ultrasound crystals and to study the masticatory tooth movement in rabbits. Therefore, the preceding chapters were organized as such to present the association between tooth and its supporting periodontium during health and disease in pigs, and during health and disuse in rabbits.

6.1.1 *Pig experimental periodontitis model*

Existing studies that involve periodontitis in pigs failed to detail the methods for induction of disease and most used a combination of mechanical removal of the alveolar bone and ligatures to induce periodontitis [170], [193]. Although pigs have been well characterized for peri-implantitis studies [192], [352], the mechanisms for induction of peri-implantitis and periodontitis are different since there is no PDL around the implants. In chapter 2 I described the details for a reliable method to induce periodontitis in pigs by using ligatures and a combination of 4 different bacteria. This method proved to induce periodontitis within 8 weeks. Clinical examination showed increased depth of periodontal pockets and increased inflammatory response around the ligated teeth. Histological examination confirmed inflammatory response at the junctional epithelium and apices of ligated teeth, and detailed CBCT analysis revealed extensive bone resorption at the alveolar crest of the ligated teeth.

6.1.2 *Periodontium during periodontal health and disease in pigs*

In chapter 2 and chapter 4 I discussed how induced experimental moderate periodontitis affects the PDL space and PDL itself in pigs and compared it to untreated younger pigs and non-ligated teeth of the same diseased animals. Although there was a significant increase in distance between the CEJ and the alveolar bone crest with age on the non-ligated side of pigs subjected to experimental periodontitis, this increase was even more for the teeth that received ligatures (Figure 4-5). This was associated with enlarged PDL space at the apex of the mesial roots. Within the experimental pigs, greater apex height was seen on the ligated teeth (range of 576-1833 μm) compared to the non-ligated teeth (range of 498-874 μm), whereas control teeth showed a range of 329-764 μm. Evidence of apical abscesses (Figure 4-13 A) in some ligated

teeth suggested that the increased apical space (Figure 4-4) was to some degree due to inflammation and related bone resorption. The non-ligated side might have been affected sub-clinically, but as discussed in Chapter 4 with regards to the changes seen in pilot P12, and non-ligated Dm3s, I cannot rule out the possibility of an age change, perhaps due to continued eruption and growth of the pigs.

Previous studies have indicated bone loss in the furcation as a common pathology during periodontal disease [353]. However, in my study the height of the PDL in the furcation region of the experimental periodontitis pigs was not significantly changed (Figure 4-4, Tables 4-1 to 4-6), nor was the width of the PDL space. It is possible that the lack of significant increase in the lateral PDL space and furcation PDL space height could be due to stabilization of the disease after 8 weeks in the pigs and thus growth of new bone in this regions [293]. This possibility could be tested by examining earlier time points in the development of disease.

6.1.3 *Tooth mobility during periodontal health and disease*

In chapter 3 I discussed how Dm3 is displaced during mastication and masseter muscle stimulation during periodontal health and disease. Masticatory muscles such as the masseter transfer force to the tooth and the supporting periodontium and thus maintain the health of the alveolar bone and PDL. As shown in chapter 2 neither the rate of mastication (Figure 2-4), nor the side of chewing was changed during the 8 weeks of developing moderate periodontitis. Furthermore, the data in chapter 3 showed that the magnitude of Dm3 displacement was not changed during moderate periodontitis either (overall averages of 192µm for control Dm3s, 140µm for non-ligated Dm3s, and 170µm for ligated Dm3s). This latter finding is surprising, in

view of the bone loss associated with periodontal disease, but can be related to the structural data from Chapter 4; these data are replotted in Figure 6-1 along with mobility data.

The mobility measurements indicated that under occlusal load from either mastication or masseter contraction, the Dm3 is probably intruded and may also tip either buccally or palatally. Apical movement (intrusion) would be resisted by the oblique PDL fibers along the root and limited by the heights of the PDL space at the root apices and at the furcation. The PDL fibers are less well organized to resist tipping except at the cervical region, but tipping would be limited by PDL space width. As seen in Figure 6-1 and Table 6-1, magnitudes of tooth movement approximate PDL space dimensions, lending credence to the idea that these dimensions control the maximum movement of the teeth under functional and para-functional loads. Importantly, the only one of these 5 dimensions that was altered by periodontal disease was the height of the space at the apex of the roots. By itself, this might have been expected to allow increased intrusion of the tooth, but in view of the fact that furcation space remained small, mobility remained unchanged.

Thus, I propose that the height of the PDL space at the apex of the roots is not a limiting factor for displacement of multi-rooted teeth under loading, nor is the height of the alveolar crest. The vertical movement of these multi-rooted teeth is mainly limited by the height of the space available at the furcation.

In vivo measurements of tooth displacement during mastication and direct correlation between tooth movement during function and its relationship to the PDL space have not been shown previously. However, *ex vivo* studies on rat molars using external loads have also indicated that the furcation plays an important role in regulating the movement of the multi-rooted teeth under vertical loads [226], [248].

An additional factor for why the displacement of Dm3 was not increased during periodontal disease, besides the evidence that the PDL space height at the furcation and around the roots did not change significantly, is that the pig Dm3 tooth has four to six roots [193], and that some of these roots showed bifurcation or even trifurcation apically (Figure 4-13 B,C). This makes the tooth very well supported in the alveolar bony socket, and thus unless the bone loss is extended to this region, there most likely would not be any significant increase in tooth movement.

6.1.4 *Alveolar bone during muscle disuse- rabbit Botox® model*

In addition to disease, disuse of the dentition affects the periodontium. In humans, pigs, and rabbits, the masseter muscle is a major source of load for the teeth and their supporting alveoli. Detailed analysis of the rabbit μCT images revealed that the tooth bearing alveolus was affected significantly by the disuse of the masseter muscle after a single injection of Botox®, but appeared to be recovered by 12 weeks later. However, repeated injections had a much more dramatic effect. Twelve weeks after the third round of injection of the toxin, the density of the mandibular bone was even less than what it was 4 weeks post injection of the first round of injection. This calls for caution when using Botox® or other treatments that result in disuse of the muscles that load the mandible.

6.2 OVERVIEW AND FUTURE DIRECTIONS

The clinical, radiographical, and histological presentation of periodontal disease in the pig model was very similar to that described in humans, however, the morphology of the roots of the pig Dm3 proved to be more complex than that of human maxillary molars, which could make

this model and the associated tooth movement more complicated and less similar to what might occur in humans. Nonetheless, the similarities in the disease progression and tissue response are very similar to humans and for the first time there is a validated and detailed protocol for establishing experimental periodontitis in pigs that can be used reliably to induce moderate periodontal disease.

Examination of the mandibular dentition indicates that both the deciduous and permanent mandibular molars of pigs are more similar to those of humans than are the maxillary molars, and so in future follow up studies it will be of interest to use the mandibular teeth to study the tooth movement direction and magnitude since it may be a better model to represent human multi-rooted teeth. Moreover, the use of ultrasound signaling to study the magnitude and direction of *in vivo* displacement of Dm3 during mastication and masseter stimulation might be less difficult on a mandibular Dm3 due to the fact that the palate would not be in the way. Presumably, the same protocol for producing periodontal disease would also work for mandibular teeth. Furthermore, taking periapical radiographs on the mandibular teeth is more reliable and repeatable than taking them on maxillary teeth due to limited space by the palate.

It will also be interesting to try to determine the peak time for periodontal damage, which was likely earlier than 8 weeks in pigs. The behavior of the periodontal tissue along with the severity of the inflammatory response might be different at the peak of disease progression compared to a more chronic state.

Histologically it is paramount to look at osteoclastic activity around ligated and non-ligated teeth not only at the alveolar crest, but also at the furcation and at the apex of the roots, in addition to examining the neutrophil abundance associated with localized inflammation in these sites. Some of the ligated Dm3s showed development of radiographic periapical lesions (Figure

4-12), but at this point it is not clear whether these are just osteoclastic bone resorptions or if this space also contains inflammatory granulocytes and is a true periodontal abscess [354]. Furthermore, because the pigs were young and still growing, the interaction of disease processes and alveolar apposition presents a complex problem in need of detailed histological exploration.

6.3 FIGURES

A

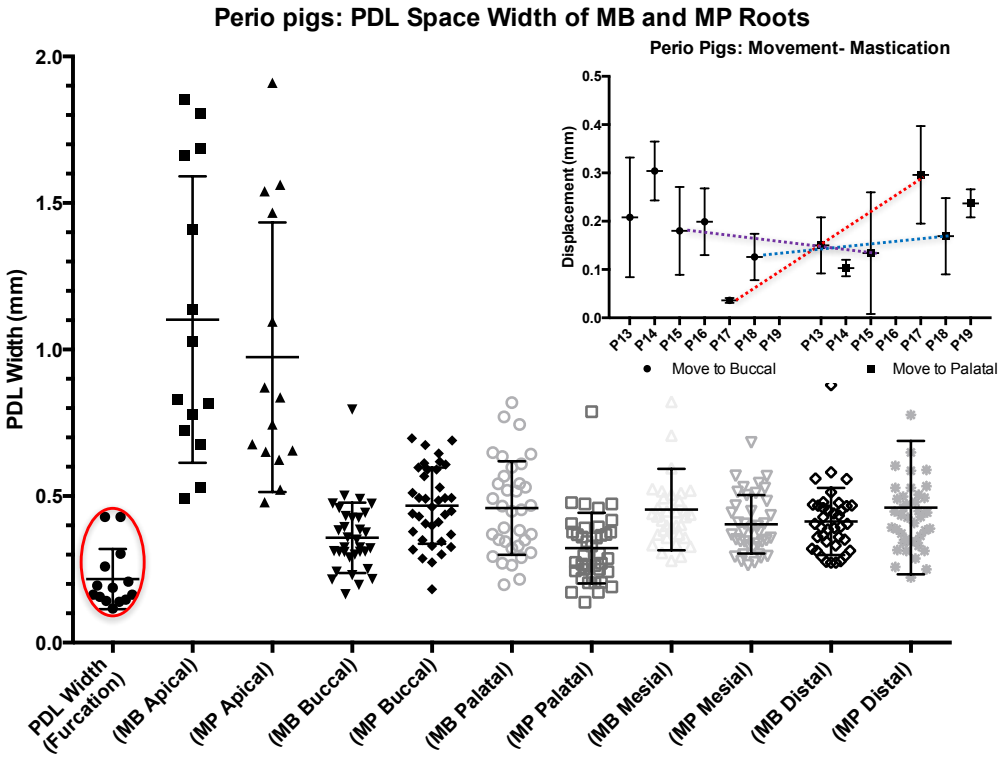

B

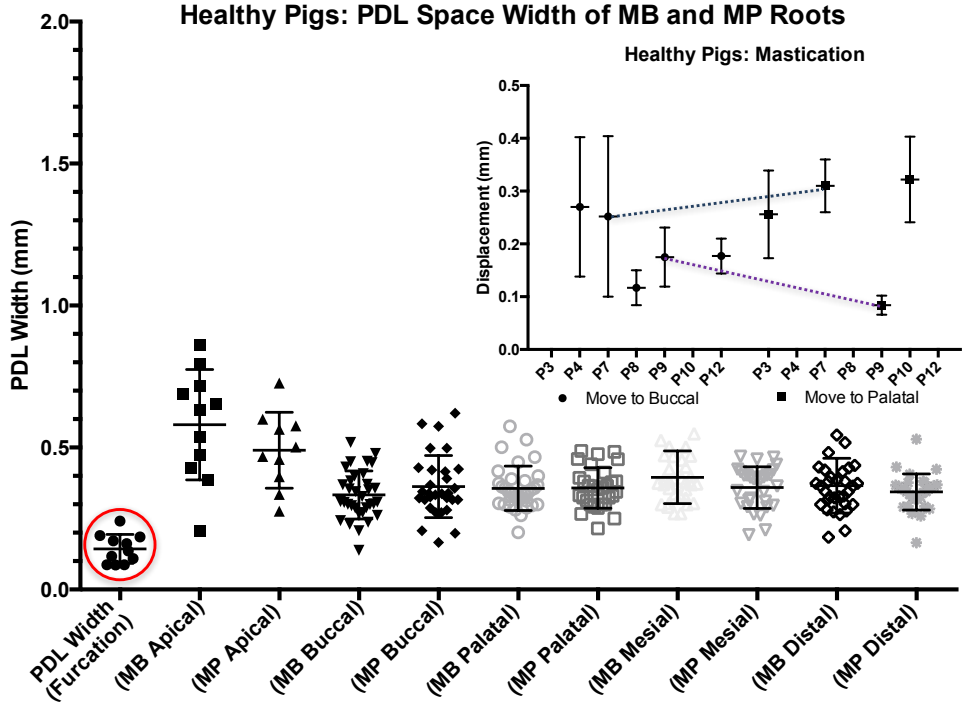

Figure 6-1: Association of tooth movement and PDL space.

Figure 6-1 Legend: Association of the PDL space of the MB and MP roots and the apex and furcation PDL height of Dm3 during periodontal health and periodontal disease with the tooth movement during mastication. Data are represented as mean and the standard deviation. It appears that the tooth movement during both health and disease is closely associated with the PDL space height at the furcation and also the lateral PDL space width, but not affected by the height of the PDL width at the apex of the roots.

Table 6-1: Summary of changes in tooth mobility and PDL and bone changes with moderate periodontitis.

Table 6-1 legend: Data are summarized from Tables 3-3, and 3-4, and 4-1 to 4-7 for the range of tooth movement and range of changes in the periodontium seen during health and moderate periodontitis of control, non-ligated, and ligated Dm3s.

Dm3 Treatment	*Tooth Mobility Range*		*PDL Space Range*			*% Root Coverage*
	Mastication (µm)	***MA Stim. (µm)***	***Furcation***	***Lateral***	***Apex***	
Control	63-322	20-302	238-426	137-698	329-764	78-82%
Non-ligated	96-199	24-139	116-303	165-819	498-874	68-69%
Ligated	36-304	34-322 (545)	147-429	137-1690	576-1833	61-63%

BIBLIOGRAPHY

[1] J. Fox, *Natural history and Diseases of Human Teeth*, 3rd ed. London, 1833.

[2] H. R. Mühlemann, "periodontometry, a method for measuring tooth mobility," *Oral Surgery, Oral Med. Oral Pathol. Oral Radiol. Endodontology*, vol. 4, no. 10, pp. 1220–33, 1951.

[3] M. E. Gher, "Non-surgical pocket therapy: dental occlusion.," *Ann. Periodontol.*, vol. 1, no. 1, pp. 567–80, Nov. 1996.

[4] M. Goellner, C. Berthold, S. Holst, A. Petschelt, M. Wichmann, and J. Schmitt, "Influence of attachment and bone loss on the mobility of incisors and canine teeth.," *Acta Odontol. Scand.*, vol. 71, no. 3–4, pp. 656–63, 2013.

[5] M. Nieri, L. Muzzi, M. Cattabriga, R. Rotundo, F. Cairo, and G. P. Pini Prato, "The prognostic value of several periodontal factors measured as radiographic bone level variation: a 10-year retrospective multilevel analysis of treated and maintained periodontal patients.," *J. Periodontol.*, vol. 73, no. 12, pp. 1485–1493, 2002.

[6] S. N. Laster L, Laudenbach KW, "An evaluation of clinical tooth mobility measurements," *J Periodontol*, vol. 46, no. 10, pp. 603–7, 1975.

[7] M. J. Perlitsh, "a systemic approach to the interpretation of tooth mobility and its clinical implications," *Dent. Clin. North Am.*, vol. 24, no. 2, pp. 177–93, 1980.

[8] T. J. O'Leary, "Tooth mobility.," *Dent. Clin. North Am.*, vol. 13, no. 3, pp. 567–79, Jul. 1969.

[9] C. S. Lear, J. S. Mackay, and A. A. Lowe, "Threshold levels for displacement of human teeth in response to laterally directed forces.," *J. Dent. Res.*, vol. 51, no. 5, pp. 1478–82.

[10] D. C. Picton, R. B. Johns, D. J. Wills, and W. I. Davies, "The relationship between the mechanisms of tooth and implant support.," *Oral Sci. Rev.*, vol. 5, pp. 3–22, 1974.

[11] D. C. Picton, "Tooth mobility--an update.," *Eur. J. Orthod.*, vol. 12, no. 1, pp. 109–15, Feb. 1990.

[12] H. R. MUEHLEMANN, S. SAVDIR, and K. H. RATEITSCHAK, "TOOTH MOBILITY--ITS CAUSES AND SIGNIFICANCE.," *J. Periodontol.*, vol. 36, pp. 148–53, 1965.

[13] F. G. Serio and C. E. Hawley, "Periodontal trauma and mobility. Diagnosis and treatment planning.," *Dent. Clin. North Am.*, vol. 43, no. 1, pp. 37–44, Jan. 1999.

[14] H. Ioi, T. Morishita, S. Nakata, A. Nakasima, and R. S. Nanda, “Evaluation of physiological tooth movements within clinically normal periodontal tissues by means of periodontal pulsation measurements.,” *J. Periodontal Res.*, vol. 37, no. 2, pp. 110–7, Apr. 2002.

[15] H. R. Mühlemann, “Tooth mobility, I. the measuring method. Initial and secondary tooth mobility,” *J. Periodontol*, vol. 25, pp. 22–29, 1954.

[16] G. Svanberg and J. Lindhe, “Experimental tooth hypermobility in the dog. A methodological study.,” *Odontol. Revy*, vol. 24, no. 3, pp. 269–82, 1973.

[17] W. Niedermeier, “Parameters of tooth mobility in cases of normal function and functional disorders of the masticatory system.,” *J. Oral Rehabil.*, vol. 20, no. 2, pp. 189–202, 1993.

[18] D. C. A. Picton, “Vertical movement of cheek teeth during biting,” *Arch. Oral Biol.*, vol. 8, no. 2, pp. 109–118, Mar. 1963.

[19] K. H. Körber, “Electronic registration of tooth movements.,” *Int. Dent. J.*, vol. 21, no. 4, pp. 466–77, Dec. 1971.

[20] D. C. A. Picton, “Some implications of normal tooth mobility during mastication,” *Arch. Oral Biol.*, vol. 9, no. 5, pp. 565–573, Sep. 1964.

[21] G. J. Parfitt, “Measurement of the physiological mobility of individual teeth in an axial direction.,” *J. Dent. Res.*, vol. 39, pp. 608–618, 1960.

[22] G. J. PARFITT, “The Dynamics of a Tooth in Function,” *J Periodontol*, vol. 32, pp. 102–7, 1961.

[23] G. K. Svanberg, G. J. King, and C. H. Gibbs, “Occlusal considerations in periodontology.,” *Periodontol. 2000*, vol. 9, pp. 106–17, Oct. 1995.

[24] M. Heners, “Syndesmotic limiting movement of the periodontal ligament.,” *Int. Dent. J.*, vol. 24, no. 2, pp. 319–327, 1974.

[25] S. M. Bien, “Hydrodynamic damping of tooth movement.,” *J. Dent. Res.*, vol. 45, no. 3, pp. 907–914, 1966.

[26] N. L.-T. Chattah, K. Kupczik, R. Shahar, J.-J. Hublin, and S. Weiner, “Structure-function relations of primate lower incisors: a study of the deformation of Macaca mulatta dentition using electronic speckle pattern interferometry (ESPI),” *J. Anat.*, vol. 218, no. 1, pp. 87–95, Jan. 2011.

[27] L. Lysell, “Qualitative and Quantitative Determination of Attrition and the Ensuing Tooth

Migraton," *Acta Odontol. Scand.*, vol. 16, no. 3, pp. 267–292, Jan. 1958.

[28] G. A. Lammie and U. Posselt, "Progressive changes in the dentition of adults.," *J. Periodontol.*, vol. 36, no. 6, pp. 443–54.

[29] J. L. Saffar, J. J. Lasfargues, and M. Cherruau, "Alveolar bone and the alveolar process: the socket that is never stable.," *Periodontol. 2000*, vol. 13, pp. 76–90, Feb. 1997.

[30] A. Nanci and D. D. Bosshardt, "Structure of periodontal tissues in health and disease*," *Periodontol. 2000*, vol. 40, no. 1, pp. 11–28, Feb. 2006.

[31] D. D. Bosshardt and N. P. Lang, "The junctional epithelium: from health to disease.," *J. Dent. Res.*, vol. 84, no. 1, pp. 9–20, Jan. 2005.

[32] H. E. Schroeder and M. A. Listgarten, "The gingival tissues: the architecture of periodontal protection.," *Periodontol. 2000*, vol. 13, pp. 91–120, Feb. 1997.

[33] Picton DCA, "The part played by the trans-septal fiber system in experimental approximal drift of the cheek teeth of monkeys," *Arch. Oral Biol.*, vol. 18, no. 6, pp. 669–80, 1973.

[34] H. E. Schroeder, S. Münzel-Pedrazzoli, and R. Page, "Correlated morphometric and biochemical analysis of gingival tissue in early chronic gingivitis in man.," *Arch. Oral Biol.*, vol. 18, no. 7, pp. 899–923, Jul. 1973.

[35] H. Zoellner and N. Hunter, "The vascular response in chronic periodontitis.," *Aust. Dent. J.*, vol. 39, no. 2, pp. 93–7, Apr. 1994.

[36] M. C. Brecx, M. Gautschi, P. Gehr, and N. P. Lang, "Variability of histologic criteria in clinically healthy human gingiva.," *J. Periodontal Res.*, vol. 22, no. 6, pp. 468–72, Nov. 1987.

[37] G. B. Anderson, R. G. Caffesse, C. E. Nasjleti, and B. A. Smith, "Correlation of periodontal probe penetration and degree of inflammation.," *Am. J. Dent.*, vol. 4, no. 4, pp. 177–83, Aug. 1991.

[38] B. K. Berkovitz, "The structure of the periodontal ligament: an update.," *Eur. J. Orthod.*, vol. 12, no. 1, pp. 51–76, Feb. 1990.

[39] R. L. MacNeil and M. J. Somerman, "Development and regeneration of the periodontium: parallels and contrasts.," *Periodontol. 2000*, vol. 19, pp. 8–20, Feb. 1999.

[40] H. Ioi, S. Nakata, A. Nakasima, A. L. Counts, and R. S. Nanda, "Changes in tooth position in humans in relation to arterial blood pressure.," *Arch. Oral Biol.*, vol. 47, no. 3, pp. 219–26, Mar. 2002.

[41] A. Mariotti, “The extracellular matrix of the periodontium: dynamic and interactive tissues.,” *Periodontol. 2000*, vol. 3, pp. 39–63, Oct. 1993.

[42] N. L. Leong, J. M. Hurng, S. I. Djomehri, S. A. Gansky, M. I. Ryder, and S. P. Ho, “Age-related adaptation of bone-PDL-tooth complex: Rattus-Norvegicus as a model system.,” *PLoS One*, vol. 7, no. 4, p. e35980, 2012.

[43] M. Bergomi, J. Cugnoni, J. Botsis, U. C. Belser, and H. W. Anselm Wiskott, “The role of the fluid phase in the viscous response of bovine periodontal ligament.,” *J. Biomech.*, vol. 43, no. 6, pp. 1146–52, Apr. 2010.

[44] M. Kagayama, Y. Sasano, I. Mizoguchi, N. Kamo, I. Takahashi, and H. Mitani, “Localization of glycosaminoglycans in periodontal ligament during physiological and experimental tooth movement.,” *J. Periodontal Res.*, vol. 31, no. 4, pp. 229–34, May 1996.

[45] S. P. Ho, R. M. Sulyanto, S. J. Marshall, and G. W. Marshall, “The cementum-dentin junction also contains glycosaminoglycans and collagen fibrils.,” *J. Struct. Biol.*, vol. 151, no. 1, pp. 69–78, Jul. 2005.

[46] T. R. Gould, A. H. Melcher, and D. M. Brunette, “Location of progenitor cells in periodontal ligament of mouse molar stimulated by wounding.,” *Anat. Rec.*, vol. 188, no. 2, pp. 133–41, Jun. 1977.

[47] S. M. Bien, “The pressure gradient in the periodontal vasculature.,” *Trans. N. Y. Acad. Sci.*, vol. 28, no. 4, pp. 496–506, Feb. 1966.

[48] A. Lewin, “direction of tooth movement in response to masticatory forces,” *J. Dent. Res.*, vol. 49, no. 3, p. 699, 1970.

[49] N. Imamura, S. Nakata, and A. Nakasima, “Changes in periodontal pulsation in relation to increasing loads on rat molars and to blood pressure.,” *Arch. Oral Biol.*, vol. 47, no. 8, pp. 599–606, Aug. 2002.

[50] E. Storey, “The nature of tooth movement.,” *Am. J. Orthod.*, vol. 63, no. 3, pp. 292–314, 1973.

[51] G. R. S. Naveh, V. Brumfeld, R. Shahar, and S. Weiner, “Tooth periodontal ligament: Direct 3D microCT visualization of the collagen network and how the network changes when the tooth is loaded,” *J. Struct. Biol.*, vol. 181, no. 2, pp. 108–115, 2013.

[52] S. P. Ho, S. J. Marshall, M. I. Ryder, and G. W. Marshall, “The tooth attachment

mechanism defined by structure, chemical composition and mechanical properties of collagen fibers in the periodontium.," *Biomaterials*, vol. 28, no. 35, pp. 5238–45, Dec. 2007.

[53] P. Sloan, "Structural organization of the fibers of the periodontal ligament," in *The Periodontal ligament in health and disease*, Oxford; New York:Pergamon Press, 1982, pp. 51–72.

[54] E. Kellner, "influence of width of periodontal membrane and cementum in regard to function," *J. Dent. Res.*, vol. 11, pp. 511–13, 1931.

[55] C. Chang, Y. Lei, Y. Ho, Y. Sung, and T. Lin, "Predicting the holistic force-displacement relation of the periodontal ligament : in-vitro experiments and finite element analysis," *Biomed. Eng. Online*, vol. 13, no. 107, pp. 1–11, 2014.

[56] G. R. S. Naveh, N. Lev-Tov Chattah, P. Zaslansky, R. Shahar, and S. Weiner, "Tooth-PDL-bone complex: Response to compressive loads encountered during mastication - A review," *Arch. Oral Biol.*, vol. 57, no. 12, pp. 1575–1584, 2012.

[57] R. Kronfeld, "Histologic Study of the Influence of Function on the Human Periodontal Membrane**From the Research Department of the Chicago College of Dental Surgery, Dental Department of Loyola University.Read before the Section on Periodontia at the Seventy-Second Ann," *J. Am. Dent. Assoc.*, vol. 18, no. 7, pp. 1242–1274, Jul. 1931.

[58] C. Gonzales, H. Hotokezaka, Y. Arai, T. Ninomiya, J. Tominaga, I. Jang, Y. Hotokezaka, M. Tanaka, and N. Yoshida, "An in vivo 3D micro-CT evaluation of tooth movement after the application of different force magnitudes in rat molar," *Angle Orthod.*, vol. 79, no. 4, pp. 703–714, 2009.

[59] G. V. Black, *A study of the Periosteum and Periodontal Membrane*. 1887.

[60] E. R. Richardson, "Comparative thickness of the human periodontal membrane of functioning versus non-functioning teeth.," *J. Oral Med.*, vol. 22, no. 4, pp. 120–6, Oct. 1967.

[61] E. D. Coolidge, "The thickness of the human periodontal memberane," *J. Am. Dent. Assoc. Dent. Cosm.*, vol. 24, no. 8, pp. 1260–70, 1937.

[62] W. Beertsen, C. A. McCulloch, and J. Sodek, "The periodontal ligament: a unique, multifunctional connective tissue.," *Periodontol. 2000*, vol. 13, pp. 20–40, Feb. 1997.

[63] S. Steigman, Y. Michaeli, M. Yitzhaki, and M. Weinreb, "A three-dimensional evaluation

of the effects of functional occlusal forces on the morphology of dental and periodontal tissues of the rat incisor.," *J. Dent. Res.*, vol. 68, no. 8, pp. 1269–1274, 1989.

[64] B. J. Denes, A. Mavropoulos, A. Bresin, and S. Kiliaridis, "Influence of masticatory hypofunction on the alveolar bone and the molar periodontal ligament space in the rat maxilla.," *Eur. J. Oral Sci.*, vol. 121, no. 6, pp. 532–7, Dec. 2013.

[65] S. Ohno, T. Doi, K. Fujimoto, C. Ijuin, N. Tanaka, K. Tanimoto, K. Honda, M. Nakahara, Y. Kato, and K. Tanne, "RGD-CAP (betaig-h3) exerts a negative regulatory function on mineralization in the human periodontal ligament.," *J. Dent. Res.*, vol. 81, no. 12, pp. 822–5, Dec. 2002.

[66] T. Yoshizawa, F. Takizawa, F. Iizawa, O. Ishibashi, H. Kawashima, A. Matsuda, N. Endo, and H. Kawashima, "Homeobox protein MSX2 acts as a molecular defense mechanism for preventing ossification in ligament fibroblasts.," *Mol. Cell. Biol.*, vol. 24, no. 8, pp. 3460–72, Apr. 2004.

[67] J. Kirkham, S. J. Brookes, R. C. Shore, W. A. Bonass, and C. Robinson, "The effect of glycosylaminoglycans on the mineralization of sheep periodontal ligament in vitro.," *Connect. Tissue Res.*, vol. 33, no. 1–3, pp. 23–9, 1995.

[68] A. Takimoto, M. Kawatsu, Y. Yoshimoto, T. Kawamoto, M. Seiryu, T. Takano-Yamamoto, Y. Hiraki, and C. Shukunami, "Scleraxis and osterix antagonistically regulate tensile force-responsive remodeling of the periodontal ligament and alveolar bone.," *Development*, vol. 142, no. 4, pp. 787–96, Feb. 2015.

[69] E. L. Niver, N. Leong, J. Greene, D. Curtis, M. I. Ryder, and S. P. Ho, "Reduced functional loads alter the physical characteristics of the bone-periodontal ligament-cementum complex.," *J. Periodontal Res.*, vol. 46, no. 6, pp. 730–41, Dec. 2011.

[70] R. J. J. Kanoza, L. Kelleher, J. Sodek, and A. H. Melcher, "A biochemical analysis of the effect of hypofunction on collagen metabolism in the rat molar periodontal ligament," *Arch. Oral Biol.*, vol. 25, no. 10, pp. 663–668, 1980.

[71] Y. Kizuki, "Effects of occlusal hypofunction on histological structure and cell activity in periodontal ligament.," *Kōkūbyō Gakkai zasshi. J. Stomatol. Soc. Japan*, vol. 76, no. 2, pp. 91–9, Jun. 2009.

[72] S. Kaneko, K. Ohashi, K. Soma, and M. Yanagishita, "Occlusal hypofunction causes changes of proteoglycan content in the rat periodontal ligament.," *J. Periodontal Res.*, vol.

36, no. 1, pp. 9–17, Feb. 2001.

[73] R. Usumi-Fujita, J. Hosomichi, N. Ono, N. Shibutani, S. Kaneko, Y. Shimizu, and T. Ono, "Occlusal hypofunction causes periodontal atrophy and VEGF/VEGFR inhibition in tooth movement.," *Angle Orthod.*, vol. 83, no. 1, pp. 48–56, Jan. 2013.

[74] A. K. L J Gathercole, "Biophysical aspects of the fibers of the periodontal ligament," in *The periodontal ligament in health and disease*, Oxford; New York:Pergamon Press, 1982, pp. 103–117.

[75] H. R. Mühlemann, "10 years of tooth mobility measurements.pdf." pp. 110–122, 1960.

[76] J. A. Bourauel C1, Freudenreich D, Vollmer D, Kobe D, Drescher D, "Simulation of orthodontic tooth movements. A comparison of numerical models.," *J Orofac Orthop*, vol. 60, no. 2, pp. 136–51, 1999.

[77] M. R. Jost-Brinkmann PG1, Tanne K, Sakuda M, "No Title[A FEM study for the biomechanical comparison of labial and palatal force application on the upper incisors. Finite element method]," *Fortschr Kieferorthop*, vol. 54, no. 2, pp. 76–82, 1993.

[78] H. R. Mühlemann, "Tooth mobility (IV). tooth mobility changes through artificial alterations of the peridontium," *J. Periodontol.*, vol. 25, pp. 198–202, 1954.

[79] B. H. F. Limeback, J. Sodek, and D. O. N. M. Brunette, "Nature of Collagens Synthesized by Monkey Periodontal-Ligament Fibroblasts in vitro," *Biochem J*, vol. 170, pp. 63–71, 1978.

[80] J. W. Rippin, "Collagen turnover in the periodontal ligament under normal and altered functional forces. II. Adult rat molars.," *J. Periodontal Res.*, vol. 13, no. 2, pp. 149–54, Mar. 1978.

[81] A. H. Melcher and M. A. Correia, "Remodelling of periodontal ligament in erupting molars of mature rats.," *J. Periodontal Res.*, vol. 6, no. 2, pp. 118–25, 1971.

[82] A. Boyde and S. J. Jones, "Scanning electron microscopy of cementum and sharpey fibre bone," *Zeitschrift für Zellforsch. und mikroskopische Anat.*, vol. 92, no. 4, pp. 536–548, 1968.

[83] A. Habbes, "Quantitative microradiographic study of the adult human alveolar bone," *Rev. Mens. suisse d'odonto-stomatologie*, vol. 77, pp. 130–142, 1967.

[84] D. D. Bosshardt, "Are cementoblasts a subpopulation of osteoblasts or a unique phenotype?," *J. Dent. Res.*, vol. 84, no. 5, pp. 390–406, May 2005.

[85] H. Zhou, R. Chernecky, and J. E. Davies, “Deposition of cement at reversal lines in rat femoral bone.,” *J. Bone Miner. Res.*, vol. 9, no. 3, pp. 367–74, Mar. 1994.

[86] M. Ona and N. Wakabayashi, “Influence of alveolar support on stress in periodontal structures.,” *J. Dent. Res.*, vol. 85, no. 12, pp. 1087–91, 2006.

[87] T. Brosh, D. Rozitsky, S. Geron, and R. Pilo, “Tensile Mechanical Properties of Swine Cortical Mandibular Bone,” *PLoS One*, vol. 9, no. 12, p. e113229, Dec. 2014.

[88] E. L. Niver, N. Leong, J. Greene, D. Curtis, M. I. Ryder, and S. P. Ho, “Reduced functional loads alter the physical characteristics of the bone-periodontal ligament-cementum complex,” *J. Periodontal Res.*, vol. 46, no. 6, pp. 730–741, Dec. 2011.

[89] P. Rygh, “Ultrastructural changes in tension zones of rat molar periodontium incident to orthodontic tooth movement.,” *Am. J. Orthod.*, vol. 70, no. 3, pp. 269–81, Sep. 1976.

[90] P. Rygh, “Ultrastructural changes in pressure zones of human periodontium incident to orthodontic tooth movement,” *Acta Odontol.*, vol. 31, no. 2, pp. 109–122, 1973.

[91] K. Reitan, “Some factors determining the evaluation of forces in orthodontics,” *Am. J. Orthod.*, vol. 43, no. 1, pp. 32–45, Jan. 1957.

[92] S. Sprogar, T. Vaupotic, A. Cör, M. Drevensek, and G. Drevensek, “The endothelin system mediates bone modeling in the late stage of orthodontic tooth movement in rats.,” *Bone*, vol. 43, no. 4, pp. 740–7, Oct. 2008.

[93] M. SC, *Textbook of periodontia*. Philadelphia: McGraw-Hill, 1950.

[94] D. W. Cohen, J. Shapiro, L. Friedman, G. C. Kyle, and S. Franklin, “A longitudinal investigation of the periodontal changes during pregnancy and fifteen months post-partum. II.,” *J. Periodontol.*, vol. 42, no. 10, pp. 653–7, Oct. 1971.

[95] K. H. Rateitschak, “Tooth mobility changes in pregnancy.,” *J. Periodontal Res.*, vol. 2, no. 3, pp. 199–206, 1967.

[96] M. S. Madan, Z. J. Liu, G. M. Gu, and G. J. King, “Effects of human relaxin on orthodontic tooth movement and periodontal ligaments in rats,” *Am. J. Orthod. Dentofac. Orthop.*, vol. 131, no. 1, pp. 1–10, 2007.

[97] H. R. Mühlemann, “tooth mobility (II). role of interdental contact points and the activation on tooth mobility.pdf,” *J. Periodontol.*, vol. 25, pp. 125–128, 1954.

[98] M. C. Manz, H. F. Morris, and S. Ochi, “An evaluation of the Periotest system. Part I: Examiner reliability and repeatability of readings. Dental Implant Clinical Group

(Planning Committee).," *Implant Dent.*, vol. 1, no. 2, pp. 142–6, 1992.

[99] E. E. W. Schulte, D. Lukas, "Periotest values and tooth mobility in periodontal disease : a comparative study," *Periodontics*, vol. 21, no. 4, pp. 289–293, 1990.

[100] W. Schulte and D. Lukas, "The Periotest method.," *Int. Dent. J.*, vol. 42, no. 6, pp. 433–40, Dec. 1992.

[101] B. d'Hoedt, D. Lukas, L. Mühlbradt, F. Scholz, W. Schulte, F. Quante, and A. Topkaya, "[Periotest methods--development and clinical trial].," *Dtsch. zahnärztliche Zeitschrift*, vol. 40, no. 2, pp. 113–25, Feb. 1985.

[102] W. Schulte, *The New Periotest method*. Dental Learning Systems Co., Newtown, OA, 1988.

[103] M. Giargia, I. Ericsson, J. Lindhe, T. Berglundh, and A. M. Neiderud, "Tooth mobility and resolution of experimental periodontitis. An experimental study in the dog.," *J. Clin. Periodontol.*, vol. 21, no. 7, pp. 457–64, Aug. 1994.

[104] H. R. Mühlemann, "Tooth mobility: a review of clinical aspects and research findings.," *J. Periodontol.*, vol. 38, no. 6, pp. Suppl:686–713, 1967.

[105] M. Goellner, J. Schmitt, S. Holst, A. Petschelt, M. Wichmann, and C. Berthold, "Correlations between tooth mobility and the Periotest method in periodontally involved teeth.," *Quintessence Int.*, vol. 44, no. 4, pp. 307–16, 2013.

[106] D.-X. Liu, H.-N. Wang, C.-L. Wang, H. Liu, P. Sun, and X. Yuan, "Modulus of elasticity of human periodontal ligament by optical measurement and numerical simulation.," *Angle Orthod.*, vol. 81, no. 2, pp. 229–36, 2011.

[107] P. Zaslansky, R. Shahar, a. a. Friesem, and S. Weiner, "Relations Between Shape, Materials Properties, and Function in Biological Materials Using Laser Speckle Interferometry: In situ Tooth Deformation," *Adv. Funct. Mater.*, vol. 16, no. 15, pp. 1925–1936, 2006.

[108] M. Goellner, J. Schmitt, M. Karl, M. Wichmann, and S. Holst, "Photogrammetric measurement of initial tooth displacement under tensile force," *Med. Eng. Phys.*, vol. 32, no. 8, pp. 883–888, 2010.

[109] M. Chiba, K. Komatsu, and S. Yamaguchi, "Axial movements of rat mandibular incisors measured under artificial respiration with halothane anaesthesia," *Arch. Oral Biol.*, vol. 40, no. 4, pp. 269–274, Apr. 1995.

[110] N. H. Berkovitz BKB, Moxham BJ, “The periodontal ligament in health and disease,” in *The effects of external forces on the periodontal ligament*, 2nd editio., London: Mosby-Wolfe, 1995, pp. 215–41.

[111] T. S. Fill, J. P. Carey, R. W. Toogood, and P. W. Major, “Experimentally determined mechanical properties of, and models for, the periodontal ligament: critical review of current literature.,” *J. Dent. Biomech.*, vol. 2011, p. 312980, 2011.

[112] M. Zeng, X. Kou, R. Yang, D. Liu, X. Wang, Y. Song, J. Zhang, Y. Yan, F. Liu, D. He, Y. Gan, and Y. Zhou, “Orthodontic Force Induces Systemic Inflammatory Monocyte Responses,” *J. Dent. Res.*, vol. 94, no. 9, pp. 1295–1302, 2015.

[113] G. J. King, S. D. Keeling, E. a McCoy, and T. H. Ward, “Measuring dental drift and orthodontic tooth movement in response to various initial forces in adult rats.,” *Am. J. Orthod. Dentofacial Orthop.*, vol. 99, no. 5, pp. 456–465, 1991.

[114] W. Profitt, *Contemporary Orthodontics*. St. Louis: CV Mosby, 1986.

[115] a. Ziegler, L. Keilig, a. Kawarizadeh, a. Jäger, and C. Bourauel, “Numerical simulation of the biomechanical behaviour of multi-rooted teeth,” *Eur. J. Orthod.*, vol. 27, no. 4, pp. 333–339, 2005.

[116] K. Reitan and E. Kvam, “Comparative behavior of human and animal tissue during experimental tooth movement.,” *Angle Orthod.*, vol. 41, no. 1, pp. 1–14, Jan. 1971.

[117] A. R. Ten Cate, D. A. Deporter, and E. Freeman, “The role of fibroblasts in the remodeling of periodontal ligament during physiologic tooth movement.,” *Am. J. Orthod.*, vol. 69, no. 2, pp. 155–68, Feb. 1976.

[118] G. R. S. Naveh and S. Weiner, “Initial orthodontic tooth movement of a multirooted tooth: a 3D study of a rat molar.,” *Orthod. Craniofac. Res.*, vol. 18, no. 3, pp. 134–42, Aug. 2015.

[119] E. M. Bearn, “Effect of different occlusal profiles on the masticatory forces transmitted by complete dentures. An evaluation.,” *Br. Dent. J.*, vol. 134, no. 1, pp. 7–10, Jan. 1973.

[120] C. H. Gibbs, P. E. Mahan, H. C. Lundeen, K. Brehnan, E. K. Walsh, and W. B. Holbrook, “Occlusal forces during chewing and swallowing as measured by sound transmission.,” *J. Prosthet. Dent.*, vol. 46, no. 4, pp. 443–9, Oct. 1981.

[121] D. J. ANDERSON, “Measurement of stress in mastication. I.,” *J. Dent. Res.*, vol. 35, no. 5, pp. 664–70, Oct. 1956.

[122] J. D. Lin, H. Özcoban, J. P. Greene, A. T. Jang, S. I. Djomehri, K. P. Fahey, L. L. Hunter, G. A. Schneider, and S. P. Ho, "Biomechanics of a bone-periodontal ligament-tooth fibrous joint.," *J. Biomech.*, vol. 46, no. 3, pp. 443–9, Feb. 2013.

[123] R. C. Williams, "Periodontal disease.," *N. Engl. J. Med.*, vol. 322, no. 6, pp. 373–82, Feb. 1990.

[124] C. Newman, Takei, Klokkevold, "Microbiology of Periodontal Disease," in *Carranza's Clinical periodontology*, Tenth edit., Elsevier Inc., 2006, pp. 134–169.

[125] S. Rovin, E. R. Costich, and H. A. Gordon, "The influence of bacteria and irritation in the initiation of periodontal disease in germfree and conventional rats.," *J. Periodontal Res.*, vol. 1, no. 3, pp. 193–204, 1966.

[126] R. Liu, H. S. Bal, T. Desta, N. Krothapalli, M. Alyassi, Q. Luan, and D. T. Graves, "Diabetes enhances periodontal bone loss through enhanced resorption and diminished bone formation.," *J. Dent. Res.*, vol. 85, no. 6, pp. 510–4, Jun. 2006.

[127] R. J. Genco, S. G. Grossi, A. Ho, F. Nishimura, and Y. Murayama, "A proposed model linking inflammation to obesity, diabetes, and periodontal infections.," *J. Periodontol.*, vol. 76, no. 11 Suppl, pp. 2075–84, Nov. 2005.

[128] P. E. Petersen and T. Yamamoto, "Improving the oral health of older people: the approach of the WHO Global Oral Health Programme.," *Community Dent. Oral Epidemiol.*, vol. 33, no. 2, pp. 81–92, Apr. 2005.

[129] J. Beck, R. Garcia, G. Heiss, P. S. Vokonas, and S. Offenbacher, "Periodontal disease and cardiovascular disease.," *J. Periodontol.*, vol. 67, no. 10 Suppl, pp. 1123–37, Oct. 1996.

[130] P. Dhadse, D. Gattani, and R. Mishra, "The link between periodontal disease and cardiovascular disease: How far we have come in last two decades ?," *J. Indian Soc. Periodontol.*, vol. 14, no. 3, p. 148, 2010.

[131] P. I. Eke, B. A. Dye, L. Wei, G. O. Thornton-Evans, and R. J. Genco, "Prevalence of Periodontitis in Adults in the United States: 2009 and 2010," *J. Dent. Res.*, vol. 91, no. 10, pp. 914–920, Oct. 2012.

[132] R. P. Darveau, "Periodontitis: a polymicrobial disruption of host homeostasis," *Nat. Rev. Microbiol.*, vol. 8, no. 7, pp. 481–490, 2010.

[133] V. Kwok and J. G. Caton, "Commentary: prognosis revisited: a system for assigning periodontal prognosis.," *J. Periodontol.*, vol. 78, no. 11, pp. 2063–2071, 2007.

[134] W. Zheng, S. Wang, J. Wang, and F. Jin, “Periodontitis promotes the proliferation and suppresses the differentiation potential of human periodontal ligament stem cells,” *Int. J. Mol. Med.*, vol. 36, pp. 915–922, 2015.

[135] T. E. Van Dyke, “The Management of Inflammation in Periodontal Disease,” *J. Periodontol.*, vol. 79, no. 8s, pp. 1601–1608, Aug. 2008.

[136] P. E. Kolenbrander, R. J. Palmer, A. H. Rickard, N. S. Jakubovics, N. I. Chalmers, and P. I. Diaz, “Bacterial interactions and successions during plaque development,” *Periodontol. 2000*, vol. 42, no. 1, pp. 47–79, 2006.

[137] S. S. Socransky and A. D. Haffajee, “The bacterial etiology of destructive periodontal disease: current concepts.,” *J. Periodontol.*, vol. 63, no. 4 Suppl, pp. 322–331, 1992.

[138] J. L. Dzink, A. C. Tanner, A. D. Haffajee, and S. S. Socransky, “Gram negative species associated with active destructive periodontal lesions.,” *J. Clin. Periodontol.*, vol. 12, no. 8, pp. 648–659, 1985.

[139] P. D. Marsh, “Microbial ecology of dental plaque and its significance in health and disease.,” *Adv. Dent. Res.*, vol. 8, no. 2, pp. 263–71, Jul. 1994.

[140] I. Yoshida-Minami, A. Suzuki, K. Kawabata, A. Okamoto, Y. Nishihara, T. Minami, S. Nagashima, I. Morisaki, and T. Ooshima, “Alveolar bone loss in rats infected with a strain of Prevotella intermedia and Fusobacterium nucleatum isolated from a child with prepubertal periodontitis.,” *J. Periodontol.*, vol. 68, no. 1, pp. 12–7, Jan. 1997.

[141] D. Polak, A. Wilensky, L. Shapira, A. Halabi, D. Goldstein, E. I. Weiss, and Y. Houri-Haddad, “Mouse model of experimental periodontitis induced by Porphyromonas gingivalis/Fusobacterium nucleatum infection: bone loss and host response.,” *J. Clin. Periodontol.*, vol. 36, no. 5, pp. 406–10, May 2009.

[142] R. S. de Molon, V. I. Mascarenhas, E. D. de Avila, L. S. Finoti, G. B. Toffoli, D. M. P. Spolidorio, R. M. Scarel-Caminaga, S. Tetradis, and J. A. Cirelli, “Long-term evaluation of oral gavage with periodontopathogens or ligature induction of experimental periodontal disease in mice.,” *Clin. Oral Investig.*, Sep. 2015.

[143] A. I. Bolstad, H. B. Jensen, and V. Bakken, “Taxonomy, biology, and periodontal aspects of Fusobacterium nucleatum.,” *Clin. Microbiol. Rev.*, vol. 9, no. 1, pp. 55–71, Jan. 1996.

[144] V. Kapatral, I. Anderson, N. Ivanova, T. Los, A. Lykidis, A. Bartman, W. Gardner, L. Zhu, O. Vasieva, L. Chu, Y. Kogan, O. Chaga, E. Goltsman, A. Bernal, N. Larsen, M. D.

Souza, T. Walunas, G. Pusch, M. Fonstein, N. Kyrpides, G. Reznik, A. Bhattacharyya, G. Grechkin, R. Haselkorn, and R. Overbeek, "Genome Sequence and Analysis of the Oral Bacterium Fusobacterium nucleatum Strain Genome Sequence and Analysis of the Oral Bacterium Fusobacterium nucleatum Strain ATCC 25586," vol. 184, no. 7, pp. 2005–2018, 2005.

[145] S. S. Socransky, A. D. Haffajee, M. A. Cugini, C. Smith, and R. L. Kent, "Microbial complexes in subgingival plaque.," *J. Clin. Periodontol.*, vol. 25, no. 2, pp. 134–44, Feb. 1998.

[146] L. Kesavalu, S. Sathishkumar, V. Bakthavatchalu, C. Matthews, D. Dawson, M. Steffen, and J. L. Ebersole, "Rat model of polymicrobial infection, immunity, and alveolar bone resorption in periodontal disease," *Infect. Immun.*, vol. 75, no. 4, pp. 1704–1712, 2007.

[147] R. S. de Molon, E. D. de Avila, and J. A. Cirelli, "Host responses induced by different animal models of periodontal disease: a literature review.," *J. Investig. Clin. Dent.*, vol. 4, no. 4, pp. 211–8, Nov. 2013.

[148] Y. Jiao, M. Hasegawa, and N. Inohara, "Emerging roles of immunostimulatory oral bacteria in periodontitis development," *Trends Microbiol.*, vol. 22, no. 3, pp. 157–163, 2014.

[149] R. P. Darveau, G. Hajishengallis, and M. A. Curtis, "Porphyromonas gingivalis as a Potential Community Activist for Disease," *J. Dent. Res.*, vol. 91, no. 9, pp. 816–820, 2012.

[150] G. Hajishengallis, "Immunomicrobial pathogenesis of periodontitis: Keystones, pathobionts, and host response," *Trends Immunol.*, vol. 35, no. 1, pp. 3–11, 2014.

[151] B. Bainbridge, R. K. Verma, C. Eastman, B. Yehia, M. Rivera, C. Moffatt, I. Bhattacharyya, R. J. Lamont, and L. Kesavalu, "Role of Porphyromonas gingivalis phosphoserine phosphatase enzyme SerB in inflammation, immune response, and induction of alveolar bone resorption in rats.," *Infect. Immun.*, vol. 78, no. 11, pp. 4560–9, Nov. 2010.

[152] W. Zhang, J. Ju, T. Rigney, and G. Tribble, "Porphyromonas gingivalis infection increases osteoclastic bone resorption and osteoblastic bone formation in a periodontitis mouse model.," *BMC Oral Health*, vol. 14, no. 1, p. 89, 2014.

[153] G. Hajishengallis, S. Liang, M. A. Payne, A. Hashim, R. Jotwani, M. A. Eskan, M. L.

McIntosh, A. Alsam, K. L. Kirkwood, J. D. Lambris, R. P. Darveau, and M. A. Curtis, "Low-abundance biofilm species orchestrates inflammatory periodontal disease through the commensal microbiota and complement.," *Cell Host Microbe*, vol. 10, no. 5, pp. 497–506, Nov. 2011.

[154] K. S. Kornman and P. B. Robertson, "Clinical and microbiological evaluation of therapy for juvenile periodontitis.," *J. Periodontol.*, vol. 56, no. 8, pp. 443–446, 1985.

[155] B. S. Michalowicz, M. Ronderos, R. Camara-Silva, A. Contreras, and J. Slots, "Human herpesviruses and Porphyromonas gingivalis are associated with juvenile periodontitis.," *J. Periodontol.*, vol. 71, no. 6, pp. 981–988, 2000.

[156] W. E. C. Moore, L. V. Holdeman, E. P. Cato, R. M. Smibert, J. a. Burmeister, K. G. Palcanis, and R. R. Ranney, "Comparative bacteriology of juvenile periodontitis," *Infect. Immun.*, vol. 48, no. 2, pp. 507–519, 1985.

[157] W. E. Moore and L. V Moore, "The bacteria of periodontal diseases.," *Periodontol. 2000*, vol. 5, pp. 66–77, 1994.

[158] P. M. Duarte, K. R. Tezolin, L. C. Figueiredo, M. Feres, and M. F. Bastos, "Microbial profile of ligature-induced periodontitis in rats," *Arch. Oral Biol.*, vol. 55, no. 2, pp. 142–147, Feb. 2010.

[159] P. E. Kolenbrander and J. London, "Adhere today, here tomorrow: Oral bacterial adherence," *J. Bacteriol.*, vol. 175, no. 11, pp. 3247–3252, 1993.

[160] R. C. Page and H. E. Schroeder, *Periodontitis in Man and Other Animals: A Comparative Review*. Karger, 1982.

[161] D. T. Graves, D. Fine, Y.-T. A. Teng, T. E. Van Dyke, and G. Hajishengallis, "The use of rodent models to investigate host-bacteria interactions related to periodontal diseases.," *J. Clin. Periodontol.*, vol. 35, no. 2, pp. 89–105, Feb. 2008.

[162] S. Rovin, E. R. Costich, and H. A. Gordon, "The influence of bacteria and irritation in the initiation of periodontal disease in germfree and conventional rats," *J. Periodontal Res.*, vol. 1, no. 3, pp. 193–203, Jun. 1966.

[163] B. Klausen, "Microbiological and immunological aspects of experimental periodontal disease in rats: a review article.," *J. Periodontol.*, vol. 62, no. 1, pp. 59–73, Jan. 1991.

[164] F. Guessous, C. Huynh, H. N'Guyen, G. Godeau, J. P. Giroud, J. Meyer, W. Hornebeck, and M. Roch-Arveiller, "An animal model for the assessment of gingival lesions," *J.*

Pharmacol. Toxicol. Methods, vol. 32, no. 3, pp. 161–167, 1994.

[165] D. C. Peruzzo, B. B. Benatti, I. B. Antunes, M. L. Andersen, E. A. Sallum, M. Z. Casati, F. H. Nociti, and G. R. Nogueira-Filho, "Chronic stress may modulate periodontal disease: a study in rats.," *J. Periodontol.*, vol. 79, no. 4, pp. 697–704, Apr. 2008.

[166] C. H. Li and S. Amar, "Morphometric, histomorphometric, and microcomputed tomographic analysis of periodontal inflammatory lesions in a murine model.," *J. Periodontol.*, vol. 78, no. 6, pp. 1120–8, Jun. 2007.

[167] K. Saadi-Thiers, O. Huck, P. Simonis, P. Tilly, J.-E. Fabre, H. Tenenbaum, and J.-L. Davideau, "Periodontal and systemic responses in various mice models of experimental periodontitis: respective roles of inflammation duration and Porphyromonas gingivalis infection.," *J. Periodontol.*, vol. 84, no. 3, pp. 396–406, Mar. 2013.

[168] R. Baron and J. L. Saffar, "A quantitative study of bone remodeling during experimental periodontal disease in the golden hamster.," *J. Periodontal Res.*, vol. 13, no. 4, pp. 309–15, Jul. 1978.

[169] B. Baroukh and J. L. Saffar, "Identification of osteoclasts and their mononuclear precursors. A comparative histological and histochemical study in hamster periodontitis.," *J. Periodontal Res.*, vol. 26, no. 3 Pt 1, pp. 161–6, May 1991.

[170] H. S. Oz and D. a. Puleo, "Animal models for periodontal disease," *J. Biomed. Biotechnol.*, vol. 2011, no. Il, pp. 13–15, 2011.

[171] M. W. Johnson, S. M. Sullivan, M. Rohrer, and M. Collier, "Regeneration of peri-implant infrabony defects using PerioGlas: a pilot study in rabbits.," *Int. J. Oral Maxillofac. Implants*, vol. 12, no. 6, pp. 835–9.

[172] K. L. Tyrrell, D. M. Citron, J. R. Jenkins, and E. J. C. Goldstein, "Periodontal Bacteria in Rabbit Mandibular and Maxillary Abscesses," *J. Clin. Microbiol.*, vol. 40, no. 3, pp. 1044–1047, Mar. 2002.

[173] D. A. W. Oortgiesen, G. J. Meijer, A. L. J. J. Bronckers, X. F. Walboomers, and J. A. Jansen, "Fenestration defects in the rabbit jaw: an inadequate model for studying periodontal regeneration.," *Tissue Eng. Part C. Methods*, vol. 16, no. 1, pp. 133–40, Feb. 2010.

[174] C. Zenobia, H. Hasturk, D. Nguyen, T. E. Van Dyke, A. Kantarci, and R. P. Darveaua, "Porphyromonas gingivalis lipid a phosphatase activity is critical for colonization and

increasing the commensal load in the rabbit ligature model," *Infect. Immun.*, vol. 82, no. 2, pp. 650–659, 2014.

[175] H. Hasturk, A. Kantarci, E. Goguet-Surmenian, A. Blackwood, C. Andry, C. N. Serhan, and T. E. Van Dyke, "Resolvin E1 regulates inflammation at the cellular and tissue level and restores tissue homeostasis in vivo.," *J. Immunol.*, vol. 179, no. 10, pp. 7021–7029, 2007.

[176] W. P. Sorensen, H. Löe, and S. P. Ramfjord, "Periodontal disease in the beagle dog. A cross sectional clinical study.," *J. Periodontal Res.*, vol. 15, no. 4, pp. 380–9, Jul. 1980.

[177] X. Struillou, H. Boutigny, A. Soueidan, and P. Layrolle, "Experimental animal models in periodontology: a review.," *Open Dent. J.*, vol. 4, pp. 37–47, 2010.

[178] S. E. Kim, E. R. Lee, Y. Lee, M. Jeong, Y. W. Park, J. S. Ahn, J. T. Ahn, and K. Seo, "A modified method for inducing periodontitis in dogs using a silk-wire twisted ligature.," *J. Vet. Sci.*, vol. 13, no. 2, pp. 193–7, Jun. 2012.

[179] S. E. Hamp and R. Lindberg, "Histopathology of spontaneous periodontitis in dogs.," *J. Periodontal Res.*, vol. 12, no. 1, pp. 46–54, Jan. 1977.

[180] J. Lindhe and G. Svanberg, "Influence of trauma from occlusion on progression of experimental periodontitis in the beagle dog.," *J. Clin. Periodontol.*, vol. 1, no. 1, pp. 3–14, 1974.

[181] M. A. Weinberg and M. Bral, "Laboratory animal models in periodontology.," *J. Clin. Periodontol.*, vol. 26, no. 6, pp. 335–40, Jun. 1999.

[182] S. Schou, P. Holmstrup, and K. S. Kornman, "Non-human primates used in studies of periodontal disease pathogenesis: a review of the literature.," *J. Periodontol.*, vol. 64, no. 6, pp. 497–508, 1993.

[183] K. S. Kornman, S. C. Holt, and P. B. Robertson, "The microbiology of ligature-induced periodontitis in the cynomolgus monkey.," *J. Periodontal Res.*, vol. 16, no. 4, pp. 363–71, Jul. 1981.

[184] J. L. Ebersole, M. Brunsvold, B. Steffensen, R. Wood, and S. C. Holt, "Effects of immunization with Porphyromonas gingivalis and Prevotella intermedia on progression of ligature-induced periodontitis in the nonhuman primate Macaca fascicularis," *Infect Immun*, vol. 59, no. 10, pp. 3351–3359, 1991.

[185] R. A. Adams, H. A. Zander, and A. M. Polson, "Cell populations in the transseptal fiber

region before, during and after experimental periodontitis in squirrel monkeys.," *J. Periodontol.*, vol. 50, no. 1, pp. 7–12, Jan. 1979.

[186] R. A. Kiel, K. S. Kornman, and P. B. Robertson, "Clinical and microbiological effects of localized ligature-induced periodontitis on non-ligated sites in the cynomolgus monkey.," *J. Periodontal Res.*, vol. 18, no. 2, pp. 200–11, Mar. 1983.

[187] E. Theilade, W. H. Wright, S. B. Jensen, and H. Löe, "Experimental gingivitis in man. II. A longitudinal clinical and bacteriological investigation.," *J. Periodontal Res.*, vol. 1, pp. 1–13, 1966.

[188] J. E. Kennedy and A. M. Polson, "Experimental marginal periodontitis in squirrel monkeys.," *J. Periodontol.*, vol. 44, no. 3, pp. 140–4, Mar. 1973.

[189] L. Heijl, B. R. Rifkin, and H. A. Zander, "Conversion of chronic gingivitis to periodontitis in squirrel monkeys.," *J. Periodontol.*, vol. 47, no. 12, pp. 710–6, Dec. 1976.

[190] A. Ziegler, "Numerical simulation of the biomechanical behaviour of multi-rooted teeth," *Eur. J. Orthod.*, vol. 27, no. 4, pp. 333–339, 2005.

[191] T. E. Van Dyke, H. Hasturk, a. Kantarci, M. O. Freire, D. Nguyen, J. Dalli, and C. N. Serhan, "Proresolving Nanomedicines Activate Bone Regeneration in Periodontitis," *J. Dent. Res.*, vol. 94, no. 1, pp. 148–156, 2014.

[192] G. Singh, R. B. O'Neal, W. A. Brennan, S. L. Strong, J. A. Horner, and T. E. Van Dyke, "Surgical treatment of induced peri-implantitis in the micro pig: clinical and histological analysis.," *J. Periodontol.*, vol. 64, no. 10, pp. 984–9, Oct. 1993.

[193] S. Wang, Y. Liu, D. Fang, and S. Shi, "The miniature pig: A useful large animal model for dental and orofacial research," *Oral Dis.*, vol. 13, no. 6, pp. 530–537, 2007.

[194] K. L. Kalkwarf and R. F. Krejci, "Effect of inflammation on periodontal attachment levels in miniature swine with mucogingival defects.," *J. Periodontol.*, vol. 54, no. 6, pp. 361–364, 1983.

[195] M. E. WEAVER, F. M. SORENSON, and E. B. JUMP, "The miniature pig as an experimental animal in dental research.," *Arch. Oral Biol.*, vol. 7, pp. 17–23.

[196] J. Appleton and T. G. Heaney, "A scanning electron microscope study of the surface features of porcine oral mucosa," *J. Periodontal Res.*, vol. 12, no. 6, pp. 430–435, Dec. 1977.

[197] G. M. Newcomb, "An ultrastructural study of epithelial specialization at the porcine

mucogingival junction.," *J. Periodontal Res.*, vol. 16, no. 1, pp. 51–65, Jan. 1981.

[198] W. C. B. Kenneth L. Kalkwarf, robert F. Krejci, "Chronic Mucogingival Defects in Miniature Swine," *J. Periodontol.*, vol. 54, no. 2, pp. 81–85, 1983.

[199] H. Meng, H. Xie, and Z. Chen, "Evaluation of ligature-induced periodontitis in minipig," *Zhonghua Kou Qiang Yi Xue Za Zhi*, vol. 31, no. 6, pp. 333–336, 1996.

[200] W. L. Ko, J. C. Wang, C. C. Chen, Y. M. Wu, and C. C. Tsai, "[TGF-beta 1 in the experimentally induced inflammatory periodontal tissues in miniature swines].," *Kaohsiung J. Med. Sci.*, vol. 15, no. 6, pp. 315–21, Jun. 1999.

[201] Y. Liu, Y. Zheng, G. Ding, D. Fang, C. Zhang, P. M. Bartold, S. Gronthos, S. Shi, and S. Wang, "Periodontal ligament stem cell-mediated treatment for periodontitis in miniature swine.," *Stem Cells*, vol. 26, no. 4, pp. 1065–1073, 2008.

[202] R. C. Page and H. E. Schroeder, "Pathogenesis of inflammatory periodontal disease. A summary of current work.," *Lab. Invest.*, vol. 34, no. 3, pp. 235–49, Mar. 1976.

[203] E.-Y. Choi, S. H. Bae, M. H. Ha, S.-H. Choe, J.-Y. Hyeon, J.-I. Choi, I. S. Choi, and S.-J. Kim, "Genistein suppresses Prevotella intermedia lipopolysaccharide-induced inflammatory response in macrophages and attenuates alveolar bone loss in ligature-induced periodontitis.," *Arch. Oral Biol.*, vol. 62, pp. 70–9, Feb. 2016.

[204] S. G. de Aquino, M. R. Guimaraes, D. R. Stach-Machado, J. A. F. da Silva, L. C. Spolidorio, and C. Rossa, "Differential regulation of MMP-13 expression in two models of experimentally induced periodontal disease in rats.," *Arch. Oral Biol.*, vol. 54, no. 7, pp. 609–17, Jul. 2009.

[205] R. Xie, A. M. Kuijpers-Jagtman, and J. C. Maltha, "Inflammatory responses in two commonly used rat models for experimental tooth movement: Comparison with ligature-induced periodontitis," *Arch. Oral Biol.*, vol. 56, no. 2, pp. 159–167, Feb. 2011.

[206] T. Shibutani, Y. Murahashi, E. Tsukada, Y. Iwayama, and J. N. Heersche, "Experimentally induced periodontitis in beagle dogs causes rapid increases in osteoclastic resorption of alveolar bone.," *J. Periodontol.*, vol. 68, no. 4, pp. 385–391, 1997.

[207] W. A. Castelli, C. E. Nasjleti, R. E. Caffesse, and R. Diaz-Perez, "Gingival response to silk, cotton, and nylon suture materials.," *Oral Surg. Oral Med. Oral Pathol.*, vol. 45, no. 2, pp. 179–85, Feb. 1978.

[208] U. E. Zappa and A. M. Polson, “Factors associated with occurrence and reversibility of connective tissue attachment loss.,” *J. Periodontol.*, vol. 59, no. 2, pp. 100–6, Feb. 1988.

[209] R. S. de Molon, E. D. de Avila, A. V. Boas Nogueira, J. A. Chaves de Souza, M. J. Avila-Campos, C. R. de Andrade, and J. A. Cirelli, “Evaluation of the host response in various models of induced periodontal disease in mice.,” *J. Periodontol.*, vol. 85, no. 3, pp. 465–77, 2014.

[210] M. S. Tonetti, M. A. Imboden, and N. P. Lang, “Neutrophil migration into the gingival sulcus is associated with transepithelial gradients of interleukin-8 and ICAM-1.,” *J. Periodontol.*, vol. 69, no. 10, pp. 1139–47, Oct. 1998.

[211] O. Takeuchi and S. Akira, “Pattern recognition receptors and inflammation.,” *Cell*, vol. 140, no. 6, pp. 805–20, Mar. 2010.

[212] A. Di Benedetto, I. Gigante, S. Colucci, and M. Grano, “Periodontal disease: Linking the primary inflammation to bone loss,” *Clin. Dev. Immunol.*, vol. 2013, 2013.

[213] S. Tanaka, N. Takahashi, N. Udagawa, T. Tamura, T. Akatsu, E. R. Stanley, T. Kurokawa, and T. Suda, “Macrophage colony-stimulating factor is indispensable for both proliferation and differentiation of osteoclast progenitors.,” *J. Clin. Invest.*, vol. 91, no. 1, pp. 257–263, Jan. 1993.

[214] T. W. Oates and D. L. Cochran, “Bone cell interactions and regulation by inflammatory mediators.,” *Curr. Opin. Periodontol.*, vol. 3, pp. 34–44, 1996.

[215] S. L. Teitelbaum, “Osteoclasts: what do they do and how do they do it?,” *Am. J. Pathol.*, vol. 170, no. 2, pp. 427–35, Feb. 2007.

[216] G. Nussbaum and L. Shapira, “How has neutrophil research improved our understanding of periodontal pathogenesis?,” *J. Clin. Periodontol.*, vol. 38 Suppl 1, pp. 49–59, Mar. 2011.

[217] M. I. Ryder, “Comparison of neutrophil functions in aggressive and chronic periodontitis.,” *Periodontol. 2000*, vol. 53, pp. 124–37, Jun. 2010.

[218] J. B. Matthews, H. J. Wright, A. Roberts, P. R. Cooper, and I. L. C. Chapple, “Hyperactivity and reactivity of peripheral blood neutrophils in chronic periodontitis.,” *Clin. Exp. Immunol.*, vol. 147, no. 2, pp. 255–64, Feb. 2007.

[219] E. Hajishengallis and G. Hajishengallis, “Neutrophil homeostasis and periodontal health in children and adults.,” *J. Dent. Res.*, vol. 93, no. 3, pp. 231–7, 2013.

[220] R. Attström, “Presence of leukocytes in crevices of healthy and chronically inflamed gingivae.,” *J. Periodontal Res.*, vol. 5, no. 1, pp. 42–7, 1970.

[221] R. Attström and J. Egelbert, “Presence of leukocytes within the gingival crevices during developing gingivitis in dogs.,” *J. Periodontal Res.*, vol. 6, no. 2, pp. 110–4, 1971.

[222] K. Irie, C. M. Novince, and R. P. Darveau, “Impact of the Oral Commensal Flora on Alveolar Bone Homeostasis.,” *J. Dent. Res.*, vol. 93, no. 8, pp. 801–806, Jun. 2014.

[223] S. Garcia de Aquino, F. R. Manzolli Leite, D. R. Stach-Machado, J. A. Francisco da Silva, L. C. Spolidorio, and C. Rossa, “Signaling pathways associated with the expression of inflammatory mediators activated during the course of two models of experimental periodontitis.,” *Life Sci.*, vol. 84, no. 21–22, pp. 745–54, May 2009.

[224] H. E. Schroeder and J. Lindhe, “Conversion of stable established gingivitis in the dog into destructive periodontitis.,” *Arch. Oral Biol.*, vol. 20, no. 12, pp. 775–82, Dec. 1975.

[225] G. Bhattarai, S. B. Poudel, S.-H. Kook, and J.-C. Lee, “Resveratrol prevents alveolar bone loss in an experimental rat model of periodontitis.,” *Acta Biomater.*, vol. 29, pp. 398–408, Jan. 2016.

[226] J. Lin, J. Lee, H. Ozcoban, G. Schneider, and S. Ho, “Biomechanical adaptation of the bone-periodontal ligament (PDL)-tooth fibrous joint as a consequence of disease.,” *J. Biomech.*, vol. 47, no. 9, pp. 2102–14, Jun. 2014.

[227] M. Ibi, A. Ishisaki, M. Yamamoto, S. Wada, T. Kozakai, A. Nakashima, J. Iida, S. Takao, Y. Izumi, A. Yokoyama, and M. Tamura, “Establishment of cell lines that exhibit pluripotency from miniature swine periodontal ligaments,” *Arch. Oral Biol.*, vol. 52, no. 10, pp. 1002–1008, 2007.

[228] R. C. Page, W. F. Ammons, L. R. Schectman, and L. A. Dillingham, “Collagen fibre bundles of the normal marginal gingiva in the marmoset,” *Arch. Oral Biol.*, vol. 19, no. 11, pp. 1039–1043, Nov. 1974.

[229] M. Giargia and J. Lindhe, “Tooth mobility and periodontal disease.,” *J. Clin. Periodontol.*, vol. 24, no. 11, pp. 785–795, 1997.

[230] F. Baelum. V, Fejerskov. O. & Manji, “Periodontai disease in adult Kenyans,” *J. Clin. Periodontol.*, vol. 15, pp. 445–452, 1988.

[231] A. M. Polson, M. E. Kantor, and H. A. Zander, “Periodontal repair after reduction of inflammation.,” *J. Periodontal Res.*, vol. 14, no. 6, pp. 520–5, Nov. 1979.

[232] W. Shefter, G. & Me Fall, “Occlusal relation and periodontal status in human adults,” *J. Periodontol.*, vol. 55, pp. 368–375, 1984.

[233] J. H. Lee, J. D. Lin, J. I. Fong, M. I. Ryder, and S. P. Ho, “The adaptive nature of the bone-periodontal ligament-cementum complex in a ligature-induced periodontitis rat model,” *Biomed Res. Int.*, vol. 2013, 2013.

[234] R. Persson and A. Svensson, “Assessment of tooth mobility using small loads. I. Technical devices and calculations of tooth mobility in periodontal health and disease.,” *J. Clin. Periodontol.*, vol. 7, no. 4, pp. 259–75, Aug. 1980.

[235] S. P. Ho, M. P. Kurylo, T. K. Fong, S. S. J. Lee, H. D. Wagner, M. I. Ryder, and G. W. Marshall, “The biomechanical characteristics of the bone-periodontal ligament-cementum complex,” *Biomaterials*, vol. 31, no. 25, pp. 6635–6646, 2010.

[236] W. S. Herring SW, Li YM, Liu ZJ, Popowics TE, Rafferty KL, *Oral Biology and Dental Models*. Taylor & Francis Group, 2011.

[237] Douglas WR, “Of pigs and men and research: a review of applications and analogies of the pig, sus scrofa, in human medical research,” *Sp. Life Sci*, vol. 3, no. 3, pp. 226–34, 1972.

[238] E. B. J. M.E. Weaver, F.M. Sorenson, “The miniature pig as an experimental animal in dental research,” *Arch. Oral Biol.*, vol. 7, pp. 17–24, 1962.

[239] Z. Sun, T. Smith, S. Kortam, D. G. Kim, B. C. Tee, and H. Fields, “Effect of bone thickness on alveolar bone-height measurements from cone-beam computed tomography images,” *Am. J. Orthod. Dentofac. Orthop.*, vol. 139, no. 2, 2011.

[240] Z.-J. Liu, K. L. Rafferty, W. Ye, and S. W. Herring, “Differential response of pig masseter to botulinum neurotoxin serotypes a and b.,” *Muscle Nerve*, vol. 52, no. 1, pp. 88–93, 2015.

[241] S. W. Herring, “TMJ anatomy and animal models,” *Journal of Musculoskeletal Neuronal Interactions*, vol. 3, no. 4. pp. 391–394, 2003.

[242] Elbrecht, “Beitrag zur Bestimmung der lockerungsgrade der Zahne,” *Parad. zeitschrift für die grenzfragen der medizin und Odontol.*, no. Pattern 2, p. 138, 1939.

[243] W. V, “Vergleichende Untersuchungen verschiedener Paradentose-Behandlungen mittels einer neucn metrischen Methode,” *Parad. zeitschrift für die grenzfragen der medizin und Odontol.*, 1942.

[244] R. S. MANLY, A. YURKSTAS, and J. B. RESWICK, “An instrument for measuring tooth mobility.,” *J. Periodontol.*, vol. 22, no. 3, pp. 148–55, Jul. 1951.

[245] D. C. A. Picton, “tilting movement of the tooth during biting.pdf,” *Arch. Oral Biol.*, vol. 7, pp. 151–159, 1962.

[246] A. Lewin, “The direction of tooth movement within the periodontal space. The omnidirectional transducer.,” *J. Dent. Assoc. South Africa*, vol. 25, no. 9, pp. 308–14, Nov. 1970.

[247] M. Yamane, M. Yamaoka, M. Hayashi, I. Furutoyo, N. Komori, and B. Ogiso, “Measuring tooth mobility with a no-contact vibration device.,” *J. Periodontal Res.*, vol. 43, no. 1, pp. 84–9, Feb. 2008.

[248] G. R. S. Naveh, R. Shahar, V. Brumfeld, and S. Weiner, “Tooth movements are guided by specific contact areas between the tooth root and the jaw bone : A dynamic 3D microCT study of the rat molar,” *J. Struct. Biol.*, vol. 177, pp. 477–483, 2012.

[249] J. L. Ebersole, F. Feuille, L. Kesavalu, and S. C. Holt, “Host modulation of tissue destruction caused by periodontopathogens: effects on a mixed microbial infection composed of Porphyromonas gingivalis and Fusobacterium nucleatum.,” *Microb. Pathog.*, vol. 23, no. 1, pp. 23–32, Jul. 1997.

[250] Y. Zubery, C. R. Dunstan, B. M. Story, L. Kesavalu, J. L. Ebersole, S. C. Holt, and B. F. Boyce, “Bone resorption caused by three periodontal pathogens in vivo in mice is mediated in part by prostaglandin.,” *Infect. Immun.*, vol. 66, no. 9, pp. 4158–62, Sep. 1998.

[251] J. H. Park, J.-K. Lee, H.-S. Um, B.-S. Chang, and S.-Y. Lee, “A periodontitis-associated multispecies model of an oral biofilm.,” *J. Periodontal Implant Sci.*, vol. 44, no. 2, pp. 79–84, 2014.

[252] S. S. Socransky and A. D. Haffajee, “Periodontal microbial ecology.,” *Periodontol. 2000*, vol. 38, pp. 135–87, 2005.

[253] A. Rawlinson, A. Eley, K. W. Bennett, and L. Goodwin, “Role of Fusobacterium nucleatum in Periodontal Health and Disease,” *Microb. Ecol. Health Dis.*, vol. 7, no. 4, pp. 201–205, 1994.

[254] B. Henderson, J. M. Ward, and D. Ready, “Aggregatibacter (Actinobacillus) actinomycetemcomitans: a triple A* periodontopathogen?,” *Periodontol. 2000*, vol. 54,

no. 1, pp. 78–105, Oct. 2010.

[255] B. de B. Bezerra, O. Andriankaja, J. Kang, S. Pacios, H. J. Bae, Y. Li, V. Tsiagbe, H. Schreiner, D. H. Fine, and D. T. Graves, "A.actinomycetemcomitans -induced periodontal disease promotes systemic and local responses in rat periodontium," *J. Clin. Periodontol.*, vol. 39, no. 4, pp. 333–341, Apr. 2012.

[256] M. E. Weaver, E. B. Jump, and C. F. McKean, "The eruption pattern of deciduous teeth in miniature swine.," *Anat. Rec.*, vol. 154, no. 1, pp. 81–6, Jan. 1966.

[257] A. Saito, S. Inagaki, R. Kimizuka, K. Okuda, Y. Hosaka, T. Nakagawa, and K. Ishihara, "Fusobacterium nucleatum enhances invasion of human gingival epithelial and aortic endothelial cells by Porphyromonas gingivalis.," *FEMS Immunol. Med. Microbiol.*, vol. 54, no. 3, pp. 349–55, Dec. 2008.

[258] A. Greer, K. Irie, A. Hashim, B. G. Leroux, A. M. Chang, M. A. Curtis, and R. P. Darveau, "Site-Specific Neutrophil Migration and CXCL2 Expression in Periodontal Tissue.," *J. Dent. Res.*, Mar. 2016.

[259] S. W. Herring, "Mastication and maturity: a longitudinal study in pigs.," *J. Dent. Res.*, vol. 56, no. 11, pp. 1377–82, Nov. 1977.

[260] M. Burmølle, D. Ren, T. Bjarnsholt, and S. J. Sørensen, "Interactions in multispecies biofilms: Do they actually matter?," *Trends Microbiol.*, vol. 22, no. 2, pp. 84–91, 2014.

[261] H. E. Schroeder and J. Lindhe, "Conditions and pathological features of rapidly destructive, experimental periodontitis in dogs.," *J. Periodontol.*, vol. 51, no. 1, pp. 6–19, Jan. 1980.

[262] J. Slots and E. Hausmann, "Longitudinal study of experimentally induced periodontal disease in Macaca arctoides: relationship between microflora and alveolar bone loss.," *Infect. Immun.*, vol. 23, no. 2, pp. 260–9, Feb. 1979.

[263] K. Nylander, B. Danielsen, O. Fejerskov, and E. Dabelsteen, "Expression of the endothelial leukocyte adhesion molecule-1 (ELAM-1) on endothelial cells in experimental gingivitis in humans.," *J. Periodontol.*, vol. 64, no. 5, pp. 355–7, May 1993.

[264] M. S. Tonetti, "Molecular factors associated with compartmentalization of gingival immune responses and transepithelial neutrophil migration.," *J. Periodontal Res.*, vol. 32, no. 1 Pt 2, pp. 104–9, Jan. 1997.

[265] M. S. Tonetti, M. A. Imboden, L. Gerber, N. P. Lang, J. Laissue, and C. Mueller,

"Localized expression of mRNA for phagocyte-specific chemotactic cytokines in human periodontal infections.," *Infect. Immun.*, vol. 62, no. 9, pp. 4005–14, Sep. 1994.

[266] C. Zenobia, X. L. Luo, A. Hashim, T. Abe, L. Jin, Y. Chang, Z. C. Jin, J. X. Sun, G. Hajishengallis, M. A. Curtis, and R. P. Darveau, "Commensal bacteria-dependent select expression of CXCL2 contributes to periodontal tissue homeostasis," *Cell. Microbiol.*, vol. 15, no. 8, pp. 1419–1426, Aug. 2013.

[267] J. Lindhe, S. Hamp, and H. Löe, "Experimental periodontitis in the beagle dog.," *J. Periodontal Res.*, vol. 8, no. 1, pp. 1–10, 1973.

[268] S. W. Herring and R. P. Scapino, "Physiology of feeding in miniature pigs.," *J. Morphol.*, vol. 141, no. 4, pp. 427–460, 1973.

[269] Z. J. Liu, J. R. Green, C. A. Moore, and S. W. Herring, "Time series analysis of jaw muscle contraction and tissue deformation during mastication in miniature pigs.," *J. Oral Rehabil.*, vol. 31, no. 1, pp. 7–17, Jan. 2004.

[270] S. W. Herring, K. L. Rafferty, Z. J. Liu, and C. D. Marshall, "Jaw muscles and the skull in mammals: the biomechanics of mastication," *Comp. Biochem. Physiol. Part A Mol. Integr. Physiol.*, vol. 131, no. 1, pp. 207–219, Dec. 2001.

[271] Z. J. Liu and S. W. Herring, "Masticatory strains on osseous and ligamentous components of the temporomandibular joint in miniature pigs.," *J. Orofac. Pain*, vol. 14, no. 4, pp. 265–78, 2000.

[272] Z. J. Liu and S. W. Herring, "Bone surface strains and internal bony pressures at the jaw joint of the miniature pig during masticatory muscle contraction," *Arch. Oral Biol.*, vol. 45, no. 2, pp. 95–112, Feb. 2000.

[273] J. V. Basmajian, *Muscles Alive, Their Functions Revealed by Electromyography*, Second Edi. 1967.

[274] R. L. Ciochon, R. A. Nisbett, and R. S. Corruccini, "Dietary consistency and craniofacial development related to masticatory function in minipigs.," *J. Craniofac. Genet. Dev. Biol.*, vol. 17, no. 2, pp. 96–102.

[275] Z. J. Liu, V. Shcherbatyy, M. Kayalioglu, and a. Seifi, "Internal kinematics of the tongue in relation to muscle activity and jaw movement in the pig," *J. Oral Rehabil.*, vol. 36, no. 9, pp. 660–674, 2009.

[276] X. Huang, G. Zhang, and S. W. Herring, "Alterations of muscle activities and jaw

movements after blocking individual jaw-closing muscles in the miniature pig.," *Arch. Oral Biol.*, vol. 38, no. 4, pp. 291–297, 1993.

[277] V. Shcherbatyy and Z.-J. Liu, "Internal Kinematics of the Tongue During Feeding in Pigs," *Anat. Rec. Adv. Integr. Anat. Evol. Biol.*, vol. 290, no. 10, pp. 1288–1299, Oct. 2007.

[278] M. M. Liu, W. Herzog, and H. H. C. M. Savelberg, "Dynamic muscle force predictions from EMG: an artificial neural network approach," *J. Electromyogr. Kinesiol.*, vol. 9, no. 6, pp. 391–400, Dec. 1999.

[279] W. L. Hylander, "Mandibular function in Galago crassicaudatus and Macaca fascicularis: an in vivo approach to stress analysis of the mandible.," *J. Morphol.*, vol. 159, no. 2, pp. 253–96, Feb. 1979.

[280] S. W. Herring, "Masticatory muscles and the skull: A comparative perspective," *Arch. Oral Biol.*, vol. 52, no. 4, pp. 296–299, Apr. 2007.

[281] D. C. A. Picton, "vertical movment of cheek teeth during biting.pdf," *Arch. Oral Biol.*, vol. 8, pp. 109–118, 1963.

[282] Y. Misawa, T. Kageyama, K. Moriyama, S. Kurihara, H. Yagasaki, T. Deguchi, H. Ozawa, and N. Sahara, "Effect of age on alveolar bone turnover adjacent to maxillary molar roots in male rats: A histomorphometric study," *Arch. Oral Biol.*, vol. 52, no. 1, pp. 44–50, Jan. 2007.

[283] M. J. Oehmke, C. R. C. Schramm, E. Knolle, N. Frickey, T. Bernhart, and H.-J. Oehmke, "Age-dependent changes of the periodontal ligament in rats.," *Microsc. Res. Tech.*, vol. 63, no. 4, pp. 198–202, Mar. 2004.

[284] E. A. Tonna, "Factors (aging) affecting bone and cementum.," *J. Periodontol.*, vol. 47, no. 5, pp. 267–80, May 1976.

[285] M. I. Cho and P. R. Garant, "Formation of multinucleated fibroblasts in the periodontal ligaments of old mice.," *Anat. Rec.*, vol. 208, no. 2, pp. 185–96, Feb. 1984.

[286] N. A. Barnett and D. J. Rowe, "A comparison of alveolar bone in young and aged mice.," *J. Periodontol.*, vol. 57, no. 7, pp. 447–52, Jul. 1986.

[287] D. Grant and S. Bernick, "The periodontium of ageing humans.," *J. Periodontol.*, vol. 43, no. 11, pp. 660–7, Nov. 1972.

[288] J.-H. Lee, J. D. Lin, J. I. Fong, M. I. Ryder, and S. P. Ho, "The adaptive nature of the

bone-periodontal ligament-cementum complex in a ligature-induced periodontitis rat model.," *Biomed Res. Int.*, vol. 2013, p. 876316, 2013.

[289] C. M. BELTING, I. SCHOUR, J. P. WEINMANN, and M. J. SHEPRO, "Age changes in the periodontal tissues of the rat molar.," *J. Dent. Res.*, vol. 32, no. 3, pp. 332–53, Jun. 1953.

[290] R. Lattouf, R. Younes, D. Lutomski, N. Naaman, G. Godeau, K. Senni, and S. Changotade, "Picrosirius red staining: a useful tool to appraise collagen networks in normal and pathological tissues.," *J. Histochem. Cytochem.*, vol. 62, no. 10, pp. 751–8, Oct. 2014.

[291] C. J. Self, "Tooth Roots and the Periodontal Ligament: Morphology, Modeling and Behavior.," University of Washington, 2015.

[292] K.-D. Yeh and T. Popowics, "Molecular and structural assessment of alveolar bone during tooth eruption and function in the miniature pig, sus scrofa.," *Anat. Histol. Embryol.*, vol. 40, no. 4, pp. 283–91, Aug. 2011.

[293] Mandee Yang, M. Baldwin, A. Salamati, and Z.-J. Liu, "Periodontal Mineralization in Experimental Periodontitis," in *IADR*, 2016.

[294] H. S. Popowics T, Yeh K, Rafferty K, "Functional cues in the development of osseous tooth support in the pig, Sus scrofa," *J Biomech*, vol. 42, no. 12, pp. 1961–1966, 2009.

[295] J. Wolff, *Das Gesetz der Transformation der Knochen*. Hirschwald, Berlin, 1892.

[296] K. L. Rafferty, Z. J. Liu, W. Ye, A. L. Navarrete, T. T. Nguyen, A. Salamati, and S. W. Herring, "Botulinum toxin in masticatory muscles: Short- and long-term effects on muscle, bone, and craniofacial function in adult rabbits," *Bone*, vol. 50, no. 3, pp. 651–662, 2012.

[297] T.-G. Kwon, H.-S. Park, S.-H. Lee, I.-S. Park, and C.-H. An, "Influence of unilateral masseter muscle atrophy on craniofacial morphology in growing rabbits.," *J. Oral Maxillofac. Surg.*, vol. 65, no. 8, pp. 1530–7, Aug. 2007.

[298] C. Y. Tsai, R. Y. Huang, C. M. Lee, W. T. Hsiao, and L. Y. Yang, "Morphologic and Bony Structural Changes in the Mandible After a Unilateral Injection of Botulinum Neurotoxin in Adult Rats," *J. Oral Maxillofac. Surg.*, vol. 68, no. 5, pp. 1081–1087, 2010.

[299] S. Ejiri, E. Toyooka, M. Tanaka, R. B. Anwar, and S. Kohno, "Histological and histomorphometrical changes in rat alveolar bone following antagonistic tooth extraction

and/or ovariectomy.," *Arch. Oral Biol.*, vol. 51, no. 11, pp. 941–50, Nov. 2006.

[300] J. Liu, Z. Jin, and Q. Li, "Effect of occlusal hypofunction and its recovery on the three-dimensional architecture of mandibular alveolar bone in growing rats.," *J. Surg. Res.*, vol. 193, no. 1, pp. 229–36, Jan. 2015.

[301] J. Liu, S.-Y. Liu, Y.-J. Zhao, X. Gu, Q. Li, Z.-L. Jin, and Y.-J. Chen, "Effects of occlusion on mandibular morphology and architecture in rats.," *J. Surg. Res.*, vol. 200, no. 2, pp. 533–43, Feb. 2016.

[302] A. Mavropoulos, P. Ammann, A. Bresin, and S. Kiliaridis, "Masticatory demands induce region-specific changes in mandibular bone density in growing rats.," *Angle Orthod.*, vol. 75, no. 4, pp. 625–30, Jul. 2005.

[303] E. Tanaka, R. Sano, N. Kawai, G. E. J. Langenbach, P. Brugman, K. Tanne, and T. M. G. J. van Eijden, "Effect of food consistency on the degree of mineralization in the rat mandible.," *Ann. Biomed. Eng.*, vol. 35, no. 9, pp. 1617–21, Sep. 2007.

[304] M. Bouvier and W. L. Hylander, "The effect of dietary consistency on gross and histologic morphology in the craniofacial region of young rats.," *Am. J. Anat.*, vol. 170, no. 1, pp. 117–26, May 1984.

[305] C. Katsaros, R. Berg, and S. Kiliaridis, "Influence of masticatory muscle function on transverse skull dimensions in the growing rat.," *J. Orofac. Orthop. = Fortschritte der Kieferorthopädie Organ/official J. Dtsch. Gesellschaft für Kieferorthopädie*, vol. 63, no. 1, pp. 5–13, Jan. 2002.

[306] K. E. Byrd, "Masticatory movements and EMG activity following electrolytic lesions of the trigeminal motor nucleus in growing guinea pigs.," *Am. J. Orthod.*, vol. 86, no. 2, pp. 146–61, Aug. 1984.

[307] K. E. Byrd, S. T. Stein, A. J. Sokoloff, and K. Shankar, "Craniofacial alterations following electrolytic lesions of the trigeminal motor nucleus in actively growing rats," *Am. J. Anat.*, vol. 189, no. 2, pp. 93–110, Oct. 1990.

[308] S. L. HOROWITZ and H. H. SHAPIRO, "Modification of skull and jaw architecture following removal of the masseter muscle in the rat.," *Am. J. Phys. Anthropol.*, vol. 13, no. 2, pp. 301–8, Jun. 1955.

[309] R. Pellizzari, O. Rossetto, G. Schiavo, and C. Montecucco, "Tetanus and botulinum neurotoxins: mechanism of action and therapeutic uses," *Philos. Trans. R. Soc. B Biol.*

Sci., vol. 354, no. 1381, pp. 259–268, Feb. 1999.

[310] A. Wheeler and H. S. Smith, "Botulinum toxins: mechanisms of action, antinociception and clinical applications.," *Toxicology*, vol. 306, pp. 124–46, Apr. 2013.

[311] O. Rossetto, A. Megighian, M. Scorzeto, and C. Montecucco, "Botulinum neurotoxins," *Toxicon*, vol. 67, pp. 31–36, Jun. 2013.

[312] D. Dressler and R. Benecke, "Pharmacology of therapeutic botulinum toxin preparations," *Disabil. Rehabil.*, vol. 29, no. 23, pp. 1761–1768, Jan. 2007.

[313] D. B. Lacy and R. C. Stevens, "Sequence homology and structural analysis of the clostridial neurotoxins," *J. Mol. Biol.*, vol. 291, no. 5, pp. 1091–1104, Sep. 1999.

[314] H. Niemann, "Clostridial neurotoxins--proposal of a common nomenclature.," *Toxicon*, vol. 30, no. 3, pp. 223–5, Mar. 1992.

[315] J. Jankovic and M. F. Brin, "Botulinum toxin: historical perspective and potential new indications.," *Muscle Nerve. Suppl.*, vol. 6, pp. S129–45, 1997.

[316] A. B. Scott, "Botulinum toxin injection into extraocular muscles as an alternative to strabismus surgery.," *Ophthalmology*, vol. 87, no. 10, pp. 1044–9, Oct. 1980.

[317] A. B. Scott, A. Rosenbaum, and C. C. Collins, "Pharmacologic weakening of extraocular muscles.," *Invest. Ophthalmol.*, vol. 12, no. 12, pp. 924–7, Dec. 1973.

[318] B. Davletov, M. Bajohrs, and T. Binz, "Beyond BOTOX: Advantages and limitations of individual botulinum neurotoxins," *Trends in Neurosciences*, vol. 28, no. 8. pp. 446–452, 2005.

[319] A. P. Tighe and G. Schiavo, "Toxicon Botulinum neurotoxins : Mechanism of action," vol. 67, pp. 87–93, 2013.

[320] C. Montecucco and G. Schiavo, "Structure and function of tetanus and botulinum neurotoxins.," *Q. Rev. Biophys.*, vol. 28, no. 4, pp. 423–72, Nov. 1995.

[321] T. J. Dickerson and K. D. Janda, "The use of small molecules to investigate molecular mechanisms and therapeutic targets for treatment of botulinum neurotoxin A intoxication.," *ACS Chem. Biol.*, vol. 1, no. 6, pp. 359–369, 2006.

[322] G. Schiavo, A. Santucci, B. R. Dasgupta, P. P. Mehta, J. Jontes, F. Benfenati, M. C. Wilson, and C. Montecucco, "Botulinum neurotoxins serotypes A and E cleave SNAP-25 at distinct COOH-terminal peptide bonds.," *FEBS Lett.*, vol. 335, no. 1, pp. 99–103, Nov. 1993.

[323] F. A. Meunier, G. Lisk, D. Sesardic, and J. O. Dolly, “Dynamics of motor nerve terminal remodeling unveiled using SNARE-cleaving botulinum toxins: The extent and duration are dictated by the sites of SNAP-25 truncation,” *Mol. Cell. Neurosci.*, vol. 22, no. 4, pp. 454–466, 2003.

[324] L. W. Duchen, “An electron microscopic study of the changes induced by botulinum toxin in the motor end-plates of slow and fast skeletal muscle fibres of the mouse,” *J. Neurol. Sci.*, vol. 14, no. 1, pp. 47–60, Sep. 1971.

[325] A. de Paiva, F. A. Meunier, J. Molgó, K. R. Aoki, and J. O. Dolly, “Functional repair of motor endplates after botulinum neurotoxin type A poisoning: biphasic switch of synaptic activity between nerve sprouts and their parent terminals.,” *Proc. Natl. Acad. Sci. U. S. A.*, vol. 96, no. 6, pp. 3200–5, Mar. 1999.

[326] O. Rossetto, M. Pirazzini, P. Bolognese, M. Rigoni, and C. Montecucco, “An update on the mechanism of action of tetanus and botulinum neurotoxins.,” *Acta Chim. Slov.*, vol. 58, no. 4, pp. 702–7, Dec. 2011.

[327] L. Barber, T. Hastings-Ison, R. Baker, H. Kerr Graham, R. Barrett, and G. Lichtwark, “The effects of botulinum toxin injection frequency on calf muscle growth in young children with spastic cerebral palsy: a 12-month prospective study,” *J. Child. Orthop.*, vol. 7, no. 5, pp. 425–433, Nov. 2013.

[328] D. Ranoux, “Botulinum toxin and painful peripheral neuropathies: what should be expected?,” *Rev. Neurol. (Paris).*, vol. 167, no. 1, pp. 46–50, Jan. 2011.

[329] J. Jankovic, “Botulinum toxin therapy for cervical dystonia.,” *Neurotox. Res.*, vol. 9, no. 2–3, pp. 145–8, Apr. 2006.

[330] J. A. Singh, “Botulinum toxin therapy for osteoarticular pain: an evidence-based review,” *Ther. Adv. Musculoskelet. Dis.*, vol. 2, no. 2, pp. 105–118, Apr. 2010.

[331] U. Wollina, “Botulinum toxin: Non-cosmetic indications and possible mechanisms of action,” *J. Cutan. Aesthet. Surg.*, vol. 1, no. 1, p. 3, 2008.

[332] D. B. Sanders, E. W. Massey, and E. G. Buckley, “Botulinum toxin for blepharospasm: single-fiber EMG studies.,” *Neurology*, vol. 36, no. 4, pp. 545–7, Apr. 1986.

[333] L. Bach-Rojecky, M. Šalković-Petrišić, and Z. Lacković, “Botulinum toxin type A reduces pain supersensitivity in experimental diabetic neuropathy: Bilateral effect after unilateral injection,” *Eur. J. Pharmacol.*, vol. 633, no. 1–3, pp. 10–14, May 2010.

[334] F. H. de M. de S. Klein, F. M. Brenner, M. S. Sato, F. M. B. R. Robert, and K. A. Helmer, "Lower facial remodeling with botulinum toxin type A for the treatment of masseter hypertrophy.," *An. Bras. Dermatol.*, vol. 89, no. 6, pp. 878–84, 2013.

[335] D. J. Lange, M. F. Brin, C. L. Warner, S. Fahn, and R. E. Lovelace, "Distant effects of local injection of botulinum toxin.," *Muscle Nerve*, vol. 10, no. 6, pp. 552–5, 1987.

[336] B. G. Lapatki, J. P. van Dijk, B. P. C. van de Warrenburg, and M. J. Zwarts, "Botulinum toxin has an increased effect when targeted toward the muscle's endplate zone: A high-density surface EMG guided study," *Clin. Neurophysiol.*, vol. 122, no. 8, pp. 1611–1616, Aug. 2011.

[337] S. K. A. Ihde and V. S. Konstantinovic, "The therapeutic use of botulinum toxin in cervical and maxillofacial conditions: an evidence-based review," *Oral Surgery, Oral Med. Oral Pathol. Oral Radiol. Endodontology*, vol. 104, no. 2, 2007.

[338] J.-D. Kün-Darbois, H. Libouban, and D. Chappard, "Botulinum toxin in masticatory muscles of the adult rat induces bone loss at the condyle and alveolar regions of the mandible associated with a bone proliferation at a muscle enthesis," *Bone*, vol. 77, pp. 75–82, Aug. 2015.

[339] C. F. Sinclair, L. E. Gurey, and A. Blitzer, "Oromandibular dystonia: long-term management with botulinum toxin.," *Laryngoscope*, vol. 123, no. 12, pp. 3078–83, Dec. 2013.

[340] Y. J. Shim, M. K. Lee, T. Kato, H. U. Park, K. Heo, and S. T. Kim, "Effects of botulinum toxin on jaw motor events during sleep in sleep bruxism patients: a polysomnographic evaluation.," *J. Clin. Sleep Med.*, vol. 10, no. 3, pp. 291–8, Mar. 2014.

[341] R. Persaud, G. Garas, S. Silva, C. Stamatoglou, P. Chatrath, and K. Patel, "An evidence-based review of botulinum toxin (Botox) applications in non-cosmetic head and neck conditions.," *JRSM Short Rep.*, vol. 4, no. 2, p. 10, Feb. 2013.

[342] C. B. Ivanhoe, J. M. Lai, and G. E. Francisco, "Bruxism after brain injury: successful treatment with botulinum toxin-A.," *Arch. Phys. Med. Rehabil.*, vol. 78, no. 11, pp. 1272–3, Nov. 1997.

[343] E. Mijiritsky, C. Mortellaro, O. Rudberg, M. Fahn, C. Basegmez, and L. Levin, "Botulinum Toxin Type A as Preoperative Treatment for Immediately Loaded Dental Implants Placed in Fresh Extraction Sockets for Full-Arch Restoration of Patients With

Bruxism.," *J. Craniofac. Surg.*, vol. 27, no. 3, pp. 668–70, May 2016.

[344] C. T. Rubin and L. E. Lanyon, "Kappa Delta Award paper. Osteoregulatory nature of mechanical stimuli: function as a determinant for adaptive remodeling in bone.," *J. Orthop. Res.*, vol. 5, no. 2, pp. 300–10, 1987.

[345] I. Rot, S. Mardesic-Brakus, W. J. Costain, M. Saraga-Babic, and B. Kablar, "Role of skeletal muscle in mandible development.," *Histol. Histopathol.*, vol. 29, no. 11, pp. 1377–94, Nov. 2014.

[346] N. Hichijo, E. Tanaka, N. Kawai, L. J. van Ruijven, and G. E. J. Langenbach, "Effects of Decreased Occlusal Loading during Growth on the Mandibular Bone Characteristics.," *PLoS One*, vol. 10, no. 6, p. e0129290, 2015.

[347] C. S. Chang, L. Bergeron, C. C. Yu, P. K. T. Chen, and Y. R. Chen, "Mandible changes evaluated by computed tomography following Botulinum Toxin A injections in square-faced patients.," *Aesthetic Plast. Surg.*, vol. 35, no. 4, pp. 452–5, Aug. 2011.

[348] K. G. Raphael, A. Tadinada, J. M. Bradshaw, M. N. Janal, D. A. Sirois, K. C. Chan, and A. G. Lurie, "Osteopenic consequences of botulinum toxin injections in the masticatory muscles: a pilot study," *J. Oral Rehabil.*, vol. 41, no. 8, pp. 555–563, Aug. 2014.

[349] M. J. Ravosa and A. S. Hogue, "Function and Fusion of the Mandibular Symphysis in Mammals: A Comparative and Experimental Perspective," in *Anthropoid Origins*, Boston, MA: Springer US, 2004, pp. 413–462.

[350] R. Huiskes, R. Ruimerman, G. H. van Lenthe, and J. D. Janssen, "Effects of mechanical forces on maintenance and adaptation of form in trabecular bone.," *Nature*, vol. 405, no. 6787, pp. 704–6, Jun. 2000.

[351] J. Kün-darbois, H. Libouban, and D. Chappard, "Botulinum toxin in masticatory muscles of the adult rat induces bone loss at the condyle and alveolar regions of the mandible associated with a bone proliferation at a muscle enthesis," *Bone*, vol. 77, pp. 75–82, 2015.

[352] J. S. Hickey, R. B. O'Neal, M. J. Scheidt, S. L. Strong, D. Turgeon, and T. E. Van Dyke, "Microbiologic characterization of ligature-induced peri-implantitis in the microswine model.," *J. Periodontol.*, vol. 62, no. 9, pp. 548–553, 1991.

[353] G. Carnevale, R. Pontoriero, and M. B. Hürzeler, "Management of furcation involvement.," *Periodontol. 2000*, vol. 9, pp. 69–89, Oct. 1995.

[354] P. Vályi and I. Gorzó, "[Periodontal abscess: etiology, diagnosis and treatment].," *Fogorv.*

Sz., vol. 97, no. 4, pp. 151–5, Aug. 2004.

CIRRICULUM VITA

ATRIYA SALAMATI

atriys@gmail.com

EDUCATION

09/09 – 07/16	**University of Washington School of Dentistry** Ph.D. in Oral Biology, GPA: 3.87 D.D.S. GPA: 3.59	**Seattle, WA** July 2016 June 2013
09/06–08/08	**University of Washington** Bachelor of Science, Biology/Physiology, GPA: 3.50/4.0 August 2008	**Seattle, WA**
09/05 - 08/06	**Everett Community College (EvCC)** Associate of Arts and Science, GPA: 3.92/4.0 Associate of Science, GPA: 3.92/4.0	**Everett, WA** August 2006 May 2006
09/04 - 08/05	**Nassau Community College** GPA: 3.97/4.0	**Garden City, NY**

AWARDS & HONORS

2016	University of Washington School of Dentistry Admissions Committee- Interviewer
2015	University of Washington Warren G. Magnuson Scholarship
2014	Sunstar Americas Preventative Dentistry Award
2013	American Association of Oral Biologists Award: In recognition of significant achievement in, and contribution to, oral science
2012	James and Joyce Oates Scholarship; Clinical Excellence with Metallic Restorations
2012	UW Dental Alumni Association Scholarship
2011	Scientific Judge for UW Research Day poster competition
2011	Certificate of Appreciation recognizing community service: UWSoD Office of Educational Partnership and Diversity
2009-2016	NIH/NIDCR T32DE07132, T90DE021984 trainee
2008- 2010	UW Dean's List
2008	Mary Gates Research Endowment Research Scholarship

2008-2015	First Aid, CPR, HIV/AIDS and Blood Born Pathogen certifications, American Red Cross
2007	Howard Hughes Medical Institution Integrative Research Intern Scholar
2006	EvCC: Transfer Student Scholarship
2006	Distinguished Tutor Award: Mathematics, Physics and Chemistry, EvCC
2006	College Reading and Learning Association, Certified Tutor, EvCC

PROFESSIONAL MEMBERSHIPS

American Academy of Pediatric Dentistry (AAPD), American Dental Association (ADA), Washington State Dental Association (WSDA), Seattle King County Dental Association (SKCDA), Academy of General Dentistry (AGD), American Association of Dental Research (AADR), International Association of Dental research (IADR), American Association for the Advancement of Science (AAAS), Eastside Young Dentist Study Club, Practice Based Research Network (PBRN).

RESEARCH EXPERIENCE

06/13 – 07/16 **Dr. Susan Herring, UW, Dept. of Orthodontics Seattle, WA**
PhD dissertation focused on measuring tooth movement during mastication using implantable piezoelectric ultrasound transducers. Research was supported by NIH/NIDCR grant T90 DE021984-03 and R21 DE023127 and SunStar Preventative dentistry award.

06/10 – 09/10 **Dr. Susan Herring, UW, Dept. of Orthodontics Seattle, WA**
Conducted research on paralysis of masseter muscle by Botulinum neurotoxin type A (Botox) and its effect on alveolar bone resorption in rabbits. Research was supported by NIH/NIDCR grant T32DE07132-27 and R01DE018142.

06/09 – 09/09 **Dr. Timothy Cox, UW, Dept. of Pediatrics and Craniofacial Medicine Seattle, WA**
Conducted research on quantifying midfacial morphology in chick embryos using Optical Projection Tomography (OPT) and 3D imaging software. Research was supported by NIH/NIDCR grant T32DE07132 and DE 018456.

01/08 – 08/08 **Dr. Celeste Berg, UW, Dept. of Genome Sciences Seattle, WA**

Conducted research with *D. melanogaster*— making new DNA constructs (rhoG4PB-Ds.Red.T4), and using this construct to analyze the process of dorsal appendage (DA) tube formation during *Drosophila* oogenesis, using confocal microscopy.

01/07 – 09/07 **Dr. Celeste Berg, UW, Dept. of Genome Sciences Seattle, WA**
Conducted research with *D. melanogaster*— making new DNA construct (Cp18FGAL4), involved cell/molecular methods: transformation, PCR, running gel, DNA sequencing, DNA purification, etc. And genetic methods: fly ovary dissection, fly injection, and crossing flies.

12/06 – 03/07 **Dr. Andrew Christie, UW, Dept. of Biology Seattle, WA**
Conducted research with *Cancer productus* crabs— dissecting midgut and immunohistochemically staining them with antibodies to localize different type of proteins that exist in this type of crab's midgut.

PEER-REVIEWED PUBLICATIONS

Rafferty KL, Liu ZJ, Ye W, Navarrete AL, Nguyen TT, **Salamati** A, Herring SW. Botulinum toxin in masticatory muscles: short- and long-term effect on muscle, bone, and craniofacial function in adult rabbits. Bone. 2012 Mar; 50 (3):651-62.

ORAL AND POSTER PRESENTATIONS

06/2016 Rafferty KL, **Salamati A,** Cunningham C, Shin DU, Herring SW. Bone Architecture in the Rabbit (*Oryctolagus cuniculus*) Mandible as a Function of Load and Age**.** Poster presentation at the International Congress of Vertebrate Morphology (ICVM) **Washington, DC**

06/2016 Yang M, Baldwin MC, **Salamati A,** Liu ZJ. Periodontal Mineralization in Experimental Periodontitis**.** Poster presentation at the IADR **Seoul, South Korea**

03/2016 **Salamati A,** Jie Chen, Cambria Cunningham, Herring SW, Liu ZJ. Quantifying *in vivo* Tooth Mobility and PDL Space Width in Pigs**.** Poster presentation at the AADR/CADR **Los Angeles, CA**

03/2015 **Salamati A,** Liu ZJ, Herring SW. Quantifying *in vivo* Tooth Mobility**.** Poster presentation at the IADR/AADR/CADR **Boston, MA**

03/2015 Chen J, Kim D, **Salamati A**, Liu ZJ. Periodontal Space, Root Size, and Alveolar Structures in Young Pigs**.** Poster presentation at the IADR/AADR/CADR **Boston, MA**

09/2014 **Salamati A,** Liu ZJ, Herring SW. Quantifying *in vivo* Tooth Mobility During Mastication: Health and Periodontal Disease. Oral presentation at the Annual Oral Health Sciences Research Symposium **Seattle, WA**

03/2012 **Salamati A,** Rafferty KL, Herring SW. Does Masseter Paralysis Lead to Alveolar Bone Resorption? Oral presentation at AADR/CADR Annual Session **Tampa, FL**

09/2010 **Salamati A,** Rafferty KL, Herring SW. Does Masseter Paralysis Lead to Alveolar Bone Resorption? Poster presentation at the University of Washington School of Dentistry (UWSoD) Research Day **Seattle, WA**

03/2010 **Salamati A,** Maga Murat, Cox L, Cox TC. Quantifying Mid-facial Morphology in Chick Embryos. Poster presentation at the UWSoD Research Day **Seattle, WA**

09/2009 **Salamati A,** Maga Murat, Cox L, Cox TC. Quantifying Mid-facial Morphology in Chick Embryos. Poster presentation at the annual AADR/CADR conference **Washington, DC**

10/2007 **Salamati A,** Berg C. Cp18-FGAL4: DNA construct for Tissue-Specific Gene Expression During Oogenesis in Drosophila *melanogaster.*UW-HHMI Research Symposium and UW Mary Gates Undergraduate Research Symposium **Seattle, WA**

TEACHING EXPERIENCE

2015-present **UW School of Dentistry Dept. of Restorative Dentistry**
Seattle, WA
Position: Affiliate Faculty
Duties: Supervise and teach senior dental students with treatment planning and restorative treatment of patients once a week in the Restorative Dentistry clinic.

2012 **Complete Denture 2nd year Prosthodontics Course Seattle, WA**
Position: Teaching Assistant (TA)
Duties: As a 3rd year dental student I taught 2nd year dental students complete denture concepts and indications, guided them to improve skills for taking final impressions, setting teeth and beautifying dentures.

2011 **Dental Anatomy Seattle, WA**
Position: Tutor
Duties: As a 2nd year dental student I helped 1st year dental students with their teeth wax-ups and learning dental anatomy after clinic hours.

2010 **Human Gross Anatomy Seattle, WA**
Position: Teaching Assistant (TA)
Duties: As a 2nd year dental student I helped teach 1st year medical and dental students with the gross anatomy dissection lab course and small group discussion and learning activities.

DENTAL LICENSE

Washington State (2013-present)

CLINICAL AND WORK EXPERIENCE

7/16 - Present **Community Health Center of Snohomish County (CHCsno) Everett, WA**
I work as a *full time* dentist floating in all 5 locations of CHCsno and provide treatment to adult and pediatric dental patients. Working in all 5 locations allows me to exercise my networking and team working skills with different providers and different dental assistants and hygienists.

06/15-present **UW School of Dentistry Dept. of Restorative Dentistry: Seattle, WA**
As an *Affiliate Faculty*, I have been volunteering to teach and supervise eight senior dental students. I supervise them with treatment planning and performing restorative dental treatments on patients once a week in the General Practice Dentistry clinic at the University of Washington. This clinical teaching experience has

allowed me to give back to my school and also staying up to date with the latest technologies and dental materials being used.

11/14 – 7/16 **Community Health Center of Snohomish County**
Everett, WA
I worked as a *per diem general dentist* one day per week floating in all 5 locations of CHCsno and see adult and pediatric patients. Even though I do not have my own patients all the time, working in all the clinics for the past two years, I see many of the same individuals come back for treatment. This has let me enjoy seeing the continuity of care and specially with my pediatric patients, it has been a joy to see them transition through primary teeth to mixed dentition, and from mixed dentition to permanent teeth.

08/13 –10/14 **A Plus Dental**
Federal Way, WA
I Worked as an *associate general dentist* on Saturdays and saw mainly pediatric patients in a private dental practice setting. I enjoyed working with children, however, due to limited pediatric training, I had to refer some cases to pediatric specialists and learned a lot from them.

11/08 – 04/09 **The EverGreen School**
Shoreline, WA
As an after school child care *provider,* I spent 15 hours a week with students in grades K-9 and provided different activities ranging from reading and storytelling, sport sessions fun movie evenings, and various other activities for them. I really enjoyed this activity as it let me be around children and enjoy their contagious energy and enthusiasm.

09/07 – 05/09 **Dr. Raymond Huey's lab. UW Dept. of Biology**
Seattle, WA
I worked as an undergraduate *research assistant* with animal physiology research on *D. melanogaster* temperature selectivity between male and female flies.

09/05 – 08/06 **Everett Community College**
Everett, WA
I *tutored* Mathematics (College Algebra and Calculus), general Chemistry and Physics. This was my first teaching experience to freshman college students which also helped me learn more as I was teaching them. I was able to get training on teaching techniques and I was certified by the College Reading and Learning Associates and was awarded the Distinguished Tutor Award in

mathematics, physics and chemistry by the Everett Community College Tutoring Center.

LEADERSHIP EXPERIENCE

2013 – Present **Zoroastrian Society of Washington State (ZSWS)**
Bellevue, WA
Position: President
Duties: As the youngest president of ZSWS, I have the responsibility of meeting with my board members several times annually, decision making, spontaneous trouble shooting, and through an efficient team work and community effort we make sure everyone is involved to keep the culture alive and pass on its values to the younger generation. This volunteer position has led me to really exercise my leadership and communication skills. I have learned a lot by being open to ideas, be creative to keep things vibrant and exciting for our younger members, resolve issues, and get things done in a timely manner through team work and by keeping our members involved and delegating responsibilities to them.

2012 – 2013 **Longview Dental Clinic**
Longview, WA
Position: Clinic Director and Site Coordinator
Duties: Scheduled student and faculty volunteers, oversaw clinic operations, and provided free dental care to low-income families of Longview 1 Saturday per quarter.

2011-2013 **Dental Action Day**
Olympia, WA
Position: Annual Dental Student Participant
Duties: Advocated for dental patients, dental students, and dentists to senators and state representatives at state Capitol.

2011-2012 **UWSoD Student Research Group**
Seattle, WA
Position: President
Duties: Selected lecturers and organized seminars in different fields of dental research for the elective course “Current Trends in Dental Research” at UW, to enhance the interest of pre-dental, dental student, and resident in dental research.

2010-2011 **Husky Smiles**
Tacoma, WA

Position: Site Coordinator and Volunteer Student Dentist
Duties: Organized volunteer students and dentists. Educated parents and children on the importance of early prevention and good oral hygiene habits, screening dentition and soft tissue, application of fluoride, and referrals. Volunteered for Shoreline and Tacoma Husky Smiles.

2007-2008 **United Way of King County and UW Carlson Leadership Center**
Seattle, WA
Position: Leader for Martin Luther King Jr. (MLK) Day of Service.
Duties: Organized volunteers for community service projects at American Red Cross.

VOLUNTEER EXPERIENCE

2016 **Snohomish County School Sealant and Fluoride Project**
Edmonds, WA
Position: Volunteer Dentist
Duties: Since starting as a full time dentist with the Community Health Center of Snohomish County, I have been able to join their team in providing oral health education to children and free fluoride and sealants to elementary school children in the city of Edmonds.

2014-present **Seattle King County Clinic**
Seattle, WA
Position: Volunteer Dentist
Duties: I volunteered for a four-day-clinic through Remote Area Medical (RAM) and Seattle King County Clinics alongside of volunteers in medical, dental, and vision specialists who provide free care to low-income patients. I was able to use my skills and provide exams and same day treatments ranging from diagnostic, restorative and emergency dental treatments to a very diverse group of adult and pediatric patients who had lined up to be seen at this free and volunteer-run clinic based in Seattle Center Key Arena.

June 2014, 2015 **Pacific Northwest Dental Conference (PNDC)**
Bellevue, WA
Position: Volunteer Dentist with Washington State Dental Associations (WSDA)
Duties: Volunteered as a lecture ambassador for various dentists.

2013-present **Research Outreach**
Seattle, WA
Position: Volunteer researcher
Duties: Our research lab has been hosting numerous research outreach activities to high school biology students and students from the Summer Medical Dental Education Program (SMDEP) to engage their interest in research, and more specifically dental research. I have helped my mentor, Dr. Herring, in teaching the students how to propose a research hypothesis and how to test their hypothesis by demonstrating and running the electromyograms (EMGs) of masseter muscles while chewing hard and soft food items and recording the muscle's activity.

2013-present **Smiles for Veterans**
Seattle, WA
Position: Volunteer Dentist
Duties: Weekend volunteer activity, with a group of other dentists and hygienists. Provide free dental care to veterans.

2013-2015 **Longview Dental Clinic**
Longview, WA
Position: Volunteer Dentist
Duties: I joined Dr. Donald Chi's team on a few trips to Longview to screen elementary school, middle school, and high school students for clinically visible caries or defective restorations, provide oral hygiene instructions and referrals to the Longview dental student clinic or other clinics as indicated, and answered any questions that the students had about their oral health.

2009-2013 **Longview Dental Clinic**
Longview, WA
Position: Volunteer Student Dentist
Duties: Provided dental care through performing exams, fillings, extractions, and periodontal therapy for the low-income families of Longview; Visited women's shelter; provided exams and preventive care, and oral hygiene instructions. Learned from Dr. Peter Milgrom how to arrest cavities with the use of silver diamine fluoride (SDF), and followed up the patients in the next visits and observed the effect of the use of SDF on carious lesions.

2011 **Walla Walla Mobile Dental Clinic**
Walla Walla, WA
Position: Volunteer Student Dentist
Duties: Outreach activity with UW Dental Education in Care of Persons with Disabilities (DECOD) program; I traveled with a group of volunteer dentists and dental students to the town of Walla Walla

and provided dental care in a dental mobile van to children who were diagnosed with Down syndrome, cerebral palsy, autism spectrum disorder, and other physically, mentally, and developmentally disabling conditions that exposed them to lower access to dental care and thus higher dental diseases. I performed extractions, fillings, deep cleanings, exams, and fluoride applications, and instructed the care givers on the importance of oral hygiene for these patients.

2010-2013 **45th Street Dental Clinic**
Seattle, WA
Position: Volunteer Student Dentist
Duties: I became interested in volunteering with this evening clinic as a 2nd year dental student. I started with assisting more senior dental students and as a 3rd and 4th year I provided exams, fillings, extractions, periodontal therapy to homeless teens. As a senior dental student, I also mentored younger student dentists with the dental procedures and treatment planning.

2010-2013 **Latina Health Fair**
Seattle, WA Position: Volunteer Student Dentist
Duties**:** During the last 3 years of dental school I attended the annual weekend long Latina Health Fair and provided dental exams, oral hygiene instructions, fluoride varnish, and referrals for kids and adults of Latina background in Seattle.

2010 **Neah Bay Indian Reservation Dental Camp**
Neah Bay, WA
Position: Dental Student Volunteer
Duties: Traveled to Neah Bay Indian Reservation during a 3-day educational outreach program with a group of volunteers and taught native Indian high school students to wax teeth, place composite restorations on plastic teeth, suture pig legs; inspired the community toward increased involvement in dentistry and answered questions.

2010 **Summer Medical Dental Education Program (SMDEP)**
Seattle, WA
Position: Volunteer Dental Student
Duties: Mentored high school students with taking alginate impressions, pouring study casts, placing composite restorations on dentoform, waxing teeth, and suturing; responded to questions about dental school.

2010 **Smile Mobile**
Lacy, WA

Position: Volunteer Student Dentist
Duties: This was a week-long volunteer activity where I was able to performed dental exam, oral hygiene instructions, prophylaxis and sealants for pediatric patients in a mobile van, sponsored by Delta Dental and Washington Dental Service Foundation.

2008-2009 **Seattle's Union Gospel Mission Dental Clinic:**
Seattle, WA
Position: Volunteer Dental Assistant
Duties: Assisted dentists in providing free dental care to homeless adult patients.

2008 **Health Care Alternative Spring Break (HCASB)**
Goldendale, WA
Position: Volunteer Dental Assistant and Intern
Duties: Shadowed and assisted in the only dental clinics in town during spring break.

2005-2009 **Seattle Children's Hospital**
Seattle, WA
Position: Volunteer
Duties: Provided emotional support to terminally ill children. Played with the children, read books for them, and kept them engaged for a few hours each week.

2005-2009 **Providence Everett Medical Center and PEMC Pharmacy**
Seattle, WA
Position: Volunteer
Duties: Helped the pharmacist re-stock the shelves and get the medication orders ready. This was a good start for me to familiarize myself with different medications.

2005-2009 **American Red Cross (Dept. Health Services & International Services)**
Seattle, WA
Position: Volunteer
Duties: Acted as a first aid and emergency responder to different events around Seattle. With the International services I helped with language section in helping those who needed Farsi translators.

ELECTIVES AND ADDITIONAL TRAINING

Summer 2015,16 **Pediatric Dentistry Externship:** In 2015 I spent 4 months observing Dr. Joel Berg at the UW Center for Pediatric Dentistry

while he treated patients including several cases treated with silver diamine fluoride (SDF). In 2016 I spent several sessions observing Dr. Joel Berg, Dr. Rebecca Slayton, and Dr. Ana Lucia Seminario while they supervised residents while treating medically compromised patients or in dental surgery center performing complex cases under general anesthesia (GA).

June 2016 **Pulp therapy and treatment of primary teeth by Dr. David Rothman:** This was a full day lecture and hands-on workshop learning different techniques in management and treatment of primary teeth, pulp therapy, and stainless steel crowns.

2014-2016 **PNDC:** Attended various lectures and earned 18 CE credits.

2014-2015 **AAPD:** Attended various lectures and earned 10 CE credits.

2014 **Botox-A Therapies for UWSoD Faculty and Graduate Students:** 4 CE credits.

2013-Present **Biomedical Research Integrity Seminars (BRI):** I have been attending these summer seminar series offered by the UW School of Medicine. Each year BRI seminars cover topics described in the NIH Guide to meet the NIH requirements for research trainees. The topics are: Conflict of Interest, Data Acquisition and Ownership, Peer Review, Responsible Authorship, and Research Misconduct.

2013-2014 **New Dentist Boot Camp:** 4 credits of CDE course received through Seattle King County Dental society.

June 2013 **AB Dental USA- Implantology Seminars:** 16 CE credits in Implant Placement and Bone Grafting Hands-On Seminar.

April 2013 **Esthetic Implant & Periodontal Plastic Surgery:** CDE sponsored though AGD.

Spring 2013 **DECOD elective:** Worked with mentally and developmentally disabled patients, performed fillings, extraction and prophylaxis. Educated them and their parents and caregivers on the importance of oral home care.(DECOD stands for: Dental Education in the Care of Persons with Disabilities).

Winter 2013 **Tucker Cast Gold Restoration Elective:** Learned the technique from leading dentists including Dr. Tucker and performed several cast gold inlays and onlays.

Winter 2013 **Honors Periodontal Surgery Selective:** Performed clinical crown lengthening surgery, distal wedge surgery, extraction with socket

preservation and bone grafts, suturing techniques, connective tissue grafts, and esthetic zone gingivectomies.

Su 2012, Sp 2013 **Oral Medicine Clinical Elective:** Shadowed Dr. Truelove and Dr. Martin and learned how to diagnose and treat patients with chronic pain, burning mouth syndrome, TMD, post traumatic facial pains, neuropathies, performed punch biopsies of oral lesions.

2012-2013 **Oral Surgery Elective Quarter, totaling 4 quarters of OS rotation:** Four academic quarters of clinical experience with simple and surgical extractions.

2012-2013 **Implant Placement and Restorations:** Clinical experience placing implant bodies and restorations.

Fall2012, 2013 **Oral Lesions Pathology Elective:** Additional training in identification and treatment of oral lesions.

Fall2012 **Bone Pathology Elective:** Additional training in identification and treatment of oral bone pathologies

Fall 2012 **Internal Medicine:** Took this course with Ortho, Perio, Pros, Endo and GPR residents for extra training in internal medicine and dealing with medical emergencies.

Summer 2012 **Harborview Hospital Oral Surgery Externship:** One-week externship in Harborview and Swedish Medical Center Oral and Maxillofacial surgery department observing jaw fixation and resection surgeries, head and neck cancer removal surgeries, trauma surgeries and performing extractions and pre- and post- operative examinations.

Summer 2012 **Pediatric dentistry External Rotation:** Two-week external rotation in Sea-Mar Tacoma community dental clinic providing fillings, pulpotomies, extractions, and limited ortho treatments for community clinic patients.

Summer 2012 **Cranial Anatomy:** Took this course with Ortho, Perio, Pros, Endo and GPR residents for extra training in head and neck anatomy. Received extra training in dissecting techniques, reviewing head and neck anatomy, and placing dental implants.

Spring 2012 **Direct Gold Foil Restoration Elective:** Learned the technique and performed several class I, class V, and class VI gold foil fillings on patients.

Spring 2011 **Implant Training course:** Required UWSoD course in implant systems, implant placement techniques, and implant restorations.